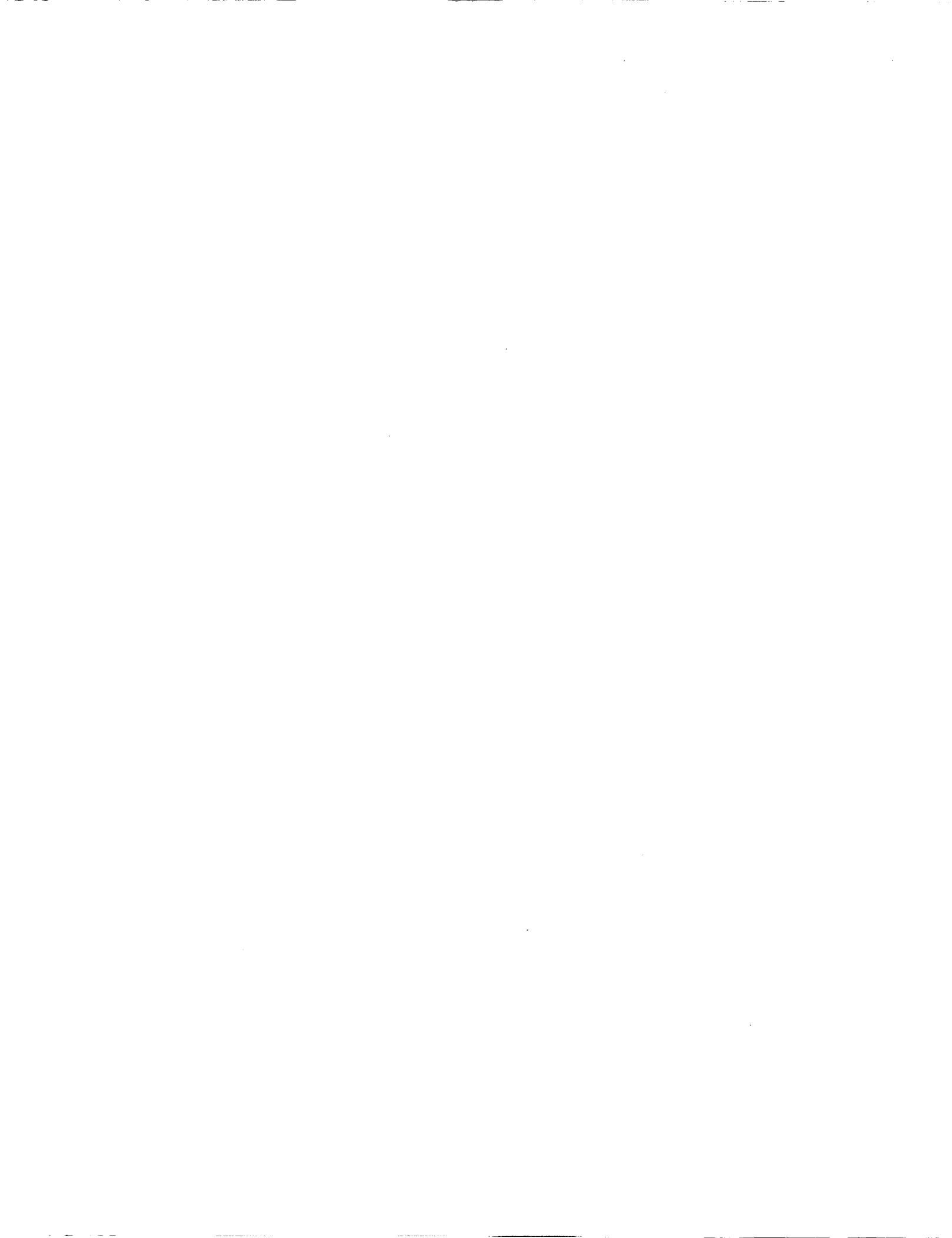


NOTE TO USERS

This reproduction is the best copy available.

UMI[®]



**Free and forced vibrations of tapered composite beams including the
effects of axial force and damping**

Hasnet Eftakher Uddin Ahmed

A Thesis
in
The department
Of
Mechanical and Industrial Engineering

Presented in partial fulfillment of the requirements for the degree of
Master of Applied science at
Concordia University
Montreal, Quebec, Canada.

October, 2008

© Hasnet Eftakher Uddin Ahmed, 2008



Library and Archives
Canada

Bibliothèque et
Archives Canada

Published Heritage
Branch

Direction du
Patrimoine de l'édition

395 Wellington Street
Ottawa ON K1A 0N4
Canada

395, rue Wellington
Ottawa ON K1A 0N4
Canada

Your file *Votre référence*
ISBN: 978-0-494-63190-4
Our file *Notre référence*
ISBN: 978-0-494-63190-4

NOTICE:

The author has granted a non-exclusive license allowing Library and Archives Canada to reproduce, publish, archive, preserve, conserve, communicate to the public by telecommunication or on the Internet, loan, distribute and sell theses worldwide, for commercial or non-commercial purposes, in microform, paper, electronic and/or any other formats.

The author retains copyright ownership and moral rights in this thesis. Neither the thesis nor substantial extracts from it may be printed or otherwise reproduced without the author's permission.

In compliance with the Canadian Privacy Act some supporting forms may have been removed from this thesis.

While these forms may be included in the document page count, their removal does not represent any loss of content from the thesis.

AVIS:

L'auteur a accordé une licence non exclusive permettant à la Bibliothèque et Archives Canada de reproduire, publier, archiver, sauvegarder, conserver, transmettre au public par télécommunication ou par l'Internet, prêter, distribuer et vendre des thèses partout dans le monde, à des fins commerciales ou autres, sur support microforme, papier, électronique et/ou autres formats.

L'auteur conserve la propriété du droit d'auteur et des droits moraux qui protègent cette thèse. Ni la thèse ni des extraits substantiels de celle-ci ne doivent être imprimés ou autrement reproduits sans son autorisation.

Conformément à la loi canadienne sur la protection de la vie privée, quelques formulaires secondaires ont été enlevés de cette thèse.

Bien que ces formulaires aient inclus dans la pagination, il n'y aura aucun contenu manquant.


Canada

**CONCORDIA UNIVERSITY
SCHOOL OF GRADUATE STUDIES**

This is to certify that the Thesis prepared,

By: Hasnet Eftakher Uddin Ahmed

Entitled: "Free and forced vibrations of tapered composite beams including the effects of axial force and damping"

And submitted in partial fulfillment of the requirements for the degree of

Master of Applied Science

Complies with the regulations of this university and meets the accepted standards with respect to originality and quality.

Signed by the Final Examination committee:

_____	Chair
_____	Examiner
_____	Examiner
_____	Examiner
_____	External
_____	Supervisor

Dr. R. Ganesan

Approved by: _____
Graduate Program Director
Department of mechanical and Industrial Engineering

Date: _____
Dean
Faculty of Engineering & Computer Science

Abstract

Free and forced vibrations of tapered composite beams including the effects of axial force and damping

Hasnet Eftakher Uddin Ahmed

Tapered composite beams formed by terminating or dropping-off some of the plies from primary structure are being used in various engineering applications since the mid-1980s. Because of their structural tailoring capabilities, damage tolerance and potential for creating significant weight savings in engineering applications such as helicopter yoke, robot arms and turbine blades, tapered composite beams have received much attention from engineers and researchers. Design of mechanical components using tapered composite beams requires a better understanding of their behavior on free and forced vibrations. In the present thesis, free and forced vibration analysis including the effects of axial force and damping of tapered composite beams is conducted using conventional, and higher-order finite elements and the Rayleigh-Ritz method. Composite beam samples are manufactured and tested for the determination of mechanical properties and damping loss factor. Conventional and higher-order finite element formulations are established based on classical laminate theory. Since conventional finite element has limitation in obtaining accurate results with fewer elements, higher-order finite element formulation is developed considering four degrees of freedom per node (deflection, rotation, curvature and gradient of curvature) to overcome that problem. Rayleigh-Ritz method is used to obtain solutions for different boundary conditions to validate the results obtained by finite element methods. A detailed parametric study is conducted to

investigate the effects of boundary conditions, laminate configuration, taper configurations, taper angle, the ratio of the length of the thick section to the length of thin section, axial force, and damping. The NCT-301 graphite-epoxy composite material is used in the experimental work, analysis, and in the parametric study.

Acknowledgements

First of all I would like to express my invaluable gratitude to Almighty creator who gave me the ability to complete this thesis. Then I wish to express my most sincere gratitude to my supervisor Dr. Rajamohan Ganesan for his time, patience, tolerance and keen guidance especially for his thesis writings correction. In a word he enhanced the value and experience of my graduate research immeasurably.

I would also like to thank Dan Jurus, Robert Oliber and Ming Xie who help me giving their time during my experimental work. I would also thank and appreciate to my officemates with whom I shared a lot time for many ideas as a good friend.

Outside my research work I wish to thank my parents and family members who have always inspired me by wishing every accomplishment in my research work. I am especially grateful to my elder sister Dr. Runa Laila who always encourages me for hard work, sincerity, patience, and honesty.

Nomenclature

A	Cross-section area
A_{avg}	Average of the end areas of the element
a_i	Co-efficient of mode shape
b	Width of the beam
c	The intercept of the centerline of the ply from the mid-plane
c_i	Co-efficient of displacement
E	Modulus of elasticity of isotropic material
E_1	Modulus of elasticity in fiber direction
E_2	Modulus of elasticity in transverse direction
d	The displacement
D_{11}	The first coefficient of bending stiffness matrix of composite beam
$D_{11}(x)$	The first coefficient of variable bending stiffness matrix of composite beam
h	Thickness of the laminate
h'_k	Distance to the top surface of k^{th} ply in tapered beam from the mid-plane
h'_{k-1}	Distance to the lower surface of k^{th} ply in tapered beam from the mid-plane
GK	Gradient of curvature
K	Curvature
k	Stiffness
L	Length of the beam
l	Length of the finite element
m	The mass per unit length

N_j	The shape function
\tilde{P}^T	Transpose of ortho-normal modal matrix
q	The generalized co-ordinate
Q_i	The generalized force
\bar{Q}_{11}	The first co-efficient of the transformed ply stiffness matrix
r	Constant of trial function for different boundary condition
s	Slope of tapered beam
T	Kinetic energy
t	Time variable
t_k	Thickness of the k^{th} ply of the laminate in x-direction
t'_k	Thickness of the k^{th} ply of the laminate in x'- direction
U	The potential energy
u_0	Mid-plane displacement in x-direction
V	The volume of the beam
v_0	Mid-plane displacement in y-direction
w	Displacement in thickness direction
W^e	Deflection of the finite element e
W	Work done
w_i^e	Degree of freedom for the finite element
x	Longitudinal direction of laminated beam
y	Transverse direction of laminated beam
z	Thickness-direction of laminated beam

α	Mass proportional constant
β	Stiffness proportional constant
ζ	Damping ratio
η	Damping loss factor
σ_x	The stress along the x - direction
ε_x	The total strain along x - direction
τ_{yz}	The shear stress along the z - direction acting on y -plane
γ_{yz}	The total change in angles (shear strain) along both y -and z - direction
θ_i	Rotation at i^{th} node
θ_x	Rotation about y -axis
ϕ	Taper angle in tapered beam
φ_i	Trial function
ρ	Density of the composite laminate
ω	Excitation frequency
ω_n	Natural frequency of the beam
ω_d	Damped natural frequency of the beam
λ	Eigen value associated with the free vibration problem
ν	Poisson's ratio
k_{ij}^e	Co-efficient of the element stiffness matrix
m_{ij}^e	Co-efficient of the element mass matrix
F_i^e	Co-efficient of the element force matrix

- [C] Damping matrix
- [d] Matrix of nodal displacement
- [F] Force matrix
- [K] Stiffness matrix
- [M] Mass matrix
- $\{f_i\}$ Force matrix after decoupling
- $\{w\}$ Vector containing nodal displacements and rotations
- $\{Z\}$ The mode shape eigen vector
- $[\]^{-1}$ Inverse of the matrix
- (Over dot) Differentiation with respect to time
- Γ A matrix defined to simplify equation in Conventional Finite Element
- Ψ A matrix defined to simplify equation in Higher-order Finite Element

Index

Abstract	iii
Acknowledgements	v
Nomenclature	vi
List of Figures.....	xvii
List of Tables	xxiv
Chapter-1	1
Introduction	1
1.1 Vibration Analysis in Mechanical Design.....	1
1.2 Composite Materials and Structures	2
1.2.1 Modeling Aspects for different composite beams	3
i) Uniform-thickness beam	3
ii) Externally tapered beam.....	3
iii) Internal mid-plane taper beam.....	4
1.4 Rayleigh-Ritz Method.....	7
1.5 Literature survey	8
1.5.1 Experimental work for determination of mechanical properties and damping loss factor of composite beams	8
1.5.2 Finite element method in vibration analysis	10
1.5.3 Vibration analysis of composite beam	11
1.6 Objectives of the Thesis	13
1.7 Layout of the thesis	14

Chapter-2	16
Experimental work.....	16
2.1 Introduction.....	16
2.2 Manufacturing of Composite Laminate	17
2.2.1 Fabrication	17
2.2.2 Autoclave curing.....	19
2.3 Tensile Test Procedure	21
2.4 Modal testing for Damping Factor.....	25
2.4.1 Experimental Procedure.....	25
2.4.2 Damping loss factor data extraction	28
2.5 Conclusion	34
Chapter-3	35
Finite element formulation for vibration analysis of composite beams.	35
3.1 Introduction.....	35
3.2 Laminated beam analysis.....	36
3.3 Conventional finite element formulation	37
3.3.1 Finite element model.....	37
3.3.2 Shape functions.....	37
3.3.3. Energy formulation based on Euler-Bernoulli beam theory for conventional finite element.....	40
3.4 Element properties for mid-plane tapered composite beam.....	45
3.5 Higher-order finite element formulation	47
3.5.1 Finite element model.....	49

3.5.2 Shape functions	49
3.5.3 Energy formulation based on Euler-Bernoulli beam theory for higher- order finite element.....	52
3.6 Analysis using Rayleigh-Ritz method	56
3.6.1 Energy formulation based on Rayleigh-Ritz method.....	57
3.6.4 Trial functions for different boundary conditions.....	59
a. Trial function for simply supported beam.....	59
b. Trial function for cantilever beam	60
c. Trial function for clamped–clamped beam	60
3.7 Vibration analysis of composite beam	60
3.7.1 Free vibration analysis	60
3.7.1.1 Natural frequencies of uniform-thickness composite beam calculated by using different finite elements	62
3.7.1.2 Natural frequencies of Beam with taper configuration-B formed from uniform-thickness beam by ply drop-off	66
3.7.2 Forced vibration analysis	68
3.7.2.1 Forced response of uniform-thickness beam calculated using different finite elements	70
3.7.2.2 Forced response of beam with taper configuration-B formed from uniform-thickness beam by ply drop-off.....	72
3.7.3 Vibration analysis considering damping properties.....	74
3.7.3.1 Natural frequencies of uniform-thickness beam without and with damping effect	76

3.7.3.2 Forced response of uniform-thickness beam without and with considering damping effect	77
3.8. Vibration analysis of composite beam including axial force effects.....	80
3.8.1 Energy formulation including axial force effects	81
3.8.2.1 Free vibration of uniform-thickness composite beam including axial force effects	82
3.8.2.2 Forced vibration response of uniform-thickness composite beam subjected to static end axial force	84
3.9 Conclusions and Discussion	86
Chapter-4	88
Free vibration analysis of tapered composite beams	88
4.1 Introduction.....	88
4.2 Effects of taper configuration on natural frequencies.....	89
4.2.1 Beam with taper configuration-A	90
Example 4.2.1	90
4.2.2 Beam with taper configuration-B.....	95
Example 4.2.2	95
4.2.3 Beam with taper configuration-C.....	99
Example 4.2.3	99
4.2.4 Beam with taper configuration-D	103
Example 4.2.4	103
4.3 Effect of laminate configuration on natural frequencies	108
Example 4.3.1	109

Example 4.3.2	112
4.4 Effects of Taper angle on natural frequencies	116
Example 4.4.1	116
Example 4.4.2	121
4.5 Effect of length ratio on natural frequencies.....	125
Example 4.5.1	126
Example 4.5.2	130
4.6 Effect of boundary condition on natural frequencies.....	132
Example 4.6.1	133
Example 4.6.2	134
4.7 Effect of axial force on natural frequencies.....	136
Example 4.7.1	136
Example 4.7.2	138
Example 4.7.3	140
Example 4.7.4	142
Example 4.7.5	147
Example 4.7.6	149
4.8 Effect of damping on natural frequencies	151
Example 4.8.1	151
Example 4.8.2	153
Example 4.8.3	156
Example 4.8.4	158
Example 4.8.5	161

Example 4.8.6	163
4.9 Conclusion and discussion.....	176
Chapter-5	178
Forced vibration analysis of tapered composite beams	178
5.1 Introduction.....	178
5.2 Effect of taper configuration on transverse displacement and rotation	179
5.2.1 Beam with taper configuration-A	179
Example 5.2.1	179
5.2.2 Beam with taper configuration-B.....	183
Example 5.2.2	183
5.2.3 Beam with taper configuration-C.....	186
Example 5.2.3	186
5.2.4 Beam with taper configuration-D	188
Example 5.2.4	188
5.3 Effect of laminate configuration on transverse displacement and rotation	194
Example 5.3.1	194
Example 5.3.2	196
5.4 Effect of Taper angle on transverse displacement and rotation.....	198
Example 5.4.1	199
Example 5.4.2	200
5.5 Effect of length ratio on transverse displacement and rotation	203
Example 5.5.1	203
Example 5.5.2	205

5.6 Effect of boundary condition on transverse displacement and rotation.....	208
Example 5.6.1	208
Example 5.6.2	211
5.7 Effect of axial force on transverse displacement and rotation	214
Example 5.7.1	215
Example 5.7.2	217
Example 5.7.3	219
Example 5.7.5	223
Example 5.7.6	227
5.8 Effect of damping on transverse displacement and rotation	230
Example 5.8.1	230
Example 5.8.2	232
Example 5.8.3	233
Example 5.8.4	235
Example 5.8.5	237
Example 5.8.6	240
5.9 Conclusion and discussion.....	242
Chapter-6	245
Conclusion	245
References.....	251
Appendix	258
MATLAB program development for vibration analysis.....	258
Flow chart for MATLAB Programming	260

List of Figures

Figure 1.1 Uniform-thickness composite beam	3
Figure 1.2 External tapered composite beam	4
Figure 1.3 Taper configurations A, B, C and D	5
Figure 2. 1 Typical cross-section of autoclave lay-up	18
Figure 2. 2 Photograph of typical Autoclave for curing of composite materials.....	20
Figure 2. 3 Cure cycle for NCT-301 graphite/epoxy composite material	21
Figure 2. 4 Photograph of typical water-cooled rotary type diamond cutter	22
Figure 2. 5 MTS machine for mechanical property testing	23
Figure 2. 6 Block diagram of instrumentation for damping loss factor measurement..	26
Figure 2. 7 Photograph of damping loss factor testing set-up	27
Figure 2. 8 Typical frequency response function for sample-1 for first excitation	29
Figure 2. 9 Typical frequency response function for sample-1 for second excitation..	29
Figure 2. 10 Typical frequency response function for sample-2 for first excitation	30
Figure 2. 11 Typical frequency response function for sample-2 for second excitation	30
Figure 2. 12 Typical frequency response function for sample-3 for first excitation	31
Figure 2. 13 Typical frequency response function for sample-3 for second excitation	31
Figure 3. 1 Finite element beam model	37
Figure 3. 2 A typical composite beam element	38
Figure 3. 3 Mid-plane tapered composite beam	46
Figure 3. 4 Ply thickness, taper angle, and intercept from mid-plane of typical ply	47

Figure 3. 5 Finite element model of a uniform-thickness beam with four degrees of freedom per node	49
Figure 3. 6 Uniform-thickness composite laminated beam with different meshes	63
Figure 3. 7 a) Uniform-thickness beam with 5-elements mesh b) Taper configuration –B beam with 3-elements mesh c) Taper configuration –B beam with 4-elements mesh d) Taper configuration –B beam with 5-elements mesh; in figures a-d, only the top half of beam is shown	66
Figure 3. 8 Frequency-displacement plot of uniform-thickness composite beam with fixed-free boundary condition	71
Figure 3. 9 Frequency-rotation plot of uniform-thickness composite beam with fixed-free boundary condition	71
Figure 3. 10 Frequency-displacement plot of laminated beam with taper configuration-B	73
Figure 3. 11 Frequency-rotation plot of laminated beam with taper configuration-B	73
Figure 3. 12 Frequency-displacement plot of uniform-thickness composite beam	78
Figure 3. 13 Frequency-rotation plot of uniform-thickness composite beam	79
Figure 3. 14 Uniform-thickness composite beam subjected to end tensile load	80
Figure 3. 15 Uniform-thickness composite beam subjected to distributed tensile load	80
Figure 3. 16 Frequency-displacement plot of uniform-thickness composite beam	85
Figure 3. 17 Frequency-rotation plot of uniform-thickness composite beam	85
Figure 4. 1 Upper half of beam with taper configuration-A with a) 3- elements mesh, b) 6- elements mesh, and c) 12- elements mesh.....	91

Figure 4. 2 Upper half of beam with taper configuration-B with a) 3- elements mesh, b) 6- elements mesh, and c) 12- elements mesh	95
Figure 4. 3 Upper half of beam with taper configuration-C with a) 3- elements mesh, b) 6- elements mesh, and c) 12- elements mesh	99
Figure 4. 4 Upper half of beam with taper configuration-D with a) 3- elements mesh, b) 6- elements mesh, and c) 12- elements mesh	103
Figure 4.5 Effects of different taper configurations on lowest four natural frequencies for different boundary conditions	107
Figure 4.6 Effects of different laminate configurations on lowest four natural frequencies for simply supported boundary condition of beam with taper configuration-D	113
Figure 4. 7 Effects of taper angle on lowest four natural frequencies for fixed-free boundary condition of beam with taper configuration-C.....	119
Figure 4. 8 Upper half of beam with taper configuration-C with 9-elements mesh of.....	126
Figure 4. 9 Effect of length ratio on lowest four natural frequencies for different boundary conditions of beam with taper configuration-C	129
Figure 4. 10 Upper half of beam with taper configuration-D with 9-elements mesh.....	130
Figure 4. 11 Effect of boundary condition on lowest four natural frequencies of beam with taper configuration-D.....	135
Figure 4. 12 Effect of applied static axial force on lowest four natural frequencies of different beam configurations for fixed-free boundary condition, a) Tensile axial force, b) Compressive axial force, and c) Axially distributed tensile force	145
Figure 4. 13 Effect of applied static axial force on lowest four natural frequencies for a) fixed-free and b) fixed-fixed boundary conditions of beam with taper configuration-D ..	146

Figure 4. 14 Effect of damping on lowest four natural frequencies for fixed-free boundary condition	160
Figure 4. 15 Effect of damping on lowest four natural frequencies for simply supported boundary condition of beam with taper configuration-B.....	162
Figure 4. 16 Effect of damping properties on lowest four natural frequencies for fixed-free boundary condition of beam with taper configuration-C for case-1	165
Figure 4. 17 Effect of damping properties on lowest four natural frequencies for fixed-free boundary condition of beam with taper configuration-C for case-2.....	167
Figure 4. 18 Effect of damping properties on lowest four natural frequencies for fixed-free boundary condition of beam with taper configuration-C for case-3	169
Figure 4. 19 Effect of damping properties on lowest four natural frequencies for fixed-free boundary condition of beam with taper configuration-D for case-1.....	171
Figure 4. 20 Effect of damping properties on lowest four natural frequencies for fixed-free boundary condition of beam with taper configuration-D for case-2.....	173
Figure 4. 21 Effect of damping properties on lowest four natural frequencies for fixed-free boundary condition of beam with taper configuration-D for case-3.....	175
Figure 5. 1 Fixed-free composite beam with taper configuration-A.....	180
Figure 5. 2 Frequency-displacement plot of beam with taper configuration-A.....	181
Figure 5. 3. Frequency-rotation plot of beam with taper configuration-A	181
Figure 5. 4 Frequency-displacement plot of beam with taper configuration-A.....	182
Figure 5. 5 Frequency-rotation plot of beam with taper configuration-A	183

Figure 5. 6	Fixed-free composite beam with taper configuration-B.....	184
Figure 5. 7	Frequency-displacement plot of beam with taper configuration-B	185
Figure 5. 8	Frequency-rotation plot of beam with taper configuration-B.....	185
Figure 5. 9	Fixed-free composite beam with taper configuration –C	186
Figure 5. 10	Frequency-displacement plot of beam with taper configuration-C.....	187
Figure 5. 11	Frequency-rotation plot of beam with taper configuration- C.....	188
Figure 5. 12	Fixed-free composite beam with taper configuration -D.....	189
Figure 5. 13	Frequency-displacement plot of beam with taper configuration-D.....	190
Figure 5. 14	Frequency-rotation plot of beam with taper configuration-D	190
Figure 5. 15	Effects of taper configuration on frequency-displacement response.....	191
Figure 5. 16	Effects of taper configuration on frequency-rotation response	192
Figure 5. 17	Steady state response curves for beam with different taper configurations	193
Figure 5. 18	Frequency-displacement plot of beam with taper configuration-C.....	195
Figure 5. 19	Frequency-rotation plot of beam with taper configuration-C.....	195
Figure 5. 20	Frequency-displacement plot of beam with taper configuration-D.....	197
Figure 5. 21	Frequency-rotation plot of beam with taper configuration-D	197
Figure 5. 22	Frequency-displacement plot of beam with taper configuration-C.....	199
Figure 5. 23	Frequency-rotation plot of beam with taper configuration-C.....	200
Figure 5. 24	Frequency-displacement plot of beam with taper configuration-D.....	201
Figure 5. 25	Frequency-rotation plot of beam with taper configuration-D	202
Figure 5. 26	Frequency-displacement plot of beam with taper configuration-C.....	204
Figure 5. 27	Frequency-rotation plot of beam with taper configuration-C.....	205
Figure 5. 28	Frequency-displacement plot of beam with taper configuration-D.....	206

Figure 5. 29 Frequency-rotation plot of beam with taper configuration-D	207
Figure 5. 30 Frequency-displacement plot of beam with taper configuration-C	209
Figure 5.31 Frequency-rotation plot of beam with taper configuration-C.....	210
Figure 5.32 Force applied on beam with taper configuration-D a) at mid-point of simply supported beam, b) at free end of (thick end) fixed- (thin end) free or cantilever beam, c) at mid-point of fixed-fixed beam, d) at free end of (thick end) free- (thin end) fixed beam, e) at mid-point of (thick end) fixed- (thin end) hinged beam, and f) at mid-point of (thick end) hinged-(thin end) fixed beam.	212
Figure 5. 33 Frequency-displacement plot of beam with taper configuration-D.....	213
Figure 5.34 Frequency-rotation plot of beam with taper configuration-D	213
Figure 5. 35 Frequency-displacement plot of beam with taper configuration-A.....	216
Figure 5. 36 Frequency-rotation plot of beam with taper configuration-A	216
Figure 5. 37 Frequency-displacement plot of beam with taper configuration-B	218
Figure 5. 38 Frequency-rotation plot of beam with taper configuration-B.....	218
Figure 5. 39 Frequency-displacement plot of beam with taper configuration-C	220
Figure 5. 40 Frequency-rotation plot of beam with taper configuration-C.....	220
Figure 5. 41 Frequency-displacement plot of beam with taper configuration-D.....	222
Figure 5. 42 Frequency-rotation plot of beam with taper configuration-D	222
Figure 5. 43 Frequency-displacement plot of beam with taper configuration-C for fixed-free boundary condition with a) Tensile axial force, b) Compressive axial force, and c) Axially distributed tensile force.....	225
Figure 5. 44 Frequency-rotation plot of beam with taper configuration-C with a) Tensile axial force, b) Compressive axial force, and c) Axially distributed tensile force.....	226

Figure 5. 45 Frequency-displacement plot of beam with taper configuration-D.....	228
Figure 5. 46 Frequency-rotation plot of beam with taper configuration-D	229
Figure 5. 47 Frequency-displacement plot of beam with taper configuration-A.....	231
Figure 5. 48 Frequency-rotation of beam with taper configuration-A.....	231
Figure 5. 49 Frequency-displacement plot of beam with taper configuration-B	232
Figure 5. 50 Frequency-rotation plot of beam with taper configuration-B.....	233
Figure 5. 51 Frequency-displacement plot of beam with taper configuration-C	234
Figure 5. 52 Frequency-rotation plot of beam with taper configuration-C.....	235
Figure 5. 53 Frequency-displacement plot of beam with taper configuration-D.....	236
Figure 5. 54 Frequency-rotation plot of beam with taper configuration-D	237
Figure 5. 55 Frequency-displacement plot of beam with taper configuration-C	238
Figure 5. 56 Frequency-rotation plot of beam with taper configuration-C for cantilever boundary condition	239
Figure 5. 57 Frequency-displacement plot of beam with taper configuration-D.....	241
Figure 5. 58 Frequency-rotation plot of beam with taper configuration-D	241

List of Tables

Table 2. 1 Tensile testing data for failure load, failure strength and longitudinal modulus of composite laminate specimen	24
Table 2. 2 Data obtained from damping loss factor measurements	33

Table 3. 1 Comparison of natural frequencies ($X 10^3$ rad/sec) of uniform-thickness beam for simply supported boundary condition.....	63
Table 3. 2 Comparison of natural frequencies ($X 10^3$ rad/sec) of uniform-thickness beam for fixed-free boundary condition.....	64
Table 3. 3 Comparison of natural frequencies ($X 10^3$ rad/sec) of uniform-thickness beam for fixed-fixed boundary condition.....	65
Table 3. 4 Comparison of natural frequencies ($X 10^3$ rad/sec) of beam with taper configuration-B with simply supported boundary condition	67
Table 3. 5 Comparison of natural frequencies ($X 10^3$ rad/sec) of beam with tapered configuration-B for fixed-free boundary condition	67
Table 3. 6 Comparison of natural frequencies ($X 10^3$ rad/sec) of beam with tapered configuration-B for fixed-fixed boundary condition	68
Table 3. 7 Comparison of un-damped and damped natural frequencies ($X 10^3$ rad/sec) of uniform-thickness beam with fixed-free boundary condition.....	77
Table 3. 8 Comparison of natural frequencies ($X 10^3$ rad/sec) obtained without and with axial force (tensile and compressive) of uniform-thickness composite beam for fixed-free boundary condition	83
Table 4. 1 Comparison of natural frequencies ($x 10^4$ rad/sec) of beam with taper configuration-A for simply supported boundary condition	92
Table 4. 2 Comparison of natural frequencies ($x 10^4$ rad/sec) of beam with taper configuration-A for fixed-free boundary condition	93

Table 4. 3 Comparison of natural frequencies ($\times 10^4$ rad/sec) of beam with taper configuration-A for fixed-fixed boundary condition	94
Table 4. 4 Comparison of natural frequencies ($\times 10^4$ rad/sec) of beam with taper configuration-B for simply supported boundary condition	96
Table 4. 5 Comparison of natural frequencies ($\times 10^4$ rad/sec) of beam with taper configuration-B for fixed-free boundary condition	97
Table 4. 6 Comparison of natural frequencies ($\times 10^4$ rad/sec) of beam with taper configuration-B for fixed-fixed boundary condition	98
Table 4.7 Comparison of natural frequencies ($\times 10^4$ rad/sec) of beam with taper configuration-C for simply supported boundary condition	100
Table 4.8 Comparison of natural frequencies ($\times 10^4$ rad/sec) of beam with taper configuration-C for fixed-free boundary condition	101
Table 4. 9 Comparison of natural frequencies ($\times 10^4$ rad/sec) of beam with taper configuration-C for fixed-fixed boundary condition	102
Table 4. 10 Comparison of natural frequencies ($\times 10^4$ rad/sec) of beam with taper configuration-D for simply supported boundary condition	104
Table 4. 11 Comparison of natural frequencies ($\times 10^4$ rad/sec) of beam with taper configuration-D for fixed-free boundary condition	105
Table 4. 12 Comparison of natural frequencies ($\times 10^4$ rad/sec) of beam with taper configuration-D for fixed-fixed boundary condition	106
Table 4.13 Comparison of natural frequencies ($\times 10^4$ rad/sec) of beam with taper configuration-C for simply supported boundary condition	109

Table 4.14 Comparison of natural frequencies ($\times 10^4$ rad/sec) of beam with taper configuration-C for fixed-free boundary condition	110
Table 4.15 Comparison of natural frequencies ($\times 10^4$ rad/sec) of beam with taper configuration-C for fixed-fixed boundary condition	111
Table 4.16 Comparison of natural frequencies ($\times 10^4$ rad/sec) of beam with taper configuration-D for simply supported boundary condition	112
Table 4. 17 Comparison of natural frequencies ($\times 10^4$ rad/sec) of beam with taper configuration-D for fixed-free boundary condition	114
Table 4. 18 Comparison of natural frequencies ($\times 10^4$ rad/sec) of beam with taper configuration-D for fixed- fixed boundary condition	115
Table 4. 19 Comparison of natural frequencies ($\times 10^4$ rad/sec) of beam with taper configuration-C for simply supported boundary condition	117
Table 4.20 Comparison of natural frequencies ($\times 10^4$ rad/sec) of beam with taper configuration-C for fixed-free boundary condition	118
Table 4. 21 Comparison of natural frequencies ($\times 10^4$ rad/sec) of beam with taper configuration-C for fixed-fixed boundary condition	120
Table 4.22 Comparison of natural frequencies ($\times 10^4$ rad/sec) of beam with taper configuration-D for simply supported boundary condition	122
Table 4. 23 Comparison of natural frequencies ($\times 10^4$ rad/sec) of beam with taper configuration-D for fixed-free boundary condition	123
Table 4. 24 Comparison of natural frequencies ($\times 10^4$ rad/sec) of beam with taper configuration-D for fixed- fixed boundary condition	124

Table 4. 25 Comparison of natural frequencies ($\times 10^4$ rad/sec) of beam with taper configuration-C for simply supported boundary condition	127
Table 4. 26 Comparison of natural frequencies ($\times 10^4$ rad/sec) of beam with taper configuration-C for fixed-free boundary condition	127
Table 4. 27 Comparison of natural frequencies ($\times 10^4$ rad/sec) of beam with taper configuration-C for fixed-fixed boundary condition	128
Table 4. 28 Comparison of natural frequencies ($\times 10^4$ rad/sec) of beam with taper configuration-D for simply supported boundary condition	131
Table 4.29 Comparison of natural frequencies ($\times 10^4$ rad/sec) of beam with taper configuration-D for fixed-free boundary condition	131
Table 4.30 Comparison of natural frequencies ($\times 10^4$ rad/sec) of beam with taper configuration-D for fixed- fixed boundary condition	132
Table 4. 31 Comparison of natural frequencies ($\times 10^4$ rad/sec) of beam with taper configuration-C for all boundary conditions.....	133
Table 4. 32 Comparison of natural frequencies ($\times 10^4$ rad/sec) of beam with taper configuration-D for all boundary conditions	134
Table 4. 33 Comparison of natural frequencies ($\times 10^4$ rad/sec) of beam with taper configuration-A for simply supported boundary condition	137
Table 4.34 Comparison of natural frequencies ($\times 10^4$ rad/sec) of beam with taper configuration-A for fixed-free boundary condition	137
Table 4.35 Comparison of natural frequencies ($\times 10^4$ rad/sec) of beam with taper configuration-A for fixed-fixed boundary condition	138

Table 4.36 Comparison of natural frequencies ($\times 10^4$ rad/sec) of beam with taper configuration-B for simply supported boundary condition	139
Table 4.37 Comparison of natural frequencies ($\times 10^4$ rad/sec) of beam with taper configuration-B for fixed-free boundary condition.	139
Table 4.38 Comparison of natural frequencies ($\times 10^4$ rad/sec) of beam with taper configuration-B for fixed- fixed boundary condition	139
Table 4.39 Comparison of natural frequencies ($\times 10^4$ rad/sec) of beam with taper configuration-C for simply supported boundary condition	140
Table 4. 40 Comparison of natural frequencies ($\times 10^4$ rad/sec) of beam with taper configuration-C for fixed-free boundary condition.	141
Table 4. 41 Comparison of natural frequencies ($\times 10^4$ rad/sec) of beam with taper configuration-C for fixed- fixed boundary condition	141
Table 4. 42 Comparison of natural frequencies ($\times 10^4$ rad/sec) of beam with taper configuration-D for simply supported boundary condition	142
Table 4.43 Comparison of natural frequencies ($\times 10^4$ rad/sec) of beam with taper configuration-D for fixed-free boundary condition.	142
Table 4.44 Comparison of natural frequencies ($\times 10^4$ rad/sec) of beam with taper configuration-D for fixed- fixed boundary condition	143
Table 4.45 Comparison of natural frequencies ($\times 10^4$ rad/sec) of beam with taper configuration-A for fixed-fixed boundary condition	148
Table 4. 46 Comparison of natural frequencies ($\times 10^4$ rad/sec) of beam with taper configuration-C for fixed-fixed boundary condition	149

Table 4.47 Comparison of natural frequencies ($\times 10^4$ rad/sec) of beam with taper configuration-D for fixed-fixed boundary condition	150
Table 4. 48 Comparison of natural frequencies ($\times 10^4$ rad/sec) of beam with taper configuration-A for simply supported boundary condition	152
Table 4.49 Comparison of natural frequencies ($\times 10^4$ rad/sec) of beam with taper configuration-A for fixed-free boundary condition	152
Table 4.50 Comparison of natural frequencies ($\times 10^4$ rad/sec) of beam with taper configuration-A for fixed-fixed boundary condition.	153
Table 4.51 Comparison of natural frequencies ($\times 10^4$ rad/sec) of beam with taper configuration-B for simply supported boundary condition	154
Table 4. 52 Comparison of natural frequencies ($\times 10^4$ rad/sec) of beam with taper configuration-B for fixed-free boundary condition	154
Table 4.53 Comparison of natural frequencies ($\times 10^4$ rad/sec) of beam with taper configuration-B for fixed-fixed boundary condition.	155
Table 4.54 Comparison of natural frequencies ($\times 10^4$ rad/sec) of beam with taper configuration-C for simply supported boundary condition	156
Table 4.55 Comparison of natural frequencies ($\times 10^4$ rad/sec) of beam with taper configuration-C for fixed-free boundary condition	157
Table 4.56 Comparison of natural frequencies ($\times 10^4$ rad/sec) of beam with taper configuration-C for fixed-fixed boundary condition.	157
Table 4. 57 Comparison of natural frequencies ($\times 10^4$ rad/sec) of beam with taper configuration-D for simply supported boundary condition	158

Table 4. 58 Comparison of natural frequencies ($\times 10^4$ rad/sec) of beam with taper configuration-D for fixed-free boundary condition	159
Table 4.59 Comparison of natural frequencies ($\times 10^4$ rad/sec) of beam with taper configuration-D for fixed- fixed boundary condition	159
Table 4.60 Comparison of natural frequencies ($\times 10^4$ rad/sec) of beam with taper configuration-B for simply supported boundary condition	161
Table 4.61 Comparison of natural frequencies ($\times 10^4$ rad/sec) of beam with taper configuration-C for fixed-free boundary condition for case-1.	164
Table 4. 62 Comparison of natural frequencies ($\times 10^4$ rad/sec) of beam with taper configuration-C for fixed-free boundary condition for case-2.	166
Table 4. 63 Comparison of natural frequencies ($\times 10^4$ rad/sec) of beam with taper configuration-C for fixed-free boundary condition for case-3.	168
Table 4. 64 Comparison of natural frequencies ($\times 10^4$ rad/sec) of beam with taper configuration-D for fixed-free boundary condition for case-1.	170
Table 4. 65 Comparison of natural frequencies ($\times 10^4$ rad/sec) of beam with taper configuration-D for fixed-free boundary condition for case-2	172
Table 4. 66 Comparison of natural frequencies ($\times 10^4$ rad/sec) of beam with taper configuration-D for fixed-free boundary condition for case-3	174

Chapter-1

Introduction

1.1 Vibration Analysis in Mechanical Design

Vibration of mechanical component and structure occurs due to elastic and inertia properties of element that involves an alternating interchange of potential and kinetic energies. Excessive alternating interchange of this potential and kinetic energies causes not only the unpredictable failure of elements but also annoyance for disturbing the normal environment [1]. Sometimes it may not harm the normal operation but if they continue to act, they can bring about fatigue failure. So most of the mechanical and structural elements such as structural failure of aircrafts, blades and disks failure in steam and gas turbine, failure of bridges etc. are associated with vibration.

The excitation to a vibratory element or structure may occur in the form of initial displacement and/or initial velocity of the mass or due to harmonically excited force. Mechanical structural elements start to vibrate due to initial displacement or velocity, when there is no continuous externally applied force on them, and this is called free vibration. Generally damping or friction from material itself or surrounding medium causes loss of energy and energy reaches a zero value, at which point the motion stops. So loss of energy or damping is an important consideration in a variety of engineering designs. But if the system is continuously under an external force, it is forced to vibrate at the same frequency as that of excited force. If the frequency of exciting force gets close to the frequency band of the natural frequencies of the structure, it experiences a vibration resonance and vibrates in large

amplitude. The resonance experience causes most of the vibrational failure or reduces the lifetime of element. Therefore, free and forced vibration analysis including damping in mechanical structure is very important and necessary to control the vibration in order to maintain the operating performance and to prevent unpredictable failures.

1.2 Composite Materials and Structures

Composite material refers to a material that is made of two or more different organic or inorganic materials to order to obtain specific material properties such as high strength and high modulus to weight ratio, corrosion resistance, thermal properties, fatigue life and wear resistance and much tolerance to damage [2]. In composite materials, one or more discontinuous phases are distributed in one continuous phase. They are permanently bonded together under heat and pressure using a hot press or autoclave. In the case of several discontinuous phases of different natures the composite is said to be a hybrid. The discontinuous phase is usually harder and with superior mechanical properties compared to those of the continuous phase. The continuous phase is called matrix where the discontinuous phase is called reinforcement (fiber, flake or lamina form). Structure made of such materials is called composite structure. Composite structures are used in different system applications such as aircraft and space structures, automobiles, submarine structure, sports equipment and medical prosthetic devices, in bar, beam and plate's structural form.

Some specific applications such as helicopter yoke, robot arms, turbine blades and satellite antenna need to be stiff at one location and flexible at another location. A typical example is a helicopter yoke, where a progressive variation in the thickness of the yoke is

required to provide high stiffness at the hub and flexibility at the middle of yoke length to accommodate for flapping. This type of structure is formed by terminating or dropping off some plies at expected location to reduce the stiffness of that structure which is called tapered composite structure [2]. These elastic tailoring properties and more significant weight saving than commonly used laminated components allow an increasing use of tapered composite in commercial and military aircraft. The first commercial composite rotor blade yoke assembly made of glass-fiber (S-2 glass)/epoxy composite was fabricated at Bell helicopter Textron that provides more safety and endures several times more flight hours than traditional titanium or steel.

1.2.1 Modeling for different composite beams

i) Uniform-thickness beam

The cross-section area of uniform-thickness beam as shown in Figure 1.1 is constant. The laminate ply orientation can be different which effect the structural properties.

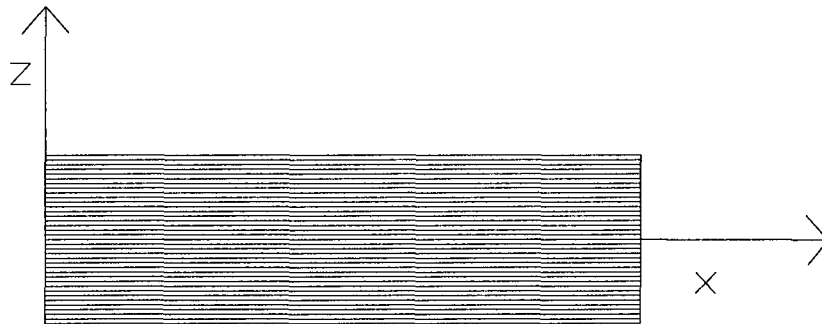


Figure 1.1 Uniform-thickness composite beam

ii) External tapered beam

Externally tapered beams as shown in Figure 1.2 can be modeled as combinations of elements with different thickness. The thickness for each element is constant. Thus each element can be considered as uniform-thickness beam.

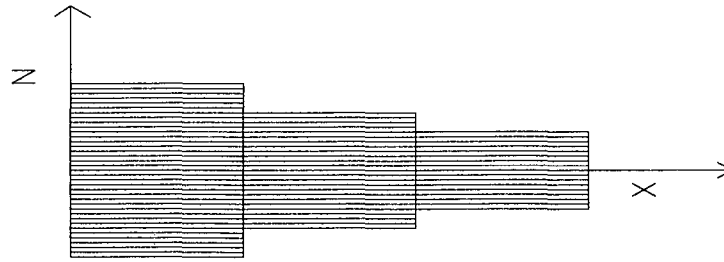


Figure 1.2 External tapered composite beam

iii) Internal mid-plane taper beam

Internal mid-plane tapered beams are in the form shown in Figure 1.3. In this case the ply in tapered element is not a straight line instead it is a function of x along the length of the element. Different types of internal mid-plane taper can be obtained by configuring the ply drop-off. In this work, four common types of taper configuration are analyzed for vibration.

Beam with taper configuration-A

This type of tapered configuration is also called basic taper. In taper configuration-A the plies are dropped-off along centerline of laminate. In Figure 1.3, 24-ply are dropped-off and the space is filled by resin that is called resin pocket.

Beam with taper configuration-B

This type of taper configuration looks like staircase arrangement. Here after a certain distance a number of plies are dropped-off from top of the laminate and vacant space is filled by resin and below the resin pocket the ply are straight and uniform.

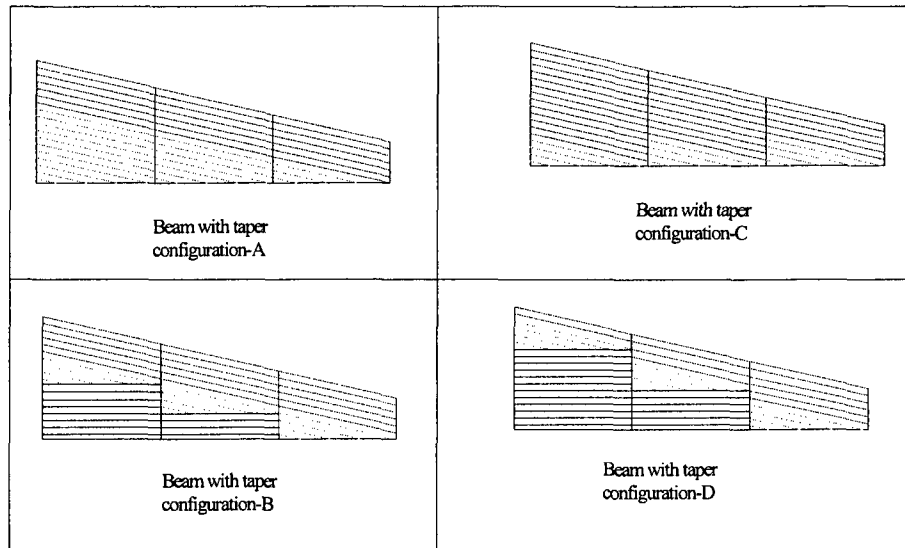


Figure 1.3 Taper configurations A, B, C and D

Beam with taper configuration-C

This type of taper configuration is also called overlapped dropped plies taper because after certain distance plies are dropped-off along center line of laminate which look like overlapping ply drop.

Beam with taper configuration-D

This type of taper configuration is also called continuous plies interspersed taper. It looks like taper configuration-B except that uniform plies make a height between the stair steps.

1.3. Finite Element Method (FEM)

Since structural configurations were changing rapidly during the last few years and the existing methods were generally insufficient to deal with variety and complexity of the new structural shapes. It was in this circumstance that the finite element method emerged as recognizable modern method in the mid-1980s.

The greatest advantage of FEM is its ability to deal with arbitrary geometry, boundary conditions as well as arbitrary shape of non-homogeneous materials that are made up of numerous different material regions. The analysis of laminated composite beam is usually based on four approaches those are classical theory of elasticity, theory of mechanics of materials, variational statement and strain energy statement. The governing equations of motions are generally non-linear partial differential equations those are difficult to solve in the closed form. But the powerful numerical technique, Finite Element Method (FEM) made possible the analysis of complex structure such as tapered composite beam by the help of modern digital computers. The basic idea in the finite element method is to find the approximate solution of complicated problem by replacing it by a simpler one [3].

The speed of convergence and accuracy of the results obtained by finite element method are strongly dependent on the selected element type. In Conventional Finite Element (CFE), a beam element is modeled using two nodes at the ends where each node has two degrees of freedom (displacement and rotation). The beam should be divided into a large number of elements to achieve the accurate results. Higher-order Finite Element (HOFE) overcomes these difficulties considering four degrees of freedom (displacement, rotation, curvature and gradient of curvature) per node. In this thesis work, both types of finite element are applied to analyze the free and force vibration of composite beam.

1.4 Rayleigh-Ritz Method

In 1877, Rayleigh published the calculation method for fundamental natural frequency of free vibration of continuum system (strings, bars, beams, membranes, plates) that is well known as Rayleigh method. He solved that problem by assuming the mode shape and setting maximum kinetic and static energy values in a cycle of motion equal to each other. In 1908, Ritz published his famous method for determining frequencies and mode shapes choosing multiple admissible displacement functions and minimizing a functional involving both potential and kinetic energy. Subsequently Rayleigh solved some problems by minimizing frequency; many research articles and books use this method (some calling the method as Rayleigh-Ritz method and others as Ritz method)[4].

The Rayleigh-Ritz or Ritz method has found tremendous use during past three decades in obtaining accurate frequencies and mode shapes for the vibration of continuum system especially for problems not amenable to exact solution of the differential equations. The method is used frequently because of the increasing capability of digital computers to set up and solve the frequency determinants arising with the method. This method can be employed to solve boundary value problem or eigen value problem by assuming a solution in the form of series of admissible functions (satisfying at least the geometric boundary conditions) each having an arbitrary co-efficient and minimizing the appropriate energy functional directly. In this thesis Rayleigh-Ritz method is employed to determine the closed form eigen value and forced response of uniform-thickness and tapered laminated composite beams. Admissible functions are taken as series of products of beam mode shape called trial function.

1.5 Literature survey

In this section a comprehensive and up-to-date literature survey is presented on relevant topics. Important works done on the experimental work of mechanical properties and damping loss factor determination of composite beams, the application of the finite element method to composite beams and on the free and forced vibration of composite beams specially related to free and forced vibration analysis by conventional, higher-order finite element, Rayleigh-Ritz method with and without considering damping and axial load effects. The literature survey is limited to the works available in English language, mostly from last two decades. The work done relevant to each topic is chronicled.

1.5.1 Experimental work for determination of mechanical properties and damping loss factor of composite beams

It is always recommended to use the updated data of any materials for the analysis. In this thesis, NCT-301 graphite epoxy materials are used for all analysis and parametric study. To know the present condition of this material, it was tested for tensile response and damping loss factor. To get the idea about mechanical properties, it was found that Ibrahim [5] studied with NCT-301 graphite epoxy material where he did some experimental work for determining notched and un-notched strength of cross-ply laminate. He studied the effect of notch size on the reliability of composite laminates based on stochastic finite element analysis.

Damping analysis of fiber-reinforced composite has not been considered as a popular research area since composite materials are designed with stiffness to weight ratio, rather than damping. Damping in laminated composite materials, where laminae are bonded with adhesive joints of very low damping capacity, is mostly due to the inelastic or visco-elastic

nature of matrix and to relative slipping at the fiber-matrix interfaces. The only reliable method for estimating damping in composite is by experimentation. Gibson et al [6] used random and impulse techniques for measurement of damping in composite materials under flexural vibration. They tested specimens of un-reinforced epoxy resin, graphite-epoxy and E-glass polyester composite in order to cover a range of damping values from low (aluminum) to intermediate (composite) to high (epoxy). Morison [7] developed a model of material damping for a fiber reinforced polymer matrix composite and experimentally predicted the loss factor and the temperature and moisture dependant structural damping of an arbitrary laminate. Hoa and Oullette [8] proposed a rule of mixture for the calculation of the loss factor for hybrid laminate where they found out the damping loss factor of individual laminate by experiment using logarithmic decrement method. Gibson [9] reviewed the progress in analytical and experimental characterization of dynamic properties of advanced materials. Adam and Bacon [10] performed a series of experiments on unidirectional fiber reinforced beams under longitudinal shear and flexural loading conditions to determine the specific damping capacity. Zabaraz et al [11] studied viscous damping approximation and transient response of laminated composite plates using finite element method. They used experimental data for the specific damping capacity (SDC) of unidirectional beams to determine the SDC of laminated plates. Wei and Kukureka [12] evaluated the damping and elastic properties of composite material and composite structures experimentally by the resonance method. Adams and Maheri [13] investigated the damping capacity of fiber-reinforced plastic and developed a damping energy equation for analysis. Damping capacity and frequency of cross ply fiber reinforced plastic composite plates were compared at room temperature by using finite element method, Rayleigh-Ritz method and an experimental

method. Sefarani and Bertholet [14] analyzed experimentally the effect of temperature on the damping properties of unidirectional glass fiber composite as a function of the frequency and fiber orientation using a cantilever beam test specimen and an impulse technique. Colakoglu [15] studied damping and vibration analysis of polyethylene fiber composite under varied temperature where he analyzed temperature dependant frequency response experimentally using a damping monitoring technique.

1.5.2 Finite element method in vibration analysis

Using finite element method, dynamic analysis of uniform-thickness and tapered composite beams has been conducted in many works. Thomas and Dokumaci [16] established improved finite elements for vibration analysis of tapered beam. To [17] used higher order tapered beam finite element for vibration analysis. Balasubramanium et al [18] estimated higher frequency using four degrees of freedom per node element for stepped beam analysis. Heyliger and Reddy [19] established a higher order beam finite element for bending and vibration problems. In this formulation, the theory assumes a cubic variation of the in-plane displacement in thickness co-ordinate and a parabolic variation of the transverse shear stress across the thickness of the beam. Gupta and Rao [20] used finite element with two nodes at the ends and two degrees of freedom per node to obtain the stiffness and mass matrices for linearly and twisted beams. Marur and Kant [21] applied higher order theory and finite element for free vibration of composite beams. Yuan and Miller [22] have developed beam finite element that includes separate rotational degrees of freedom for each lamina but do not require additional axial or transverse degrees of freedom. Manjunatha and Kant [23] presented a set of higher order theories with C^0 finite elements having five, six and seven degrees of freedom per node. Prathap and Vnayak [24] analyzed vibrations of laminated

beams using higher order theory. Shi and Lam [25] studied an efficient finite element modeling technique based on the higher order theories for the analysis of composite beam. They present a third order beam theory using Hamilton's principle. Cleghorn and Tabarrok [26] presented a finite element model for free vibration of linearly tapered beams. Rao and Ganesan [27] applied conventional finite element formulation to determine the natural frequency of linearly tapered beams. Most recently Nigam [28] used hierarchical finite element method to investigate the dynamic response of laminated composite beams. Zabihollah [29] studied free vibration and buckling analysis of tapered composite beams using both conventional and advanced finite element formulations.

1.5.3 Vibration analysis of composite beam

Most of the works of vibration analysis related to composite materials are on laminated plates and shells. Though applicability of composite beams as structural components in many important engineering applications is growing ever fast, works on this is not sufficient especially on forced vibration.

Abarcar and Cunniff [30] obtained experimental results for natural frequencies and mode shapes of cantilevered graphite-epoxy and boron epoxy composite beams. They established an interaction between bending and twisting. Miller and Adams [31] studied the vibration characteristic of orthotropic fixed-free beams using classical laminate theory. Cheng and Yang [32] investigated the static and dynamic response of symmetrically laminated beams. Chanrashekhara et al [33] analyzed the free vibration of composite beams including the effects of rotary inertia and shear deformation. Hodges et al [34] studied the free vibration of composite beams using exact integration method and mixed finite element method.

Krishanaswamy et al [35] obtained the analytical solution to vibration of laminated composite beams. Zeng [36] established composite element method of vibration analysis of beam structure. Reddy and Khedir [37] studied free vibration behaviour of cross-ply laminate to show the comparison between shear deformation theory and classical laminate theory under various boundary conditions. Abramovich and Livshits [38] established analytical solutions for free vibration of non-symmetric cross-ply laminated beams. Houmat [39] investigated the vibration of Timoshenko beams considering four-node element with variable degrees of freedom where he described element transverse displacement and cross-sectional rotations by cubic polynomial plus a variable number of trigonometric sine terms. Singh and Abdelnassar [40] examined the free vibration response of composite beams considering a third order shear deformation theory. Chen and Sun [41] investigated the impact response of composite laminate with and without initial stresses using finite element method. They developed a nine-node iso-parametric quadrilateral element based on the Mindlin plate theory and the Von Karman large deflection assumptions. Lips et al [42] modeled composite structures (a bond line with a single layer of elements) to obtain accurate frequency response predictions using finite element methods. They examined the effect bonded lap joints have on the frequency response of a given structure where the test article developed consist of carbon fiber composite sections joined with epoxy single lap joints. Amit and Yadav [43] investigated forced nonlinear random vibration of a simply supported cross-ply laminated composite plate analytically using Kirchoff-Love plate theory and Von-Karman nonlinear strain displacement formulations. Asghar et al [44] studied forced vibration analysis developed by the modal superposition technique and the layer wise theory of Reddy is used to study the low velocity impact response of laminated plates. Cheung et al

[45] proposed a computationally efficient and highly accurate numerical method to analyze the vibrations of symmetrically laminated rectangular composite plates with intermediate line supports. The governing eigen frequency equation is derived using Rayleigh-Ritz method. He developed a set of admissible functions from the static solutions of a beam with intermediate point supports under a series of sinusoidal loads. Kadivar et al [46] studied the forced vibration of an unsymmetrical laminated composite beam subjected to moving loads. They studied a one-dimensional element with 24 degrees of freedom, which includes the effects of transverse shear deformation; rotary and higher order inertia to get the response. Beytullah et al [47] investigated the dynamic behavior of composite cylindrical helical rods subjected to time dependent loads theoretically in the Laplace domain. Azrar et al [48] studied the forced non-linear response of C-C and S-S beams using spectral analysis, Lagrange's equations and harmonic balanced method. They proposed a method to solve the multidimensional duffing equation and obtained a set of non-linear algebraic equation whose numerical solutions leads in each case to the basic function contribution co-efficient to the displacement response function based on harmonic balance method. These coefficients depend on the excitation frequency and the distribution of the applied loads. Farouk [49] analyzed free and forced vibrations of non-uniform composite beams in the Laplace domain. He adopted Timoshenko beam theory in the derivation of governing equation. He obtained ordinary differential equation in scalar form and solved numerically.

1.6 Objectives of the Thesis

The objectives of the present thesis are 1) to develop and compare the conventional and higher-order finite element formulation for free and forced vibration analysis; 2) to investigate the natural frequencies and modal displacement and rotation response of composite beams with different types of taper and laminate configurations; 3) to develop the

element method; 4) to investigate the natural frequencies and the modal displacement and rotation response of composite beams considering the damping properties; 5) to investigate the effects of concentrated and distributed static axial loads on frequencies and modal displacement and rotation response; and 6) to conduct a detailed parametric study of the tapered composite beam.

Free and forced vibration analyses with and without damping for composite beams are developed based on classical laminate theory by using conventional and higher-order finite elements. Both formulations are analyzed for their performance in free and forced vibration response. Approximation solution using Rayleigh-Ritz method is also developed to compare the results. The developed methodology gives more accurate and converging results, and is extremely advantageous in the analysis of composite beam structures.

1.7 Layout of the thesis

The present chapter provided a brief introduction and literature survey on experimental work for determination of mechanical properties and damping loss factor of composite beams, and on free and forced vibration analysis of uniform-thickness and tapered composite beam using conventional and higher-order finite elements and Rayleigh-Ritz method.

In Chapter 2, a detailed experimental work procedure is described for the determination of mechanical and damping properties of laminated composite beam. Several samples are made and tested to compare the tensile properties of a specific laminate with that of un-notched cross-ply specimens of ref. [5]. Then several samples are made and tested for the damping loss factor properties of composite beam.

In Chapter 3 formulation for free and forced vibration analysis of composite beams is developed based on classical laminate theory using conventional and higher-order finite elements. Then, formulation for free and forced vibrations analysis of composite beams is developed using Rayleigh-Ritz method based on classical laminate theory. Trial functions for different support conditions are determined. A sample example application is then presented to show how these finite element formulations are used to determine the natural frequencies and modal response of uniform-thickness composite beam and tapered beam.

In Chapter 4, natural frequencies of different internally tapered composite beams are determined for different boundary conditions by using these formulations. Then concentrated and distributed static axial forces are applied on beam and the natural frequencies of different internally tapered composite beams are determined. Finally a detailed comparison is arranged in tables and graphs for comparison among these types of taper configurations including the effects of different taper angles, composite laminate configuration, axial forces, and damping.

In Chapter 5 a detailed parametric study is presented for forced vibration analysis which includes the effects of different taper angles, composite laminate configuration effects and the effects of concentrated and distributed static axial loads and different boundary conditions for different taper configurations of composite beams. A comparison similar to that in chapter 4 is also presented.

Chapter 6 brings the thesis to its end by providing an overall conclusion of the present work and some recommendation for future work.

Chapter-2

Experimental work

2.1 Introduction

The use of composite materials in aerospace structures, automobiles, turbine blades, helicopter blades, robot arms, and other mechanical structures has grown very rapidly from 20th century. Most of the applications with a high degree of structural complexity are limited to dealing with various types of loading in different environmental conditions. There is significant randomness in properties of composite laminate due to manufacturing and testing conditions. Therefore, several material specimens are required to make and test to get the material properties.

In this chapter detailed procedures of manufacturing and testing of the composite laminate for evaluating the material properties are described. Pre-impregnated NCT-301 graphite/epoxy material supplied by Newported Company, USA is used in the present thesis for all experiments and analysis. The composite laminate should be tested according to ASTM specification D 3039M-00 and ASTM specification D 3518M-94-01 to get the ply mechanical properties (longitudinal modulus E_1 , transverse modulus E_2 , shear modulus G_{12} , Poisson's ratio ν_{12}). Due to lack of sufficient material quantity in the laboratory and to the fact that in order to purchase the new material it takes about few months, only one plate (12" x12") was manufactured (using the existing quantity of the material at that time) for preparing laminate tensile testing specimens. After getting the testing data of longitudinal Young's modulus E_1 , failure load and failure strength, the data are compared with that given in ref. [5]. Though the material was aged, still its damping properties were used in the

modal testing. Procedure followed to do the test at room temperature is available in ASTM E 756–98 [50].

2.2 Manufacturing of Composite Laminate

The manufacturing of composite laminates can be categorized into two phases:

- 1) Fabrication
- 2) Processing

2.2.1 Fabrication

In the fabrication phase the fiber reinforcement and matrix material are placed or shaped into a structural form. In the present work a flat plate is manufactured from layers or plies of pre-impregnated NCT-301 graphite/epoxy material.

Tooling: All fabrication methods require tools to provide the shape of the composite structure/laminate during the processing. In this case a flat aluminum tool is used to manufacture flat composite plate.

Secondary Materials for laminate curing preparation: Many secondary or specialty materials are used in composite manufacturing such as release agent, release films, bleeder plies, breather ply, vacuum bags and sealant tape. Each of these materials provides specific function. A cross-section of typical lay-up of a composite structure prepared for autoclave processing is shown in Figure 2.1.

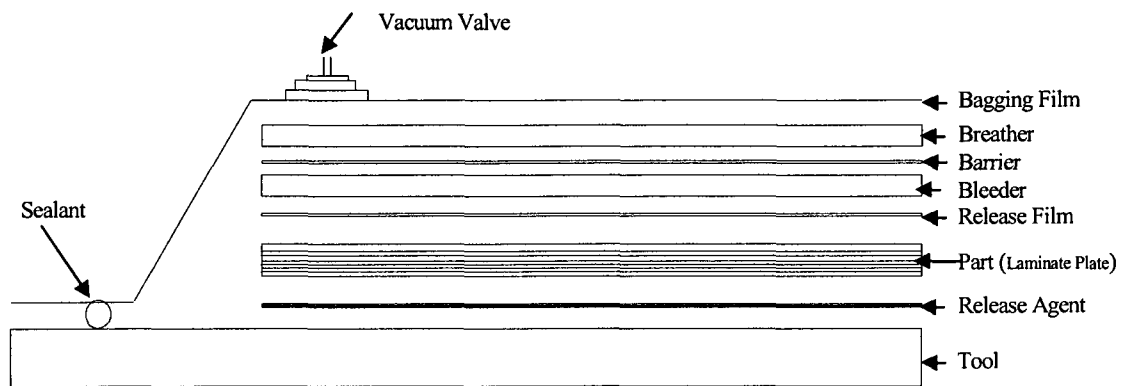


Figure 2. 1 Typical cross-section of autoclave lay-up

Hand lay-up

The hand lay-up of pre-impregnated materials is the oldest and most commonly used method where the production volume is low and other forms of production would prove to be expensive. Each step in hand lay-up of a flat composite laminate must follow in successive fashion in order to obtain a high quality composite laminate after final processing. The major steps that are followed in the hand lay-up of prepreg are briefly highlighted:

- At first the pre-impregnated material is cut from the prepreg roll according to the required dimension of respective specimen.
- The surface of the plate is cleaned and a release agent is applied followed by one layer of the release film. This allows the part to easily separate from the mold after curing.
- A ply is oriented and placed upon the tool and subsequent plies are placed on top of the laminate according to the laminate configuration. Compaction pressure is applied by the use of a roller device to adhere the plies and remove entrapped air that could lead to voids or delamination in between the layers.

- After completing the ply gathering, a sheet of porous release film, the bleeder ply, the breather plies and vacuum valve are placed on top of the laminate one after one according to Figure 2.1.
- When putting of the lay-up of all of the secondary material plies is completed, the sealant tape is placed around the periphery of the laid laminate and the vacuum bag is placed over the entire lay up.
- The entire assembly is placed inside an autoclave and the vacuum valve is connected with vacuum pump of the autoclave to check the leaks between sealant and vacuum bag before starting the autoclave for processing.

2.2.2 Autoclave curing

The autoclave is a large metal pressure vessel with thermal insulation shown in Figure 2.2. The autoclave is used to provide the necessary heat and pressure required to consolidate and cure the composite part [51]. The major advantages of the autoclave are that it represents a flexible method to apply required pressure and temperature to a composite part, which is precisely controlled by computer.

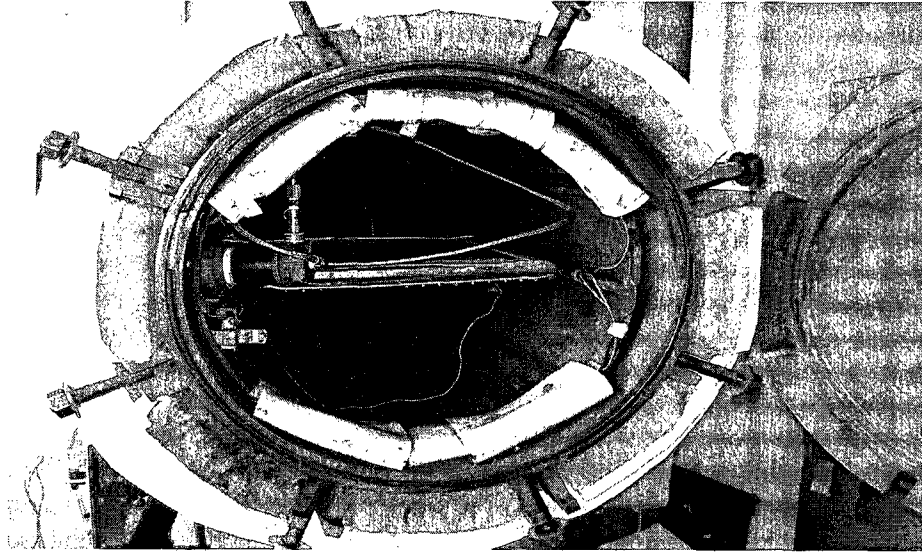


Figure 2. 2 Photograph of typical Autoclave for curing of composite materials

The cure temperature and pressure are selected to meet the following requirements:

- To cure the resin uniformly and to attain a specified degree of cure in the shortest possible time.
- To maintain the temperature of any part inside the prepreg which should not exceed a prescribed limit during the cure.
- To have sufficient pressure to squeeze out all the excess resin from every ply before the resin becomes gel at any location inside the prepreg.
- Pressurization also helps to bond layers and remove persistent voids in the matrix.

In autoclave the temperature plays an important role in initiation of cross-linking and acceleration of curing process. The cure cycle is a two-step process. The laminate is heated from room temperature to 106°C at constant rate and it is held at this temperature for a period of 20 minutes (first dwell). The purpose of the first dwell is to allow the entrapped air, water vapor or volatiles to escape from the matrix material and to allow matrix flow. In step two or second dwell the temperature is again increased to 145°C and held constant for about

an hour. In this step cross-linking of the resin takes place and the strength and mechanical properties are developed. A constant 60-psi pressure is maintained inside the autoclave throughout the processing time. Then the laminate is cooled to room temperature at constant rate. A typical cure cycle for NCT-301 graphite/epoxy composite is shown in Figure 2.3.

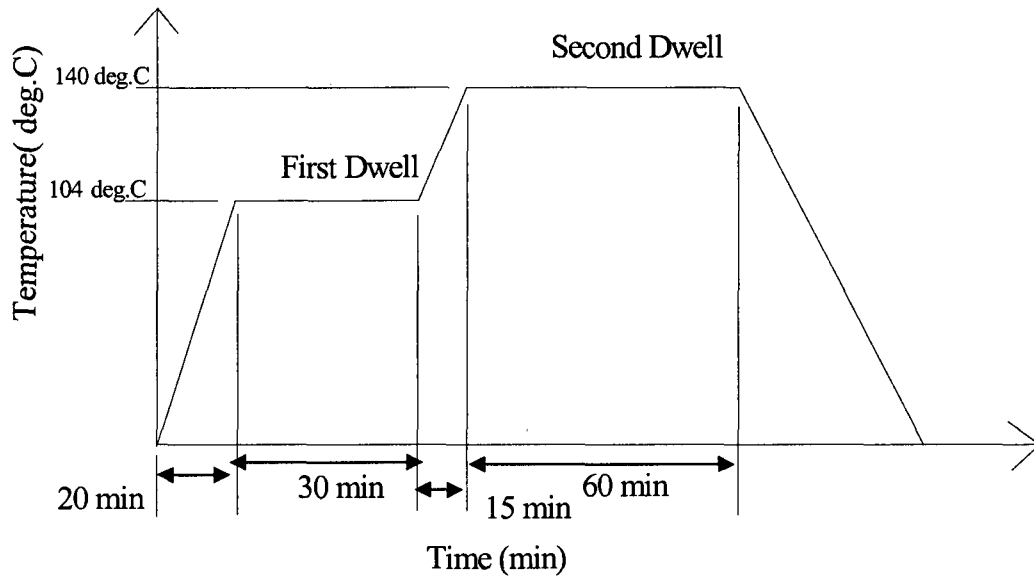


Figure 2. 3 Cure cycle for NCT-301 graphite/epoxy composite material

2.3 Tensile Test Procedure

Uniaxial tensile tests are conducted on cross-ply laminate to determine the laminate longitudinal Young's modulus E_1 , failure load and failure strength. These values are also compared with ref [5]. First the laminate made by autoclave curing is prepared and cut to the required size by using water-cooled rotary type diamond cutter shown in Figure 2.4.

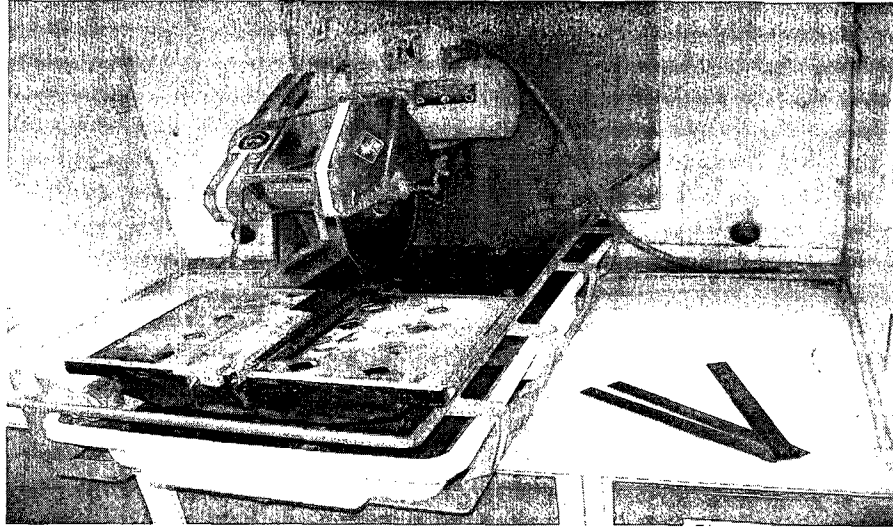


Figure 2. 4 Photograph of typical water-cooled rotary type diamond cutter

Three specimens of the $[0/90]_{4s}$ laminate configuration are tested to get longitudinal Young's modulus E_1 , failure load and failure strength values. Specimen dimension was 270mm (gauge length-180mm) X 38.9mm X 2mm. The specimen is gripped with double sided sand paper to the universal MTS machine as shown in Figure 2.5. The specification of the machine is 100 Kilo-Newton capacity, hydraulic grip control. Specimen is loaded until failure at a loading rate of 50lb/sec.

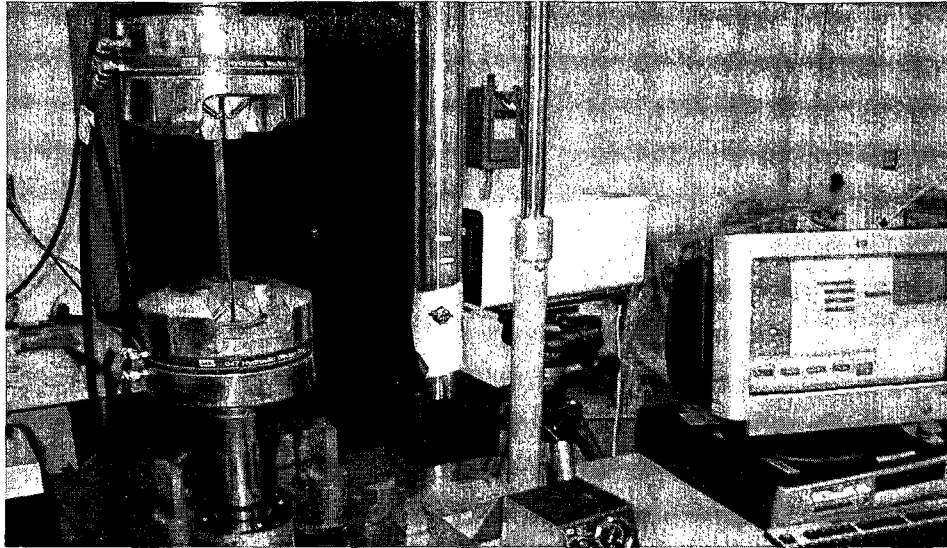


Figure 2. 5 MTS machine for mechanical property testing

A continuous record of loading P and deformation was obtained by an appropriate data acquisition system on computer attached with the MTS testing machine at some predefined time interval. Then the longitudinal direction stress is calculated by using the formula

$$\sigma_x = \frac{P_x}{A} \quad (2.1)$$

where A is cross-section of beam specimen. Longitudinal strain is calculated dividing the deformation by total gauge length. Then longitudinal stress versus longitudinal strain is plotted. The slope of this curve in the linear region is the longitudinal Young's modulus E_1 . Calculated longitudinal modulus values, failure load, failure strength are compared with ref [5] in Table 2.1.

Table 2. 1 Tensile testing data for failure load, failure strength and longitudinal modulus of composite laminate specimen

Specimen No.	Failure load (N)	Failure Strength (MPa)	Longitudinal modulus E_1 (GPa)	Mean Failure load (N) [5]	Mean Failure Strength (MPa) [5]	Longitudinal modulus [5] E_1 (GPa)
1	60884.2	780.5644	50.69			
2	53482.5	687.4357	48.62			
3	62577.1	802.27	51.68			
Mean Value	58981.26	756.7567	50.33	80496	1073.40	71.755

From Table 2.1 one can observe that there is a significant difference in laminate properties when compared with ref [5]. Longer shelf life could be one of the reasons for this difference of results. Properties such as damping loss factor can also undergo some change with time and preservation conditions. However, the testing will help to get the properties of the material according to its current condition.

2.4 Modal testing for Damping Factor

Damping characteristic in composite materials is an important factor of the dynamic behaviour of structures, controlling the resonant and near resonant vibrations and thus prolonging the structure service life under fatigue and impact loading. Generally composite materials have more damping capacity than metals. Damping in vibrating composite structures refers to a complex physical dynamic nature inducing from both constituent level (visco-elastic behaviour of matrix, damping at the fiber-matrix interface) and laminate level (layer orientation, inter-laminar effects, stacking sequence, etc.) [52].

It is still difficult to determine accurately the damping parameters by an analytical approach. The experimental prediction is therefore very desirable. In a broad class of composite structures, the distinguishing characteristic of the damping mechanism is its strong dependence on the eigen frequencies such that it exhibits little damping at high frequency level [53].

2.4.1 Experimental Procedure

This experiment is done to get the damping loss factor of cross-ply composite beam. Block diagram of instrumentation with models, which were used for damping loss factor measurement, is shown in Figure 2.6.

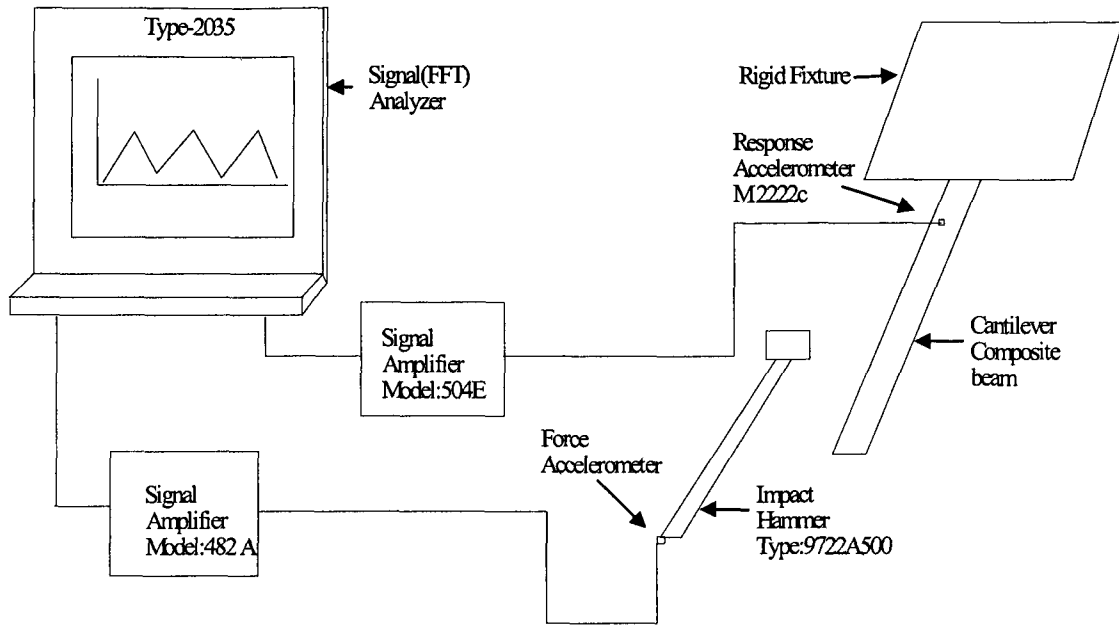


Figure 2. 6 Block diagram of instrumentation for damping loss factor measurement

Main apparatus used in the experiment are as follows:

- a. *Test fixture:* The test fixture consists of a rigid mounting support which provides a clamp for the root end of the beam.
- b. *Accelerometer/Transducer:* Two accelerometers are utilized. One accelerometer is applied for the excitation force and the other is used to measure the response of the beam. In the experiment an impact hammer that consists of a hammer with a force accelerometer built into the head of the hammer is used as excitation source.
- c. *Amplifier:* Two amplifiers are used to amplify the input signal of transducer by the two individual data channel from the force excitation impact hammer and response accelerometer.

- d. *Analyzer*: The function of this equipment is simply to measure the signals developed by the transducer in order to ascertain the magnitudes of the excitation force and response.

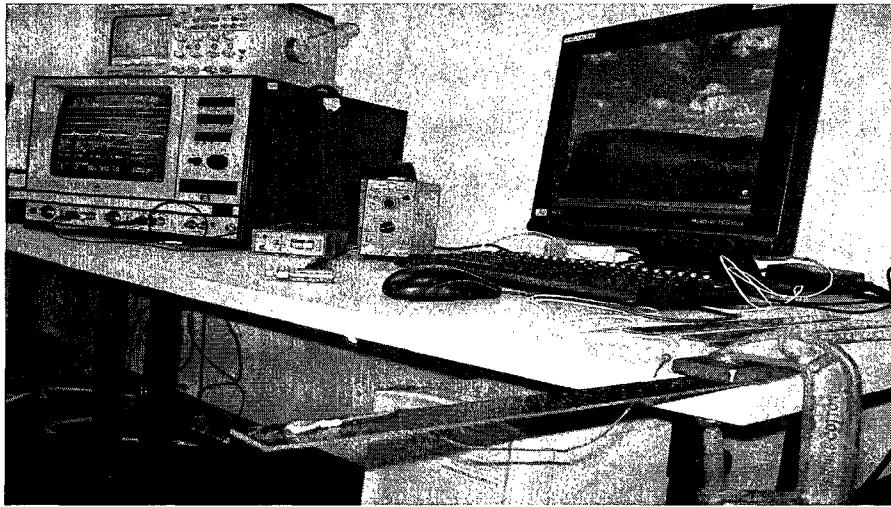


Figure 2. 7 Photograph of damping loss factor testing set-up

In this work the test specimens are prepared from the NCT-301 graphite/epoxy cross-ply laminate beam with dimensions of 250 mm x 25 mm x 2 mm. The composite beam is mounted on a corner of a big rigid table with vise/fixture providing sufficient clamping force at the root of the beam to simulate fixed end, similar to cantilevered boundary condition. The beam is excited by the impact hammer and provides signal to the amplifier. Response accelerometer is attached at free end of the beam with wax glue and provides the response to the amplifier. Two separate amplifiers amplify the signals from the force transducer and response transducer and they are fed to the FFT (Fast Fourier Transform) analyzer, which can display the FRF (Frequency Response Function) plot. The photograph of the experimental set-up is shown in Figure 2.7.

2.4.2 Damping loss factor data extraction

The testing is done in Dual Channel Spectrum averaging mode. Data were taken in a range of 0-1600 Hz frequencies in frequency span of 2Hz. The delay time was set as 500 mSec. The loss factor is calculated by using half power bandwidth technique [60]. For a structure with less damping loss, the peak $|H(\omega)|$ at resonance is well defined. The modal damping loss factor η is related to frequencies corresponding to the two points on the FRF plot, where

$$|H(\omega_a)| = |H(\omega_b)| = \frac{|H(\omega_d)|}{\sqrt{2}} \quad (2.2)$$

where ω_d , ω_a , and ω_b are the damped natural frequency at resonance, frequency found from 3-dB down point before and after the resonance frequency respectively. The frequency difference between the upper 3dB down point and the lower 3 dB point is the half power bandwidth of the mode. The modal damping loss factor η is the ratio of the half power bandwidth to the resonant frequency.

$$\eta = \frac{\omega_b - \omega_a}{\omega_d} \quad (2.3)$$

Total of three specimens of composite laminate beam were excited and damping loss factor was found out in this modal testing experiment. Each specimen was excited several times. It was taken care that the response only from beam is observed when it was excited. Among many excitations only two best excitations (based on smooth FRF curve found from proper excitation) were taken for data exaction for each specimen. Typical FRF graphs for these three specimens made of NCT-301 graphite/epoxy composite beam are shown in Figures 2.8-2.13.

The following two FRF graphs were taken from two separate excitations of the first specimen. The peaks represent the resonant frequencies of the composite beam. In first excitation, FRF shows the peaks corresponding to 34.3 dB in 220 Hz and 33.8 dB at 1234 Hz. In second excitation, FRF shows the peaks corresponding to 33.9 dB at 220 Hz and 35.9 dB at 1234 Hz.

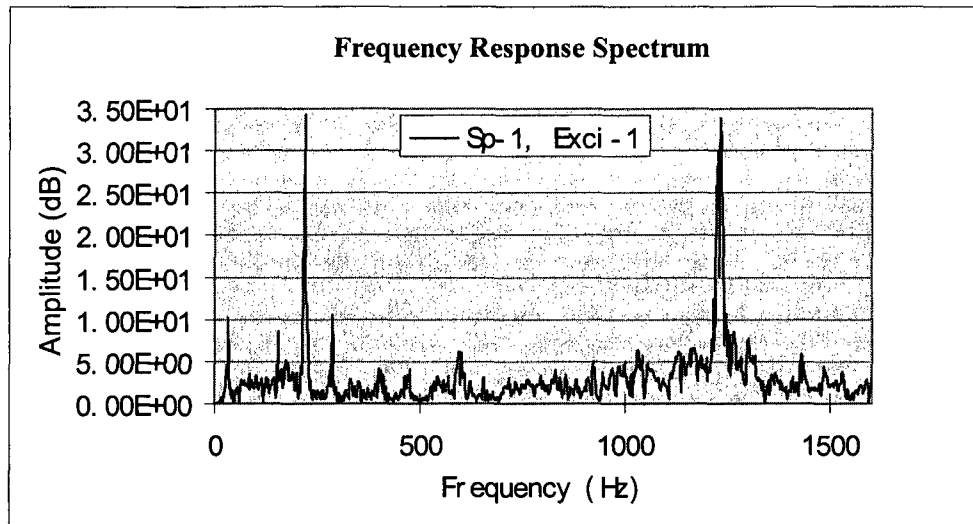


Figure 2. 8 Typical frequency response function for sample-1 for first excitation

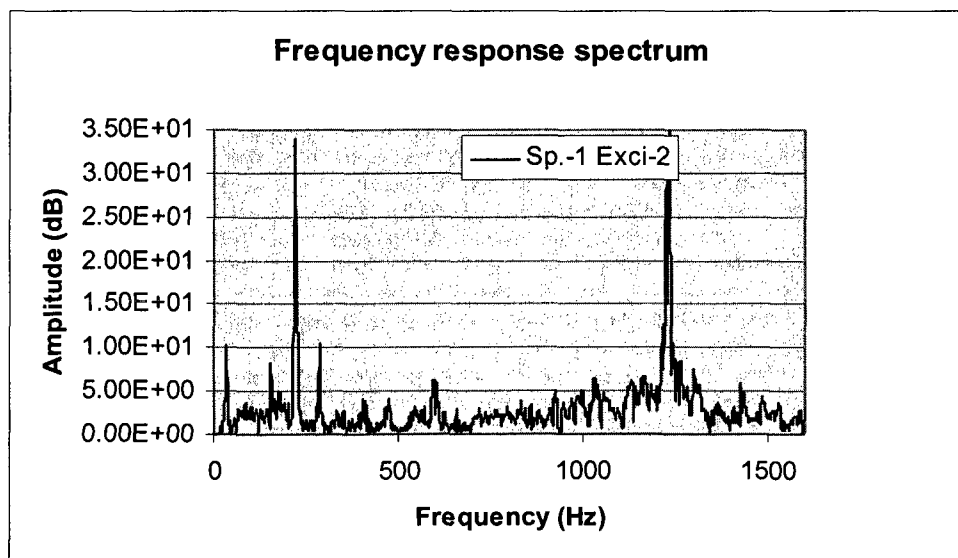


Figure 2. 9 Typical frequency response function for sample-1 for second excitation

The following two FRF graphs were taken from two separate excitations of the second specimen. In first excitation, FRF shows the peaks corresponding to 19.3 dB at 220 Hz and 23.4 dB at 1236 Hz. In second excitation, FRF shows the peaks corresponding to 20.1 dB at 220 Hz and 23.2 dB at 1236 Hz.

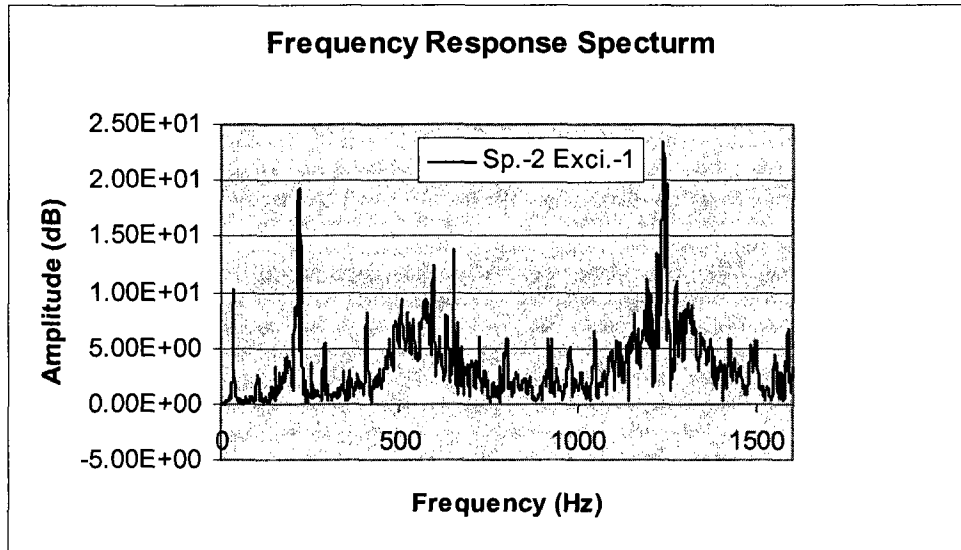


Figure 2. 10 Typical frequency response function for sample-2 for first excitation

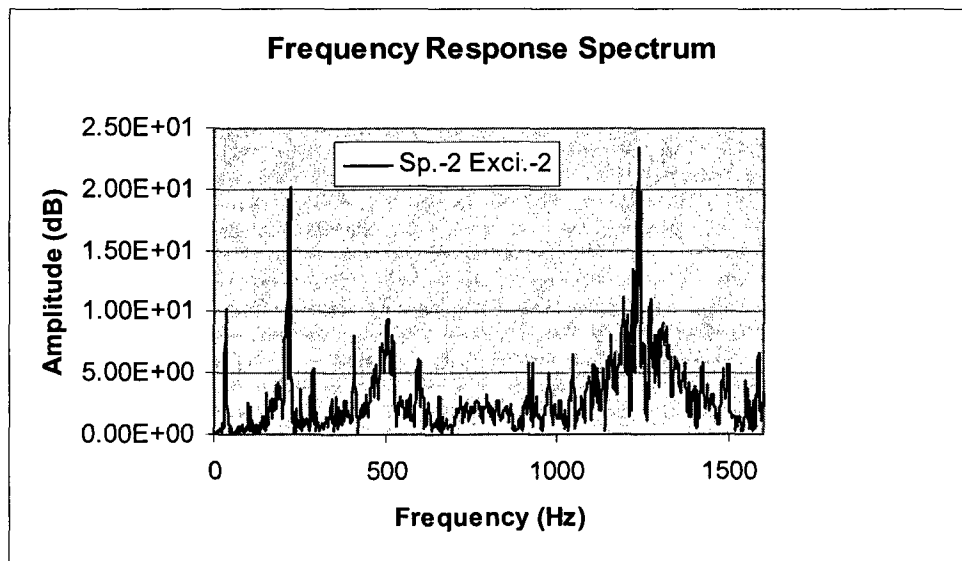


Figure 2. 11 Typical frequency response function for sample-2 for second excitation

The following two FRF graphs were taken from two separate excitations of the third specimen. In first excitation, FRF shows the peaks corresponding to 49.9 dB at 220 Hz and 19.2 dB in 1232 Hz. In second excitation, FFR shows the peaks are in 56.1 dB in 220 Hz and 20.6 dB in 1232 Hz.

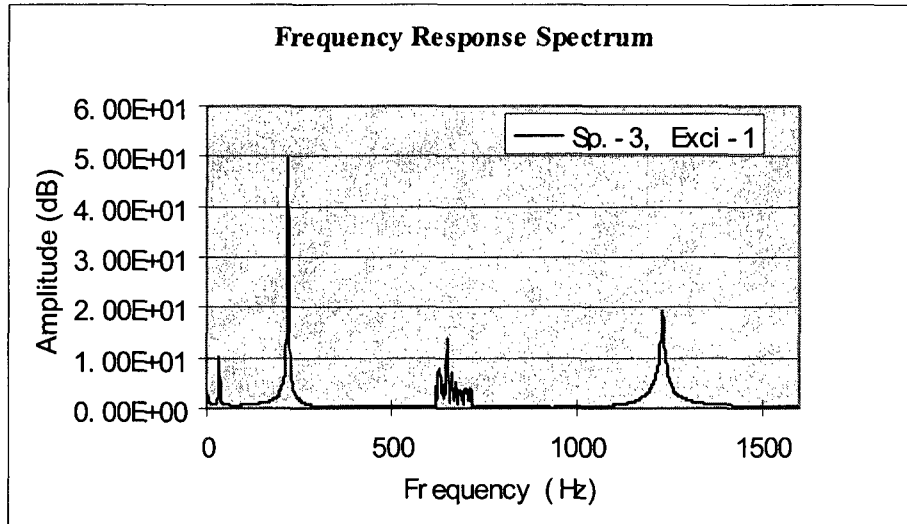


Figure 2. 12 Typical frequency response function for sample-3 for first excitation

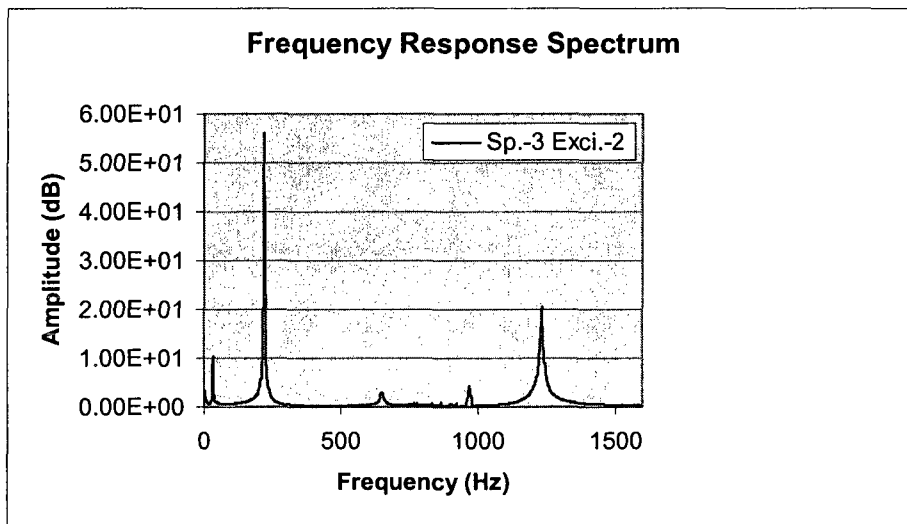


Figure 2. 13 Typical frequency response function for sample-3 for second excitation

Though FRF plots that were obtained with a little bit different shapes from different specimens, extracted data for damping loss factor for the above-mentioned composite material are almost same. Because difference in the performance of the excitation caused the different shapes of FRF plot. The damping ratios ζ are calculated from damping loss factor by dividing by two for each resonance mode of vibration of composite laminate beam respectively.

$$\zeta_i = \frac{\eta_i}{2} \quad (2.4)$$

Then mass proportional damping constant (α) and stiffness proportional damping constants (β) are calculated by using these damping ratios. Equation used to calculate these is in the following [11].

$$\frac{\alpha}{2\omega_i} + \frac{\beta\omega_i}{2} = \zeta_i \quad \text{where } i=1,2. \quad (2.5)$$

By getting two linear equations for first and second mode, one can solve those for α and β . The best two extracted values of damping loss factor (η), damping ratio (ζ), mass proportional damping constant (α) and stiffness proportional damping constant (β) from three specimens in terms of less coherence are given in Table 2.2.

Table 2. 2 Data obtained from damping loss factor measurements

	η_1	ζ_1	η_2	ζ_2	α	β
Sp.-1 Exci-1	0.0112	0.0056	0.0053	0.0026	2.3201	2.735 $\times 10^{-6}$
Sp.-1 Exci-2	0.0111	0.0056	0.0042	0.0021	2.3590	1.8342 $\times 10^{-6}$
Sp.-2 Exci-1	0.0089	0.00445	0.0048	0.0024	1.8157	2.7169 $\times 10^{-6}$
Sp.-2 Exci-2	0.0091	0.00455	0.0058	0.0029	1.82219	3.5127 $\times 10^{-6}$
Sp.-3 Exci-1	0.0121	0.00605	0.0055	0.0028	2.5204	2.8267 $\times 10^{-6}$
Sp.-3 Exci-2	0.0110	0.0055	0.0044	0.0022	2.3326	2.026 $\times 10^{-6}$

In the Table 2.2, Sp.-1 stands for first specimen and Exci.-1 stands for first excitation and so on. Thus calculated damping properties are used to calculate average proportional mass and stiffness constants that are used in the finite element analysis to form a Rayleigh damping matrix [C] as a linear combination of mass and stiffness matrices.

2.5 Conclusion

In this chapter experimental determination of mechanical properties of composite material (NCT-301) was described in detail. Damping loss factor (η) is extracted from the FRF plots by using half power bandwidth method [50]. It is observed that there is noticeable difference in tensile test data when compared with reference [5]. New values of longitudinal modulus, and failure load, failure strength are less than the available data. It was figured out that material properties could change over time due to preservation conditions. So it was concluded that data extracted for damping loss factor could also be a bit different for new NCT-301 material. Since damping loss factor for two subsequent modes of above-mentioned composite material were not found in the literature, the calculated damping loss data obtained from the testing will be used in vibration analysis of composite materials considering damping in the following chapters. But the values of other mechanical properties such as longitudinal modulus E_1 , transverse modulus E_2 , shear modulus G_{12} , major Poisson's ratio ν_{12} and minor Poisson's ratio ν_{21} , density ρ will be taken from the ref [29].

Chapter-3

Finite element formulation for vibration analysis of composite beams

3.1 Introduction

Mechanical structures require the development of necessary tools for modeling the mechanical behaviour in design and analysis. When their behaviour is to be predicted under various loadings, there is a need for accurate analysis of those loading effects. The in-service loadings on aerospace and automobile structures are mostly dynamic in nature. Therefore, advanced analytical and numerical techniques are required for the calculation of the dynamic response characteristics of structures in order that they can be designed against failure due to dynamic loads. In this chapter, free and forced vibration analysis of laminated beam is conducted using conventional finite element, higher-order finite element, and Rayleigh-Ritz formulation where Lagrange's equations are used to obtain the equation of motion.

Section 3.2 describes the one-dimensional analysis of laminated beams. Conventional finite element formulation is carried out based on Euler-Bernoulli beam theory for uniform-thickness composite beam in section 3.3. Section 3.4 explains element properties for mid-plane tapered composite beam. Higher-order finite element formulation is carried out based on Euler-Bernoulli beam theory for uniform-thickness composite beam in section 3.5. In section 3.6, the formulation based on Rayleigh-Ritz method for both uniform-thickness and tapered composite beams using the classical laminate theory is developed. The stiffness, damping and mass matrices thus generated are used in the free and forced vibration analysis of laminated composite beams as explained in details in section 3.7. A set of problems is solved considering uniform- thickness and tapered laminated composite beams with different

boundary conditions and the results are compared with existing solutions. In section 3.8 finite element formulation is developed considering the axial forces that are applied at the ends of the beam and distributed over the beam span. The problem of a uniform-thickness beam with fixed-free boundary condition subjected to axial force acting at the ends of the beam is solved for natural frequencies and forced response in terms of transverse displacement and rotation. Finally a discussion of these results that were obtained based on different finite element formulations is provided.

3.2 Laminated beam analysis

A beam is a solid structural member most commonly used in almost all mechanical structures or systems. In practical structures, it can take up a great variety of loads such as transverse load applied between its supports, transverse shear, biaxial bending and even torsion. Such complicated actions are typical of spatial beams, which are used in three-dimensional frameworks and are subjected to applied forces along arbitrary directions.

A plane beam resists primarily loading applied in one plane and has cross-section that is symmetric with respect to that plane. One-dimensional mathematical model of plane beam is considered on the basis of beam theories. In laminated plane beams the width (dimension along y-axis) is small compared to the length (dimension along x-axis). Therefore, changes in width direction are negligible and hence the kinematics of a plane straight beam is defined by the transverse displacement $w(x)$ and cross-section rotation $\theta(x)$ functions. The stiffness co-efficients of the laminated beam are determined based on classical laminate theory (for Euler-Bernoulli beam theory).

3.3 Conventional finite element formulation

3.3.1 Finite element model

The finite element model for the laminated beam as shown in Figure 3.1 is constructed using the three-step procedure given in reference [54]. First the domain (the length of the beam) is divided into a set of sub-domains. This sub-domain is called beam element and the interfaces of the elements at the ends are called nodes.

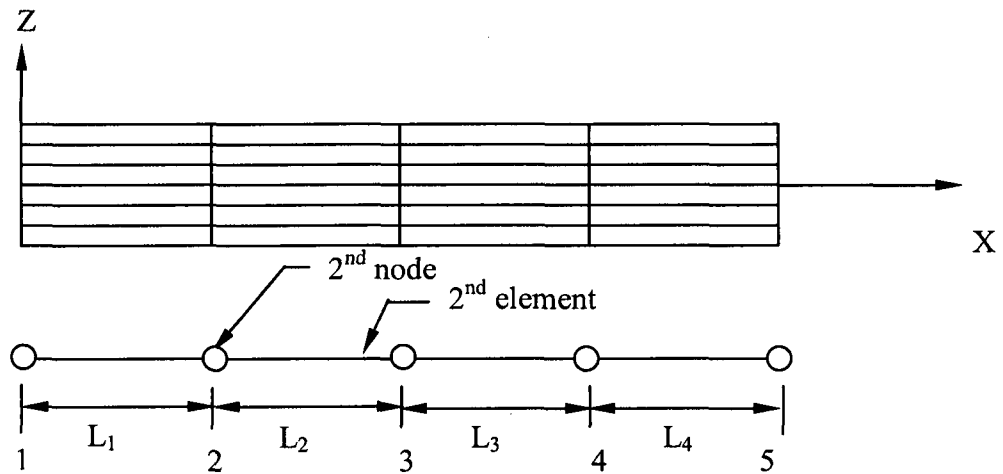


Figure 3. 1 Finite element beam model

3.3.2 Shape functions

For the development of the general equation of the beam, it is required to express the deflection in the form of polynomial. A fourth order polynomial is needed since there are four boundary conditions at two nodes (w and θ , that are respectively the deflection and rotation, for each node). For a typical beam element as shown in Figure 3.2,

$$w(x,t) = c_1 + c_2x + c_3x^2 + c_4x^3 \quad (3.1)$$

Differentiating the above equation yields the slope,

$$\theta(x,t) = c_2 + 2c_3x + 3c_4x^2 \quad (3.2)$$

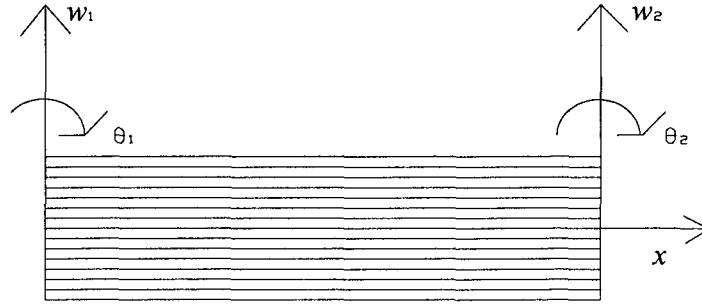


Figure 3. 2 A typical composite beam element

Since deflection w and slope θ must be continuous everywhere in the domain, they should be continuous at each and every interface between elements. So the deflection w and slope θ at nodes 1 and 2 are given as:

$$w(0, t) = w_1$$

$$w(l, t) = w_2$$

$$\theta(0, t) = \left[-\frac{dw}{dx} \right]_{(x=0)} = \theta_1 \quad (3.3 \text{ a-d})$$

$$\theta(l, t) = \left[-\frac{dw}{dx} \right]_{(x=l)} = \theta_2$$

Since the polynomial should satisfy the essential boundary conditions, one can write boundary conditions to determine the co-efficients using equation (3.3 a-d)

$$w_1 = c_1$$

$$\theta_1 = -c_2$$

$$w_2 = c_1 + c_2 l + c_3 l^2 + c_4 l^3 \quad (3.4 \text{ a-d})$$

$$\theta_2 = -c_2 - 2c_3 l - 3c_4 l^2$$

Rewriting the above four equations in matrix form, one gets the following:

$$\begin{Bmatrix} w_1 \\ \theta_1 \\ w_2 \\ \theta_2 \end{Bmatrix} = \begin{bmatrix} 1 & 0 & 0 & 0 \\ 0 & -1 & 0 & 0 \\ 1 & l & l^2 & l^3 \\ 0 & -1 & -2l & -3l^2 \end{bmatrix} \begin{Bmatrix} c_1 \\ c_2 \\ c_3 \\ c_4 \end{Bmatrix} \quad (3.5)$$

In short form equation (3.5) can be written as:

$$\{d\} = [\Gamma]\{c\} \quad (3.6)$$

By inverting $[\Gamma]$ and pre-multiplying $\{d\}$ with $[\Gamma]^{-1}$, one can obtain $\{c\}$ as follows:

$\{c\} = [\Gamma]^{-1} \{d\}$. Substituting $\{c\}$ into equation (3.1), one can approximate the deflection of the beam by the following equation:

$$w(x,t) = w_1 N_1 + \theta_1 N_2 + w_2 N_3 + \theta_2 N_4 \quad (3.7)$$

where N_j ($j=1,2,3,4$) denote the shape functions. The shape functions have been obtained using MATLAB software as follows.

$$\begin{aligned} N_1 &= 1 - 3\frac{x^2}{l^2} + 2\frac{x^3}{l^3} \\ N_2 &= -x + 2\frac{x^2}{l} - \frac{x^3}{l^2} \\ N_3 &= 3\frac{x^2}{l^2} - 2\frac{x^3}{l^3} \\ N_4 &= \frac{x^2}{l} - \frac{x^3}{l^2} \end{aligned} \quad (3.8 \text{ a-d})$$

3.3.3. Energy formulation based on Euler-Bernoulli beam theory for conventional finite element

Euler-Bernoulli beam theory is also defined as classical beam theory. This beam model accounts for bending moment effects on stress and deformation. Transverse shear forces are recovered from equilibrium but their effect on beam deformations is neglected. The fundamental assumption is that cross-section remains plane and normal to the deformed longitudinal axis.

The potential energy of an elastic solid is given by [55].

$$U = \frac{1}{2} \iiint (\sigma_x \varepsilon_x + \sigma_y \varepsilon_y + \sigma_z \varepsilon_z + \tau_{yz} \gamma_{yz} + \tau_{xz} \gamma_{xz} + \tau_{xy} \gamma_{xy}) dx dy dz \quad (3.9)$$

where σ_x denotes the stress along the x direction, ε_x denotes the total strain along x -direction, τ_{yz} denotes the shear stress along the z direction acting on y -plane, γ_{yz} denotes the shear strain corresponding to y and z -directions, and so on. Taking into account the basic assumptions of classical laminated plate theory,

$$\sigma_z = \tau_{yz} = \tau_{xz} = 0 \quad (3.10)$$

The right hand side of the equation (3.9) can be written as

$$U = \frac{1}{2} \iiint (\sigma_x \varepsilon_x + \sigma_y \varepsilon_y + \tau_{xy} \gamma_{xy}) dx dy dz \quad (3.11)$$

For pure bending of a beam, ε_y and γ_{xy} are ignored. The potential energy expression can be simplified to

$$U = \frac{1}{2} \int_x \int_A \sigma_x \varepsilon_x dA dx \quad (3.12)$$

where dA denotes the cross-section of beam. The relation between stress and strain is given by $\sigma_x = \bar{Q}_{11} \varepsilon_x$, where \bar{Q}_{11} is the first co-efficient of the transformed ply stiffness matrix.

$$U = \frac{1}{2} \int \int_{x,z} (\bar{Q}_{11} \varepsilon_{xp}) \varepsilon_{xp} b dz dx \quad (3.13)$$

where ε_{xp} denotes the strain of each ply along x - direction.

$$U = \frac{1}{2} \int \int_{x,z} \bar{Q}_{11} \varepsilon_{xp}^2 dz dx \quad (3.14)$$

The axial displacement can be written as

$$u(x, z) = -z \frac{\partial w}{\partial x} \quad (3.15)$$

For a ply, the strain is given by,

$$\varepsilon_{xp} = -z_p \frac{\partial^2 w}{\partial x^2} \quad (3.16)$$

Substituting equation (3.16) in equation (3.14) one gets

$$U = \frac{1}{2} \int \int_{x,z} \bar{Q}_{11} (-z_p \frac{\partial^2 w}{\partial x^2})^2 dz dx \quad (3.17)$$

$$U = \frac{1}{2} \int \int_{x,z} \bar{Q}_{11} z_p^2 dz (\frac{\partial^2 w}{\partial x^2})^2 dx \quad (3.18)$$

From classical laminated plate theory,

$$D_{11} = \int_{-\frac{h}{2}}^{\frac{h}{2}} \bar{Q}_{11} z^2 dz \quad (3.19)$$

where h denotes the laminate thickness.

Therefore the potential energy is given by,

$$U = \frac{1}{2} \int_x b D_{11} (\frac{\partial^2 w}{\partial x^2})^2 dx \quad (3.20)$$

Substituting the displacement equation in equation (3.20) one gets

$$U = \frac{1}{2} \int_x bD_{11} \left[\frac{\partial^2 (N_1 w_1 + N_2 \theta_1 + N_3 w_2 + N_4 \theta_2)}{\partial x^2} \right]^2 dx \quad (3.22)$$

The generalized co-ordinates for the beam element can be taken to be w_1, θ_1, w_2 and θ_2 .

Therefore

$$\begin{aligned} q_1 &= w_1 \\ q_2 &= \theta_1 \\ q_3 &= w_2 \\ q_4 &= \theta_2 \end{aligned} \quad (3.23 \text{ a-d})$$

The potential energy expression changes to

$$U = \frac{1}{2} \int_x bD_{11} \left[\frac{\partial^2 (N_1 q_1 + N_2 q_2 + N_3 q_3 + N_4 q_4)}{\partial x^2} \right]^2 dx \quad (3.24)$$

Differentiating the above equation with respect to first generalized co-ordinate, q_1 , one gets

$$\frac{\partial U}{\partial q_1} = \frac{1}{2} \int_x bD_{11} \cdot 2 \left[\frac{\partial^2 (N_1 q_1 + N_2 q_2 + N_3 q_3 + N_4 q_4)}{\partial x^2} \right] \frac{\partial^2 N_1}{\partial x^2} dx \quad (3.25)$$

$$\begin{aligned} \frac{\partial U}{\partial q_1} &= \left(\int_x bD_{11} \frac{d^2 N_1}{dx^2} \cdot \frac{d^2 N_1}{dx^2} dx \right) q_1 + \left(\int_x bD_{11} \frac{d^2 N_2}{dx^2} \cdot \frac{d^2 N_1}{dx^2} dx \right) q_2 \\ &+ \left(\int_x bD_{11} \frac{d^2 N_3}{dx^2} \cdot \frac{d^2 N_1}{dx^2} dx \right) q_3 + \left(\int_x bD_{11} \frac{d^2 N_4}{dx^2} \cdot \frac{d^2 N_1}{dx^2} dx \right) q_4 \end{aligned} \quad (3.26)$$

$$\frac{\partial U}{\partial q_1} = k_{11} q_1 + k_{12} q_2 + k_{13} q_3 + k_{14} q_4 \quad (3.27)$$

Similarly, differentiating the potential energy expression with respect to second, third and fourth generalized co-ordinates, one can get

$$\frac{\partial U}{\partial q_2} = k_{21} q_1 + k_{22} q_2 + k_{23} q_3 + k_{24} q_4 \quad (3.28)$$

$$\frac{\partial U}{\partial q_3} = k_{31}q_1 + k_{32}q_2 + k_{33}q_3 + k_{34}q_4 \quad (3.29)$$

$$\frac{\partial U}{\partial q_4} = k_{41}q_1 + k_{42}q_2 + k_{43}q_3 + k_{44}q_4 \quad (3.30)$$

Equation (3.27), (3.28), (3.29) and (3.30) can be written together in matrix form as

$$\left\{ \frac{\partial U}{\partial q} \right\} = \begin{Bmatrix} \frac{\partial U}{\partial q_1} \\ \frac{\partial U}{\partial q_2} \\ \frac{\partial U}{\partial q_3} \\ \frac{\partial U}{\partial q_4} \end{Bmatrix} = \begin{bmatrix} k_{11} & k_{12} & k_{13} & k_{14} \\ k_{21} & k_{22} & k_{23} & k_{24} \\ k_{31} & k_{32} & k_{33} & k_{34} \\ k_{41} & k_{42} & k_{43} & k_{44} \end{bmatrix} \begin{Bmatrix} q_1 \\ q_2 \\ q_3 \\ q_4 \end{Bmatrix} \quad (3.31)$$

In general one can write the above equation in short form as,

$$\left\{ \frac{\partial U}{\partial q} \right\} = [k] \{q\} \quad (3.32)$$

$$\text{where } k_{ij} = \int_0^l bD_{11} \frac{d^2 N_i}{dx^2} \frac{d^2 N_j}{dx^2} dx \quad (3.33)$$

The kinetic energy denoted as T , of an elastic body in terms of the xyz coordinate system can be written as,

$$T = \frac{1}{2} \iiint \rho \left[\left(\frac{\partial u}{\partial t} \right)^2 + \left(\frac{\partial v}{\partial t} \right)^2 + \left(\frac{\partial w}{\partial t} \right)^2 \right] dx dy dz \quad (3.34)$$

where ρ is the density of the material and the displacements u , v and w are along x , y and z directions.

Substituting equation (3.15), into equation (3.34), the kinetic energy can be written as

$$T = \frac{1}{2} \iiint \rho \left[\left(-z \frac{\partial^2 w}{\partial x \partial t} \right)^2 + \left(\frac{\partial w}{\partial t} \right)^2 \right] dx dy dz \quad (3.35)$$

since v is neglected in Euler-Bernoulli theory.

Considering that the rotary inertia terms are negligible, the equation for the kinetic energy becomes

$$T = \frac{1}{2} \iint b \rho \left(\frac{\partial w}{\partial t} \right)^2 dx dz \quad (3.36)$$

$$T = \frac{1}{2} \int \rho A \left(\frac{\partial (N_1 q_1 + N_2 q_2 + N_3 q_3 + N_4 q_4)}{\partial t} \right)^2 dx \quad (3.37)$$

$$T = \frac{1}{2} \sum_i \sum_j \dot{q}_i \dot{q}_j \int \rho A N_i N_j dx \quad (3.38)$$

where A is the cross section of the beam and $\dot{}$ denotes time differentiation.

The kinetic energy expression can be rewritten as

$$T = \frac{1}{2} \sum_i \sum_j \dot{q}_i \dot{q}_j m_{ij} \quad (3.39)$$

$$\text{where } m_{ij} = \int_0^l \rho A N_i N_j dx \quad (3.40)$$

Partially differentiating equation (3.39) with respect to each \dot{q} term and then differentiating the whole term with respect to time t , one can obtain

$$\begin{Bmatrix} \frac{d}{dt} \left(\frac{\partial T}{\partial \dot{q}_1} \right) \\ \frac{d}{dt} \left(\frac{\partial T}{\partial \dot{q}_2} \right) \\ \frac{d}{dt} \left(\frac{\partial T}{\partial \dot{q}_3} \right) \\ \frac{d}{dt} \left(\frac{\partial T}{\partial \dot{q}_4} \right) \end{Bmatrix} = \begin{bmatrix} m_{11} & m_{12} & m_{13} & m_{14} \\ m_{21} & m_{22} & m_{23} & m_{24} \\ m_{31} & m_{32} & m_{33} & m_{34} \\ m_{41} & m_{42} & m_{43} & m_{44} \end{bmatrix} \begin{Bmatrix} \ddot{q}_1 \\ \ddot{q}_2 \\ \ddot{q}_3 \\ \ddot{q}_4 \end{Bmatrix} \quad (3.41)$$

In general one can write the above equation as,

$$\left\{ \frac{d}{dt} \left(\frac{\partial T}{\partial \dot{q}} \right) \right\} = [m] \{ \ddot{q} \} \quad (3.42)$$

Differentiating equation (3.39) with respect to generalized co-ordinate one can get

$$\frac{\partial T}{\partial q_i} = 0 \quad (3.43)$$

The virtual work due to virtual displacement is [56].

$$\partial W = \sum_{j=0}^n F_j \cdot \left(\sum_{i=1}^4 N_i(x_j) \partial q_i \right) \quad (3.44)$$

where virtual displacement $\partial w = \sum_{i=1}^4 N_i(x) \partial q_i$ and F_j is force applied on beam span.

$$\text{The generalized force is } Q_i = \frac{\partial W}{\partial q_i} = \sum_{j=0}^n F_j N_i(x_j) \quad (3.45)$$

where Q_i is referred to as the generalized force. If a force F_1 is applied at one point of beam, the generalized force Q_1 will be applied force F_1 with respect to that generalized co-ordinate.

3.4 Element properties for mid-plane tapered composite beam

In the case of mid-plane tapered composite beam as shown in Figure 3.3, the cross-section area and the value of D_{11} are not constant throughout the length in the tapered section of the beam as there are ply drop-off at specific distances.

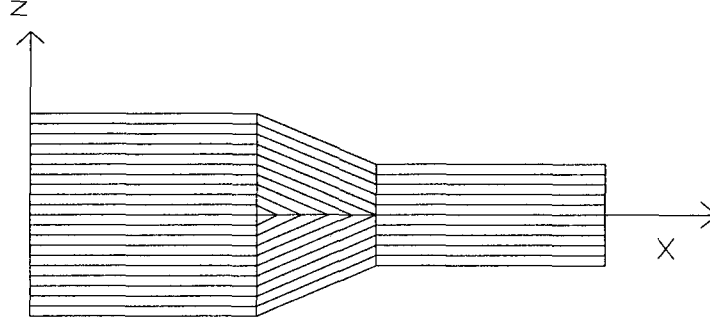


Figure 3. 3 Mid-plane tapered composite beam

One can write the stiffness co-efficients of a mid-plane tapered composite beam as [29]

$$k_{ij} = \int_0^l b D_{11}(x) \cos^4(\phi) \frac{d^2 N_i}{dx^2} \frac{d^2 N_j}{dx^2} dx \quad (3.46)$$

where ϕ denotes the taper angle. According to classical laminated theory, the bending or flexural laminate stiffness relating the bending moment to curvature, $D_{11}(x)$ can be written as [57]

$$D_{11}(x) = \sum_{k=1}^n \left[t'_k \bar{z}_k^2 + \frac{t_k^3}{12} \right] (\bar{Q}_{11})_k \quad (3.47)$$

where \bar{Q}_{11} is the first co-efficient of the transformed ply stiffness matrix and t'_k for k^{th} ply is given by

$$t'_k = h'_k - h'_{k-1} = \frac{t_k}{\cos(\phi)} \quad (3.48)$$

where h'_k , h'_{k-1} , t'_k and t'_{k-1} are shown in Figure 3.4 and the term \bar{z}_k is the distance between the centerline of the inclined ply and the mid-plane of the laminate for the k_{th} ply and it is given by $\bar{z}_k = sx + c$ (3.49)

where c is the intercept of the center line of the ply from the mid-plane line and s is the slope of the line that is given as $s = -\tan(\phi)$, as can be seen in Figure 3.4.

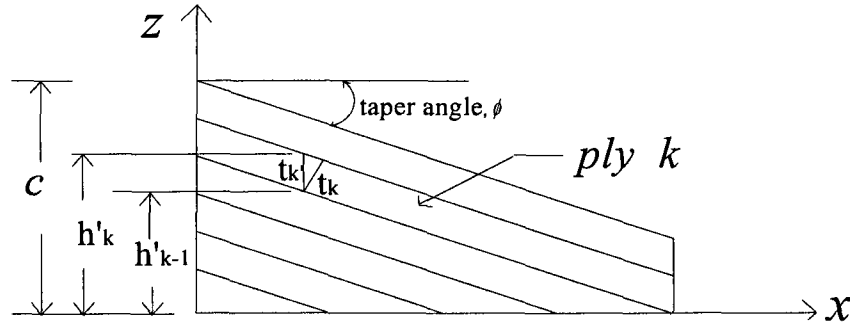


Figure 3. 4 Ply thickness, taper angle, and intercept from mid-plane of typical ply

Equation (3.47) can be rewritten as

$$D_{11}(x) = \sum_{k=1}^n \left[\frac{t_k}{\cos(\phi)} (sx + c)_k^2 + \frac{t_k^3}{12 \cos^3(\phi)} \right] (\bar{Q}_{11})_k \quad (3.50)$$

By substituting this variable bending or flexural laminate stiffness and the shape functions into equation (3.46), the stiffness matrix $[k]$ is obtained by performing the integration as specified. Integration has been performed using MATLAB software to determine the stiffness matrix for symmetric mid-plane tapered composite beam.

To construct mass matrix for a tapered beam, one should consider the decreasing value of area due to the ply drop-off. In mass matrix, the area for an element is considered as the average of both the end areas.

$$m_{ij} = \int_0^l \rho A_{avg} N_i N_j dx \quad (3.51)$$

A_{avg} denotes the average of the end areas of the element.

It has been shown [15] that more accurate results than that of lower degrees of freedom can be obtained by increasing the number of degrees of freedom. Then a finite element can consider both the essential or geometric boundary conditions (deflection and slope) and natural or force boundary conditions (curvature and gradient of curvature) at each node of the beam element. Such an element is called as higher-order finite element. It also removed the limitations of advanced finite element formulation given in ref. [29] for forced vibration analysis.

In higher-order finite element formulation for the analysis of composite beams, a beam element with two nodes at the ends and four degrees of freedom per node is considered. The transverse displacement w , the slope $\frac{\partial w}{\partial x}$, the curvature $\frac{\partial^2 w}{\partial x^2}$, and the gradient of curvature $\frac{\partial^3 w}{\partial x^3}$ are considered as the degrees of freedom for each node. Then a seventh degree polynomial displacement function is required to satisfy the boundary conditions. This element represents the entire physical situation involved in any combination of displacement, rotation and curvature conditions.

3.5.1 Finite element model

The domain (the length of the beam) is divided into a set of sub-domains. This sub-domain is called beam element and the interfaces of the elements at the ends are called nodes. In the higher-order finite element formulation, four degrees of freedom (curvature and gradient of curvature as natural boundary conditions and deflection and slope as geometric boundary conditions) are considered for each node. Thus there are eight degrees of freedom per element. A finite element model of a uniform-thickness beam with four degrees of freedom per node is shown in Figure 3.5.

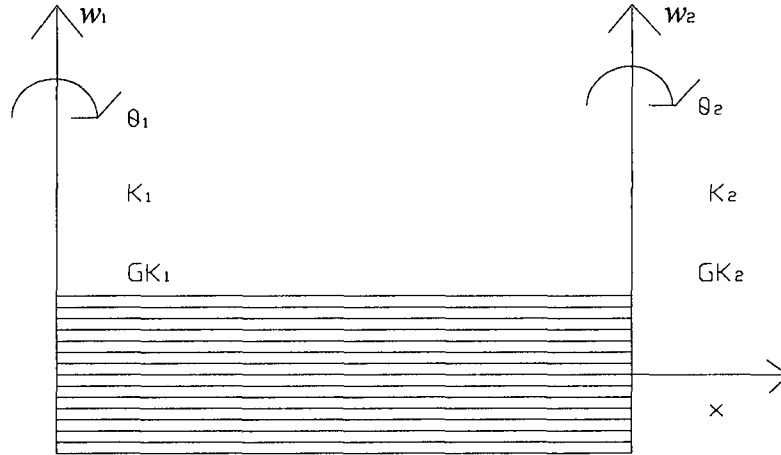


Figure 3. 5 Finite element model of a uniform-thickness beam with four degrees of freedom per node

3.5.2 Shape functions

For the development of the general equation of the beam in higher-order finite element formulation, it is required to express the deflection in the form of polynomial.

The deflection w , is approximated by a seventh order polynomial as follows:

$$w(x) = c_0 + c_1x + c_2x^2 + c_3x^3 + c_4x^4 + c_5x^5 + c_6x^6 + c_7x^7 \quad (3.52)$$

In matrix form equation (3.52) can be written as

$$[w] = [X][c] \quad (3.53)$$

where $[X]$ is a vector which is given by $[X] = [1 \ x \ x^2 \ x^3 \ x^4 \ x^5 \ x^6 \ x^7]$ and $[c]$ is column matrix of co-efficients.

Then rotation, curvature and gradient of curvature as a function of deflection w are given as follows:

$$\theta(x) = -\frac{dw(x)}{dx} = -(c_1 + 2c_2x + 3c_3x^2 + 4c_4x^3 + 5c_5x^4 + 6c_6x^5 + 7c_7x^6) \quad (3.54)$$

$$K(x) = -\frac{d^2w(x)}{dx^2} = -(2c_2 + 6c_3x + 12c_4x^2 + 20c_5x^3 + 30c_6x^4 + 42c_7x^5) \quad (3.55)$$

$$GK(x) = \frac{d^3w(x)}{dx^3} = 6c_3 + 24c_4x + 60c_5x^2 + 120c_6x^3 + 210c_7x^4 \quad (3.56)$$

To evaluate the above relations at the two ends of the element, one can choose the first node at $x=0$ and the second node at $x=l$.

To evaluate the co-efficient c_i , one can use the following boundary conditions:

$$w(0) = w_1^e = c_0$$

$$\theta(0) = \theta_1 = -\frac{dw}{dx} = -c_1$$

$$K(0) = K_1 = -\frac{d^2w}{dx^2} = -2c_2$$

$$GK(0) = GK_1 = \frac{d^3w}{dx^3} = 6c_3$$

$$w(l) = w_2^e = c_0 + c_1l + c_2l^2 + c_3l^3 + c_4l^4 + c_5l^5 + c_6l^6 + c_7l^7 \quad (3.57 \text{ a-h})$$

$$\theta(l) = \theta_2 = -[c_1 + 2c_2l + 3c_3l^2 + 4c_4l^3 + 5c_5l^4 + 6c_6l^5 + 7c_7l^6]$$

$$K(l) = K_2 = -[2c_2 + 6c_3l + 12c_4l^2 + 20c_5l^3 + 30c_6l^4 + 42c_7l^5]$$

$$GK(l) = GK_2 = [6c_3 + 24c_4l + 60c_5l^2 + 120c_6l^3 + 210c_7l^4]$$

In matrix form, the equations can be written as:

$$\begin{Bmatrix} w_1 \\ \theta_1 \\ GK_1 \\ K_1 \\ w_2 \\ \theta_2 \\ GK_2 \\ K_2 \end{Bmatrix} = \begin{bmatrix} 1 & 0 & 0 & 0 & 0 & 0 & 0 & 0 \\ 0 & -1 & 0 & 0 & 0 & 0 & 0 & 0 \\ 0 & 0 & 0 & 6 & 0 & 0 & 0 & 0 \\ 0 & 0 & -2 & 0 & 0 & 0 & 0 & 0 \\ 1 & l & l^2 & l^3 & l^4 & l^5 & l^6 & l^7 \\ 0 & -1 & -2l & -3l^2 & -4l^3 & -5l^4 & -6l^5 & -7l^6 \\ 0 & 0 & 0 & 6 & 24l & 60l^2 & 120l^3 & 210l^4 \\ 0 & 0 & -2 & -6l & -12l^2 & -20l^3 & -30l^4 & -42l^5 \end{bmatrix} \begin{Bmatrix} c_1 \\ c_2 \\ c_3 \\ c_4 \\ c_5 \\ c_6 \\ c_7 \\ c_8 \end{Bmatrix} \quad (3.58)$$

where it is considered that gradient of curvature and curvature are analogous to shear force and bending moment respectively.

In short form equation (3.58) can be written as:

$$\{d\} = [\Psi]\{c\} \quad (3.59)$$

Using shape functions $w(x)$ can be approximated as

$$\{w\} = [N]\{d\} \quad (3.60)$$

where $[N]$ is a vector containing shape functions. Substituting for $\{d\}$, from equation (3.59) into equation (3.60), one can get

$$\{w\} = [N][\Psi]\{c\} \quad (3.61)$$

Substituting $\{w\}$ from equation (3.53) into left side, discarding $[c]$, and multiplying by

$[\Psi]^{-1}$ in both side of equation (3.61), the resultant equation leads to

$$[X][\Psi]^{-1} = [N][\Psi][\Psi]^{-1} \quad (3.62)$$

Finally, shape functions can be obtained by solving the following equation

$$[N] = [X][\Psi]^{-1} \quad (3.63)$$

By using MATLAB software, the shape functions are obtained as follows,

$$\begin{aligned}
 N_1 &= 1 - 35 \frac{x^4}{l^4} + 84 \frac{x^5}{l^5} - 70 \frac{x^6}{l^6} + 20 \frac{x^7}{l^7} \\
 N_2 &= -x + 20 \frac{x^4}{l^3} - 45 \frac{x^5}{l^4} + 36 \frac{x^6}{l^5} - 10 \frac{x^7}{l^6} \\
 N_3 &= \frac{x^3}{6} - \frac{2x^4}{3l} + \frac{x^5}{l^2} - \frac{2x^6}{3l^3} + \frac{x^7}{6l^4} \\
 N_4 &= -\frac{x^2}{2} + \frac{5x^4}{l^2} - \frac{10x^5}{l^3} + \frac{15x^6}{2l^4} - \frac{2x^7}{l^5} \\
 N_5 &= \frac{35x^4}{l^4} - \frac{84x^5}{l^5} + \frac{70x^6}{l^6} - \frac{20x^7}{l^7} \\
 N_6 &= \frac{15x^4}{l^3} - \frac{39x^5}{l^4} + \frac{34x^6}{l^5} - \frac{10x^7}{l^6} \\
 N_7 &= -\frac{x^4}{6l} + \frac{x^5}{2l^2} - \frac{x^6}{2l^3} + \frac{x^7}{6l^4} \\
 N_8 &= \frac{5x^4}{2l^2} + \frac{7x^5}{l^3} - \frac{13x^6}{2l^4} + \frac{2x^7}{l^5}
 \end{aligned} \tag{3.64 a-h}$$

3.5.3 Energy formulation based on Euler-Bernoulli beam theory for higher- order finite element

The potential energy of an elastic solid written in Cartesian co-ordinate system is given by equation (3.9).

Taking into account the basic assumptions of pure bending of a beam and classical lamination theory, the potential energy expression can be simplified as given by equation (3.20). One can write,

$$w = N_1 w_1 + N_2 \theta_1 + N_3 GK_1 + N_4 K_1 + N_5 w_2 + N_6 \theta_2 + N_7 GK_2 + N_8 K_2 \tag{3.65}$$

Substituting this displacement expression in equation (3.20) one gets

$$U = \frac{1}{2} \int bD_{11} \left[\frac{d^2}{dx^2} N_1 w_1 + N_2 \theta_1 + N_3 GK_1 + N_4 K_1 + N_5 w_2 + N_6 \theta_2 + N_7 GK_2 + N_8 K_2 \right]^2 dx \quad (3.66)$$

Now one can write the displacement as a function of shape functions and generalized co-ordinate,

$$w = N_1 q_1 + N_2 q_2 + N_3 q_3 + N_4 q_4 + N_5 q_5 + N_6 q_6 + N_7 q_7 + N_8 q_8 \quad (3.67)$$

So the potential energy will be

$$U = \frac{1}{2} \int bD_{11} \left[\frac{d^2}{dx^2} (N_1 q_1 + N_2 q_2 + N_3 q_3 + N_4 q_4 + N_5 q_5 + N_6 q_6 + N_7 q_7 + N_8 q_8) \right]^2 dx \quad (3.68)$$

Differentiating the potential energy with respect to first generalized co-ordinate, q_1 one can

get,

$$\frac{\partial U}{\partial q_1} = \frac{1}{2} \int bD_{11} \cdot 2 \left[\frac{d^2}{dx^2} (N_1 q_1 + N_2 q_2 + N_3 q_3 + N_4 q_4 + N_5 q_5 + N_6 q_6 + N_7 q_7 + N_8 q_8) \right] \frac{d^2 N_1}{dx^2} dx \quad (3.69)$$

$$\begin{aligned} \frac{\partial U}{\partial q_1} &= \left(\int bD_{11} \frac{d^2 N_1}{dx^2} \cdot \frac{d^2 N_1}{dx^2} dx \right) q_1 + \left(\int bD_{11} \frac{d^2 N_2}{dx^2} \cdot \frac{d^2 N_1}{dx^2} dx \right) q_2 \\ &+ \left(\int bD_{11} \frac{d^2 N_3}{dx^2} \cdot \frac{d^2 N_1}{dx^2} dx \right) q_3 + \left(\int bD_{11} \frac{d^2 N_4}{dx^2} \cdot \frac{d^2 N_1}{dx^2} dx \right) q_4 + \\ &\left(\int bD_{11} \frac{d^2 N_5}{dx^2} \cdot \frac{d^2 N_1}{dx^2} dx \right) q_5 + \left(\int bD_{11} \frac{d^2 N_6}{dx^2} \cdot \frac{d^2 N_1}{dx^2} dx \right) q_6 + \\ &\left(\int bD_{11} \frac{d^2 N_7}{dx^2} \cdot \frac{d^2 N_1}{dx^2} dx \right) q_7 + \left(\int bD_{11} \frac{d^2 N_8}{dx^2} \cdot \frac{d^2 N_1}{dx^2} dx \right) q_8 \end{aligned} \quad (3.70)$$

$$\begin{aligned} \frac{\partial U}{\partial q_1} &= k_{11} q_1 + k_{12} q_2 + k_{13} q_3 + k_{14} q_4 + k_{15} q_5 \\ &+ k_{16} q_6 + k_{17} q_7 + k_{18} q_8 \end{aligned} \quad (3.71)$$

Similarly one can get,

$$\frac{\partial U}{\partial q_2} = k_{21}q_1 + k_{22}q_2 + k_{23}q_3 + k_{24}q_4 + k_{25}q_5 + k_{26}q_6 + k_{27}q_7 + k_{28}q_8$$

$$\frac{\partial U}{\partial q_3} = k_{31}q_1 + k_{32}q_2 + k_{33}q_3 + k_{34}q_4 + k_{35}q_5 + k_{36}q_6 + k_{37}q_7 + k_{38}q_8$$

$$\frac{\partial U}{\partial q_4} = k_{41}q_1 + k_{42}q_2 + k_{43}q_3 + k_{44}q_4 + k_{45}q_5 + k_{46}q_6 + k_{47}q_7 + k_{48}q_8$$

$$\frac{\partial U}{\partial q_5} = k_{51}q_1 + k_{52}q_2 + k_{53}q_3 + k_{54}q_4 + k_{55}q_5 + k_{56}q_6 + k_{57}q_7 + k_{58}q_8$$

$$\frac{\partial U}{\partial q_6} = k_{61}q_1 + k_{62}q_2 + k_{63}q_3 + k_{64}q_4 + k_{65}q_5 + k_{66}q_6 + k_{67}q_7 + k_{68}q_8 \quad (3.72 \text{ a-g})$$

$$\frac{\partial U}{\partial q_7} = k_{71}q_1 + k_{72}q_2 + k_{73}q_3 + k_{74}q_4 + k_{75}q_5 + k_{76}q_6 + k_{77}q_7 + k_{78}q_8$$

$$\frac{\partial U}{\partial q_8} = k_{81}q_1 + k_{82}q_2 + k_{83}q_3 + k_{84}q_4 + k_{85}q_5 + k_{86}q_6 + k_{87}q_7 + k_{88}q_8$$

Now assembling the equation (3.71) and equation (3.72 a-g) in matrix form, one can

write as follows:

$$\left\{ \frac{\partial U}{\partial q} \right\} = \begin{Bmatrix} \frac{\partial U}{\partial q_1} \\ \frac{\partial U}{\partial q_2} \\ \frac{\partial U}{\partial q_3} \\ \frac{\partial U}{\partial q_4} \\ \frac{\partial U}{\partial q_5} \\ \frac{\partial U}{\partial q_6} \\ \frac{\partial U}{\partial q_7} \\ \frac{\partial U}{\partial q_8} \end{Bmatrix} = \begin{bmatrix} k_{11} & k_{12} & k_{13} & k_{14} & k_{15} & k_{16} & k_{17} & k_{18} \\ k_{21} & k_{22} & k_{23} & k_{24} & k_{25} & k_{26} & k_{27} & k_{28} \\ k_{31} & k_{32} & k_{33} & k_{34} & k_{35} & k_{36} & k_{37} & k_{38} \\ k_{41} & k_{42} & k_{43} & k_{44} & k_{45} & k_{46} & k_{47} & k_{48} \\ k_{51} & k_{52} & k_{53} & k_{54} & k_{55} & k_{56} & k_{57} & k_{58} \\ k_{61} & k_{62} & k_{63} & k_{64} & k_{65} & k_{66} & k_{67} & k_{68} \\ k_{71} & k_{72} & k_{73} & k_{74} & k_{75} & k_{76} & k_{77} & k_{78} \\ k_{81} & k_{82} & k_{83} & k_{84} & k_{85} & k_{86} & k_{87} & k_{88} \end{bmatrix} \begin{Bmatrix} q_1 \\ q_2 \\ q_3 \\ q_4 \\ q_5 \\ q_6 \\ q_7 \\ q_8 \end{Bmatrix} \quad (3.73)$$

In general for higher-order finite element one can write as

$$\frac{\partial U}{\partial q_i} = \sum_{j=1}^8 k_{ij} q_j \quad (3.74)$$

$$\text{where } k_{ij} = \int_0^l b D_{11} \frac{d^2 N_i}{dx^2} \frac{d^2 N_j}{dx^2} dx$$

The kinetic energy T , of an elastic body in terms of the xyz co-ordinate system can be written as equation (3.34). Now in the case of pure bending based on the classical laminate theory, considering that the rotary inertia terms are negligible, which means ignoring the first term of equation (3.35) leads to the kinetic energy as equation (3.36). Substituting the displacement equation for higher-order finite element in equation (3.36), one gets

$$T = \frac{1}{2} \iint b \rho \left[\left(\frac{\partial(N_1 w_1 + N_2 \theta_1 + N_3 G K_1 + N_4 K_1 + N_5 w_2 + N_6 \theta_2 + N_7 G K_2 + N_8 K_2)}{\partial t} \right)^2 \right] dx dz \quad (3.75)$$

Considering the general displacement equation (3.67) which is as a function of shape functions and generalized co-ordinate, the kinetic energy equation changes to

$$T = \frac{1}{2} \iint b \rho \left[\left(\frac{\partial(N_1 q_1 + N_2 q_2 + N_3 q_3 + N_4 q_4 + N_5 q_5 + N_6 q_6 + N_7 q_7 + N_8 q_8)}{\partial t} \right)^2 \right] dx dz \quad (3.76)$$

$$T = \frac{1}{2} \int \rho A \left[\left(\frac{\partial(N_1 q_1 + N_2 q_2 + N_3 q_3 + N_4 q_4 + N_5 q_5 + N_6 q_6 + N_7 q_7 + N_8 q_8)}{\partial t} \right)^2 \right] dx \quad (3.77)$$

Now equation (3.77) for the kinetic energy expression can be written as equation (3.38).

Partially differentiating equation (3.38) with respect to \dot{q} and then differentiating the whole term with respect to time t , one can obtain

$$\left\{ \frac{d}{dt} \left(\frac{\partial T}{\partial \dot{q}} \right) \right\} = \begin{Bmatrix} \frac{d}{dt} \left(\frac{\partial T}{\partial \dot{q}_1} \right) \\ \frac{d}{dt} \left(\frac{\partial T}{\partial \dot{q}_2} \right) \\ \frac{d}{dt} \left(\frac{\partial T}{\partial \dot{q}_3} \right) \\ \frac{d}{dt} \left(\frac{\partial T}{\partial \dot{q}_4} \right) \\ \frac{d}{dt} \left(\frac{\partial T}{\partial \dot{q}_5} \right) \\ \frac{d}{dt} \left(\frac{\partial T}{\partial \dot{q}_6} \right) \\ \frac{d}{dt} \left(\frac{\partial T}{\partial \dot{q}_7} \right) \\ \frac{d}{dt} \left(\frac{\partial T}{\partial \dot{q}_8} \right) \end{Bmatrix} = \begin{bmatrix} m_{11} & m_{12} & m_{13} & m_{14} & m_{15} & m_{16} & m_{17} & m_{18} \\ m_{21} & m_{22} & m_{23} & m_{24} & m_{25} & m_{26} & m_{27} & m_{28} \\ m_{31} & m_{32} & m_{33} & m_{34} & m_{35} & m_{36} & m_{37} & m_{38} \\ m_{41} & m_{42} & m_{43} & m_{44} & m_{45} & m_{46} & m_{47} & m_{48} \\ m_{51} & m_{52} & m_{53} & m_{54} & m_{55} & m_{56} & m_{57} & m_{58} \\ m_{61} & m_{62} & m_{63} & m_{64} & m_{65} & m_{66} & m_{67} & m_{68} \\ m_{71} & m_{72} & m_{73} & m_{74} & m_{75} & m_{76} & m_{77} & m_{78} \\ m_{81} & m_{82} & m_{83} & m_{84} & m_{85} & m_{86} & m_{87} & m_{88} \end{bmatrix} \begin{Bmatrix} \ddot{q}_1 \\ \ddot{q}_2 \\ \ddot{q}_3 \\ \ddot{q}_4 \\ \ddot{q}_5 \\ \ddot{q}_6 \\ \ddot{q}_7 \\ \ddot{q}_8 \end{Bmatrix} \quad (3.78)$$

In general one can write the equation (3.78) as in the form of equation (3.42). Differentiating equation (3.38) with respect to generalized co-ordinate one can get equation (3.43). Equation (3.45) can be written for generalized force but with shape function that correspond to higher-order finite element.

3.6 Analysis using Rayleigh-Ritz method

There exist no exact solutions for the natural frequency, mode shape and forced response for many systems. Even when they exist they are often cumbersome to use, often requiring solution for transcendental equations to determine the natural frequency and subsequent evaluation of infinite series to evaluate the system response. For these reasons, approximate solutions such as the Galerkin method, and the Rayleigh-Ritz method were developed using variational principles. In this thesis, Rayleigh-Ritz method is used to find the natural frequency and forced response of laminated composite beam.

Rayleigh-Ritz method is the extension of Rayleigh's method that provides a means of obtaining a more accurate value for the fundamental frequency as well as approximations to the high frequencies and mode shapes. In this method single shape function is replaced by a series of shape functions multiplied by constant co-efficients. The success of the method depends on the choice of the shape functions that should satisfy the geometric boundary conditions [56].

3.6.1 Energy formulation based on Rayleigh-Ritz method

In this section, the formulations based on Rayleigh-Ritz method for uniform-thickness and tapered composite beams are derived using the classical laminate theory. The potential energy of an elastic solid written in Cartesian co-ordinate is given by equation (3.9). Taking into account the basic assumptions of pure bending of a beam and classical lamination theory, the potential energy can be simplified as given by equation (3.20). The approximate solution is given by single summation series [58].

$$w(x,t) = \sum_{i=1}^n c_i \varphi_i e^{i\omega t} \quad (3.79)$$

where c_i is the undetermined co-efficient, t refers to time, ω is the natural frequency of vibration and φ_i is the shape or trial function which should be determined by satisfying the geometric boundary conditions.

Substituting the approximation expression for the deflection into potential energy equation (3.20) one gets

$$U = \frac{1}{2} \int bD_{11} \frac{d^2 \left(\sum_{i=1}^n c_i \varphi_i e^{i\omega t} \right)}{dx^2} \frac{d^2 \left(\sum_{j=1}^n c_j \varphi_j e^{i\omega t} \right)}{dx^2} dx \quad (3.80)$$

$$U = \frac{1}{2} \sum_{i=1}^n \sum_{j=1}^n \int bD_{11} \frac{d^2(c_i \varphi_i) e^{i\omega t}}{dx^2} \frac{d^2(c_j \varphi_j) e^{i\omega t}}{dx^2} dx \quad (3.81)$$

$$U = \frac{1}{2} \sum_{i=1}^n \sum_{j=1}^n \int bD_{11} c_i c_j e^{2i\omega t} \frac{d^2 \varphi_i}{dx^2} \frac{d^2 \varphi_j}{dx^2} dx \quad (3.82)$$

The kinetic energy T , of an elastic body in terms of the xyz co-ordinate system can be written as equation (3.34). Now in the case of pure bending based on the classical laminate theory, considering that the rotary inertia terms are negligible, which means ignoring the first term of equation (3.35) leads to the kinetic energy as equation (3.36). Substituting the expression for the deflection into equation (3.36), kinetic energy is expressed as,

$$T = \frac{1}{2} \iint \rho b \left[\frac{\partial(w(x,t))}{\partial t} \right]^2 dx dz \quad (3.83)$$

$$T = \frac{1}{2} \int \rho A \frac{\partial w_i}{\partial t} \frac{\partial w_j}{\partial t} dx \quad (3.84)$$

$$T = \frac{1}{2} \sum_{i=1}^n \sum_{j=1}^n \int \rho A \frac{\partial((c_i \varphi_i) e^{i\omega t})}{\partial t} \frac{\partial((c_j \varphi_j) e^{i\omega t})}{\partial t} dx \quad (3.85)$$

$$T = -\omega^2 \frac{1}{2} \sum_{i=1}^n \sum_{j=1}^n \int \rho A c_i c_j \varphi_i \varphi_j e^{2i\omega t} dx \quad (3.86)$$

The work done by external transverse force F applied at $x = x_0$ is

$$W_f = F \times w(x_0) \quad (3.87)$$

$$W_f = F_0 e^{i\omega t} \times \sum_{i=1}^n \varphi_{i(x=x_0)} c_i e^{i\omega t} \quad (3.88)$$

$$W = \sum_{i=1}^n F_0 \varphi_{i(x=x_0)} e^{2i\omega t} c_i \quad (3.89)$$

The total potential energy is given by

$$\Pi = (U - W + T) \quad (3.90)$$

Substituting the equations (3.82), (3.86) and (3.89) in equation (3.90) and using the principle of minimum potential energy leads to a minimization problem relative to undetermined coefficients.

$$\begin{aligned} \Pi = & \frac{1}{2} \sum_{i=1}^n \sum_{j=1}^n \int bD_{11} c_i c_j e^{2i\omega t} \frac{d^2 \varphi_i}{dx^2} \frac{d^2 \varphi_j}{dx^2} dx - \sum_{i=1}^n F_0 \varphi_{i(x=x_0)} e^{2i\omega t} c_i \\ & - \omega^2 \frac{1}{2} \sum_{i=1}^n \sum_{j=1}^n \int \rho A c_i c_j \varphi_i \varphi_j e^{2i\omega t} dx \end{aligned} \quad (3.91)$$

One can impose the stationary conditions:

$$\frac{\partial \Pi}{\partial c_i} = 0 \quad (3.92)$$

This leads to

$$\sum_{i=1}^n \sum_{j=1}^n \left(\int bD_{11} \frac{d^2 \varphi_i}{dx^2} \frac{d^2 \varphi_j}{dx^2} dx \right) c_j - \omega^2 \sum_{i=1}^n \sum_{j=1}^n \left(\int \rho A \varphi_i \varphi_j dx \right) c_j = \sum_{i=1}^n F_0 \varphi_{i(x=x_0)} \quad (3.93)$$

From the above formulation, one can get a set of n linear simultaneous equations that can be used for free and force vibration analysis.

3.6.4 Trial functions for different boundary conditions

a. Trial function for simply supported beam

In the case of a beam of length, L that is simply supported at two ends, the boundary conditions are

$$w_{(x=0)} = 0 \text{ and } w_{(x=l)} = 0 \text{ but } \frac{dw}{dx}_{(x=0)} \neq 0 \text{ and } \frac{dw}{dx}_{(x=l)} \neq 0 \quad (3.94)$$

The boundary conditions are satisfied by the trial functions of equation (3.79).

$$\text{where trial function } \varphi_r(x) = (L-x) \sin \frac{r\pi x}{2L}, \quad r = 1, 2, 3, 4, \dots \quad (3.95)$$

b. Trial function for cantilever beam

In the case of a beam of length, L that is fixed at one end and free at the other end, the boundary conditions are

$$w_{(x=0)} = 0 \text{ and } w_{(x=l)} \neq 0 \text{ but } \frac{\partial w}{\partial x}_{(x=0)} = 0 \text{ and } \frac{\partial w}{\partial x}_{(x=l)} \neq 0 \quad (3.96)$$

The boundary conditions are satisfied by the trial functions of equation (3.79).

$$\text{where trial function } \varphi_i(x) = x \sin \frac{r\pi x}{4L}, \quad r = 1, 2, 3, 4, \dots \quad (3.97)$$

c. Trial function for clamped–clamped beam

In the case of a beam of length, L that is clamped at the two ends, the boundary conditions are:

$$w_{(x=0)} = 0 \text{ and } w_{(x=l)} = 0 ; \frac{\partial w}{\partial x}_{(x=0)} = 0 \text{ and } \frac{\partial w}{\partial x}_{(x=l)} = 0 \quad (3.98)$$

The boundary conditions are satisfied by trial functions of equation (3.79).

$$\text{where trial function } \varphi_i(x) = rx^{(r+1)}(L-x)^2, r = 1, 2, 3, 4, \dots \quad (3.99)$$

3.7 Vibration analysis of composite beam

3.7.1 Free vibration analysis

All systems possessing mass and elasticity are capable of free vibration. In this work for the vibration analysis of composite beams, Lagrange's equation is used to derive the equation of motion. The Lagrange's equation is given as [56]

$$\frac{d}{dt} \left(\frac{\partial T}{\partial \dot{q}_i} \right) - \frac{\partial T}{\partial q_i} + \frac{\partial U}{\partial q_i} = Q_i \quad (3.100)$$

Substituting for different terms, $\left\{ \frac{d}{dt} \left(\frac{\partial T}{\partial \dot{q}_i} \right) \right\} = [M] \{ \ddot{q} \}$, $\frac{\partial T}{\partial q_i} = 0$ and $\frac{\partial U}{\partial q_i} = [K] \{ q \}$ from

equations (3.32), (3.42) and (3.43) (equations (3.74) and (3.78) for higher-order finite

element) and generalized force equal to zero), of Lagrange's equation, equation (3.100) changes to

$$[M]\{\dot{w}\} + [K]\{w\} = \{0\} \quad (3.101)$$

where, $[M]$, $[K]$, $\{w\}$ are the mass matrix, stiffness matrix and displacement matrix respectively. To find the natural motion of a structure, the form of response or solution can be assumed as

$$\{w(t)\} = \{Z\} e^{i\omega t} \quad (3.102)$$

where $\{Z\}$ is the mode shape (eigen) vector and ω is the natural frequency of the motion.

The general solution is a linear combination of each mode:

$$\{w(t)\} = a_1 \{Z_1\} e^{i\omega_1 t} + a_2 \{Z_2\} e^{i\omega_2 t} + a_3 \{Z_3\} e^{i\omega_3 t} + \dots + a_n \{Z_n\} e^{i\omega_n t} \quad (3.103)$$

where each constant (a_i) can be evaluated from the initial conditions. Substituting equation (3.103) into equation (3.101) yields

$$([K] - \omega^2 [M])\{Z\} e^{i\omega t} = 0 \quad (3.104)$$

The above equation has a nontrivial solution if $\|[K] - \omega^2 [M]\|$ becomes singular. In other words, there exist n number of ω^2 ($\omega_1^2, \omega_2^2, \dots, \omega_n^2$) which satisfy the following equation:

$$\|[K] - \lambda [M]\|\{Z\} = \{0\} \quad (3.105)$$

where $\lambda = \omega^2$ is the eigen value of the system.

In the following section, a set of problems has been solved for free vibration of different types of composite beam. Comparisons with existing results and the results obtained in the present work using exact solution, conventional finite element, higher-order finite element and Rayleigh-Ritz formulation are presented in tables. All the data used in the examples are in SI unit.

3.7.1.1 Natural frequencies of uniform-thickness composite beam calculated by using different finite elements

Example 3.7.1.1

The uniform-thickness composite beam is made of 36 plies NCT/301 graphite-epoxy material that is meshed with three, four and five equal length elements as shown in Figure 3.6. Mechanical properties of the NCT/301 graphite-epoxy material are: $E_1 = 113.9$ GPa, $E_2 = 7.98$ GPa, Poisson's ratio $\nu_{21} = 0.018$, $\nu_{12} = 0.288$, shear modulus $G_{12} = 3.138$ GPa, density $\rho = 1480$ kg/m³. Elastic modulus of epoxy resin (E_r) is equal to 3.902 GPa and Poisson's ratio (ν) is to be 0.37. The geometric properties of the beam are: length, L is 0.25 m; individual ply thickness (t_k) is 0.000125m, and width (b) is unity. Three types of boundary conditions such as simply supported, fixed-free (or cantilever) and fixed-fixed (both ends clamped) are applied. The first four lowest frequencies are calculated using closed form (exact) solution, conventional finite element, higher-order finite element, and Rayleigh-Ritz formulation and the results are compared with the results given in reference [29] in Tables 3.1 to 3.3.

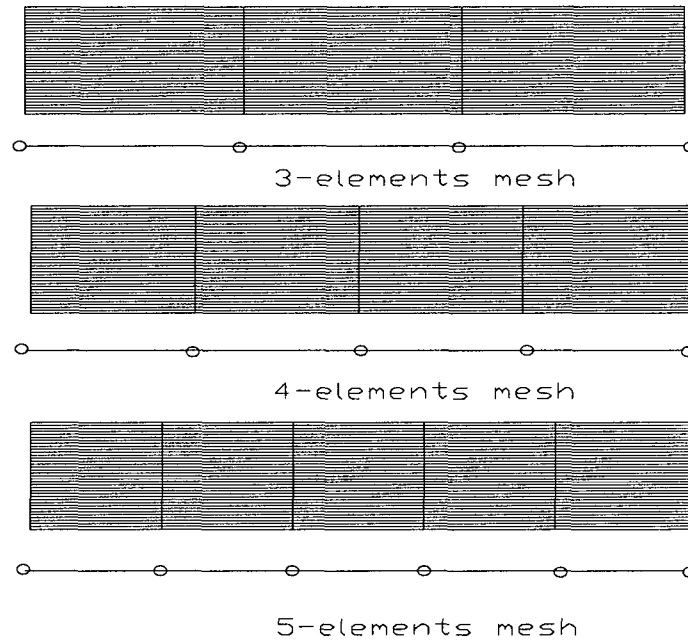


Figure 3. 6 Uniform-thickness composite laminated beam with different meshes

Table 3. 1 Comparison of natural frequencies ($\times 10^3$ rad/sec) of uniform-thickness beam for simply supported boundary condition

Method	Mode-1	Mode-2	Mode-3	Mode-4
Exact solution	1.366	5.466	12.300	21.867
CFE (3-E)	1.367	5.529	13.646	25.374
CFE (4-E)	1.366	5.486	12.519	24.260
CFE (5-E)	1.366	5.473	12.392	22.361
HOFE (3-E)	1.366	5.466	12.300	21.867
HOFE (4-E)	1.366	5.466	12.300	21.867
HOFE (5-E)	1.366	5.466	12.300	21.867
Rayleigh-Ritz (6-T)	1.390	5.495	12.346	21.959
Rayleigh-Ritz (7-T)	1.386	5.490	12.332	21.932
Rayleigh-Ritz (8-T)	1.384	5.486	12.325	21.604
Exact solution Ref[29]	1.366	5.466	12.300	
CEF-3E Ref [29]	1.368	5.531	13.652	

In Table 3.1 and in all tables that follows CFE stands for conventional finite element, HOFE stands for higher-order finite element, n-E stands for number of element, and n-T stands for number of terms used in trial function of Rayleigh-Ritz method.

Table 3. 2 Comparison of natural frequencies ($\times 10^3$ rad/sec) of uniform-thickness beam for fixed-free boundary condition

Method	Mode-1	Mode-2	Mode-3	Mode-4
Exact solution	0.486	3.051	8.544	
CFE (3-E)	0.486	3.059	8.646	19.471
CFE (4-E)	0.486	3.053	8.606	16.977
CFE (5-E)	0.486	3.051	8.570	16.931
HOFE (3-E)	0.486	3.051	8.543	16.741
HOFE (4-E)	0.486	3.051	8.543	16.741
HOFE (5-E)	0.486	3.051	8.543	16.741
Rayleigh-Ritz (6-T)	0.487	3.068	8.695	18.202
Rayleigh-Ritz (7-T)	0.487	3.061	8.628	17.208
Rayleigh-Ritz (8-T)	0.486	3.058	8.589	14.944
Exact solution Ref[29]	0.486	3.051	8.543	
CEF-3E Ref [29]	0.487	3.061	8.650	

Table 3. 3 Comparison of natural frequencies ($X 10^3$ rad/sec) of uniform-thickness beam for fixed-fixed boundary condition

Method	Mode-1	Mode-2	Mode-3	Mode-4
Exact solution	3.100	8.539	16.743	
CFE (3-E)	3.109	8.707	20.251	40.24
CFE (4-E)	3.101	8.615	17.092	32.337
CFE (5-E)	3.098	8.570	16.966	28.267
HOFE (3-E)	3.098	8.540	16.742	27.675
HOFE (4-E)	3.098	8.540	16.742	27.675
HOFE (5-E)	3.098	8.540	16.742	27.675
Rayleigh-Ritz (6-T)	3.098	8.540	16.773	27.850
Rayleigh-Ritz (7-T)	3.098	8.540	16.742	27.850
Rayleigh-Ritz (8-T)	3.098	8.540	16.742	27.679
Exact solution Ref[29]	3.100	8.539	16.743	
CEF-3E Ref [29]	3.111	8.711	20.259	

From the Tables 3.1 to 3.3, it is observed that natural frequencies for conventional finite element, higher-order finite element and Rayleigh-Ritz formulation of uniform-thickness beam with three different boundary conditions are converging well which means percentage of difference is negligible. Comparison among the boundary conditions shows that first four lowest natural frequencies with fixed-fixed boundary condition are highest in values where first four lowest natural frequencies with fixed-free condition are lowest in values.

3.7.1.2 Natural frequencies of Beam with taper configuration-B formed from uniform-thickness beam by ply drop-off

Example 3.7.1.2

A beam with the same data as that of example 3.7.1.2 but with sets of plies drop-off is solved to investigate the effects on frequencies. Beam of taper configuration-B is formed from uniform-thickness beam as shown in Figure 3.7. The beam is made of 36 plies at thick section and after dropping off 6, 8 and 10 plies; it ends with 30, 28 and 26 plies respectively at thin section. Since the total length is kept constant, therefore drop off plies result in increasing the taper angle that is adjusted by thickness ratio. The tapered section of beam is meshed with three, four and five equal length elements resulting from drop-off of 6, 8 and 10 plies respectively.

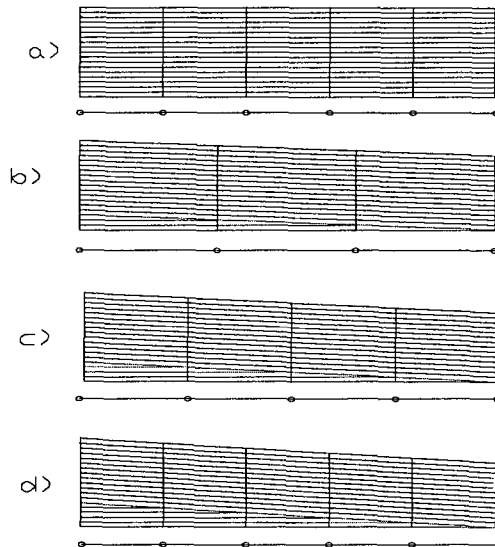


Figure 3. 7 a) Uniform-thickness beam with 5-elements mesh b) Taper configuration –B beam with 3-elements mesh c) Taper configuration –B beam with 4-elements mesh d) Taper configuration –B beam with 5-elements mesh; in figures a-d, only the top half of beam is shown

Ply drop-off occurs consistently from top to bottom in a staircase arrangement. Dropped-off plies are replaced by resin pocket. By using the mechanical properties described in example 3.7.1.1, the example 3.7.1.2 is solved to find the natural frequencies for simply supported, fixed-free and fixed-fixed boundary conditions. The results are obtained for uniform-thickness beam with 36-ply using exact (closed form) solution and beam with taper configuration-B of different number of ply drop-off using higher-order finite element. First four lowest frequencies for all boundary conditions are presented in Tables 3.4 to 3.6.

Table 3. 4 Comparison of natural frequencies ($\times 10^3$ rad/sec) of beam with taper configuration-B with simply supported boundary condition

Method	Mode-1	Mode-2	Mode-3	Mode-4
Exact solution (UTB)	1.366	5.466	12.300	21.867
HOFE (6-DOP)	1.348	5.587	11.249	
HOFE (8-DOP)	1.268	5.484	11.683	19.161
HOFE (10-DOP)	1.209	5.188	11.975	19.459

Table 3. 5 Comparison of natural frequencies ($\times 10^3$ rad/sec) of beam with taper configuration-B for fixed-free boundary condition

Method	Mode-1	Mode-2	Mode-3	Mode-4
Exact solution (UTB)	0.486	3.051	8.544	
HOFE (6-DOP)	0.463	2.536	6.520	13.638
HOFE (8-DOP)	0.480	2.637	7.052	16.752
HOFE (10-DOP)	0.498	2.662	7.162	20.741

In Tables 3.4-3.6 UTB denotes uniform-thickness beam, HOFE denotes higher-order finite element and n-DOP denotes number of drop-off plies.

Table 3. 6 Comparison of natural frequencies ($X 10^3$ rad/sec) of beam with taper configuration-B for fixed-fixed boundary condition

Method	Mode-1	Mode-2	Mode-3	Mode-4
Exact solution (UTB)	3.100	8.539	16.743	
HOFE (6-DOP)	2.921	7.984	14.458	22.445
HOFE (8-DOP)	2.845	7.907	13.427	22.627
HOFE (10-DOP)	2.742	7.846	12.850	21.310

From the above Tables 3.4 to 3.6, one can see that, natural frequencies obtained using higher-order finite element with three different boundary conditions for beam with taper configuration-B are decreasing with the increasing of number of plies drop-off from uniform-thickness beam. Comparison among the boundary conditions shows that natural frequencies with fixed-fixed boundary condition are highest where natural frequencies with fixed-free condition are lowest.

3.7.2 Forced vibration analysis

The forced vibration response with reference to discrete number of nodal coordinates of the composite beam is determined in this section. These coordinate are the translational displacement and rotation defined at the nodes of the finite elements of the beam. Lagrange's equation is used to get the equation of motion. The equations of motion for a linear system without considering the damping effects can be written as

$$[M]\{\ddot{w}\} + [K]\{w\} = \{F\} \quad (3.106)$$

$[M]$, $[K]$, $\{F\}$ and $\{w\}$ are respectively mass matrix, stiffness matrix, force matrix and displacement matrix of beam. Mode superposition method is considered for forced vibration of composite beam in this thesis. By making the co-ordinate transformation, one can write,

$$\{w\}=[\tilde{P}]\{y\} \quad (3.107)$$

where \tilde{P} denotes orthonormal modal matrix. Substituting equation (3.107) and pre-multiplying by \tilde{P}^T on both side of equation (3.106), leads to

$$[\tilde{P}]^T[M][\tilde{P}]\{\ddot{y}\}+[\tilde{P}]^T[K][\tilde{P}]\{y\}=[\tilde{P}]^T\{F\} \quad (3.108)$$

The normal modes or the eigenvectors of the system can be shown to be orthogonal with respect to the mass and stiffness matrices [56]. By taking the advantages of this property, equation (3.108) can be written as decoupled 2nd order differential equation.

$$\{\ddot{y}\}_i + \text{diag}(\lambda)_i \{y\}_i = \{f_i\} \quad (3.109)$$

which is a second order of differential equation, can be solved as single degree of freedom of forced vibration response.

$$y_i = y_i(0) \cos \omega_i t + \frac{\dot{y}(0) \sin \omega_i t}{\omega_i} + \frac{f_i \sin \omega t}{\omega_i^2 - \omega^2} \quad (3.110)$$

Substituting the value of y form equation (3.110) in equation (3.107), one can get forced vibration response.

In the following section, a set of problems has been solved for forced vibration of composite beam. Results are compared with using conventional and higher-order finite elements and Rayleigh-Ritz (approximation) method. All the data used in the examples are in SI unit system.

3.7.2.1 Forced response of uniform-thickness beam calculated using different finite elements

Example 3.7.2.1

The example 3.7.1.1 that is already used to find the natural frequencies is taken to conduct forced response analysis in terms of transverse displacement and rotation of beam at the free end of uniform-thickness beam as shown in Figure 3.6. The beam is meshed into five elements for analysis. The ply of composite beam is made of NCT/301 graphite-epoxy material whose mechanical and physical properties are used to find the stiffness and mass matrices. A sinusoidal force of magnitude 2 N and a sinusoidal moment of magnitude 2 N-m with excitation frequency ω are applied at free end of cantilever beam. The forced response in terms of the magnitude of sinusoidal transverse displacement and the magnitude of sinusoidal rotation are observed for different values of excitation frequency ratio to first natural frequency (ω_{1n} is 0.0486×10^4 rad/sec) in Figures 3.8 and 3.9.

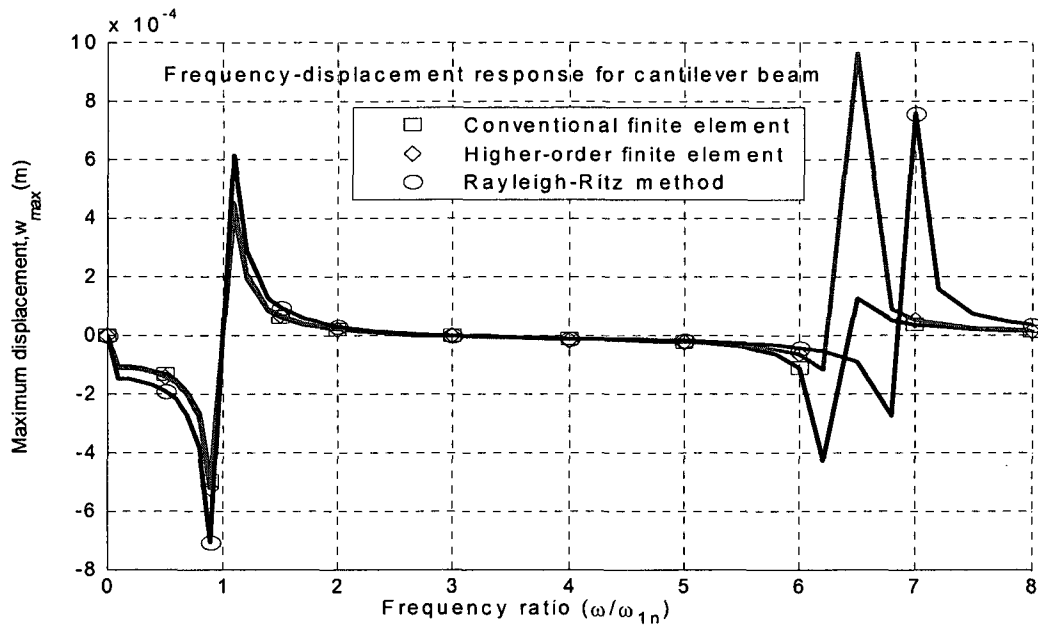


Figure 3. 8 Frequency-displacement plot of uniform-thickness composite beam with fixed-free boundary condition

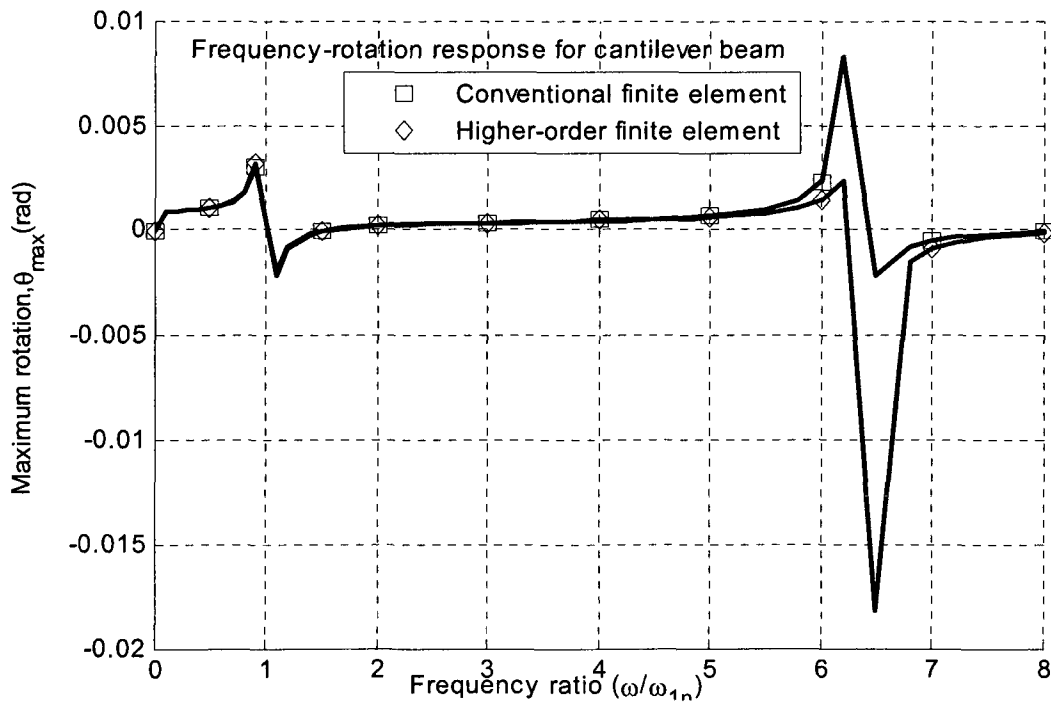


Figure 3. 9 Frequency-rotation plot of uniform-thickness composite beam with fixed-free boundary condition

From the Figures 3.8 and 3.9, one can see that forced response in terms of transverse displacement and rotation for different frequency ratio values for conventional finite element, higher-order finite element and Rayleigh-Ritz formulation of uniform-thickness beam with fixed-free boundary condition are converging well. One can observe that transverse displacement and rotation for fixed-free boundary condition is highest where excitation frequency nears the natural frequency.

3.7.2.2 Forced response of beam with taper configuration-B formed from uniform-thickness beam by ply drop-off

Example 3.7.2.2

Example 3.7.2.2 is solved to investigate the effects on forced response of beam with taper configuration-B that is formed from uniform-thickness beam by ply drop-off as shown in Figure 3.7. The beam is made of 36 plies in thick section and after dropping off 6, 8 and 10 plies, it ends with 30, 28 and 26 plies in thin section respectively. The beam is meshed into three, four and five elements for analysis, plies drop-off occur consistently from top to bottom. Dropped-off plies are replaced by resin pocket. The ply of composite beam is made of NCT/301 graphite-epoxy whose mechanical and physical properties are used to find the stiffness and mass matrices. A sinusoidal force of magnitude 2 N and a sinusoidal moment of magnitude 2 N-m with excitation frequency ω are applied at free end of cantilever beam. The forced response in terms of the magnitude of sinusoidal transverse displacement and the magnitude of sinusoidal rotation are observed for different values of excitation frequency ratio to first natural frequency shown in Figures 3.10 and 3.11.

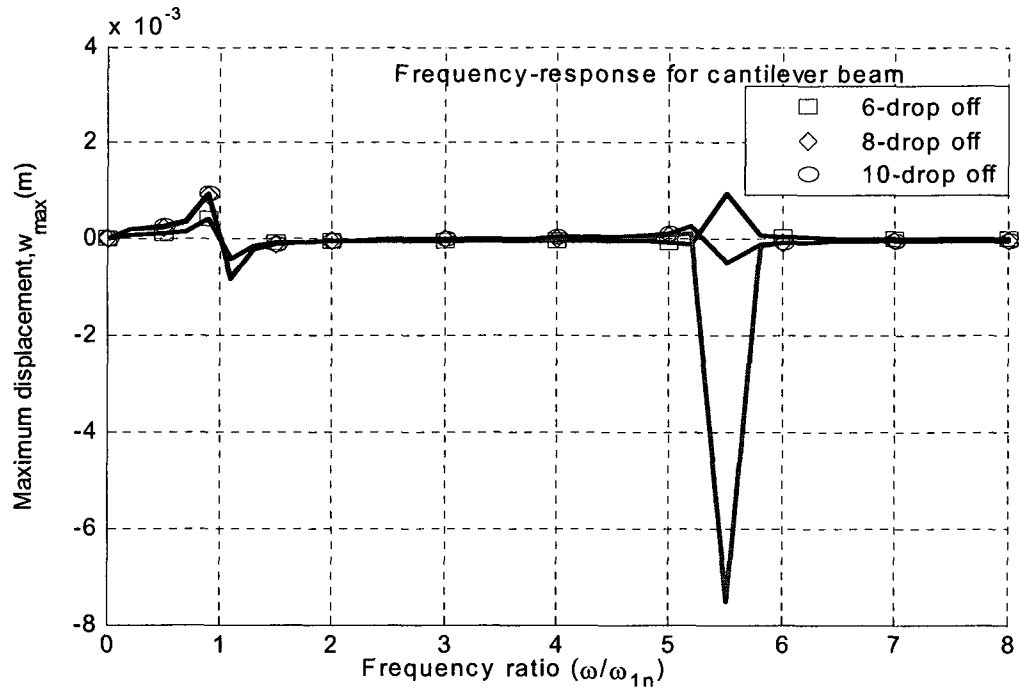


Figure 3. 10 Frequency-displacement plot of laminated beam with taper configuration-B

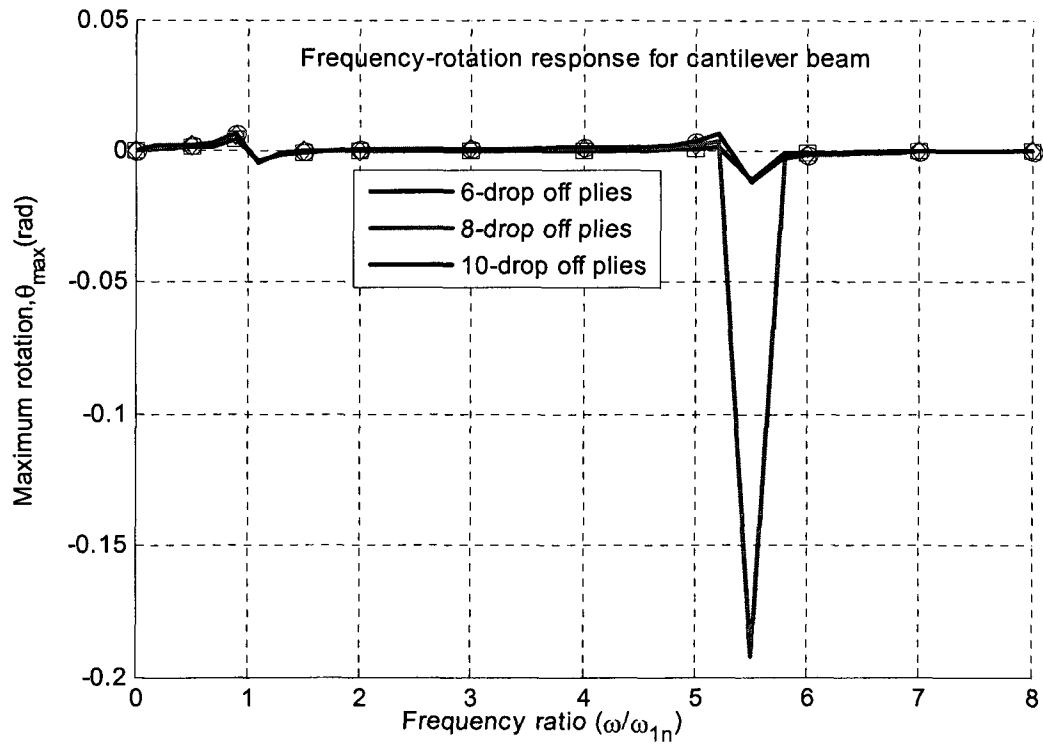


Figure 3. 11 Frequency-rotation plot of laminated beam with taper configuration-B

From the Figures 3.10 and 3.11, one can see that forced response in terms of transverse displacement and rotation obtained using higher-order finite element for fixed-free boundary condition for beam with taper configuration-B are increasing with the increasing of number of plies drop-off. One can also observe that transverse displacement and rotation for fixed-free boundary condition is highest when excitation frequency nears the natural frequency.

3.7.3 Vibration analysis considering damping properties

The definition of damping of composite materials is mostly based on the macroscopic response rather than the microscopic mechanisms governing the energy dissipation process [59]. To investigate the concept of an equivalent viscous damping mechanism for a multiple degree of freedom system that is damped by a non-viscous process, the finite element model given by equation (3.106) is augmented with a viscous term

$$[M]\{\ddot{q}\} + [C]\{\dot{q}\} + [K]\{q\} = \{F\} \quad (3.111)$$

where $[C]$ is a damping matrix.

The difficulty with modeling damping in this fashion is that modal analysis cannot in general be used to solve equation (3.111) because damping provides additional coupling between the equations of motion. As a result, this cannot be always decoupled by the modal transformation. Modal analysis can be used directly to solve equation (3.111), if the damping matrix $[C]$ can be written as a linear combination of the mass and stiffness matrices [60],

$$[C] = \alpha[M] + \beta[K] \quad (3.112)$$

where α and β are mass proportional constant and stiffness proportional constant respectively. Substitution of equation (3.112) into equation (3.111) yields

$$[M]\{\ddot{q}\} + (\alpha[M] + \beta[K])\{\dot{q}\} + [K]\{q\} = \{F\} \quad (3.113)$$

By taking the advantages of orthogonal properties, substituting equation (3.107) in equation (3.113) and pre-multiply \tilde{P}^T on both side of equation, equation (3.113) leads

$$[\tilde{p}]^T [M][\tilde{P}]\{\ddot{y}\} + [\tilde{P}]^T (\alpha[M] + \beta[K])[\tilde{P}]\{\dot{y}\} + [\tilde{P}]^T [K][\tilde{P}]\{y\} = [\tilde{P}]^T \{F\} \quad (3.114)$$

$$\{\ddot{y}\} + (\alpha[I] + \beta[\Lambda])\{\dot{y}\} + \Lambda\{y\} = \{f\} \quad (3.115)$$

where Λ stands for ω^2 .

This corresponds to the n decoupled modal equations

$$\ddot{y}_i + 2\zeta_i \omega_i \dot{y}_i + \omega_i^2 y_i = f_i \quad (3.116)$$

$$\text{where } 2\zeta_i \omega_i = \alpha + \beta \omega_i^2 \quad (3.117)$$

Considering the response of equation (3.116) as viscously damped single degree of freedom system subject to harmonic excitation, the solution of equation will be

$$y_i = e^{-\zeta_i \omega_i t} \left[\frac{\dot{y}(0) + \zeta_i \omega_i y(0)}{\omega_{di}} \sin \omega_{di} t + y(0) \cos \omega_{di} t \right] + \frac{f_0}{\sqrt{(\omega_{ni}^2 - \omega^2)^2 + (2\zeta_i \omega_{ni} \omega)^2}} \sin(\omega t - \tan^{-1} \frac{2\zeta_i \omega_n \omega}{\omega_{ni}^2 - \omega^2}) \quad (3.118)$$

$$\text{where } \omega_{di} = \omega_n \sqrt{1 - \zeta_i^2} \quad (3.119)$$

Substituting the value of y form equation (3.118) in equation (3.107), one can get forced vibration response with damping effects.

Next a set of problems has been solved for free and forced vibration of uniform-thickness composite beams without and with considering damping loss properties. The results are obtained considering higher-order finite element. Results are compared with Rayleigh-Ritz method.

3.7.3.1 Natural frequencies of uniform-thickness beam without and with damping effect

Example 3.7.3.1

The common example which is already used to find the natural frequency and force response without considering damping loss properties, is taken to solve for free and forced response considering damping properties of (example 3.7.3.1) for uniform-thickness beam as shown in Figure 3.6. The beam is meshed into five elements for analysis. The ply of composite beam is made of NCT/301 graphite-epoxy whose mechanical and physical properties are used to find the stiffness and mass matrices. The mass proportional constant and stiffness proportional constant those are found by modal testing experiment (described in chapter-2) are 2.195 and 2.6085×10^{-6} respectively.

First four lowest frequencies for fixed-free boundary condition are obtained and compared with frequencies obtained without considering damping by using higher-order finite element and Rayleigh-Ritz method.

Table 3. 7 Comparison of un-damped and damped natural frequencies ($X 10^3$ rad/sec) of uniform-thickness beam with fixed-free boundary condition

	Mode-1	Mode-2	Mode-3	Mode-4
HOFE -UND (5-E)	0.486	3.051	8.543	16.741
HOFE -D (5-E)	0.486	3.044	8.495	16.557
Rayleigh-Ritz UND (7-T)	0.487	3.061	8.628	17.208
Rayleigh-Ritz-D(7-T)	0.486	3.055	8.579	17.014

UND denotes un-damped; D denotes damped; n-E denotes number of element; n-T denotes number of terms used in the trial function of Rayleigh-Ritz method. From the Table 3.7 one can see that, natural frequencies obtained considering the damping properties of materials for uniform-thickness beam in fixed-free boundary condition are less than the frequencies obtained without considering damping loss of composite materials. One can also see that natural frequencies for higher-order finite element and Rayleigh-Ritz formulation of uniform-thickness beam converge well.

3.7.3.2 Forced response of uniform-thickness beam without and with considering damping effect

Example 3.7.3.2

The common example which is already used to find the natural frequency and force response without considering damping loss properties, is taken to solve for free and forced response considering damping loss factor of (example 3.7.3.2) uniform-thickness beam as shown in Figure 3.6. The beam is meshed into five elements for analysis. The ply of

composite beam is made of NCT/301 graphite-epoxy material whose mechanical and physical properties are used to find the stiffness and mass matrices.

The mass proportional constant and stiffness proportional constant those are found by modal testing experiment (described in chapter-2) are 2.195 and 2.6085×10^{-6} respectively. A sinusoidal force of magnitude 2 N and a sinusoidal moment of magnitude 2 N-m with excitation frequency ω are applied at free end of cantilever beam. The forced response in terms of the magnitude of sinusoidal transverse displacement and the magnitude of sinusoidal rotation are observed for different values of excitation frequency ratio to first natural frequency (ω_{1n} is 0.0486×10^4 rad/sec) by using higher-order finite element and they are shown in Figures 3.12 and 3.13.

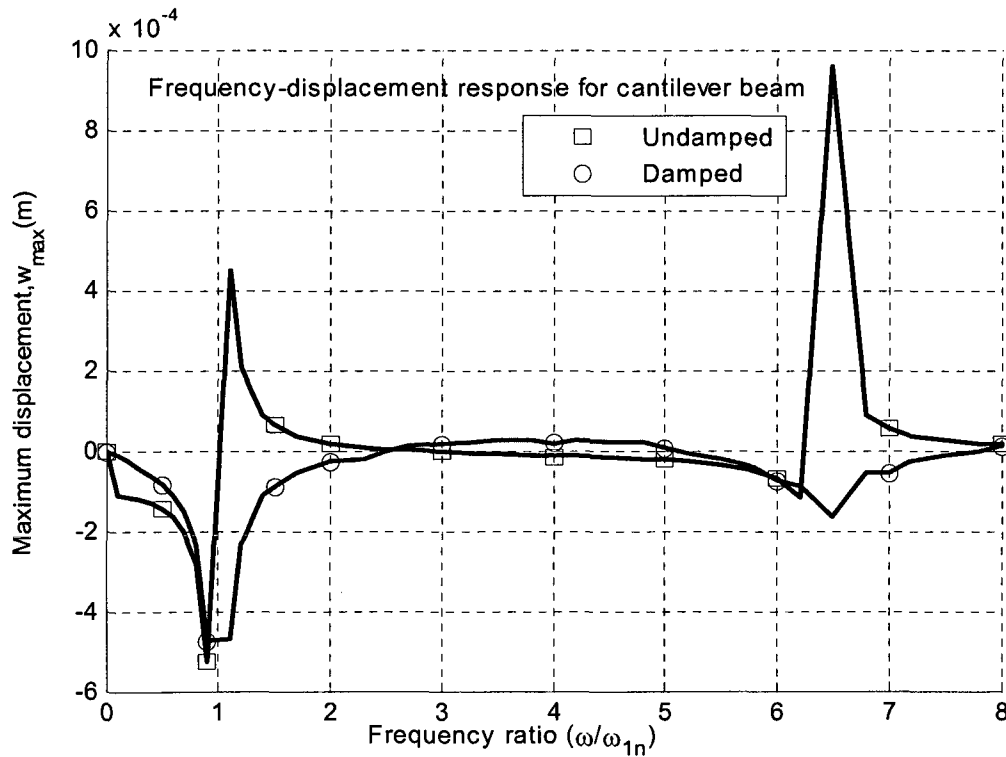


Figure 3. 12 Frequency-displacement plot of uniform-thickness composite beam

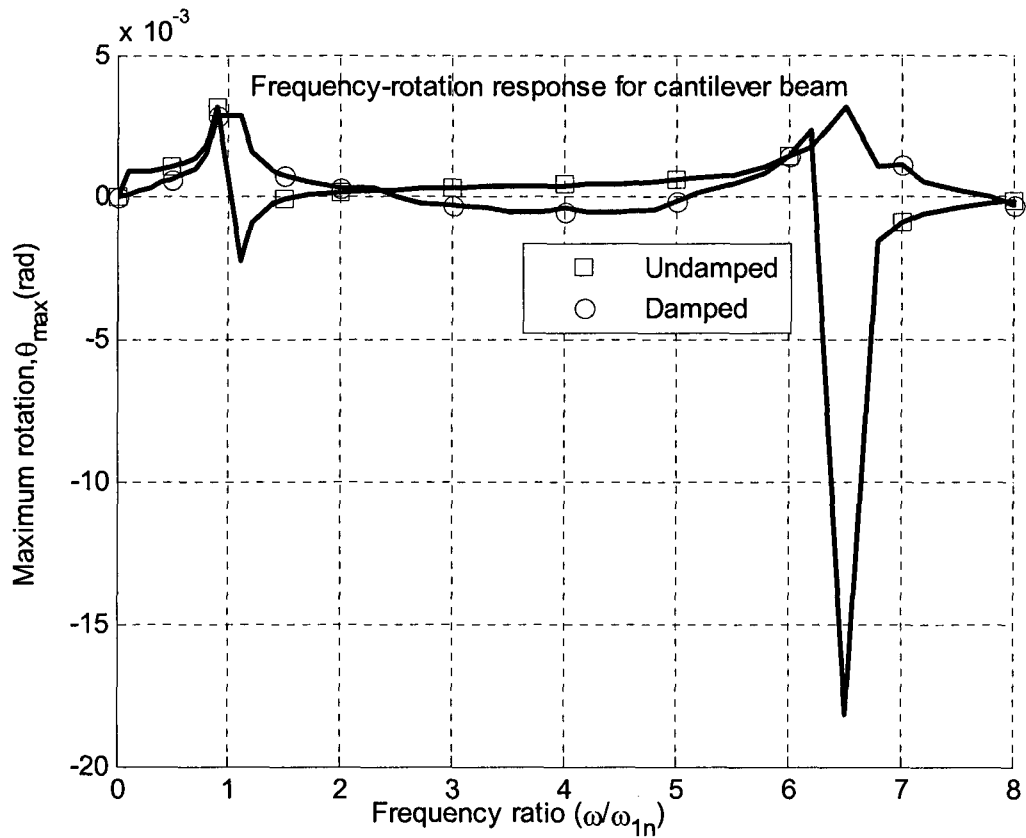


Figure 3. 13 Frequency-rotation plot of uniform-thickness composite beam

From the Figures 3.12 and 3.13, one can see that force response for transverse displacement and rotation obtained using higher order finite element in fixed-free boundary condition for uniform are increasing with the loss of damping of materials. One can observe that transverse displacement and rotation response for fixed-free boundary condition is almost flat after the first natural frequency.

3.8. Vibration analysis of composite beam including axial force effects

In the previous sections 3.3.3 and 3.5.3, the energy formulations of a composite beam for vibration analysis are derived based on classical laminate theory without considering any additional force acting on the beam. In this section, axial force acting on the beam that affects the vibration is considered. The axial force is considered acting as concentrated force at the ends and force distributed over of the beam as shown in Figure 3.14 and Figure 3.15 respectively. The energy formulations for free and forced vibration analysis of composite beam subjected to both concentrated and distributed axial force will be derived based on classical laminate theory of beam (Euler- Bernoulli beams).

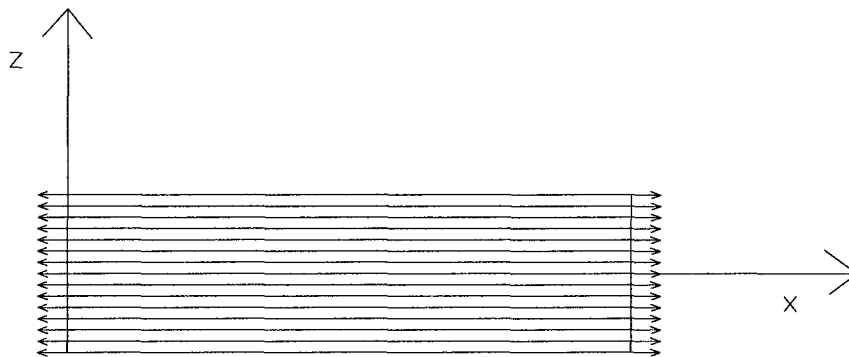


Figure 3. 14 Uniform-thickness composite beam subjected to end tensile load

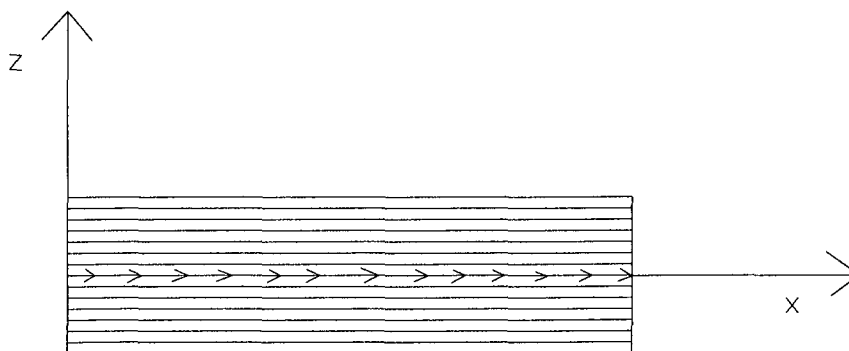


Figure 3. 15 Uniform-thickness composite beam subjected to distributed tensile load

3.8.1 Energy formulation including axial force effects

The potential energy of an elastic solid written in Cartesian co-ordinates is given by equation (3.9). Now when the actions exerted upon the composite laminate beam (transverse deformation) by in-plane loads is considered for energy formulation. The potential energy produced from the in plane loads N_x , N_y and N_{xy} due to a deflection w is [55],

$$U_a = \frac{1}{2} \int \int [N_x \left(\frac{\partial w}{\partial x}\right)^2 + 2N_{xy} \frac{\partial w}{\partial x} \frac{\partial w}{\partial y} + N_y \left(\frac{\partial w}{\partial y}\right)^2] dx dy \quad (3.120)$$

As this analysis is considered for beam, only N_x is acting on it. The potential energy due to end force can be reduced to

$$U_{ca} = \frac{1}{2} N_x \int \int \left[\left(\frac{\partial w}{\partial x}\right)^2\right] dx dy \quad (3.121)$$

$$U_{ca} = \frac{1}{2} N_x \int \left[b \left(\frac{\partial w}{\partial x}\right)^2\right] dx \quad (3.122)$$

The potential energy due to distributed axial load can be written as follows:

$$U_{da} = \frac{1}{2} \int \left[b N_x(x) \left(\frac{\partial w}{\partial x}\right)^2\right] dx \quad (3.123)$$

Taking into account the basic assumptions of pure bending of a beam and classical lamination theory, the total potential energy can be simplified including distributed and concentrated axial loads. So the total potential energy equation leads to

$$U_T = U + U_{ca} + U_{da} \quad (3.124)$$

$$U_T = \frac{1}{2} \int_x b D_{11} \left(\frac{\partial^2 w}{\partial x^2}\right)_{xp} dx + \frac{1}{2} N_x \int \left[b \left(\frac{\partial w}{\partial x}\right)^2\right] dx + \frac{1}{2} \int \left[b N_x(x) \left(\frac{\partial w}{\partial x}\right)^2\right] dx \quad (3.125)$$

Now differentiating the total potential energy with respect to generalized co-ordinate, one can get,

$$\frac{\partial U_T}{\partial q_i} = K_{ij}q_j + K_{ijca}q_j + K_{ijda}q_j \quad (3.126)$$

The kinetic energy T can be written as same as equation (3.39) that for a beam subjected to pure bending without axial force. Partially differentiating equation (3.39) with respect to \dot{q} and then differentiating the whole term with respect to time t , one can obtain equation (3.42). Differentiating equation (3.39) with respect to generalized co-ordinate one can get (3.43). Substituting equations (3.126), (3.42), (3.43), and (3.45) into equation (3.100), one can get an equation like equation (3.106) which can be solved for natural frequencies and forced response.

A couple of problems have been solved for free and forced vibration of uniform-thickness composite beams without and with considering axial force (tensile and compressive). The results are obtained considering higher-order finite element.

3.8.2.1 Free vibration of uniform-thickness composite beam including axial force effects

Example 3.8.2.1

The common example 3.7.1.1 which is already used to find the natural frequency and force response without considering axial force acted on both ends of the beam as tensile or compressive, is taken to solve for free and forced response analysis considering damping loss factor of (example 3.8.2.1) uniform-thickness beam as shown in Figure 3.6. The beam is meshed into five elements for analysis.

The ply of composite beam is made of NCT/301 graphite-epoxy whose mechanical and physical properties are used to find the stiffness and mass matrices. Axial force 2000N/m applied at the ends of the beam is considered for both tensile and compressive condition that is much smaller than corresponding buckling loads. First four lowest frequencies for fixed-free boundary condition are obtained by using higher-order finite element and are compared with that obtained without end axial force for both tensile and compressive forces by higher-order finite element in Table 3.8.

Table 3. 8 Comparison of natural frequencies ($X 10^3$ rad/sec) obtained without and with axial force (tensile and compressive) of uniform-thickness composite beam for fixed-free boundary condition

	Mode-1	Mode-2	Mode-3	Mode-4
WOA	0.486	3.051	8.543	16.741
WAT	0.5302	3.1017	8.586	16.782
WAC	0.437	2.9996	8.499	16.7008

WOA denotes “without axial force”, WAT denotes “with axial tensile force” and WAC denotes with “axial compressive force”. From the Table 3.8 one can see that, natural frequencies obtained considering the additional end axial force acting at the end of uniform-thickness beam with fixed-free boundary condition are more or less than the frequencies obtained without considering any axial force. In addition, one can see that the tensile axial force applied at the ends of beam increases the frequency and the compressive axial force applied at the ends of beam decreases the frequency.

3.8.2.2 Forced vibration response of uniform-thickness composite beam subjected to static end axial force

Example 3.8.2.2

The common example 3.7.1.2 that is already used to find the force response without considering end axial force acting on both sides of the beam, is taken to solve (example 3.8.2.2) for force response including the effect of the axial force applied at the ends of uniform-thickness beam. The beam is meshed into five elements for analysis. The ply of composite beam is made of NCT/301 graphite-epoxy and resin whose mechanical and physical properties are used to find the stiffness and mass matrices. End axial force of 2000N/m is considered for both tensile and compressive condition. This force is far less than the critical buckling load of the beam.

A sinusoidal force of magnitude 2 N and a sinusoidal moment of magnitude 2 N-m with excitation frequency ω are applied at free end of cantilever beam. The forced response in terms of the magnitude of sinusoidal transverse displacement and the magnitude of sinusoidal rotation are observed for different values of excitation frequency ratio to first natural frequency (ω_{1n} is 0.0486×10^4 rad/sec) by using higher-order finite element and is shown in Figure 3.16 and Figure 3.17.

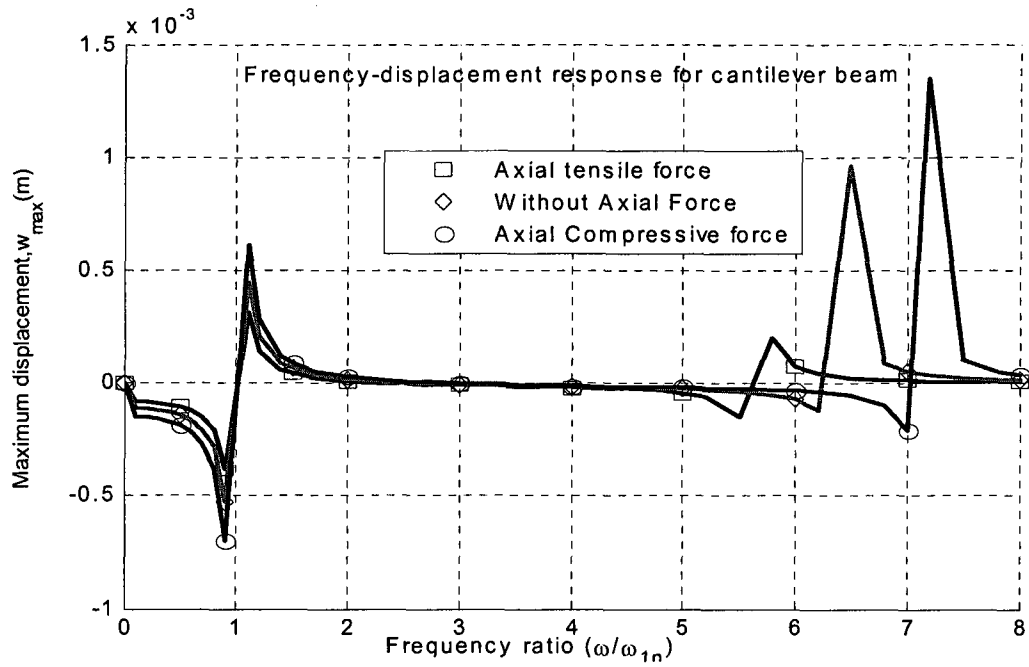


Figure 3. 16 Frequency-displacement plot of uniform-thickness composite beam

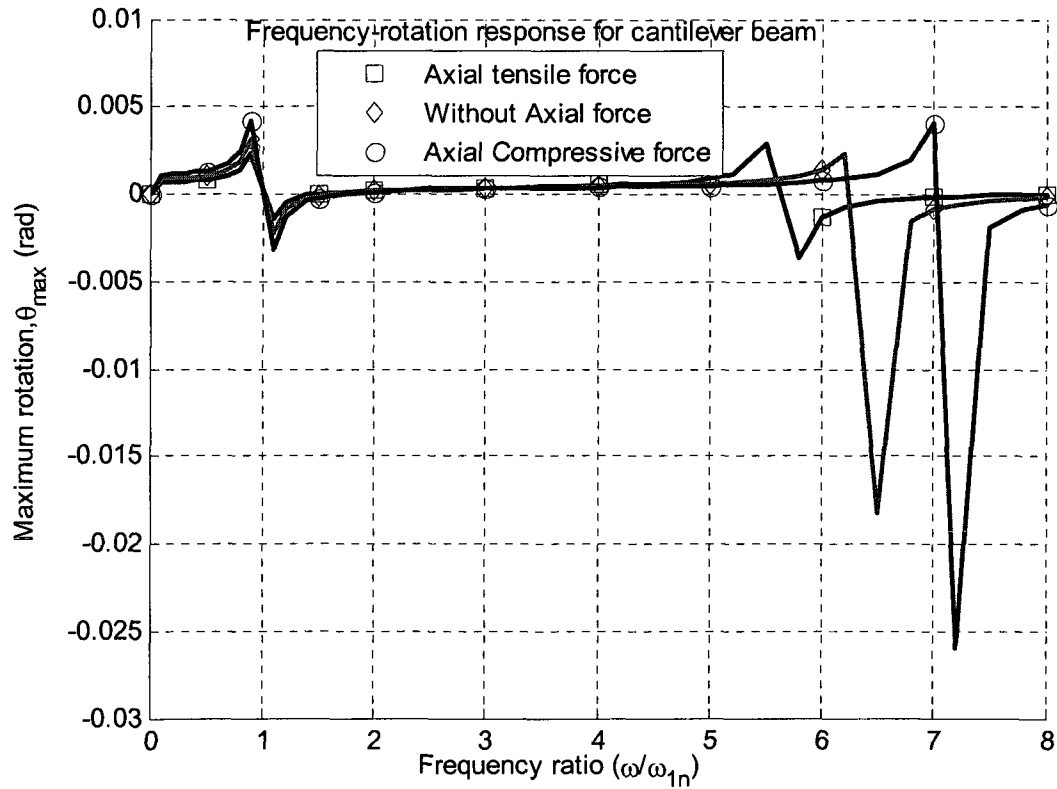


Figure 3. 17 Frequency-rotation plot of uniform-thickness composite beam

From the Figures 3.16 and 3.17, one can see that forced response in terms of transverse displacement and rotation obtained considering the additional end axial force acting at the end of uniform-thickness beam with fixed-free boundary condition are more or less than that obtained without considering any axial force. One can observe that when the tensile axial force applied at the ends of beams, transverse displacement and rotation are lowest and when the compressive axial force applied at the ends of beam, transverse displacement and rotation are highest.

3.9 Conclusions and Discussion

In this chapter, free and forced vibration analysis for different types of composite beam such as uniform-thickness beam and tapered composite beam have been carried out using conventional finite element, higher-order finite element and Rayleigh-Ritz method. Finite element formulation is developed based on energy method for Euler-Bernoulli's beam where Lagrange's equation is used to obtain the equations of motion. Energy formulation is described in detail in respective section to obtain the stiffness, mass and force matrices. Damping properties and axial force effects are considered to investigate the effects of these on natural frequencies and forced response. Then a set of examples is solved for every formulation to justify the formulation. The first four lowest natural frequencies and forced response (both transverse displacement and rotation) are obtained and presented in tables and graphs respectively for uniform-thickness and tapered composite beams.

By observing the results, we see the comparison of natural frequencies for conventional finite element, higher-order finite element and Rayleigh-Ritz formulation of uniform-thickness beam with three different boundary conditions and they were converging

well. Natural frequencies obtained for beam with taper configuration-B decrease with the increasing number of plies drop-off from that of uniform-thickness beam. Comparison among the boundary conditions shows that natural frequencies with fixed-fixed boundary condition are highest where natural frequencies with fixed-free condition are lowest.

Forced response in terms of transverse displacement and rotation are increasing with the decreasing of natural frequency and materials stiffness for both uniform- thickness beam and beam with taper configuration (resulting from plies drop-off from uniform-thickness beam).

The damped frequencies are found to be lower than the natural frequencies obtained considering un-damped case. Forced response in terms of transverse displacement and rotation are found to be less when considering damping.

Natural frequencies obtained considering the axial force acting at the end of uniform-thickness beam with fixed-free boundary condition are more for tensile axial force and less for compressive axial force than the frequencies obtained considering without any axial force.

Forced response in terms of transverse displacement and rotation obtained considering the axial compressive force acting at the end of uniform-thickness beam are more than the transverse displacement and rotation obtained without considering any axial force. Forced response in terms of transverse displacement and rotation obtained considering the axial tensile force acting at the end of uniform-thickness beam are less than the transverse displacement and rotation obtained without considering any axial force.

Chapter-4

Free vibration analysis of tapered composite beams

4.1 Introduction

Laminated beams having non-uniform configurations such as tapered and stepped are increasingly finding applications in modern industries. Therefore, there is a need for accurate prediction of dynamic response characteristics of such composite structures in order that they can be designed against failure due to dynamic loads.

In the previous chapter, the finite element modeling procedures and approximate method of analysis were established for uniform-thickness and mid-plane internally tapered composite beams. First, the conventional finite element formulation was developed in which the geometric boundary conditions (associated with essential boundary conditions) were considered in the interpolation functions. Second, the higher-order finite element formulation was developed which considers not only the geometric degrees of freedom, but also the generalized force boundary conditions (associated with natural boundary conditions) in the interpolation functions. Next, solution using Rayleigh-Ritz method was developed assuming the deflection to be a sum of several functions multiplied by constants. These developed formulations are employed for a comprehensive parametric study of free vibration of different types of tapered composite beams in this chapter.

The material chosen is NCT/301 graphite-epoxy that is available in the laboratory of Concordia center for composites. The properties of the material are given in all problems. The specifications of composite beam (ply orientations) and geometric properties (total number of plies in different sections, taper angle and length) are given in detail in individual

problems. Symmetric laminate is considered in all problems. As the beam is symmetric, only upper half of the beam properties are considered for vibration analysis.

The results are summarized in tables to interpret the results. Also a comparison is done with the help of plotting. Each subsection is ended with a short interpretation right after the problem. Finally, overall conclusions based on individual types of problems are provided that serve as factors to be considered in calculating the optimal results. These conclusions can guide the designer on the choice of different parameters involved in the analysis.

4.2 Effects of taper configuration on natural frequencies

The design of a tapered structure involves consideration of stiffness, static strength, dynamic stability and damage tolerance. For designing a tapered beam, laminate configuration, ply orientation and taper angle are major considerations. The beam will have a thick uniform section, a tapered section and a thin uniform section. The length of tapered section depends on the taper angle and usually is much smaller than the lengths of the other two sections. Different internal tapered beams (configuration-A, configuration-B, configuration-C and configuration-D) are formed in practice and they are considered for analysis of free vibration response. A set of problems is solved for vibration analysis of composite beams of different tapers. The problems are solved using conventional finite element, higher-order finite element and Rayleigh-Ritz method and compared. The results are summarized in tables and figures to interpret the results. All the data used in this thesis are in SI unit system.

4.2.1 Beam with taper configuration-A

Example 4.2.1

Beam with taper configuration-A as shown in Figure 4.1 is considered to solve the example 4.2.1. The beam is made of 36 plies at thick section and after dropping off 24 plies, it ends with 12 plies at thin section. The configuration of the thick section is $[0/90]_9$, and it is $[0/90]_{3s}$ at thin section. The beam is meshed into three, six and twelve elements of equal length for analysis, resulting from 4, 2, and 1 dropped-off plies in each element respectively. Though dropped-off plies are replaced by resin pocket, resin pocket is divided into imaginary layers with the same thickness of lamina. As these imaginary layers are not of same length, integration limits for different calculations are considered according to appropriate position of ending.

The ply of composite beam is made of NCT/301 graphite-epoxy material. Mechanical properties of the graphite-epoxy are: E_1 is 113.9 GPa, E_2 is 7.9856 GPa, Poisson's ratio ν_{21} is 0.0178, ν_{12} is 0.288, shear modulus G_{12} is 3.138 GPa, Density ρ is 1480 kg/m³. Elastic modulus of epoxy resin (E_r) is 3.902 GPa and Poisson's ratio (ν) is 0.37.

The geometric properties of the beam are: length L (m) is 0.0345 m (corresponding to fixed taper angle and beam thickness), individual ply thickness (t_k) is 0.000125m, width (b) is unity, and taper angle (ϕ) is 2.5°.

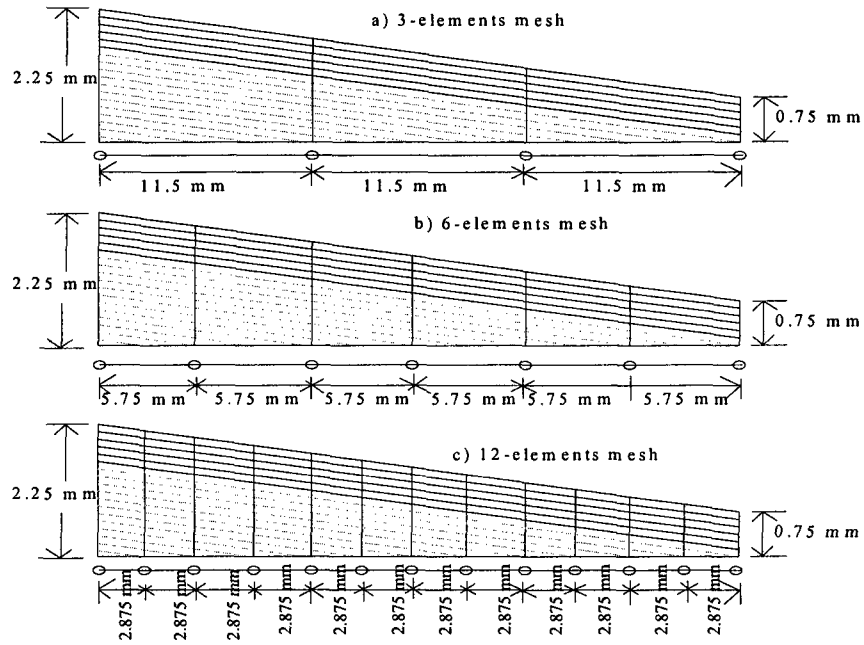


Figure 4. 1 Upper half of beam with taper configuration-A with a) 3- elements mesh, b) 6- elements mesh, and c) 12- elements mesh

By using the properties described in the above, the problem is solved to find the natural frequencies of taper configuration-A for simply supported, fixed-free and fixed-fixed boundary conditions. The first four lowest frequencies for all boundary conditions are compared and results are presented in Tables 4.1 - 4.3.

Table 4. 1 Comparison of natural frequencies ($\times 10^4$ rad/sec) of beam with taper configuration-A for simply supported boundary condition

	Mode No.	3-elements mesh	6-elements mesh	12-elements mesh
Conventional finite element	Mode-1	4.2858	4.2696	4.2681
	Mode-2	17.9550	17.5348	17.5022
	Mode-3	40.9420	39.4485	39.1829
	Mode-4	80.0459	70.8250	69.5000
Higher-order finite element	Mode-1	4.2623	4.2559	4.2527
	Mode-2	17.5370	17.4351	17.4172
	Mode-3	38.4039	39.0425	38.9803
	Mode-4	69.1892	69.2889	69.0901
		5-terms	6-terms	7-terms
Rayleigh-Ritz Method	Mode-1	4.2589	4.2446	4.2303
	Mode-2	16.7736	16.7278	16.7117
	Mode-3	37.4204	37.4096	37.3976
	Mode-4	73.4496	66.3725	66.3725

Table 4. 2 Comparison of natural frequencies ($\times 10^4$ rad/sec) of beam with taper configuration-A for fixed-free boundary condition

	Mode No.	3-elements mesh	6-elements mesh	12-elements mesh
Conventional finite element	Mode-1	2.5626	2.6199	2.6349
	Mode-2	11.2849	11.5311	11.6133
	Mode-3	29.4621	28.8551	29.0281
	Mode-4	59.2593	54.8650	54.9424
Higher-order finite element	Mode-1	2.5497	2.5998	2.6107
	Mode-2	11.2285	11.4748	11.5448
	Mode-3	28.6584	28.6951	28.8744
	Mode-4	53.5376	54.3627	54.6452
		5-terms	6-terms	7-terms
Rayleigh-Ritz Method	Mode-1	2.5180	2.5180	2.5180
	Mode-2	12.8986	12.8894	12.8869
	Mode-3	33.9266	33.9232	33.8926
	Mode-4	70.1266	65.3378	65.3366

Table 4. 3 Comparison of natural frequencies ($\times 10^4$ rad/sec) of beam with taper configuration-A for fixed-fixed boundary condition

	Mode No.	3-elements mesh	6-elements mesh	12-elements mesh
Conventional finite element	Mode-1	9.9982	9.7216	9.6971
	Mode-2	29.5688	27.0201	26.8546
	Mode-3	66.9271	53.5419	52.7769
	Mode-4	138.7700	90.2598	87.4195
Higher-order finite element	Mode-1	9.6736	9.6489	9.6383
	Mode-2	27.1137	26.7277	26.6999
	Mode-3	51.8179	52.5262	52.4559
	Mode-4	86.6127	87.1265	86.7977
		5-terms	6-terms	7-terms
Rayleigh-Ritz Method	Mode-1	9.7036	9.7035	9.7035
	Mode-2	26.660	26.6461	26.6453
	Mode-3	52.6338	52.2813	52.1488
	Mode-4	89.3744	88.4211	86.7458

From Tables 4.1-4.3, one can see that natural frequencies calculated using different finite elements for beam with taper configuration-A for all boundary conditions are converging well. Another important observation is that natural frequencies for fixed-free beam are lowest and for double clamped or fixed-fixed are highest for all modes respectively.

4.2.2 Beam with taper configuration-B

Example 4.2.2

Example 4.2.2 is solved for beam with taper configuration-B as shown in Figure 4.2. The beam is made of 36 plies at thick section and after dropping off 24 plies, it ends with 12 plies at thin section.

The beam is meshed into three, six and twelve elements of equal length for analysis, plies drop-off occur consistently from top to bottom in a staircase arrangement. Dropped-off plies are replaced by resin pocket; resin pocket is divided into imaginary layers in each element with the same thickness of lamina. Integration limits for different calculations are considered according to appropriate position of imaginary ply ending.

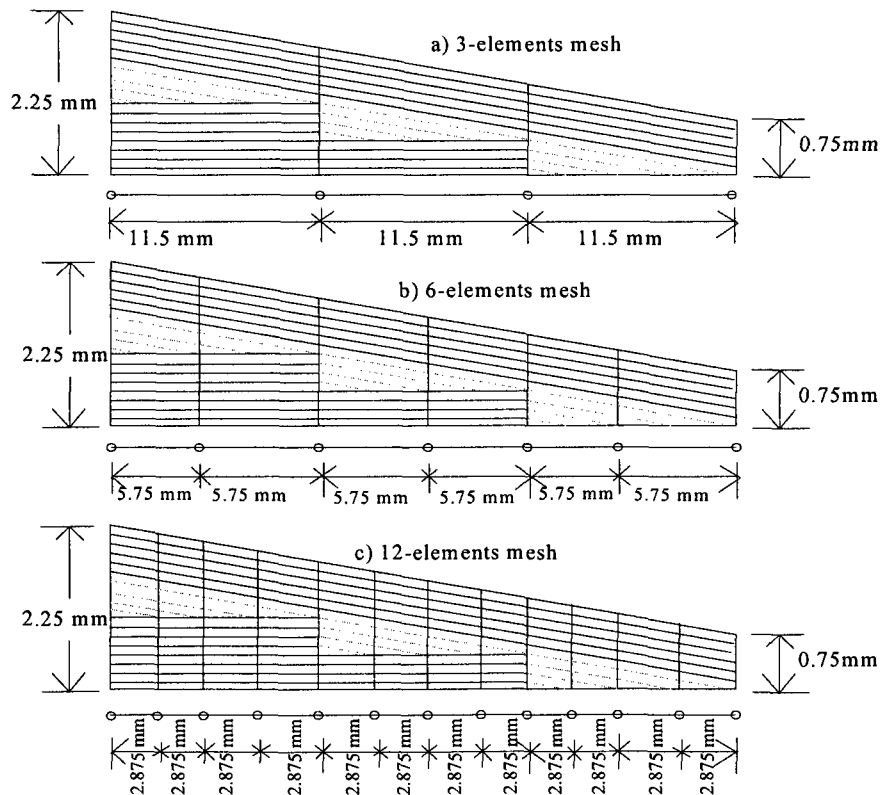


Figure 4. 2 Upper half of beam with taper configuration-B with a) 3- elements mesh, b) 6- elements mesh, and c) 12- elements mesh

By using the mechanical and geometric properties described in Example 4.2.1, the problem is solved to find the natural frequencies for simply supported, fixed-free and fixed-fixed boundary conditions. The results are presented in Tables 4.4- 4.6 and first four lowest frequencies for all boundary conditions are compared.

Table 4. 4 Comparison of natural frequencies ($\times 10^4$ rad/sec) of beam with taper configuration-B for simply supported boundary condition

	Mode No.	3-elements mesh	6-elements mesh	12-elements mesh
Conventional finite element	Mode-1	4.5620	4.5417	4.5403
	Mode-2	22.0237	20.5585	18.7760
	Mode-3	36.0830	51.8119	43.8864
	Mode-4	61.4687	95.5087	81.3516
Higher- order finite element	Mode-1	4.5157	4.5105	4.5306
	Mode-2	18.4262	18.2508	17.7351
	Mode-3	40.3867	40.9487	39.6125
	Mode-4	72.2595	71.9776	69.4286
		5-terms	6-terms	7-terms
Rayleigh-Ritz Method	Mode-1	4.5379	4.5281	4.5129
	Mode-2	18.4564	18.3997	18.3994
	Mode-3	40.1403	40.1340	40.0943
	Mode-4	76.7818	71.7793	71.6527

Table 4. 5 Comparison of natural frequencies ($\times 10^4$ rad/sec) of beam with taper configuration-B for fixed-free boundary condition

	Mode No.	3-elements mesh	6-elements mesh	12-elements mesh
Conventional finite element	Mode-1	2.7740	2.7353	2.8394
	Mode-2	11.2322	11.8492	12.0568
	Mode-3	29.6919	30.7040	30.4511
	Mode-4	66.5374	61.8766	59.8188
Higher-order finite element	Mode-1	2.8021	2.8410	2.8674
	Mode-2	11.8808	12.0377	11.8142
	Mode-3	29.9102	29.8216	29.1083
	Mode-4	55.9999	56.8462	55.3228
		5-terms	6-terms	7-terms
Rayleigh-Ritz Method	Mode-1	2.7159	2.7156	2.7151
	Mode-2	11.6960	11.6913	11.6894
	Mode-3	29.8880	29.8880	29.8755
	Mode-4	58.3052	56.0164	56.0162

Table 4. 6 Comparison of natural frequencies ($\times 10^4$ rad/sec) of beam with taper configuration-B for fixed-fixed boundary condition

	Mode No.	3-elements mesh	6-elements mesh	12-elements mesh
Conventional finite element	Mode-1	10.0340	10.4050	10.1750
	Mode-2	28.6456	31.0729	28.6821
	Mode-3	60.7868	65.8171	59.0518
	Mode-4	130.372	109.1310	101.9280
Higher-order finite element	Mode-1	10.29119	10.1285	9.8561
	Mode-2	28.5792	27.7911	26.8954
	Mode-3	54.9170	53.0146	53.1272
	Mode-4	91.0711	90.7206	87.3191
		5-terms	6-terms	7-terms
Rayleigh-Ritz Method	Mode-1	10.0588	10.0573	10.0572
	Mode-2	2.1352	28.1332	28.1260
	Mode-3	54.1915	54.0318	54.0023
	Mode-4	91.8375	91.1748	89.9167

From Tables 4.4 - 4.6, one can see that natural frequencies calculated using different finite elements for beam with taper configuration-B for all boundary conditions are converging well. Another important observation is that natural frequency for fixed-free beam is lowest and for double clamped or fixed-fixed is highest for all modes respectively.

4.2.3 Beam with taper configuration-C

Example 4.2.3

Example 4.2.3 is solved for beam with taper configuration-C as shown in Figure 4.3. The beam is meshed into three, six and twelve elements of equal length for analysis, plies drop-off occur near the middle plane of beam. Dropped-off plies are replaced by resin pocket; resin pocket is divided into imaginary layers in each element with the same thickness of lamina. Integration limits for different calculations are considered according to appropriate position of imaginary ply ending.

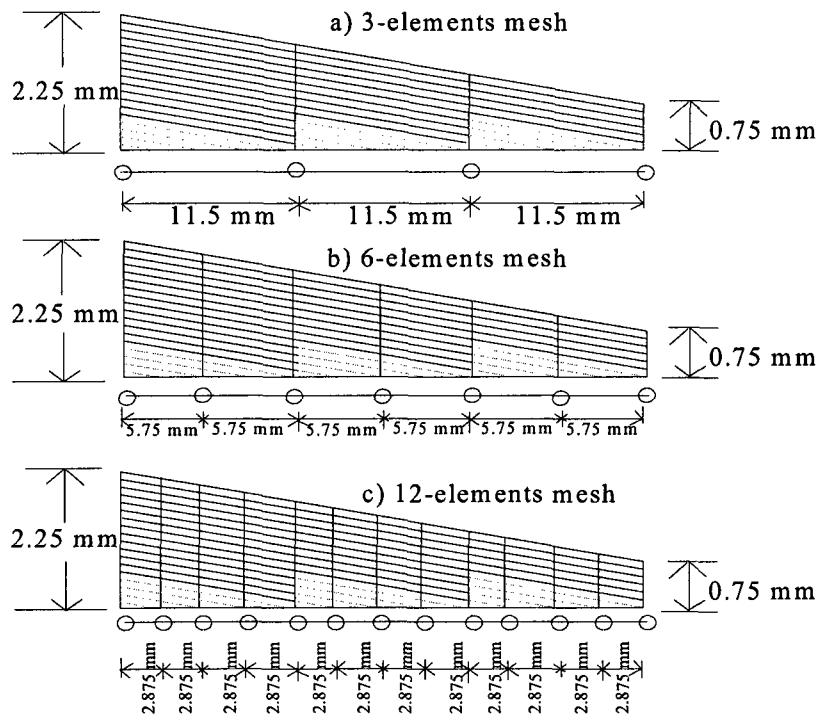


Figure 4. 3 Upper half of beam with taper configuration-C with a) 3- elements mesh, b) 6- elements mesh, and c) 12- elements mesh

By using the mechanical and geometric properties described in Example 4.2.1, the problem is solved to find the natural frequencies for simply supported, fixed-free and fixed-fixed boundary conditions. The results are presented in Tables 4.7 - 4.9 and first four lowest frequencies for all boundary conditions are compared.

Table 4.7 Comparison of natural frequencies ($\times 10^4$ rad/sec) of beam with taper configuration-C for simply supported boundary condition

	Mode No.	3-elements mesh	6-elements mesh	12-elements mesh
Conventional finite element	Mode-1	4.4584	4.2838	4.5203
	Mode-2	22.0971	19.6170	19.2789
	Mode-3	35.2454	48.2989	45.1144
	Mode-4	62.1887	86.9207	84.2137
Higher-order finite element	Mode-1	4.4628	4.4537	4.4752
	Mode-2	18.6621	18.5369	18.2687
	Mode-3	40.8959	41.6979	42.3035
	Mode-4	73.6041	73.6882	73.2632
		5-terms	6-terms	7-terms
Rayleigh-Ritz Method	Mode-1	4.4784	4.4637	4.4425
	Mode-2	17.6983	17.6157	17.6095
	Mode-3	38.8529	38.7887	38.7336
	Mode-4	77.1363	69.5652	69.5643

Table 4.8 Comparison of natural frequencies ($\times 10^4$ rad/sec) of beam with taper configuration-C for fixed-free boundary condition

	Mode No.	3-elements mesh	6-elements mesh	12-elements mesh
Conventional finite element	Mode-1	2.7068	2.8669	2.9549
	Mode-2	11.3412	11.5120	12.5410
	Mode-3	30.4753	28.6966	31.6047
	Mode-4	64.8351	56.1765	61.7094
Higher-order finite element	Mode-1	2.8741	2.8369	2.8244
	Mode-2	12.0934	12.3725	12.7897
	Mode-3	30.6002	30.5637	30.2017
	Mode-4	57.0692	58.0778	59.1343
		5-terms	6-terms	7-terms
Rayleigh-Ritz Method	Mode-1	2.8447	2.8447	2.8447
	Mode-2	13.0675	13.0598	13.0577
	Mode-3	33.2505	33.2482	33.2204
	Mode-4	65.5679	62.5872	62.5852

Table 4. 9 Comparison of natural frequencies ($\times 10^4$ rad/sec) of beam with taper configuration-C for fixed-fixed boundary condition

	Mode No.	3-elements mesh	6-elements mesh	12-elements mesh
Conventional finite element	Mode-1	10.8195	10.7798	10.5546
	Mode-2	31.0342	31.4717	29.8230
	Mode-3	63.9129	63.5531	60.9670
	Mode-4	138.5300	98.9848	105.5860
Higher-order finite element	Mode-1	10.4357	10.4132	10.4273
	Mode-2	29.0178	28.5754	30.6978
	Mode-3	55.3247	56.2269	61.9033
	Mode-4	92.2916	92.9352	100.0800
		5-terms	6-terms	7-terms
Rayleigh-Ritz Method	Mode-1	10.4801	10.4797	10.4794
	Mode-2	28.5848	28.5844	28.5844
	Mode-3	54.9271	54.8212	54.7591
	Mode-4	94.5890	92.5481	91.6527

From Tables 4.7-4.9, one can see that natural frequencies calculated using different finite elements for beam with taper configuration-C for all boundary conditions are converging well. Another important observation is that natural frequencies for fixed-free beam are lowest and for double clamped or fixed-fixed are highest for all modes respectively.

4.2.4 Beam with taper configuration-D

Example 4.2.4

Example 4.2.4 is solved for beam with taper configuration-D as shown in Figure 4.4. The beam is made of 36 plies at thick section and after dropping off 24 plies, it ends with 12 plies at thin section.

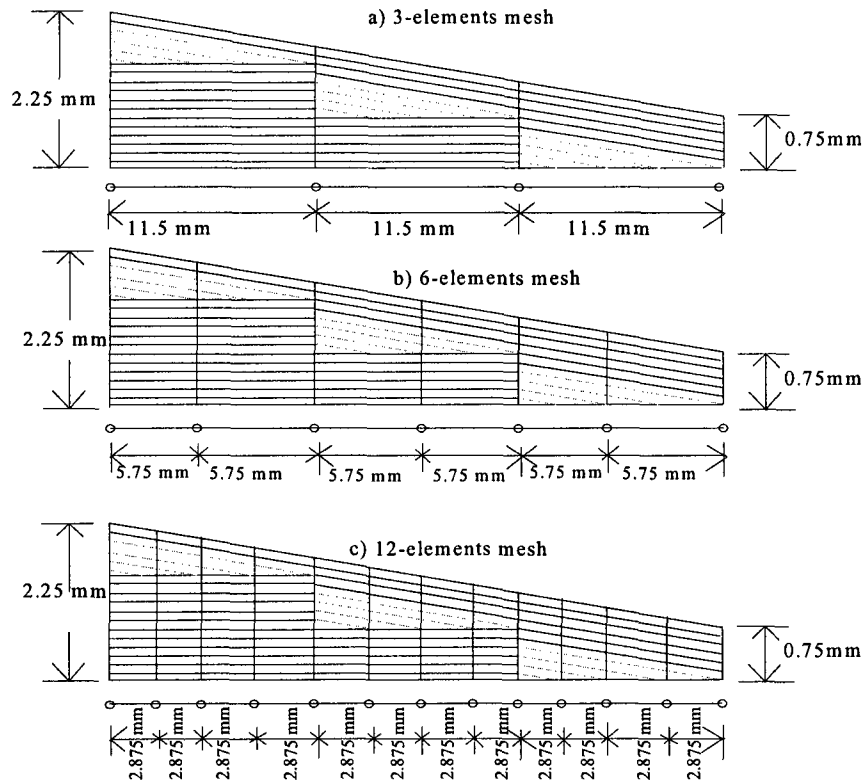


Figure 4. 4 Upper half of beam with taper configuration-D with a) 3- elements mesh, b) 6- elements mesh, and c) 12- elements mesh

The beam is symmetric and meshed into three, six and twelve elements for analysis. Ply drop-off appearance looks like that of taper configuration-B except that there is a ply difference above the resin pocket corresponding to specific element. By using the mechanical and geometric properties described in Example 4.2.1, the problem is solved to find the natural frequencies for simply supported, fixed-free and fixed-fixed boundary conditions.

The results are presented in Tables 4.10-4.12 and first four lowest frequencies for all boundary conditions are compared.

Table 4. 10 Comparison of natural frequencies ($\times 10^4$ rad/sec) of beam with taper configuration-D for simply supported boundary condition

	Mode No.	3-elements mesh	6-elements mesh	12-elements mesh
Conventional finite element	Mode-1	5.1576	5.17774	5.1320
	Mode-2	24.9619	22.8579	21.6346
	Mode-3	43.7041	57.0612	50.1385
	Mode-4	65.6226	106.664	93.5380
Higher-order finite element	Mode-1	5.1386	5.1673	5.1732
	Mode-2	20.7265	21.5256	21.5338
	Mode-3	45.3079	48.6968	48.7402
	Mode-4	80.5905	85.0560	85.1541
		5-terms	6-terms	7-terms
Rayleigh-Ritz Method	Mode-1	5.1360	5.1149	5.1133
	Mode-2	25.4821	25.4737	25.4736
	Mode-3	58.4958	57.5122	57.4093
	Mode-4	112.318	106.379	105.376

Table 4. 11 Comparison of natural frequencies ($\times 10^4$ rad/sec) of beam with taper configuration-D for fixed-free boundary condition

	Mode No.	3-elements mesh	6-elements mesh	12-elements mesh
Conventional finite element	Mode-1	2.6966	2.7688	2.8236
	Mode-2	13.1356	12.7642	13.2406
	Mode-3	33.9963	34.2183	34.9084
	Mode-4	75.3676	68.7625	68.667
Higher-order finite element	Mode-1	2.7997	2.7010	2.8816
	Mode-2	12.7427	10.7070	11.2947
	Mode-3	33.1539	25.9296	27.2641
	Mode-4	62.7518	50.1510	52.4998
		5-terms	6-terms	7-terms
Rayleigh-Ritz Method	Mode-1	2.7875	2.7791	2.7732
	Mode-2	9.7060	9.7060	9.7059
	Mode-3	27.6040	25.6675	25.5570
	Mode-4	55.5870	66.3469	49.0986

Table 4. 12 Comparison of natural frequencies ($\times 10^4$ rad/sec) of beam with taper configuration-D for fixed-fixed boundary condition

	Mode No.	3-elements mesh	6-elements mesh	12-elements mesh
Conventional finite element	Mode-1	11.1358	11.3317	11.4625
	Mode-2	31.4620	34.3274	33.0267
	Mode-3	68.3596	72.5525	67.6632
	Mode-4	140.3970	120.7700	117.1990
Higher-order finite element	Mode-1	11.2488	11.2438	11.6828
	Mode-2	31.7595	30.4811	31.7390
	Mode-3	61.4682	60.1612	62.8098
	Mode-4	101.4540	95.9521	101.6720
		5-terms	6-terms	7-terms
Rayleigh-Ritz Method	Mode-1	11.3597	11.3574	11.3558
	Mode-2	31.9551	31.9326	31.8658
	Mode-3	66.1598	65.1073	65.0442
	Mode-4	132.1880	112.0270	110.1420

From Tables 4.10-4.12, one can see that natural frequencies calculated using different finite elements for beam with taper configuration-D for all boundary conditions are converging well. Another important observation is that natural frequencies for fixed-free beam are lowest and for double clamped or fixed-fixed are highest for all modes respectively.

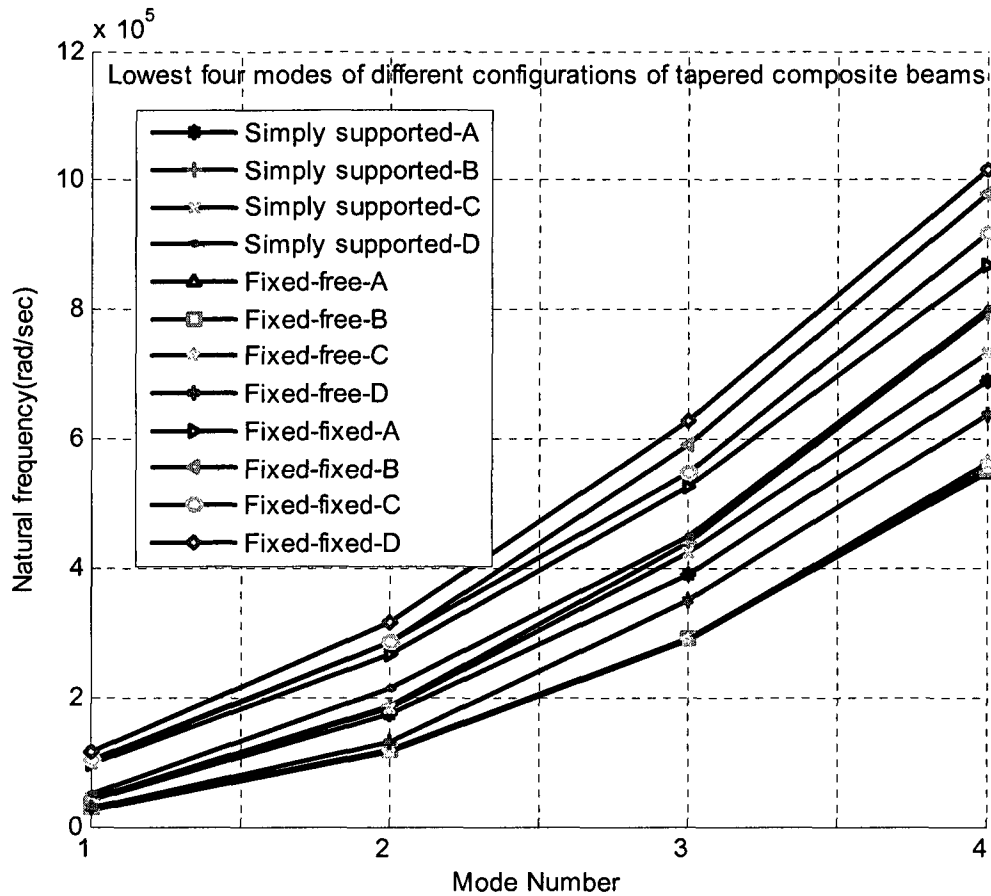


Figure 4.5 Effects of different taper configurations on lowest four natural frequencies for different boundary conditions

One can observe the first four lowest natural frequencies for all taper configurations beam for different boundary conditions respectively from the Figure 4.5 at a glance. The results obtained for different types of taper configuration for all boundary conditions show that natural frequencies obtained from taper configuration-D gives the highest values; then taper configuration-B, C and A ranked second, third and fourth respectively. This difference in frequency is expected from the inside geometry variation; the location of plies drop-off. Because frequencies calculated for different taper configurations depend on the stiffness of the beam that is dependant on D_{11} .

The D_{11} is dependant on mechanical properties and height of the ply from the mid-plane of the beam. As different taper configurations are considered according to plies drop-off at different locations, these are giving different stiffness. One can see from the Figures 4.1 to 4.4 for different taper configuration that configuration-D is more stiff due to more uniform plies in different elements. Then taper configuration-B gives second highest stiffness considering its number and location of uniform plies and resin pocket. Beam with taper configuration-C gives less stiffness than configuration-B because plies drop-off near mid-plane makes resin pocket that does affect much the total stiffness. Taper configuration-A gives the lowest stiffness compared to others as it is made with a big resin pocket. Natural frequencies of taper configuration-C are in between the natural frequencies of taper configurations-B and A due to the reason that plies drop-off near mid-plane of beam makes it all taper plies. Observation among the boundary conditions is that first four lower natural frequencies for fixed-free beam are lowest and for double clamped or fixed-fixed are highest for all beams. Simply supported beam gives the frequency values in between those that compared to these two boundary conditions.

4.3 Effect of laminate configuration on natural frequencies

To investigate the effects of different laminate configurations, the beam with taper configurations-C and D are considered. The beam is with 36 and 12 plies at thick and thin sections respectively, which results in 24 drop-off plies. The laminate configurations considered are: 1) LC-1 that has $[0/90]_{9s}$ configuration at thick section and $[0/90]_{3s}$ configuration at thin section; 2) LC-2 that has $[\pm 45]_{9s}$ configuration at thick section and $[\pm 45]_{3s}$ configuration at thin section; 3) LC-3 that has $[0_4 / \pm 45_7]_s$ configuration at thick section and $[0_4 / \pm 45]_s$ configuration at thin section.

Example 4.3.1

By using the properties described in Example-4.2.1, the example 4.3.1 is solved to find the natural frequencies for simply supported, fixed-free and fixed-fixed boundary conditions of beam with taper configuration-C. The first four lowest frequencies for all boundary conditions are obtained considering 12-elements of equal length mesh and 5-terms for Rayleigh-Ritz method and results are presented in Tables 4.13 - 4.15.

Table 4.13 Comparison of natural frequencies ($\times 10^4$ rad/sec) of beam with taper configuration-C for simply supported boundary condition

LC	Mode No.	Conventional finite element (12-elements mesh)	Higher-order finite element (12-elements mesh)	Rayleigh-Ritz Method (5-terms)
1	Mode-1	4.5203	4.4752	4.4784
	Mode-2	19.2789	18.2687	17.6983
	Mode-3	45.1144	42.3035	38.8529
	Mode-4	84.2137	73.2632	77.1363
2	Mode-1	3.2406	3.1777	3.2204
	Mode-2	13.8227	13.0443	12.7286
	Mode-3	32.2302	30.0497	27.7535
	Mode-4	60.2901	52.1670	55.3538
3	Mode-1	5.3238	5.2582	5.4554
	Mode-2	22.4870	21.0523	21.6036
	Mode-3	52.4763	49.0475	47.4870
	Mode-4	98.1883	84.8510	94.6475

Table 4.14 Comparison of natural frequencies ($\times 10^4$ rad/sec) of beam with taper configuration-C for fixed-free boundary condition

LC	Mode No.	Conventional finite element (12-elements mesh)	Higher-order finite element (12-elements mesh)	Rayleigh-Ritz Method (5-terms)
1	Mode-1	2.9549	2.9244	2.8447
	Mode-2	12.5410	12.7897	13.0675
	Mode-3	31.6047	30.2017	33.2505
	Mode-4	61.7094	59.1343	65.5679
2	Mode-1	2.1453	2.1163	1.8822
	Mode-2	9.0315	9.1451	8.3095
	Mode-3	22.7104	21.5898	20.9147
	Mode-4	44.1034	42.0851	39.2866
3	Mode-1	3.3109	3.2562	3.1914
	Mode-2	14.4936	14.7865	14.0705
	Mode-3	36.8338	34.8481	35.3903
	Mode-4	71.8461	68.4017	67.3767

Table 4.15 Comparison of natural frequencies ($\times 10^4 \text{rad/sec}$) of beam with taper configuration-C for fixed-fixed boundary condition

LC	Mode No.	Conventional finite element (12-elements mesh)	Higher-order finite element (12-elements mesh)	Rayleigh-Ritz Method (5-terms)
1	Mode-1	10.5546	10.4273	10.4801
	Mode-2	29.8230	30.6978	28.5848
	Mode-3	60.9670	61.9033	54.9271
	Mode-4	105.5860	100.0800	94.5890
2	Mode-1	7.5470	7.4329	7.1788
	Mode-2	21.3567	21.9990	19.6409
	Mode-3	43.5321	44.1832	37.4063
	Mode-4	75.5036	71.4824	65.3657
3	Mode-1	12.2050	12.0516	12.2757
	Mode-2	34.6706	35.0717	33.4247
	Mode-3	70.8230	71.1757	64.1135
	Mode-4	122.9690	115.6040	111.4880

As one can observe from the Tables 4.13-4.15, natural frequencies of LC-3 laminate configuration are highest and they are lowest for LC-2 for all boundary conditions respectively. Another important observation is that natural frequencies for fixed-free beam are lowest and for fixed-fixed (double clamped) are highest for beam with taper configuration-C.

Example 4.3.2

By using the properties described in Example-4.2.1, the example 4.3.2 is solved to find the natural frequencies for simply supported, fixed-free and fixed-fixed boundary conditions of beam with taper configuration-D. The first four lowest frequencies for all boundary conditions are obtained considering 12-elements mesh and 5-terms for Rayleigh-Ritz method and results are presented in Tables 4.16 - 4.18.

Table 4.16 Comparison of natural frequencies ($\times 10^4$ rad/sec) of beam with taper configuration-D for simply supported boundary condition

LC	Mode No.	Conventional finite element (12-elements mesh)	Higher-order finite element (12-elements mesh)	Rayleigh-Ritz Method (5-terms)
1	Mode-1	5.1320	5.1732	5.1360
	Mode-2	21.6346	21.5338	25.4821
	Mode-3	50.1385	48.7402	58.4958
	Mode-4	93.5380	85.1541	112.318
2	Mode-1	3.7110	3.6631	3.7402
	Mode-2	15.6443	15.3618	18.8195
	Mode-3	36.2483	35.2031	43.2589
	Mode-4	67.6835	60.8450	84.0258
3	Mode-1	6.5123	6.9215	6.6590
	Mode-2	26.9132	28.6048	33.1692
	Mode-3	62.9011	64.6318	76.1782
	Mode-4	117.5860	114.2610	146.4710

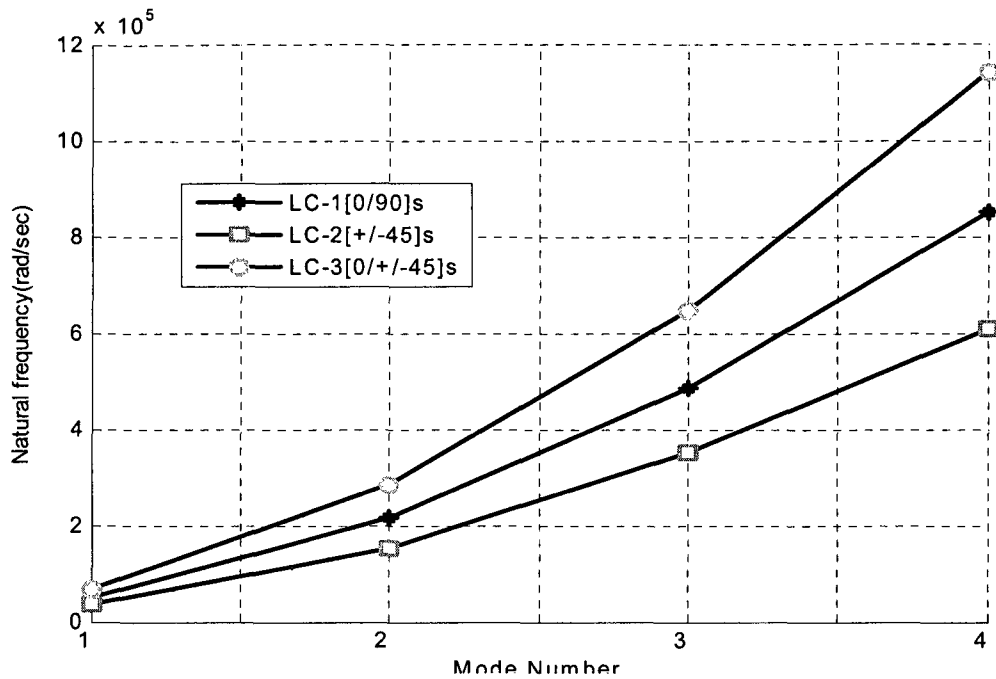


Figure 4.6 Effects of different laminate configurations on lowest four natural frequencies for simply supported boundary condition of beam with taper configuration-D

One can observe the effects of different laminate configurations on natural frequencies of beam with taper configuration-D for simply supported boundary condition from the Figure 4.6. The results obtained for different types of laminate configuration show that natural frequencies obtained from laminate configuration LC-3 gives the highest values; then laminate configuration LC-1 ranked second and laminate configuration LC-2 gives the lowest values. This difference in frequency is expected from the laminate configuration variation. Because frequency calculated for different laminate configuration depends on the stiffness of the beam that is dependant on D_{11} . The D_{11} is directly dependant on Q_{11} of the ply. As different laminate configurations of composite beams give different stiffnesses according to sequence of ply orientation in the laminate, it gives different natural frequency values.

Table 4. 17 Comparison of natural frequencies ($\times 10^4$ rad/sec) of beam with taper configuration-D for fixed-free boundary condition

LC	Mode No.	Conventional finite element (12-elements mesh)	Higher-order finite element (12-elements mesh)	Rayleigh-Ritz Method (5-terms)
1	Mode-1	2.8236	2.8316	2.7875
	Mode-2	13.2406	11.2947	9.7060
	Mode-3	34.9084	27.2641	27.6040
	Mode-4	68.667	52.4998	55.5870
2	Mode-1	2.0671	2.4228	2.1041
	Mode-2	9.6268	9.6814	6.8702
	Mode-3	25.2931	23.2770	18.9780
	Mode-4	49.6574	45.3952	111.4960
3	Mode-1	3.5474	3.9412	3.7133
	Mode-2	16.7944	18.1835	12.2504
	Mode-3	43.5343	46.5458	33.3895
	Mode-4	85.8679	89.5021	182.1560

Table 4. 18 Comparison of natural frequencies ($\times 10^4$ rad/sec) of beam with taper configuration-D for fixed- fixed boundary condition

LC	Mode No.	Conventional finite element (12-elements mesh)	Higher-order finite element (12-elements mesh)	Rayleigh-Ritz Method (5-terms)
1	Mode-1	11.4625	11.6828	11.3597
	Mode-2	33.0267	31.7390	31.9551
	Mode-3	67.6632	62.8098	66.1598
	Mode-4	117.1990	101.6720	132.1880
2	Mode-1	8.2993	9.6073	8.4430
	Mode-2	23.8964	26.0252	23.8892
	Mode-3	48.9092	52.0764	49.1108
	Mode-4	84.7785	84.7945	101.0710
3	Mode-1	14.3985	16.2051	14.7036
	Mode-2	41.2471	44.5531	41.3987
	Mode-3	84.7568	87.9044	85.64.85
	Mode-4	147.2390	144.8930	172.742

As one can observe from the Tables 4.16-4.18, the natural frequencies of LC-3 laminate configuration are highest and they are lowest for LC-2 for all boundary conditions respectively. Another important observation is that natural frequencies for fixed-free beam are lowest and for fixed-fixed (double clamped) are highest for beam with taper configuration-D.

4.4 Effects of Taper angle on natural frequencies

To investigate the effects of taper angle on natural frequency, the beam with taper configurations-C and D are considered. The geometric properties of the beams are: It was considered with 36 and 12 plies at thick and thin sections respectively, which results in 24 drop-off plies, height at thick section (h_1) is 0.0045m; height at thin section (h_2) is 0.0015m; individual ply thickness (t_k) is 0.000125m, width (b) is unity, and taper angle (ϕ) for tapered section have been increased from 1° to 3° .

Though the thickness ratio is kept constant, therefore increasing the taper angle results in decreasing the length in tapered section. The tapered section of beam is meshed with twelve equal length elements.

Example 4.4.1

By using the properties described in Example-4.2.1, the example 4.4.1 is solved to find the natural frequencies for simply supported, fixed-free and fixed-fixed boundary conditions of beam with taper configuration-C. The first four lowest frequencies for all boundary conditions are obtained considering 12-elements mesh and 5-terms for Rayleigh-Ritz method and results are presented in Tables 4.19 - 4.21.

Table 4. 19 Comparison of natural frequencies ($\times 10^4$ rad/sec) of beam with taper configuration-C for simply supported boundary condition

Taper angle (ϕ°)	Mode No.	Conventional finite element (12-elements mesh)	Higher-order finite element (12-elements mesh)	Rayleigh-Ritz Method (5-terms)
1	Mode-1	0.7233	0.7161	0.7155
	Mode-2	3.0850	2.9233	2.8275
	Mode-3	7.2192	6.7694	6.2073
	Mode-4	13.4760	11.7237	12.3237
1.5	Mode-1	1.6274	1.6112	1.6104
	Mode-2	6.9411	6.5773	6.3642
	Mode-3	16.2428	15.2308	13.9714
	Mode-4	30.3200	26.3774	27.7380
2	Mode-1	2.8931	2.8643	2.8644
	Mode-2	12.3392	11.6926	11.3198
	Mode-3	28.8749	27.0757	24.8502
	Mode-4	53.8998	46.8911	49.3362
2.5	Mode-1	4.5203	4.4752	4.4784
	Mode-2	19.2789	18.2687	17.6983
	Mode-3	45.1144	42.3035	38.8529
	Mode-4	84.2137	73.2632	77.1363
3	Mode-1	6.5088	6.4439	6.4539
	Mode-2	27.7597	26.3051	25.5052
	Mode-3	64.9603	60.9128	55.9913
	Mode-4	121.2590	105.4920	111.1620

Table 4.20 Comparison of natural frequencies ($\times 10^4$ rad/sec) of beam with taper configuration-C for fixed-free boundary condition

Taper angle (ϕ°)	Mode No.	Conventional finite element (12-elements mesh)	Higher-order finite element (12-elements mesh)	Rayleigh-Ritz Method (5-terms)
1	Mode-1	0.4728	0.4679	0.4544
	Mode-2	2.0068	2.0466	2.0877
	Mode-3	5.0574	4.8329	5.3122
	Mode-4	9.8748	9.4627	10.4755
1.5	Mode-1	1.0639	1.0529	1.0229
	Mode-2	4.5152	4.6047	4.6990
	Mode-3	11.3788	10.8737	11.9568
	Mode-4	22.2176	21.2905	23.5780
2	Mode-1	1.8913	1.8717	1.8195
	Mode-2	8.0267	8.1858	8.3579
	Mode-3	20.2282	19.3302	21.2669
	Mode-4	39.4962	37.8481	41.9371
2.5	Mode-1	2.9549	2.9244	2.8447
	Mode-2	12.5410	12.7897	13.0675
	Mode-3	31.6047	30.2017	33.2505
	Mode-4	61.7094	59.1343	65.5679
3	Mode-1	4.2549	4.2109	4.0996
	Mode-2	18.0578	18.4159	18.8316
	Mode-3	45.5076	43.4875	47.9175
	Mode-4	88.8554	85.1475	94.4904

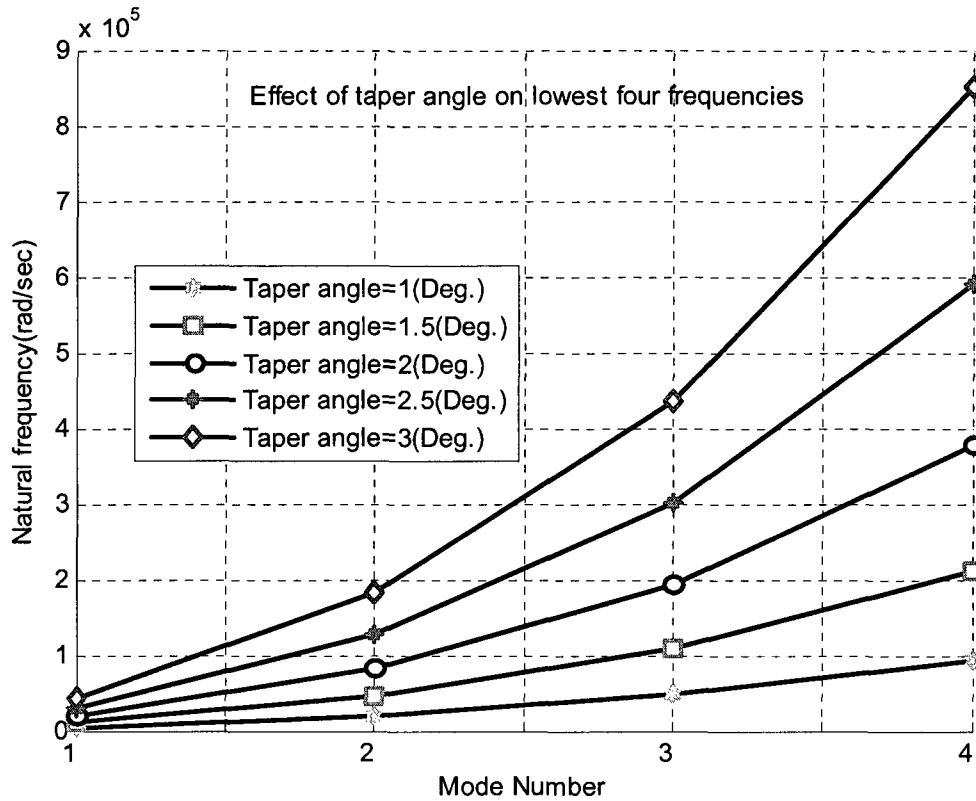


Figure 4. 7 Effects of taper angle on lowest four natural frequencies for fixed-free boundary condition of beam with taper configuration-C

One can observe the effects of taper angle on natural frequencies of beam with taper configuration-B for simply supported boundary condition from the Figure 4.7. The results obtained for different values of taper angle show that natural frequencies obtained for highest taper angle are the highest in value and the lowest taper angle values gives the lowest values of frequencies. The frequency is increasing with the increasing of taper angle, because the length of the beam decreases which makes it stiffer that results in higher natural frequency and vice versa.

Table 4. 21 Comparison of natural frequencies ($\times 10^4 \text{rad/sec}$) of beam with taper configuration-C for fixed-fixed boundary condition

Taper angle (ϕ°)	Mode No.	Conventional finite element (12-elements mesh)	Higher-order finite element (12-elements mesh)	Rayleigh-Ritz Method (5-terms)
1	Mode-1	1.6889	1.526	1.674
	Mode-2	4.772	4.536	4.566
	Mode-3	9.756	9.084	8.775
	Mode-4	16.896	14.705	15.112
1.5	Mode-1	3.800	3.434	3.768
	Mode-2	10.737	10.206	10.279
	Mode-3	21.950	20.440	19.751
	Mode-4	38.014	33.087	34.014
2	Mode-1	6.755	6.105	6.703
	Mode-2	19.087	18.143	18.282
	Mode-3	39.021	36.336	35.131
	Mode-4	67.579	58.818	60.498
2.5	Mode-1	10.554	10.427	10.480
	Mode-2	29.823	30.697	28.584
	Mode-3	60.967	61.903	54.927
	Mode-4	105.586	100.080	94.589
3	Mode-1	15.197	13.736	15.103
	Mode-2	42.942	40.818	41.193
	Mode-3	87.786	81.747	79.155
	Mode-4	152.034	132.326	136.313

As one can observe from the Tables 4.19-4.21, the natural frequencies of beam with higher taper angle are the highest in values and the lowest taper angle values gives the lowest values of frequencies for all boundary conditions respectively. Another important observation is that natural frequency for fixed-free beam is lowest and for fixed-fixed (double clamped) is highest for beam with taper configuration-C.

Example 4.4.2

By using the properties described in Example-4.2.1, the example 4.4.2 is solved to find the natural frequencies for simply supported, fixed-free and fixed-fixed boundary conditions of beam with taper configuration-D. The first four lowest frequencies for all boundary conditions are obtained considering 12-elements mesh and 5-terms for Rayleigh-Ritz method and results are presented in Tables 4.22 - 4.24.

Table 4.22 Comparison of natural frequencies ($\times 10^4$ rad/sec) of beam with taper configuration-D for simply supported boundary condition

Taper angle (ϕ°)	Mode No.	Conventional finite element (12-elements mesh)	Higher-order finite element (12-elements mesh)	Rayleigh-Ritz Method (5-terms)
1	Mode-1	0.821	0.827	0.820
	Mode-2	3.461	3.445	4.071
	Mode-3	8.021	7.799	9.346
	Mode-4	14.964	13.626	17.946
1.5	Mode-1	1.847	1.862	1.867
	Mode-2	7.787	7.752	9.164
	Mode-3	18.047	17.548	21.037
	Mode-4	33.671	30.658	40.392
2	Mode-1	3.284	3.311	3.285
	Mode-2	13.845	13.782	16.299
	Mode-3	32.086	31.195	37.415
	Mode-4	59.862	54.501	71.841
2.5	Mode-1	5.132	5.173	5.136
	Mode-2	21.634	21.533	25.482
	Mode-3	50.138	48.740	58.495
	Mode-4	93.538	85.154	112.318
3	Mode-1	7.390	7.448	7.401
	Mode-2	31.155	31.006	36.720
	Mode-3	72.204	70.181	84.293
	Mode-4	134.700	122.610	161.850

Table 4. 23 Comparison of natural frequencies ($\times 10^4$ rad/sec) of beam with taper configuration-D for fixed-free boundary condition

Taper angle (ϕ°)	Mode No.	Conventional finite element (12-elements mesh)	Higher-order finite element (12-elements mesh)	Rayleigh-Ritz Method (5-terms)
1	Mode-1	0.4516	0.4531	0.4454
	Mode-2	2.1182	1.8073	1.5509
	Mode-3	5.5848	4.3628	4.4107
	Mode-4	10.9853	8.4010	24.8575
1.5	Mode-1	1.0162	1.0195	1.0025
	Mode-2	4.70661	4.0664	3.4906
	Mode-3	12.5661	9.8160	9.9273
	Mode-4	24.7177	18.9018	55.9489
2	Mode-1	1.8068	1.8125	1.7830
	Mode-2	8.4733	7.2289	6.2083
	Mode-3	22.3405	17.4500	17.6566
	Mode-4	43.9444	33.6017	99.5133
2.5	Mode-1	2.8236	2.8316	2.7875
	Mode-2	13.2406	11.2947	9.7060
	Mode-3	34.9084	27.2641	2.7604
	Mode-4	68.667	52.4998	155.587
3	Mode-1	4.0667	4.0776	4.0166
	Mode-2	19.0676	16.2632	13.9865
	Mode-3	50.2705	39.2576	39.7790
	Mode-4	98.8866	75.5946	224.217

Table 4. 24 Comparison of natural frequencies ($\times 10^4 \text{rad/sec}$) of beam with taper configuration-D for fixed- fixed boundary condition

Taper angle (ϕ°)	Mode No.	Conventional finite element (12-elements mesh)	Higher-order finite element (12-elements mesh)	Rayleigh-Ritz Method (5-terms)
1	Mode-1	1.83337	1.8694	1.8151
	Mode-2	5.2837	5.0789	5.1060
	Mode-3	10.8246	10.0509	10.5719
	Mode-4	18.7500	16.2696	21.1220
1.5	Mode-1	4.1260	4.2062	4.0854
	Mode-2	11.8888	11.4272	11.4922
	Mode-3	24.3562	22.6138	23.7940
	Mode-4	42.1884	54.5680	47.5395
2	Mode-1	7.3355	7.4773	7.2661
	Mode-2	21.1362	20.3141	20.4396
	Mode-3	43.3019	40.2005	42.3188
	Mode-4	75.0042	65.0737	84.5522
2.5	Mode-1	11.4625	11.6828	11.3597
	Mode-2	33.0267	31.7390	31.9551
	Mode-3	67.6632	62.8098	66.1598
	Mode-4	117.199	101.672	132.188
3	Mode-1	16.5070	16.8220	16.3691
	Mode-2	47.5609	45.7010	46.0475
	Mode-3	97.4421	90.4399	95.3349
	Mode-4	168.776	146.398	190.484

As one can observe from the Tables 4.22-4.24, the natural frequencies of beam with higher taper angle are the highest in values and the lowest taper angle values gives the lowest values of frequencies for all boundary conditions respectively. Another important observation is that natural frequency for fixed-free beam is lowest and for fixed-fixed (double clamped) is highest for beam with taper configuration-D beam.

4.5 Effect of length ratio on natural frequencies

To study the length ratio (L_{thick} / L_{thin}) effect on natural frequencies, the beam with taper configurations-C and D are considered as shown in Figures 4.8 and 4.10. The ply of composite beam is made of NCT/301 graphite-epoxy and the beam consists of 36 plies. The configuration of the thick section is $[0/90]_{9s}$ and it is $[0/90]_{3s}$ at thin section.

The geometric properties of the beams are: the beam is considered with 36 and 12 plies at thick and thin sections respectively, which results in 24 drop-off plies, it is considered with 9-elements mesh and the length of each element section is 0.0115m, so the total length of the beam is 0.1035m, height at thick section (h_1) is 0.0045m, height at thin section (h_2) is 0.0015m, individual ply thickness (t_k) is 0.000125m, width (b) is unity and taper angle (ϕ) for tapered section is considered as 2.5°.

Though the thickness ratio, taper angle and total length are kept constant, changing length ratio is adjusted by using changing lengths of thick and thin sections in different length ratio. When length ratio is 2, it is that length of thick section is twice that of thin section. When length ratio is ½, it is that length of thick section is half of the length of thin section. When length ratio is 1, the length of thick section is equal to the length of thin section.

Example 4.5.1

By using the properties described in Example-4.2.1, the example 4.5.1 is solved to find the natural frequencies at simply supported, fixed-free and fixed-fixed boundary conditions of beam with taper configuration-C. The first four lowest frequencies for all boundary conditions are obtained considering 9-elements mesh and 5-terms for Rayleigh-Ritz method and results are presented in Tables 4.25 - 4.27.

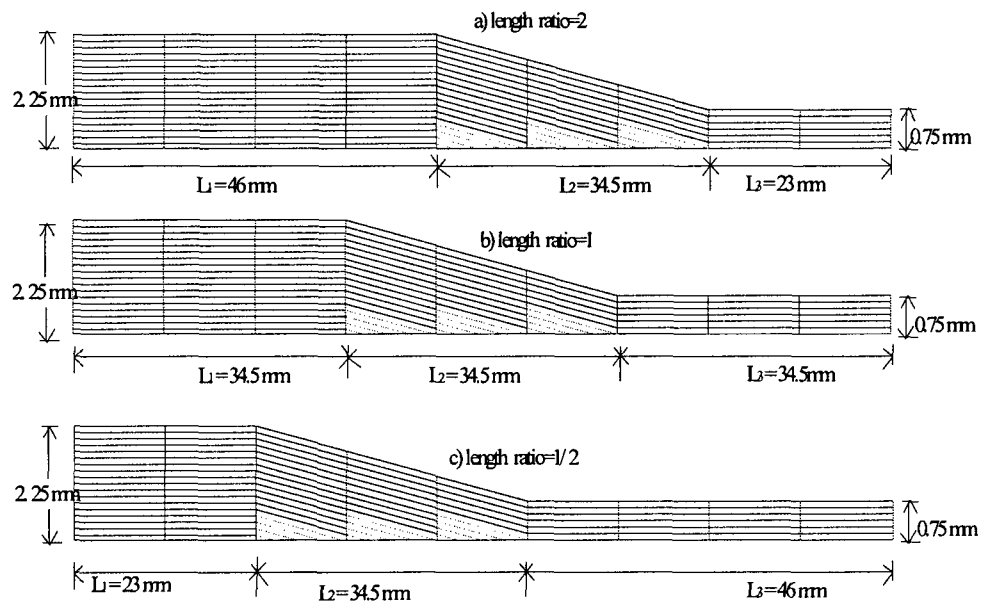


Figure 4. 8 Upper half of beam with taper configuration-C with 9-elements mesh of
a) length ratio = 2, b) length ratio = 1, and c) length ratio =1/ 2

Table 4. 25 Comparison of natural frequencies ($\times 10^4$ rad/sec) of beam with taper configuration-C for simply supported boundary condition

	Mode No.	Length ratio=2	Length ratio=1	Length ratio=1/2
CFE	Mode-1	0.4474	0.3698	0.3372
	Mode-2	2.2416	2.0473	1.7153
	Mode-3	4.7877	4.2494	3.8270
	Mode-4	8.3875	7.4626	6.7672
HOFE	Mode-1	0.4566	0.3736	0.3351
	Mode-2	2.2811	2.1083	1.7507
	Mode-3	4.7521	4.2902	3.9515
	Mode-4	8.2275	7.5793	6.8456

Table 4. 26 Comparison of natural frequencies ($\times 10^4$ rad/sec) of beam with taper configuration-C for fixed-free boundary condition

	Mode No.	Length ratio=2	Length ratio=1	Length ratio=1/2
CFE	Mode-1	0.4314	0.3698	0.3091
	Mode-2	1.3336	2.0473	1.1231
	Mode-3	3.3648	4.2494	2.7119
	Mode-4	6.4565	7.4626	5.1557
HOEF	Mode-1	0.4265	0.3926	0.3104
	Mode-2	1.3543	1.1203	1.1293
	Mode-3	3.4371	3.1419	2.7342
	Mode-4	6.5572	5.8481	5.2997

Table 4. 27 Comparison of natural frequencies ($\times 10^4$ rad/sec) of beam with taper configuration-C for fixed-fixed boundary condition

	Mode No.	Length ratio=2	Length ratio=1	Length ratio=1/2
CFE	Mode-1	1.1012	1.0846	1.1410
	Mode-2	3.3594	3.0780	2.7250
	Mode-3	6.4872	5.7721	5.1559
	Mode-4	10.6512	9.4569	8.5042
HOEF	Mode-1	1.1139	1.0856	1.1471
	Mode-2	3.4357	3.1704	2.7473
	Mode-3	6.5888	5.8556	5.2986
	Mode-4	10.8754	9.5500	8.6367

* CFE-Conventional finite element, HOFE-Higher order finite element.

As one can observe from the Tables 4.25-4.27, the natural frequencies of beam with higher length ratio are higher and they are lower for beam with lower length ratio for all boundary conditions. Another important observation is that natural frequencies for fixed-free beam are lowest and for fixed-fixed (double clamped) are highest for beam with taper configuration-C.

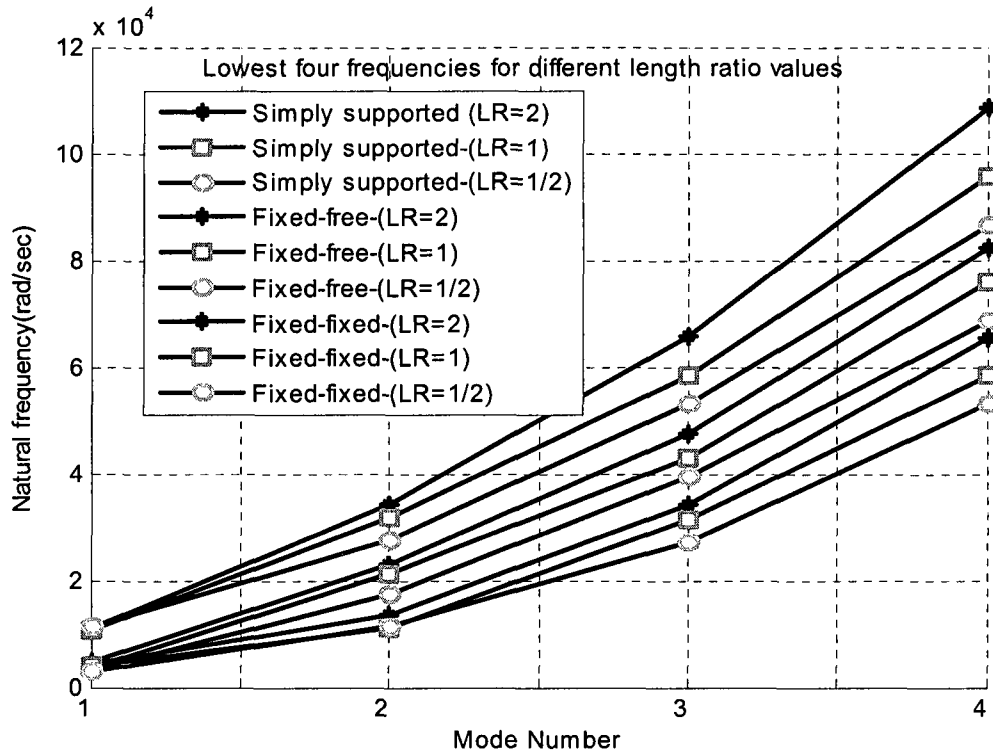


Figure 4. 9 Effect of length ratio on lowest four natural frequencies for different boundary conditions of beam with taper configuration-C

One can observe the effect of length ratio on natural frequencies of beam with taper configuration-C for different boundary conditions from the Figure 4.9. The results obtained for different values of length ratio show that natural frequencies obtained from highest length ratio are the highest and the lowest length ratio gives the lowest values of frequencies. The frequency is increasing with the increasing of length ratio, because the length of thick section increases, which makes the beam stiffer that results in higher natural frequencies and vice versa.

Example 4.5.2

By using the properties described in Example-4.2.1, the example 4.5.2 is solved to find the natural frequencies at simply supported, fixed-free and fixed-fixed boundary conditions of beam with taper configuration-D. The first four lowest frequencies for all boundary conditions are obtained considering 9-elements mesh and 5-terms for Rayleigh-Ritz method and results are presented in Tables 4.28 - 4.30.

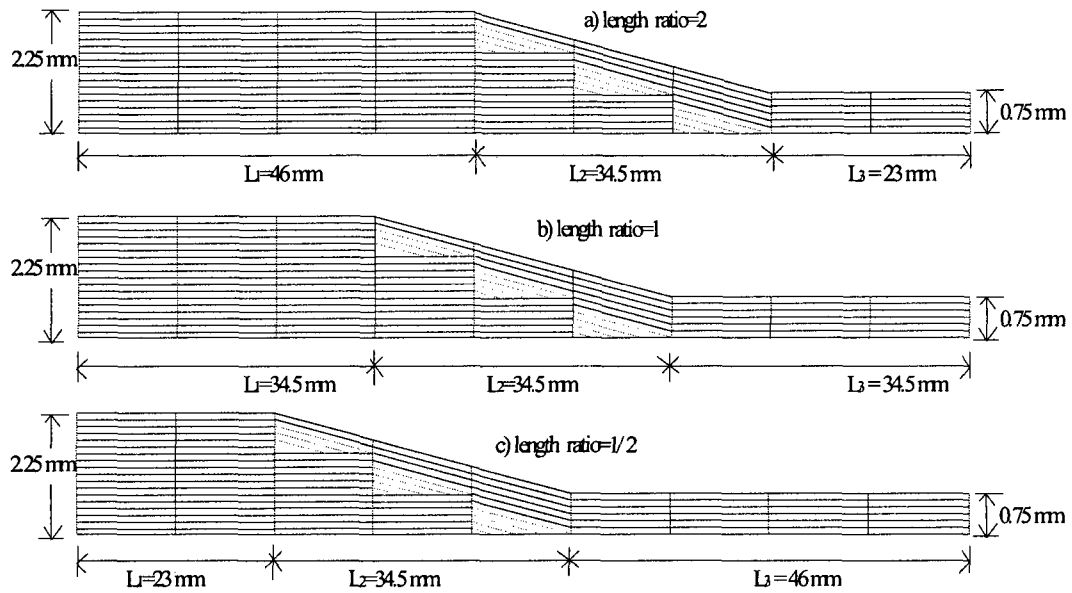


Figure 4. 10 Upper half of beam with taper configuration-D with 9-elements mesh

a) length ratio = 2, b) length ratio = 1, and c) length ratio = 1/ 2

Table 4. 28 Comparison of natural frequencies ($\times 10^4$ rad/sec) of beam with taper configuration-D for simply supported boundary condition

	Mode No.	Length ratio=2	Length ratio=1	Length ratio=1/2
CFE	Mode-1	0.6007	0.5019	0.4553
	Mode-2	2.3029	2.1871	1.8767
	Mode-3	5.0138	4.2610	4.2299
	Mode-4	8.6698	7.8495	7.1751
HOEF	Mode-1	0.6681	0.50176	0.4234
	Mode-2	3.0900	1.9191	1.2094
	Mode-3	4.0499	4.8536	3.4491
	Mode-4	7.3995	5.9560	6.3091

Table 4.29 Comparison of natural frequencies ($\times 10^4$ rad/sec) of beam with taper configuration-D for fixed-free boundary condition

	Mode No.	Length ratio=2	Length ratio=1	Length ratio=1/2
CFE	Mode-1	0.4683	0.3975	0.3082
	Mode-2	1.3924	1.1399	1.2141
	Mode-3	3.4676	3.2622	2.9460
	Mode-4	6.7701	5.8393	5.7597
HOEF	Mode-1	0.6172	0.4208	0.2446
	Mode-2	1.0234	1.0562	1.4212
	Mode-3	4.2351	2.7096	2.0382
	Mode-4	5.4614	6.0322	4.2415

Table 4.30 Comparison of natural frequencies ($\times 10^4$ rad/sec) of beam with taper configuration-D for fixed- fixed boundary condition

	Mode No.	Length ratio=2	Length ratio=1	Length ratio=1/2
CFE	Mode-1	1.1840	1.1145	1.2402
	Mode-2	3.4757	3.2910	2.9543
	Mode-3	6.8077	5.8467	5.7597
	Mode-4	1.10164	9.8673	9.1506
HOEF	Mode-1	1.1911	1.0664	1.4459
	Mode-2	4.2583	2.7470	2.0385
	Mode-3	5.5389	6.0289	4.2397
	Mode-4	8.3065	7.5693	7.0488

* CFE-Conventional finite element, HOFE-Higher order finite element.

As one can observe from the Tables 4.28-4.30, the natural frequencies of beam with higher length ratio values are the higher values and lower frequencies for beam with lower length ratio values for all boundary conditions respectively. Another important observation is that natural frequencies for fixed-free beam are the lowest and they are the highest for fixed-fixed (double clamped) for beam with taper configuration-D.

4.6 Effect of boundary condition on natural frequencies

To study the boundary condition effect on natural frequencies, the beam with taper configuration-C and D are considered as shown in Figures 4.3 and 4.4. The ply of composite beam is made of NCT/301 graphite-epoxy and the beam consists of 36 plies. The configuration of the thick sections is $[0/90]_{9s}$ and it is $[0/90]_{3s}$ in thin section.

The geometric properties of the beams are: It is considered with 36 and 12 plies at thick and thin sections respectively, which results in 24 drop-off plies, it is considered with 12-elements mesh and the length the beam is 0.0345m, height at thick section (h_1) is 0.0045m, height at thin section (h_2) is 0.0015m, individual ply thickness (t_k) is 0.000125m, width (b) is unity, and taper angle (ϕ) is 2.5°.

Example 4.6.1

By using the properties described in Example-4.2.1, the example 4.6.1 is solved to find the natural frequencies for (Thin end) fixed- (thick end) free, (Thick end) fixed- (thin end) hinged and (Thick end) hinged- (thin end) fixed boundary conditions of beam with taper configuration-C. The first four lowest frequencies for all boundary conditions are obtained considering 12-elements mesh and results are presented in Table 4.31.

Table 4. 31 Comparison of natural frequencies ($\times 10^4$ rad/sec) of beam with taper configuration-C for all boundary conditions

	Mode No.	(Thin)fixed- (thick)free	(Thick)fixed-(thin) hinged	(Thick) hinged- (thin) fixed
CFE	Mode-1	0.1309	1.3256	0.9938
	Mode-2	1.3565	4.0590	3.7105
	Mode-3	4.4729	8.6473	8.2364
	Mode-4	9.3939	15.4292	14.8824

- CFE-Conventional finite element

As one can observe from the Table 4.31, natural frequencies of beam with (Thin end) fixed- (thick end) free boundary condition are higher and they are lower for beam with (Thick end) hinged- (thin end) fixed boundary condition respectively for beam with taper configuration- C.

Example 4.6.2

By using the properties described in Example-4.2.1, the example 4.6.2 is solved to find the natural frequencies for (Thin end) fixed- (thick end) free, (Thick end) fixed- (thin end) hinged and (Thick end) hinged- (thin end) fixed boundary conditions of beam with taper configuration-D. The first four lowest frequencies for all boundary conditions are obtained considering 12-elements mesh and results are presented in Table 4.32.

Table 4. 32 Comparison of natural frequencies ($\times 10^4$ rad/sec) of beam with taper configuration-D for all boundary conditions

	Mode No.	(Thin)fixed- (thick)free	(Thick)fixed-(thin) hinged	(Thick) hinged- (thin) fixed
CFE	Mode-1	0.1585	1.2709	1.0324
	Mode-2	1.4312	3.9916	3.7849
	Mode-3	4.5857	8.5872	8.2813
	Mode-4	9.4997	15.3298	14.9606

*CFE-Conventional finite element

As one can observe from the Table 4.32, natural frequencies of beam with (Thin end) fixed-(thick end) free boundary condition are higher and they are lower for beam with (Thick end) hinged- (thin end) fixed boundary condition respectively for beam with taper configuration- D.

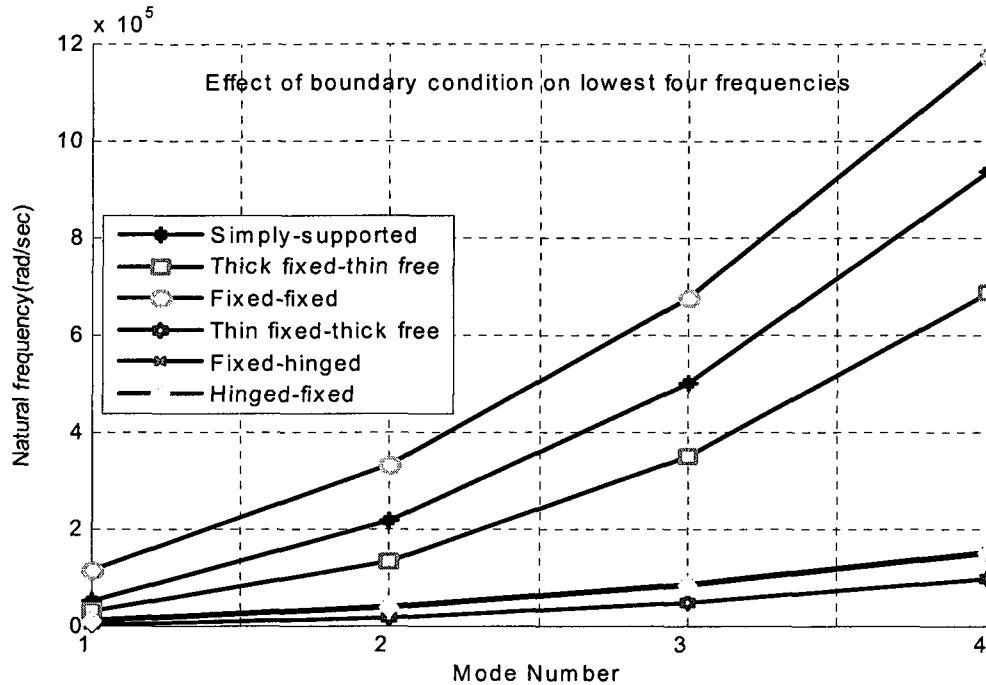


Figure 4. 11 Effect of boundary condition on lowest four natural frequencies of beam with taper configuration-D

One can observe the effects of boundary condition on natural frequencies of beam with taper configuration-D from the Figure 4.11. It shows that the beam with fixed-fixed boundary condition gives the highest natural frequencies which means that for this boundary condition the beam gets highest stiffness. Beam with (thin end) fixed- (thick end) free boundary condition gives the lowest natural frequencies which means that for this boundary condition the beam gets lowest stiffness. Then beam with simply supported, and (thick end) fixed- (thin end) free boundary conditions ranked second and third positions. Then beam with (thick end) fixed- (thin end) hinged and (thick end) hinged- (thin end) fixed boundary conditions give almost the same values of natural frequencies. That's why in the figure the corresponding curves overlap each other and they cannot be distinguished.

4.7 Effect of axial force on natural frequencies

To investigate the effect of applied axial (static) force on natural frequencies beam with taper configurations-A, B, C, and D are considered as shown in Figures 4.1-4.4. The ply of composite beam is made of NCT/301 graphite-epoxy and the beam consists of 36 plies. The configuration of the thick section is $[0/90]_{9s}$ and it is $[0/90]_{3s}$ at thin section. The geometric properties of the beams are: It is considered with 36 and 12 plies at thick and thin sections respectively, which results in 24 drop-off plies, it is considered with 12-elements mesh and the length the beam is 0.0345m, height at thick section (h_1) is 0.0045m, height at thin section (h_2) is 0.0015m, individual ply thickness (t_k) is 0.000125m, width (b) is unity, and taper angle (ϕ) is 2.5°.

Concentrated axial tensile (or compressive) force of 10000 N (less than the critical buckling load [29] for any type of taper configuration for any boundary condition) is applied at both ends of the beam and axially distributed tensile force of 10x N/m is applied over the beam span. The natural frequencies are calculated for all cases separately.

Example 4.7.1

By using the properties described in Example-4.2.1, the example 4.7.1 is solved to find the natural frequencies for simply supported, fixed-free and fixed-fixed boundary conditions of beam with taper configuration-A. The first four lowest frequencies for all boundary conditions are obtained considering 12-element mesh using higher-order finite element and results are presented in Tables 4.33 - 4.35.

Table 4. 33 Comparison of natural frequencies ($\times 10^4$ rad/sec) of beam with taper configuration-A for simply supported boundary condition

Mode No.	WOAF	WATF	WACF	WADTF
Mode-1	4.2527	4.4182	4.0798	4.2656
Mode-2	17.4172	17.5960	17.2362	17.5668
Mode-3	38.9803	39.1596	38.8000	38.4859
Mode-4	69.0901	69.2632	68.9166	69.3069

In Table 4.33 and in all tables of the present section, WOAF stands for ‘Without Axial Force’, WATF stands for ‘With Axial Tensile Force’, WACF stands for ‘With Axial Compressive Force’, and WADTF stands for ‘With Axially Distributed Tensile Force’.

Table 4.34 Comparison of natural frequencies ($\times 10^4$ rad/sec) of beam with taper configuration-A for fixed-free boundary condition

Mode No.	WOAF	WATF	WACF	WADTF
Mode-1	2.6107	2.8098	2.3798	2.5591
Mode-2	11.5448	11.8558	11.2189	11.2449
Mode-3	28.8744	29.1696	28.5745	28.6913
Mode-4	54.6452	54.9172	54.3712	53.6463

Table 4.35 Comparison of natural frequencies ($\times 10^4$ rad/sec) of beam with taper configuration-A for fixed-fixed boundary condition

Mode No.	WOAF	WATF	WACF	WADTF
Mode-1	9.6383	9.7316	9.5339	9.6998
Mode-2	26.6999	26.8263	26.5728	27.1687
Mode-3	52.4559	52.5910	52.3205	51.9630
Mode-4	86.7977	86.9332	86.6619	86.8507

As one can observe from the Tables 4.33-4.35, the natural frequencies of beam with axial tensile force are higher and the natural frequencies of beam with axial compressive force are lower than the natural frequencies of beam without axial force for all boundary conditions. Another interesting observation is that natural frequencies with axially distributed tensile force are higher for simply supported and fixed-fixed boundary conditions while for fixed-free beam are lower than the natural frequencies of beam without axial force with taper configuration-A.

Example 4.7.2

By using the properties described in Example-4.2.1, the example 4.7.2 is solved to find the natural frequencies for simply supported, fixed-free and fixed-fixed boundary conditions of beam with taper configuration-B. The first four lowest frequencies for all boundary conditions are obtained considering 12-elements mesh using higher-order finite element and results are presented in Tables 4.36 - 4.38.

Table 4.36 Comparison of natural frequencies ($\times 10^4$ rad/sec) of beam with taper configuration-B for simply supported boundary condition

Mode No.	WOAF	WATF	WACF	WADTF
Mode-1	4.5306	4.6822	4.3729	4.5596
Mode-2	17.7351	17.9090	17.5588	18.6742
Mode-3	39.6125	39.7879	39.4360	40.7678
Mode-4	69.4286	69.6017	69.2548	71.8041

Table 4.37 Comparison of natural frequencies ($\times 10^4$ rad/sec) of beam with taper configuration-B for fixed-free boundary condition.

Mode No.	WOAF	WATF	WACF	WADTF
Mode-1	2.8674	3.0509	2.6571	2.7734
Mode-2	11.8142	12.1165	11.4973	11.8362
Mode-3	29.1083	29.4034	28.8081	30.0957
Mode-4	55.3228	55.5932	55.0500	56.8168

Table 4.38 Comparison of natural frequencies ($\times 10^4$ rad/sec) of beam with taper configuration-B for fixed- fixed boundary condition

Mode No.	WOAF	WATF	WACF	WADTF
Mode-1	9.8561	9.9454	9.7657	10.2173
Mode-2	26.8954	27.0202	26.7698	28.4117
Mode-3	53.1272	53.2618	52.9920	54.8858
Mode-4	87.3191	87.4568	87.1823	89.7913

As one can observe from the Tables 4.36-4.38 the natural frequencies of beam with axial tensile force are higher and the natural frequencies of beam with axial compressive force are lower than the natural frequencies of beam without axial force for all boundary conditions. Another interesting observation is that natural frequencies with axially distributed tensile force are higher for simply supported and fixed-fixed boundary conditions while for fixed-free beam are lower than the natural frequencies of beam without axial force with taper configuration-B.

Example 4.7.3

By using the properties described in Example-4.2.1, the example 4.7.3 is solved to find the natural frequencies for simply supported, fixed-free and fixed-fixed boundary conditions of beam with taper configuration-C. The first four lowest frequencies for all boundary conditions are obtained considering 12-elements mesh using higher-order finite element and results are presented in Tables 4.39 - 4.41.

Table 4.39 Comparison of natural frequencies ($\times 10^4$ rad/sec) of beam with taper configuration-C for simply supported boundary condition

Mode No.	WOAF	WATF	WACF	WADTF
Mode-1	4.4752	4.6253	4.3188	4.4790
Mode-2	18.2687	18.4344	18.1011	18.7274
Mode-3	42.3035	42.4861	42.1197	41.0020
Mode-4	73.2632	73.4322	73.0938	73.8754

Table 4. 40 Comparison of natural frequencies ($\times 10^4$ rad/sec) of beam with taper configuration-C for fixed-free boundary condition.

Mode No.	WOAF	WATF	WACF	WADTF
Mode-1	2.9244	3.0777	2.7517	2.8753
Mode-2	12.7897	13.1377	12.4209	12.1266
Mode-3	30.2017	30.4919	29.9074	30.7535
Mode-4	59.1343	59.4361	58.8295	57.5790

Table 4. 41 Comparison of natural frequencies ($\times 10^4$ rad/sec) of beam with taper configuration-C for fixed- fixed boundary condition

Mode No.	WOAF	WATF	WACF	WADTF
Mode-1	10.4273	10.5038	10.3501	10.4610
Mode-2	30.6978	30.7993	30.5958	29.1176
Mode-3	61.9033	62.0162	61.7901	55.4786
Mode-4	100.0800	100.2010	99.9646	92.6641

As one can observe from the Tables 4.39-4.41, the natural frequencies of beam with axial tensile force are higher and the natural frequencies of beam with axial compressive force are lower than the natural frequencies of beam without axial force for all boundary conditions. Another interesting observation is that natural frequencies with axially distributed tensile force are higher for simply supported and fixed-fixed boundary conditions while for fixed-free beam are lower than the natural frequencies of beam without axial force with taper configuration-C.

Example 4.7.4

By using the properties described in Example-4.2.1, the example 4.7.4 is solved to find the natural frequencies for simply supported, fixed-free and fixed-fixed boundary conditions of beam with taper configuration-D. The first four lowest frequencies for all boundary conditions are obtained considering 12-elements mesh using higher-order finite element and results are presented in Tables 4.42 - 4.44.

Table 4. 42 Comparison of natural frequencies ($\times 10^4$ rad/sec) of beam with taper configuration-D for simply supported boundary condition

Mode No.	WOAF	WATF	WACF	WADTF
Mode-1	5.1732	5.3139	5.0282	5.2992
Mode-2	21.5338	21.6851	21.3811	22.0223
Mode-3	48.7402	48.8907	48.5891	43.3654
Mode-4	85.1541	85.3001	85.0077	56.3360

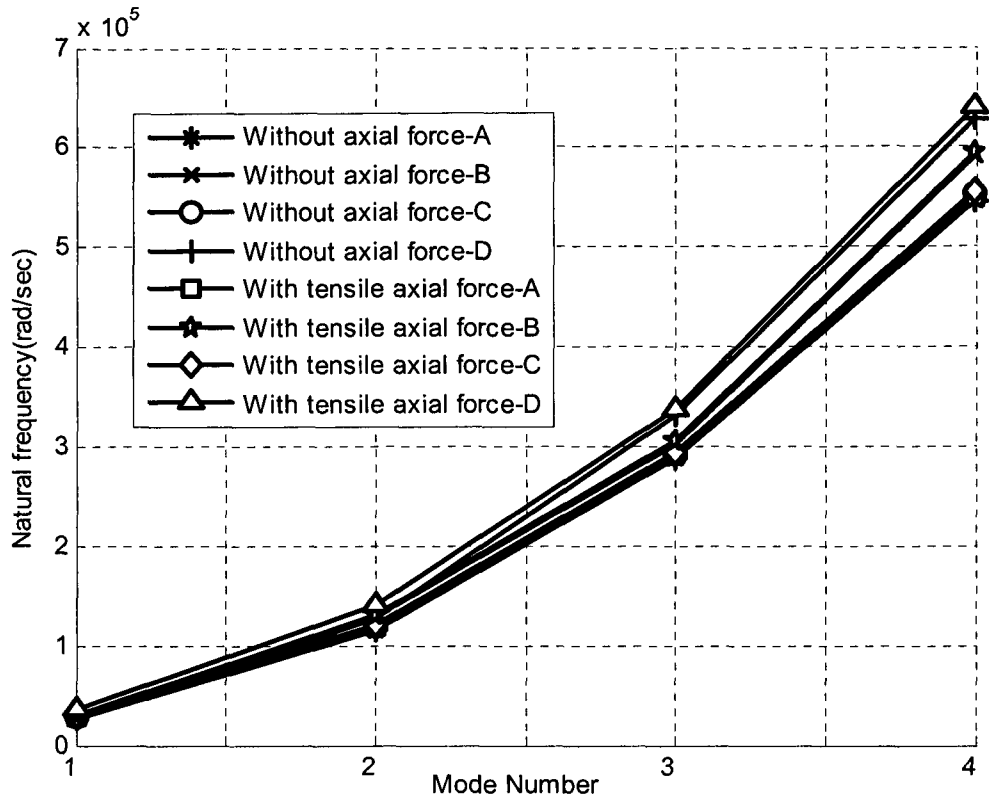
Table 4.43 Comparison of natural frequencies ($\times 10^4$ rad/sec) of beam with taper configuration-D for fixed-free boundary condition.

Mode No.	WOAF	WATF	WACF	WADTF
Mode-1	2.7997	3.5433	2.4421	2.4906
Mode-2	12.7427	14.0389	10.6877	10.2991
Mode-3	33.1539	33.6477	26.7190	25.4069
Mode-4	62.7518	64.0402	51.9969	58.6197

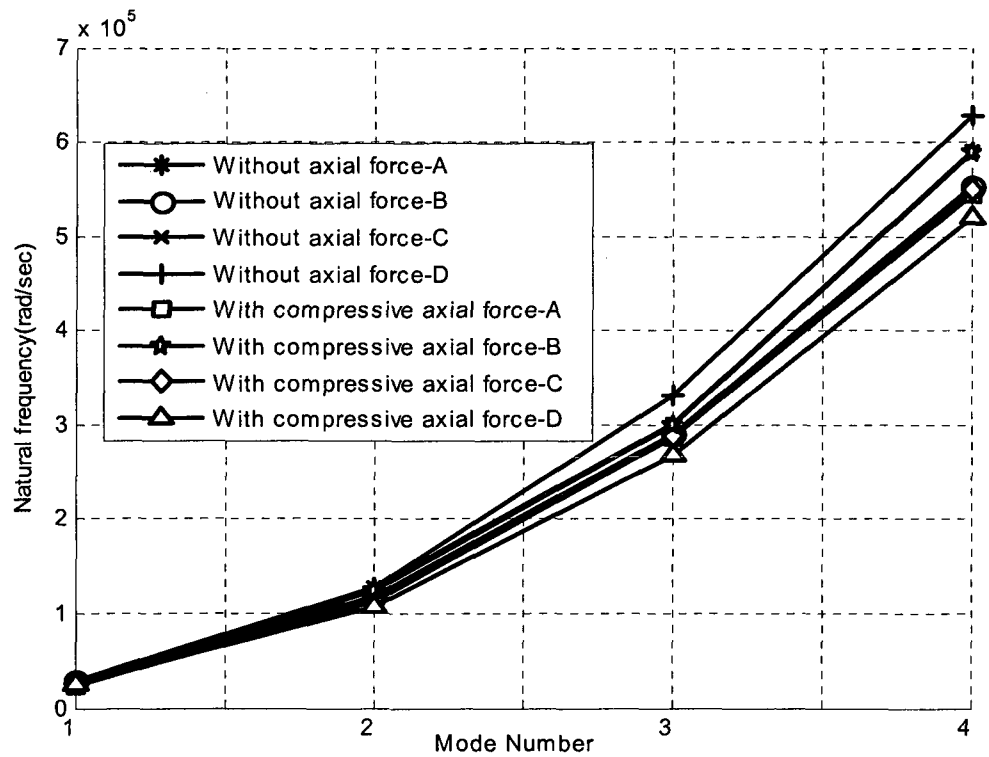
Table 4.44 Comparison of natural frequencies ($\times 10^4$ rad/sec) of beam with taper configuration-D for fixed- fixed boundary condition

Mode No.	WOAF	WATF	WACF	WADTF
Mode-1	11.6828	12.8267	9.7021	11.8736
Mode-2	31.7390	33.3609	28.2808	29.0816
Mode-3	62.8098	64.5596	57.7166	60.2187
Mode-4	101.6720	103.5130	94.3874	105.9320

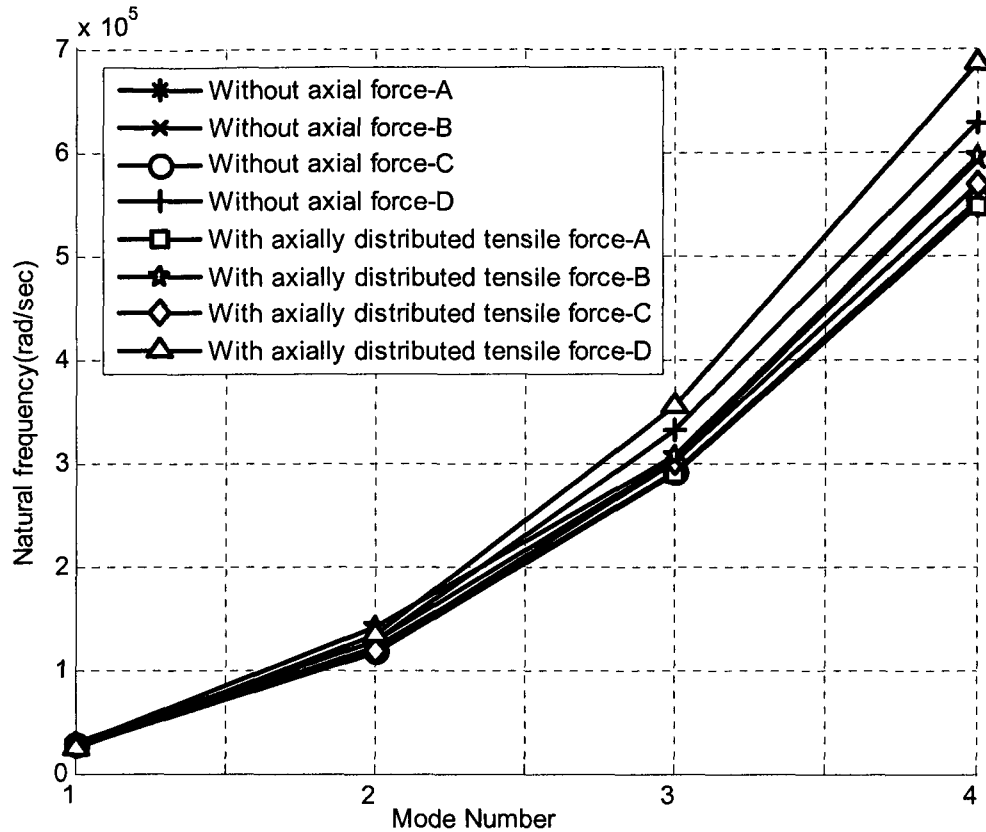
As one can observe from the Tables 4.42-4.44, the natural frequencies of beam with axial tensile force are higher and the natural frequencies of beam with axial compressive force are lower than the natural frequencies of beam without axial force for all boundary conditions. Another interesting observation is that natural frequencies with axially distributed tensile force are higher for simply supported and fixed-fixed boundary conditions while for fixed-free beam are lower than the natural frequencies of beam without axial force with taper configuration-D.



a) Effect of axial tensile force on lowest four natural frequencies



b) Effect of axial compressive force on lowest four natural frequencies



c) Effect of axially distributed tensile force on lowest four natural frequencies

Figure 4. 12 Effect of applied static axial force on lowest four natural frequencies of different beam configurations for fixed-free boundary condition, a) Tensile axial force, b) Compressive axial force, and c) Axially distributed tensile force

One can observe the effect of axial force on natural frequencies for different taper configurations beam for fixed-free boundary condition from the Figure 4.12 at a glance. The results obtained for the beam with and without axial force show that the effect of axial force on natural frequencies obtained for beam with configuration-D are highest and beam with configuration-A are lowest for axial tensile, axial compressive and axially distributed tensile force.

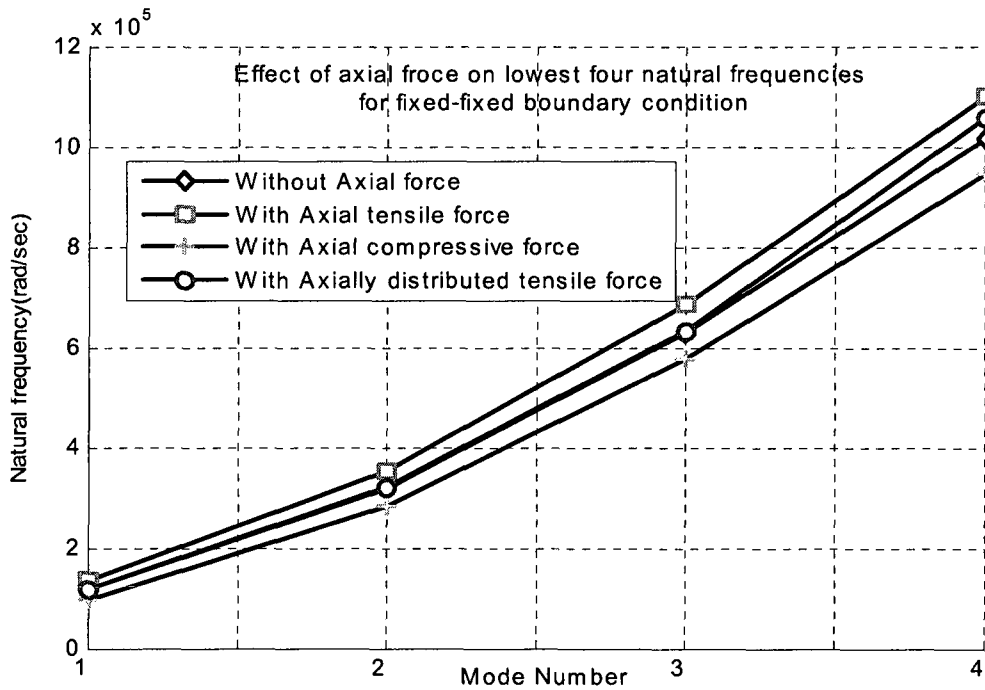
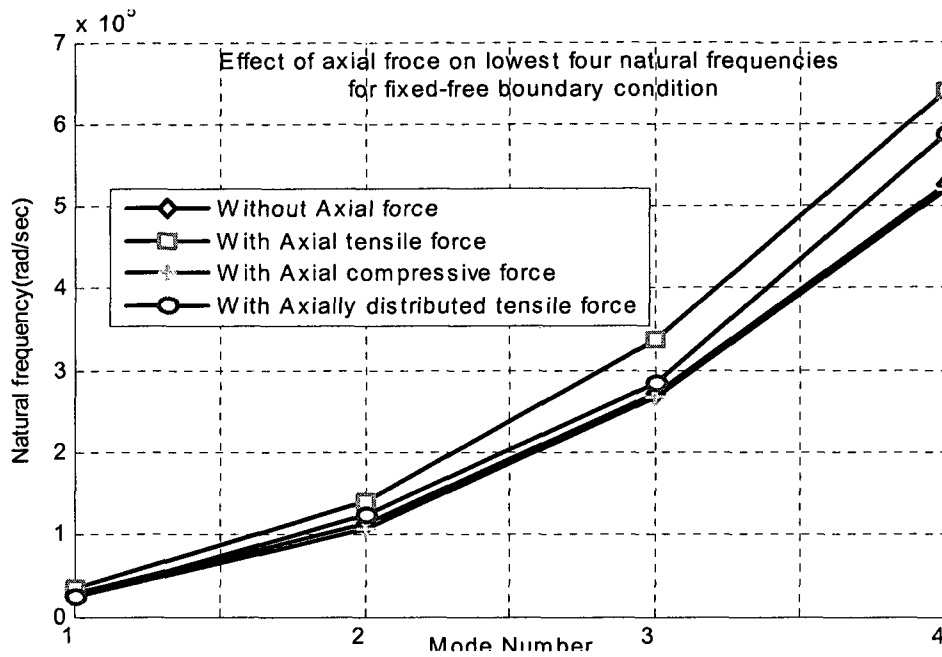


Figure 4. 13 Effect of applied static axial force on lowest four natural frequencies for a) fixed-free and b) fixed-fixed boundary conditions of beam with taper configuration-D

One can observe the effect of applied static axial force on natural frequencies of beam with taper configuration-D for fixed-free and fixed-fixed boundary conditions from the Figure 4.13. The results obtained for the beam with and without axial force show that natural frequencies obtained from considering the axial tensile force are more and considering the axial compressive force are less than the natural frequencies obtained without considering axial force. The results obtained for the beam with and without axially distributed tensile force show that natural frequencies obtained from considering the axially distributed tensile force are a little bit more up to first three natural frequencies than the natural frequencies obtained without considering axial force but the fourth lowest natural frequencies increases significantly for both boundary conditions.

Example 4.7.5

By using the properties described in Example-4.2.1, the example 4.7.5 is solved to investigate the effect of different laminate configuration on the natural frequencies for fixed-fixed boundary conditions of beam with taper configuration-A. The first four lowest frequencies are obtained considering 12-element mesh using higher-order finite element and results are presented in Table 4.45.

Table 4.45 Comparison of natural frequencies ($\times 10^4$ rad/sec) of beam with taper configuration-A for fixed-fixed boundary condition

	Mode No.	LC-1	LC-2	LC-3
WOAF	Mode-1	9.6383	6.9107	11.7199
	Mode-2	26.6999	19.1358	32.4743
	Mode-3	52.4559	37.5878	63.8079
	Mode-4	86.7977	62.1890	105.588
WATF	Mode-1	9.7316	7.0413	11.7966
	Mode-2	26.8263	19.3134	32.5781
	Mode-3	52.5910	37.7779	63.9188
	Mode-4	86.9332	62.3799	105.6990
WACF	Mode-1	9.5339	6.7770	11.6426
	Mode-2	26.5728	18.9561	32.3701
	Mode-3	52.3205	37.3965	63.6969
	Mode-4	86.6619	61.9974	105.4770

One can observe the effect of axial force on natural frequencies for different laminate configurations of beam with taper configuration-A for fixed-fixed boundary condition from the Table 4.45. The natural frequencies of beam with tensile axial force are higher than the natural frequencies of beam without axial force and the natural frequencies of beam with compressive axial force are lower than the natural frequencies of beam without axial force for all laminate configurations respectively.

Example 4.7.6

By using the properties described in Example-4.2.1, the example 4.7.6 is solved to investigate the effect of different concentrated axial force on the natural frequencies for fixed-fixed boundary conditions of beam with taper configuration-C and D. The load is increased by 10%, 20%, 50% and 100% of 10000 N for both tensile and compressive cases. The first four lowest frequencies are obtained considering 12-elements mesh using higher-order finite element and results are presented in Tables 4.46 – 4.47.

Table 4. 46 Comparison of natural frequencies ($\times 10^4$ rad/sec) of beam with taper configuration-C for fixed-fixed boundary condition

Axial Load	Mode No.	WOAF	WATF	% of difference with WOAF	WACF	% of difference with WOAF
10000 N/m (T/C)	Mode-1	10.4273	10.5038	0.7337	10.3501	0.7404
	Mode-2	30.6978	30.7993	0.3306	30.5958	0.3323
	Mode-3	61.9033	62.0162	0.1824	61.7901	0.1829
	Mode-4	100.0800	100.2010	0.1209	99.9646	0.1153
11000 N/m (T/C)	Mode-1	10.4273	10.5114	0.8065	10.3423	0.8152
	Mode-2	30.6978	30.8095	0.3639	30.5856	0.3655
	Mode-3	61.9033	62.0275	0.2006	61.7788	0.2011
	Mode-4	100.0800	100.2130	0.1329	99.9528	0.1271
12000 N/m (T/C)	Mode-1	10.4273	10.5190	0.8794	10.3346	0.889
	Mode-2	30.6978	30.8196	0.3968	30.5754	0.3987
	Mode-3	61.9033	62.0388	0.2189	61.7674	0.2195
	Mode-4	100.0800	100.224	0.1439	99.9410	0.1389
15000 N/m (T/C)	Mode-1	10.4273	10.5418	1.0981	10.3112	1.1134
	Mode-2	30.6978	30.8500	0.4958	30.5447	0.4987
	Mode-3	61.9033	62.0726	0.2735	61.7334	0.2745
	Mode-4	100.0800	100.2600	0.1799	99.9054	0.1745
20000 N/m (T/C)	Mode-1	10.4273	10.5795	1.4596	10.2720	1.4894
	Mode-2	30.6978	30.9005	0.6603	30.4934	0.6658
	Mode-3	61.9033	62.1289	0.3644	61.6766	0.3662
	Mode-4	100.0800	100.3190	0.2388	99.8462	0.2336

Table 4.47 Comparison of natural frequencies ($\times 10^4$ rad/sec) of beam with taper configuration-D for fixed-fixed boundary condition

Axial Load	Mode No.	WOAF	WATF	% of difference with WOAF	WACF	% of difference with WOAF
10000 N/m (T/C)	Mode-1	11.6828	12.8267	9.791	9.7021	16.95
	Mode-2	31.7390	33.3609	5.11	28.2808	10.9
	Mode-3	62.8098	64.5596	2.786	57.7166	8.109
	Mode-4	101.6720	103.5130	1.811	94.3874	7.165
11000 N/m (T/C)	Mode-1	11.6828	12.9340	10.71	9.5470	18.28
	Mode-2	31.7390	33.5178	5.604	28.0884	11.5
	Mode-3	62.8098	64.7313	3.059	57.5184	8.424
	Mode-4	101.6720	103.6950	1.99	94.1840	7.365
12000 N/m (T/C)	Mode-1	11.6828	13.0401	11.62	9.3887	19.64
	Mode-2	31.7390	33.6739	6.096	27.8944	12.11
	Mode-3	62.8098	64.9025	3.332	57.3194	8.741
	Mode-4	101.6720	103.8770	2.169	93.9801	7.565
15000 N/m (T/C)	Mode-1	11.6828	13.3520	14.29	8.8925	23.88
	Mode-2	31.7390	34.1368	7.555	27.3026	13.98
	Mode-3	62.8098	65.4127	4.144	56.7170	9.70
	Mode-4	101.6720	104.4190	2.702	93.3654	8.17
20000 N/m (T/C)	Mode-1	11.6828	13.8518	18.57	7.9769	31.72
	Mode-2	31.7390	34.8915	9.933	26.2815	17.19
	Mode-3	62.8098	66.2520	5.48	55.6952	11.33
	Mode-4	101.6720	105.3160	3.584	92.3307	9.18

As one can observe from the Tables 4.46- 4.47, that the percentage of difference of natural frequencies does not change much for beam with configuration-C where this effect is more for beam with taper configuration-D with the increment of the value of axial force. It can be also observed that percentage of difference is decreasing with the increasing of natural frequency mode number.

4.8 Effect of damping on natural frequencies

To investigate the effect of damping on natural frequencies, beam with taper configurations-A, B, C and D are considered as shown in Figures 4.1-4.4. The ply of composite beam is made of NCT/301 graphite-epoxy and the beam consists of 36 plies. The configuration of the thick sections is $[0/90]_{9s}$, and it is $[0/90]_{3s}$ in thin section.

The geometric properties of the beams are: It is considered with 36 and 12 plies at thick and thin sections respectively, which results in 24 drop-off plies. It is considered with 12-elements mesh and the length the beam is 0.0345m, height at thick section (h_1) is 0.0045m, height at thin section (h_2) is 0.0015m, individual ply thickness (t_k) is 0.000125m, width (b) is unity, and taper angle (ϕ) is 2.5° . The mass proportional constant, (α) and stiffness proportional constant (β) are 2.195 and 2.6085×10^{-6} respectively.

Example 4.8.1

By using the properties described in Example-4.2.1, the example 4.8.1 is solved to find the natural frequencies for simply supported, fixed-free and fixed-fixed boundary conditions of beam with taper configuration-A. The first four lowest frequencies for all boundary conditions are obtained considering 12-elements mesh and 5-terms for Rayleigh-Ritz method and results are presented in Tables 4.48 - 4.50.

Table 4. 48 Comparison of natural frequencies ($\times 10^4$ rad/sec) of beam with taper configuration-A for simply supported boundary condition

	Mode No.	Conventional finite element	Higher-order finite element	Rayleigh-Ritz Method
DA	Mode-1	4.1475	4.1330	4.1389
	Mode-2	15.3752	15.3125	14.8256
	Mode-3	27.3987	27.3306	26.7743
	Mode-4	51.2566	51.7266	45.0584
UNDA	Mode-1	4.2681	4.2527	4.2589
	Mode-2	17.5022	17.4172	16.7736
	Mode-3	39.1829	38.9803	37.4204
	Mode-4	69.5000	69.0901	73.4496

*DA-Damped, UNDA-Undamped

Table 4.49 Comparison of natural frequencies ($\times 10^4$ rad/sec) of beam with taper configuration-A for fixed-free boundary condition

	Mode No.	Conventional finite element	Higher-order finite element	Rayleigh-Ritz Method
DA	Mode-1	2.5891	2.5658	2.4763
	Mode-2	10.6976	10.6401	11.7636
	Mode-3	22.8824	22.7980	25.3318
	Mode-4	29.2493	29.2894	29.4899
UNDA	Mode-1	2.6349	2.6107	2.5180
	Mode-2	11.6133	11.5448	12.8986
	Mode-3	29.0281	28.8744	33.9266
	Mode-4	54.9424	54.6452	70.1266

*DA-Damped, UNDA-Un-damped

Table 4.50 Comparison of natural frequencies ($\times 10^4 \text{rad/sec}$) of beam with taper configuration-A for fixed-fixed boundary condition

	Mode No.	Conventional finite element	Higher-order finite element	Rayleigh-Ritz Method
DA	Mode-1	9.0631	9.0121	9.0648
	Mode-2	21.6466	21.5553	21.5316
	Mode-3	29.4932	29.4801	29.4712
	Mode-4	32.7292	31.5423	36.3773
UNDA	Mode-1	9.6971	9.6383	9.7036
	Mode-2	26.8546	26.6999	26.660
	Mode-3	52.7769	52.4559	52.6338
	Mode-4	87.4195	86.7977	89.3744

*DA-Damped, UNDA-Un-damped

As one can observe from the Tables 4.48-4.50, the natural frequencies of un-damped beam are higher than the natural frequencies with damping for all boundary conditions. Another important observation is that natural frequencies for fixed-free beam are the lowest and for fixed-fixed (double clamped) they are highest for beam with taper configuration-A.

Example 4.8.2

By using the properties described in Example-4.2.1, the example 4.8.2 is solved to find the natural frequencies for simply supported, fixed-free and fixed-fixed boundary conditions of beam with taper configuration-B. The first four lowest frequencies for all boundary conditions are obtained considering 12-elements mesh and 5-terms for Rayleigh-Ritz method and results are presented in Tables 4.51 - 4.53.

Table 4.51 Comparison of natural frequencies ($\times 10^4$ rad/sec) of beam with taper configuration-B for simply supported boundary condition

	Mode No.	Conventional finite element	Higher-order finite element	Rayleigh-Ritz Method
DA	Mode-1	4.4038	4.3947	4.4015
	Mode-2	16.3157	15.5491	16.0822
	Mode-3	28.6981	27.5399	27.7074
	Mode-4	60.0972	51.3402	39.2112
UNDA	Mode-1	4.5403	4.5306	4.5379
	Mode-2	18.7760	17.7351	18.4564
	Mode-3	43.8864	39.6125	40.1403
	Mode-4	81.3516	69.4286	76.7818

Table 4. 52 Comparison of natural frequencies ($\times 10^4$ rad/sec) of beam with taper configuration-B for fixed-free boundary condition

	Mode No.	Conventional finite element	Higher-order finite element	Rayleigh-Ritz Method
DA	Mode-1	2.7863	2.8132	2.6673
	Mode-2	11.0682	10.8658	10.7669
	Mode-3	23.6430	22.9263	23.3467
	Mode-4	28.0454	29.1929	28.5369
UNDA	Mode-1	2.8394	2.8674	2.7159
	Mode-2	12.0568	11.8142	11.6960
	Mode-3	30.4511	29.1083	29.8880
	Mode-4	59.8188	55.3228	58.3052

Table 4.53 Comparison of natural frequencies ($\times 10^4$ rad/sec) of beam with taper configuration-B for fixed-fixed boundary condition

	Mode No.	Conventional finite element	Higher-order finite element	Rayleigh-Ritz Method
DA	Mode-1	9.4757	9.2008	9.3757
	Mode-2	22.6916	21.6706	22.3854
	Mode-3	28.3088	29.4406	29.3438
	Mode-4	58.4996	52.5385	40.8436
UNDA	Mode-1	10.1750	9.8561	10.0588
	Mode-2	28.6821	26.8954	2.1352
	Mode-3	59.0518	53.1272	54.1915
	Mode-4	101.928	87.3191	91.8375

*DA-Damped, UNDA-Un-damped

As one can observe from the Tables 4.51-4.53, the natural frequencies of un-damped beam are higher than the natural frequencies with damping for all boundary conditions. Another important observation is that natural frequencies for fixed-free beam are the lowest and for fixed-fixed (double clamped) they are highest for beam with taper configuration-B.

Example 4.8.3

By using the properties described in Example-4.2.1, the example 4.8.3 is solved to find the natural frequencies for simply supported, fixed-free and fixed-fixed boundary conditions of beam with taper configuration-C. The first four lowest frequencies for all boundary conditions are obtained considering 12-elements mesh and 5-terms for Rayleigh-Ritz method and results are presented in Tables 4.54 - 4.56.

Table 4.54 Comparison of natural frequencies ($\times 10^4$ rad/sec) of beam with taper configuration-C for simply supported boundary condition

	Mode No.	Conventional finite element	Higher-order finite element	Rayleigh-Ritz Method
DA	Mode-1	4.3849	4.3426	4.3456
	Mode-2	16.6798	15.9443	15.5217
	Mode-3	28.9433	28.3229	27.2873
	Mode-4	48.9433	54.4850	60.005
UNDA	Mode-1	4.5203	4.4752	4.4784
	Mode-2	19.2789	18.2687	17.6983
	Mode-3	45.1144	42.3035	38.8529
	Mode-4	84.2137	73.2632	77.1363

*DA-Damped, UNDA-Un-damped

Table 4.55 Comparison of natural frequencies ($\times 10^4$ rad/sec) of beam with taper configuration-C for fixed-free boundary condition

	Mode No.	Conventional finite element	Higher-order finite element	Rayleigh-Ritz Method
DA	Mode-1	2.8974	2.8680	2.7914
	Mode-2	11.4695	11.6742	11.9018
	Mode-3	24.2305	23.5125	25.0225
	Mode-4	27.2608	28.2819	28.9527
UNDA	Mode-1	2.9549	2.9244	2.8447
	Mode-2	12.5410	12.7897	13.0675
	Mode-3	31.6047	30.2017	33.2505
	Mode-4	61.7094	59.1343	65.5679

Table 4.56 Comparison of natural frequencies ($\times 10^4$ rad/sec) of beam with taper configuration-C for fixed-fixed boundary condition

	Mode No.	Conventional finite element	Higher-order finite element	Rayleigh-Ritz Method
DA	Mode-1	9.8011	9.6922	9.7374
	Mode-2	23.3121	23.7732	22.6376
	Mode-3	27.5929	27.1687	29.2515
	Mode-4	64.8392	55.3028	45.7245
UNDA	Mode-1	10.5546	10.4273	10.4801
	Mode-2	29.8230	30.6978	28.5848
	Mode-3	60.9670	61.9033	54.9271
	Mode-4	105.586	100.08	94.5890

As one can observe from the Tables 4.54-4.56, the natural frequencies of un-damped beam are higher than the natural frequencies with damping for all boundary conditions. Another important observation is that natural frequencies for fixed-free beam are the lowest and for fixed-fixed (double clamped) they are highest for beam with taper configuration-C.

Example 4.8.4

By using the properties described in Example-4.2.1, the example 4.8.4 is solved to find the natural frequencies for simply supported, fixed-free and fixed-fixed boundary conditions of beam with taper configuration-D. The first four lowest frequencies for all boundary conditions are obtained considering 12-elements mesh and 5-terms for Rayleigh-Ritz method and results are presented in Tables 4.57- 4.59.

Table 4. 57 Comparison of natural frequencies ($\times 10^4$ rad/sec) of beam with taper configuration-D for simply supported boundary condition

	Mode No.	Conventional finite element	Higher-order finite element	Rayleigh-Ritz Method
DA	Mode-1	4.9572	4.9956	4.9609
	Mode-2	18.3298	18.2611	20.8213
	Mode-3	29.4951	29.4184	28.4813
	Mode-4	73.8702	78.3223	76.5831
UNDA	Mode-1	5.1320	5.1732	5.1360
	Mode-2	21.6346	21.5338	25.4821
	Mode-3	50.1385	48.7402	58.4958
	Mode-4	93.5380	85.1541	112.318

Table 4. 58 Comparison of natural frequencies ($\times 10^4$ rad/sec) of beam with taper configuration-D for fixed-free boundary condition

	Mode No.	Conventional finite element	Higher-order finite element	Rayleigh-Ritz Method
DA	Mode-1	2.7710	2.7790	2.7363
	Mode-2	12.0431	10.4295	9.0708
	Mode-3	25.7638	21.8861	22.0830
	Mode-4	32.1882	29.4780	35.7845
UNDA	Mode-1	2.8236	2.8316	2.7875
	Mode-2	13.2406	11.2947	9.7060
	Mode-3	34.9084	27.2641	2.7604
	Mode-4	68.667	52.4998	155.587

Table 4.59 Comparison of natural frequencies ($\times 10^4$ rad/sec) of beam with taper configuration-D for fixed- fixed boundary condition

	Mode No.	Conventional finite element	Higher-order finite element	Rayleigh-Ritz Method
DA	Mode-1	10.5709	10.7559	10.4844
	Mode-2	24.9181	24.2972	24.4037
	Mode-3	29.1938	26.7071	28.4978
	Mode-4	85.2068	58.0562	62.4812
UNDA	Mode-1	11.4625	11.6828	11.3597
	Mode-2	33.0267	31.7390	31.9551
	Mode-3	67.6632	62.8098	66.1598
	Mode-4	117.199	101.672	132.188

As one can observe from the Tables 4.57-4.59, the natural frequencies of un-damped beam are higher than the natural frequencies with damping for all boundary conditions. Another important observation is that natural frequencies for fixed-free beam are the lowest and they are highest for fixed-fixed (double clamped) for beam with taper configuration-D.

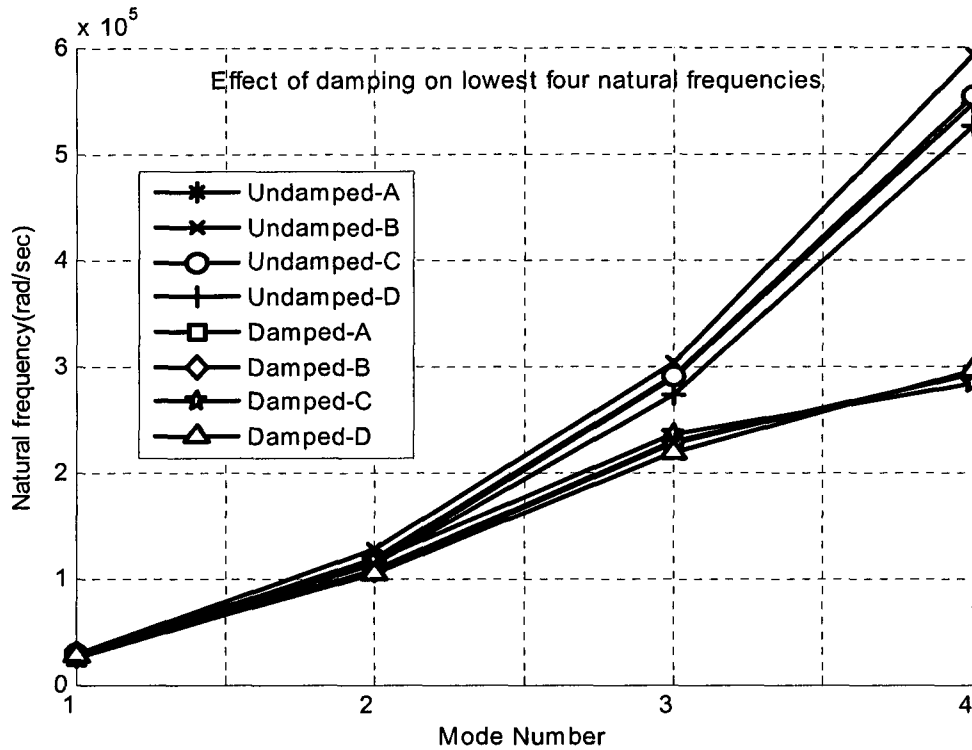


Figure 4. 14 Effect of damping on lowest four natural frequencies for fixed-free boundary condition

One can observe the effect of damping loss factor on natural frequencies of beam for different taper configurations for fixed-free boundary condition from the Figure 4.14. The results obtained for the beam with and without damping show that natural frequencies obtained considering damping loss are less than the natural frequencies obtained considering without damping loss but for fourth mode it is very significant for all taper configurations.

Example 4.8.5

By using the properties described in Example-4.2.1, the example 4.8.5 is solved to find the natural frequencies of different laminate configurations of beam with taper configuration-B for simply supported boundary condition. The first four lowest frequencies are obtained considering 12-elements mesh using higher-order finite element and results are presented in Table 4.60.

Table 4.60 Comparison of natural frequencies ($\times 10^4$ rad/sec) of beam with taper configuration-B for simply supported boundary condition

	Mode No.	LC-1	LC-2	LC-3
DA	Mode-1	4.3947	3.3363	5.2020
	Mode-2	15.5491	11.6691	18.2226
	Mode-3	27.5399	22.4955	29.3610
	Mode-4	51.3402	39.4758	65.8523
UNDA	Mode-1	4.5306	3.4132	5.3953
	Mode-2	17.7351	12.7835	21.4827
	Mode-3	39.6125	28.3306	48.0817
	Mode-4	69.4286	49.6576	84.2981

As one can observe from the Tables 4.60, One can observe the effects of different laminate configurations on damped natural frequencies of beam with taper configuration-B for simply supported boundary condition. The results obtained for different types of laminate configuration show that like un-damped natural frequencies, damped frequencies obtained

from laminate configuration LC-3 gives the highest values; then laminate configuration LC-1 ranked second and laminate configuration LC-2 gives the lowest values.

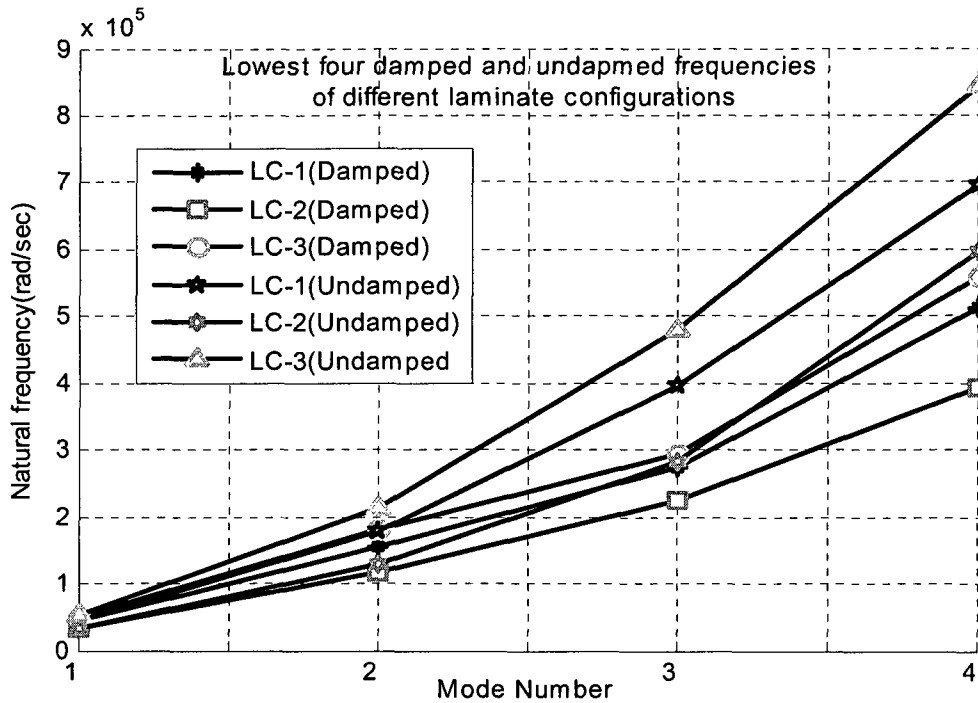


Figure 4. 15 Effect of damping on lowest four natural frequencies for simply supported boundary condition of beam with taper configuration-B

One can observe the effect of damping on natural frequencies for different laminate configurations of beam with taper configuration-B for simply supported boundary condition from the Figure 4.15. The difference between damped and un-damped natural frequencies for 3rd and 4th modes is more significant while for other modes the difference is a little bit less.

Example 4.8.6

By using the properties described in Example-4.2.1, the example 4.8.6 is solved to find the natural frequencies with the variation of damping properties of beam with taper configurations-C and D for fixed-free boundary condition. The properties is observed in three

different cases: Case-1) The value of both the mass proportional constant, (α) and stiffness proportional constant (β) were increased by 10%, 20%, 50%, 75%, 100% of the original value, Cases-2) when mass proportional constant is increased by 10%, 20%, 50%, 75%, 100% of the original value and stiffness proportional constant is kept constant, and Case-3) when stiffness proportional constant is increased by 10%, 20%, 50%, 75%, 100% of the original value and mass proportional constant is kept constant respectively and the effect on damped frequencies was observed. The first four lowest frequencies are obtained considering 12-elements mesh using higher-order finite element and percentage of difference is calculated with respect to un-damped natural frequencies and results are presented in Tables 4.61-4.66.

Table 4.61 Comparison of natural frequencies ($\times 10^4$ rad/sec) of beam with taper configuration-C for fixed-free boundary condition for case-1.

α and β	Mode No.	Damped	Un-damped	% of difference
$\alpha = 2.195$ $\beta = 2.608 \times 10^{-6}$	Mode-1	2.8680	2.9244	1.967
	Mode-2	11.6742	12.7897	9.555
	Mode-3	23.5125	30.2017	28.45
	Mode-4	28.2819	59.1343	109.1
$\alpha = 2.4145$ $\beta = 2.869 \times 10^{-6}$	Mode-1	2.8623	2.9244	2.17
	Mode-2	11.5568	12.7897	10.67
	Mode-3	22.7356	30.2017	32.84
	Mode-4	28.0254	59.1343	111
$\alpha = 2.634$ $\beta = 3.130 \times 10^{-6}$	Mode-1	2.8566	2.9244	2.373
	Mode-2	11.4381	12.7897	11.82
	Mode-3	21.9312	30.2017	37.71
	Mode-4	26.1360	59.1343	126.3
$\alpha = 3.2925$ $\beta = 3.912 \times 10^{-6}$	Mode-1	2.8394	2.9244	2.994
	Mode-2	11.0745	12.7897	15.49
	Mode-3	19.3181	30.2017	56.34
	Mode-4	24.4228	59.1343	152.5
$\alpha = 3.84125$ $\beta = 4.568 \times 10^{-6}$	Mode-1	2.8250	2.9244	3.519
	Mode-2	10.7621	12.7897	18.84
	Mode-3	16.8334	30.2017	79.42
	Mode-4	23.1696	59.1343	155.2
$\alpha = 4.39$ $\beta = 5.217 \times 10^{-6}$	Mode-1	2.8105	2.9244	4.053
	Mode-2	10.4403	12.7897	22.5
	Mode-3	13.9118	30.2017	117.1
	Mode-4	22.5560	59.1343	162.2

It is observed from the Table 4.61 that with the increment of both the value of mass proportional constant and stiffness proportional constant, the percentage of difference of damped frequencies does not change linearly. It is also observed that change in fourth and third modes of damped natural frequencies is a little bit more significant with un-damped natural frequencies than the first and second modes.

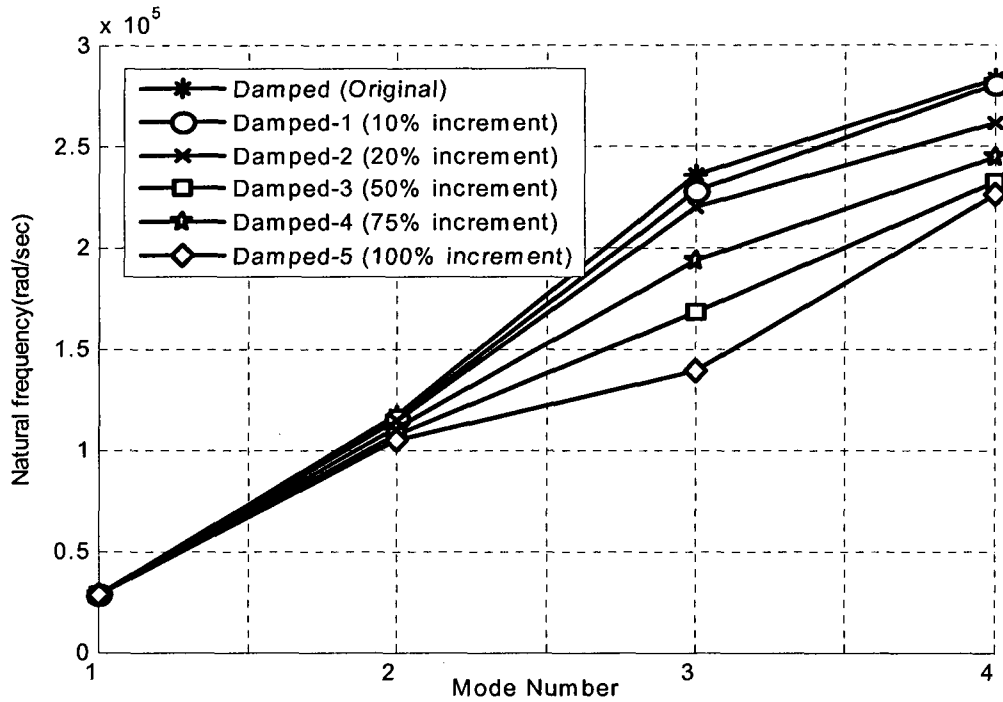


Figure 4. 16 Effect of damping properties on lowest four natural frequencies for fixed-free boundary condition of beam with taper configuration-C for case-1

One can observe the effect of different values of stiffness and mass proportional constant on damped natural frequencies of beam with taper configuration-C for fixed-free boundary condition from the Figure 4.16. The results obtained for the beam with different values of stiffness and mass proportional constant show that damped natural frequencies obtained considering different values of stiffness and mass proportional constant are almost same up to 2nd mode but difference among the 3rd and 4th modes are little bit more.

Table 4. 62 Comparison of natural frequencies ($\times 10^4$ rad/sec) of beam with taper configuration-C for fixed-free boundary condition for case-2

α and β	Mode No.	Damped	Un-damped	% of difference
$\alpha = 2.195$ $\beta = 2.6085 \times 10^{-6}$	Mode-1	2.8680	2.9244	1.967
	Mode-2	11.6742	12.7897	9.555
	Mode-3	23.5125	30.2017	28.45
	Mode-4	28.2819	59.1343	109.1
$\alpha = 2.4145$ $\beta = 2.6085 \times 10^{-6}$	Mode-1	2.8619	2.9244	2.184
	Mode-2	11.6677	12.7897	9.616
	Mode-3	23.5048	30.2017	28.49
	Mode-4	28.2694	59.1343	109.2
$\alpha = 2.634$ $\beta = 2.6085 \times 10^{-6}$	Mode-1	2.8614	2.9244	2.202
	Mode-2	11.6671	12.7897	9.622
	Mode-3	23.5041	30.2017	28.5
	Mode-4	28.2683	59.1343	109.2
$\alpha = 3.2925$ $\beta = 2.6085 \times 10^{-6}$	Mode-1	2.8597	2.9244	2.262
	Mode-2	11.6653	12.7897	9.639
	Mode-3	23.5020	30.2017	28.51
	Mode-4	28.2648	59.1343	109.2
$\alpha = 3.84125$ $\beta = 2.6085 \times 10^{-6}$	Mode-1	2.8583	2.9244	2.313
	Mode-2	11.6638	12.7897	9.653
	Mode-3	23.5003	30.2017	28.52
	Mode-4	28.2619	59.1343	109.2
$\alpha = 4.39$ $\beta = 2.6085 \times 10^{-6}$	Mode-1	2.8569	2.9244	2.363
	Mode-2	11.6623	12.7897	9.667
	Mode-3	23.4985	30.2017	28.53
	Mode-4	28.2591	59.1343	109.3

It is observed from the Table 4.62 that with the increment of the value of mass proportional constant and by keeping original value of stiffness proportional constant, the percentage of difference of damped frequencies does not change more. It is also observed that change in fourth and third modes of damped natural frequencies is a little bit more significant with the un-damped natural frequencies than the first and second modes.

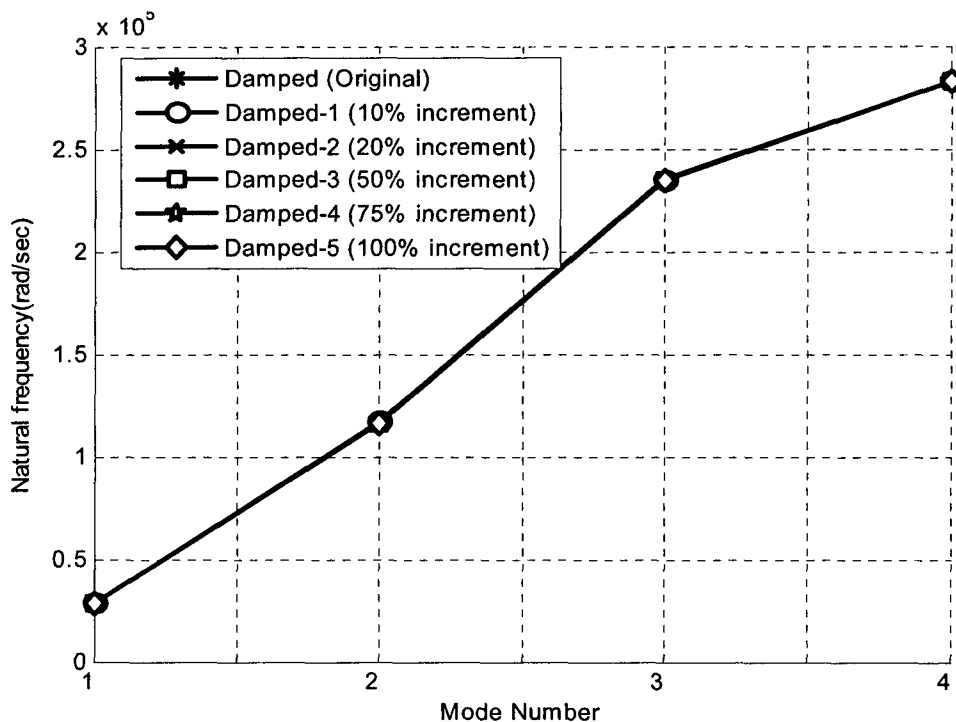


Figure 4. 17 Effect of damping properties on lowest four natural frequencies for fixed-free boundary condition of beam with taper configuration-C for case-2

One can observe the effect of different values of mass proportional constant while stiffness proportional constant is kept original value on natural frequencies of beam with taper configuration-C for fixed-free boundary condition from the Figure 4.17. The results obtained for different increment of mass proportional constant show that changes in damped natural frequencies is very very less; even it cannot be distinguished from the Figure 4.17.

Table 4. 63 Comparison of natural frequencies ($\times 10^4$ rad/sec) of beam with taper configuration-C for fixed-free boundary condition for case-3

α and β	Mode No.	Damped	Un-damped	% of difference
$\alpha = 2.195$ $\beta = 2.608 \times 10^{-6}$	Mode-1	2.8680	2.9244	1.967
	Mode-2	11.6742	12.7897	9.555
	Mode-3	23.5125	30.2017	28.45
	Mode-4	28.2819	59.1343	109.1
$\alpha = 2.195$ $\beta = 2.869 \times 10^{-6}$	Mode-1	2.8623	2.9244	2.17
	Mode-2	11.5568	12.7897	10.67
	Mode-3	22.7356	30.2017	32.84
	Mode-4	28.0254	59.1343	156.8
$\alpha = 2.195$ $\beta = 3.130 \times 10^{-6}$	Mode-1	2.8566	2.9244	2.373
	Mode-2	11.4381	12.7897	11.82
	Mode-3	21.9312	30.2017	37.71
	Mode-4	26.1391	59.1343	126.2
$\alpha = 2.195$ $\beta = 3.913 \times 10^{-6}$	Mode-1	2.8395	2.9244	2.99
	Mode-2	11.0745	12.7897	15.49
	Mode-3	19.3181	30.2017	56.34
	Mode-4	23.4227	59.1343	152.5
$\alpha = 2.195$ $\beta = 4.565 \times 10^{-6}$	Mode-1	2.8251	2.9244	3.515
	Mode-2	10.7621	12.7897	18.84
	Mode-3	16.8335	30.2017	79.41
	Mode-4	21.9695	59.1343	169.2
$\alpha = 2.195$ $\beta = 5.217 \times 10^{-6}$	Mode-1	2.8106	2.9244	4.049
	Mode-2	10.4404	12.7897	22.5
	Mode-3	13.9119	30.2017	117.1
	Mode-4	20.5559	59.1343	187.7

It is observed from the Table 4.63 that with the increment of the value of stiffness proportional constant and mass proportional constant is kept constant the percentage of difference of damped frequencies does not change linearly. It is also observed that change in fourth and third modes of damped natural frequencies is a little bit more significant with undamped natural frequencies than the first and second modes.

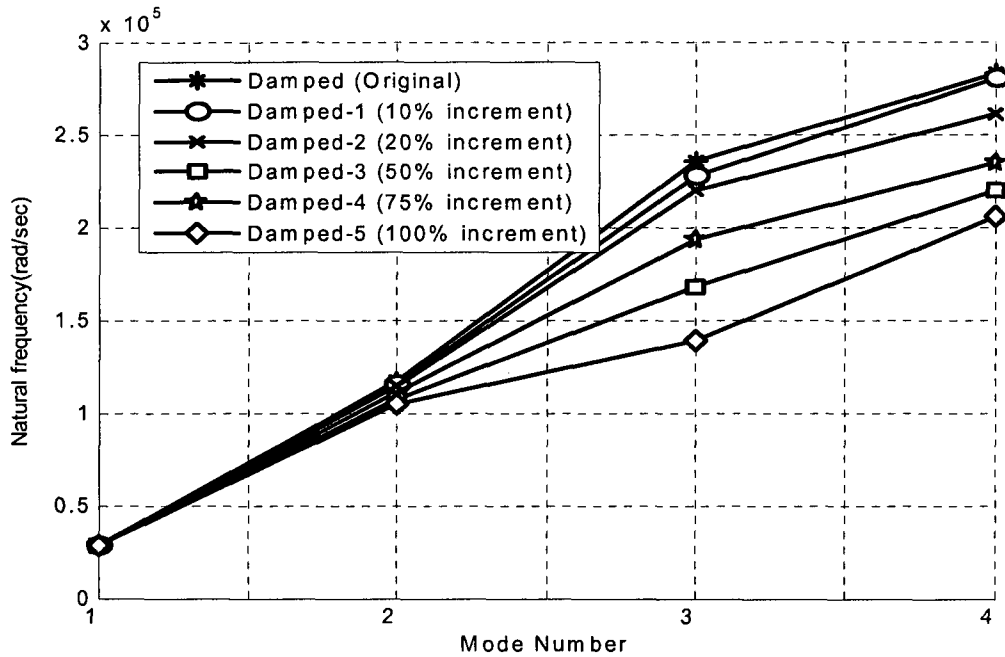


Figure 4. 18 Effect of damping properties on lowest four natural frequencies for fixed-free boundary condition of beam with taper configuration-C for case-3

One can observe the effect of different values of stiffness proportional constant while mass proportional constant is kept constant on damped natural frequencies of beam with taper configuration-C for fixed-free boundary condition from the Figure 4.18. The results obtained for the beam with different values of stiffness proportional constant while mass proportional constant is kept constant show that damped natural frequencies obtained considering different values of stiffness and mass proportional constant are almost same up to 2nd mode but difference among the 3rd and 4th modes are little bit more.

Table 4. 64 Comparison of natural frequencies ($\times 10^4$ rad/sec) of beam with taper configuration-D for fixed-free boundary condition for case-1.

α and β	Mode No.	Damped	Un-damped	% of difference
$\alpha = 2.195$ $\beta = 2.608 \times 10^{-6}$	Mode-1	2.7790	2.8316	1.893
	Mode-2	10.4295	11.2947	8.296
	Mode-3	21.8861	27.2641	24.57
	Mode-4	29.4780	52.4998	78.1
$\alpha = 2.4145$ $\beta = 2.869 \times 10^{-6}$	Mode-1	2.7737	2.8316	2.087
	Mode-2	10.3391	11.2947	9.243
	Mode-3	21.2737	27.2641	28.16
	Mode-4	26.0811	52.4998	101.3
$\alpha = 2.634$ $\beta = 3.130 \times 10^{-6}$	Mode-1	2.7683	2.8316	2.287
	Mode-2	10.2478	11.2947	10.22
	Mode-3	20.6431	27.2641	32.07
	Mode-4	24.1697	52.4998	136.8
$\alpha = 3.2925$ $\beta = 3.912 \times 10^{-6}$	Mode-1	2.7522	2.8316	2.885
	Mode-2	9.9689	11.2947	13.3
	Mode-3	18.6237	27.2641	46.39
	Mode-4	21.8641	52.4998	140.1
$\alpha = 3.84125$ $\beta = 4.568 \times 10^{-6}$	Mode-1	2.7387	2.8316	3.392
	Mode-2	9.7304	11.2947	16.08
	Mode-3	16.7559	27.2641	62.71
	Mode-4	20.3773	52.4998	145.6
$\alpha = 4.39$ $\beta = 5.217 \times 10^{-6}$	Mode-1	2.7251	2.8316	3.908
	Mode-2	9.4859	11.2947	19.07
	Mode-3	14.6519	27.2641	86.08
	Mode-4	19.1113	52.4998	174.7

It is observed from the Table 4.64 that with the increment of both the value of mass proportional constant and stiffness proportional constant, the percentage of difference of damped frequencies does not change linearly. It is also observed that change in fourth and third modes of damped natural frequencies is a little bit more significant with un-damped natural frequencies than the first and second modes.

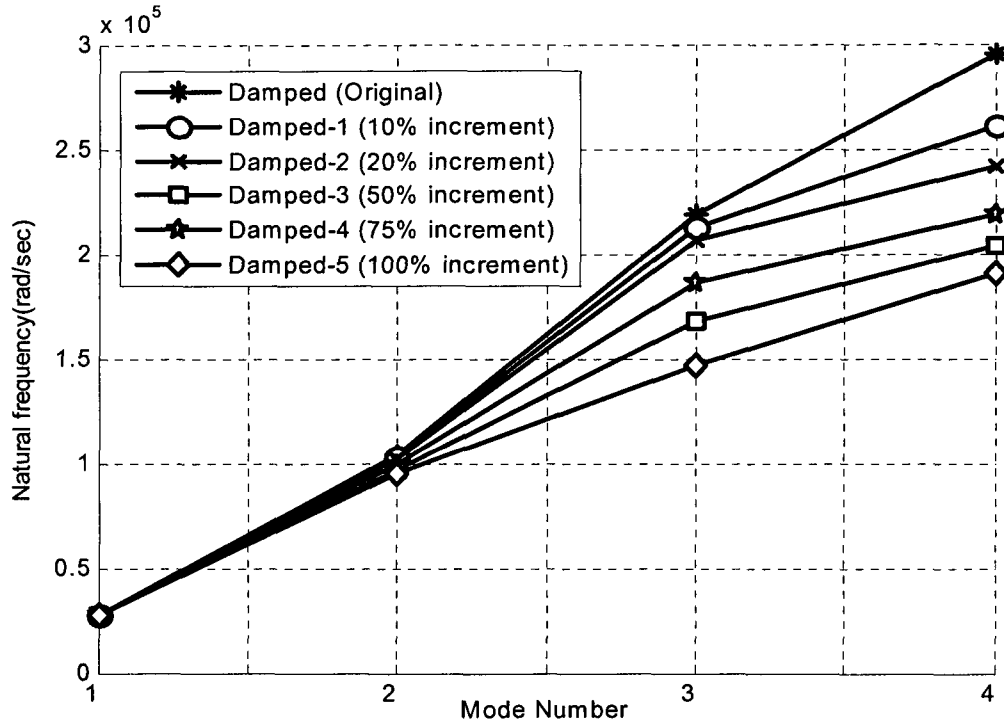


Figure 4. 19 Effect of damping properties on lowest four natural frequencies for fixed-free boundary condition of beam with taper configuration-D for case-1

One can observe the effect of different values of stiffness and mass proportional constant on damped natural frequencies of beam with taper configuration-D for fixed-free boundary condition from the Figure 4.19. The results obtained for the beam with different values of stiffness and mass proportional constant show that damped natural frequencies obtained considering different values of stiffness and mass proportional constant are almost same up to 2nd mode but difference among the 3rd and 4th modes are little bit more.

Table 4. 65 Comparison of natural frequencies ($\times 10^4$ rad/sec) of beam with taper configuration-D for fixed-free boundary condition for case-2

α and β	Mode No.	Damped	Un-damped	% of difference
$\alpha = 2.195$ $\beta = 2.608 \times 10^{-6}$	Mode-1	2.7790	2.8316	1.893
	Mode-2	10.4295	11.2947	8.296
	Mode-3	21.8861	27.2641	24.57
	Mode-4	29.4780	52.4998	78.1
$\alpha = 2.4145$ $\beta = 2.608 \times 10^{-6}$	Mode-1	2.7729	2.8316	2.117
	Mode-2	10.4231	11.2947	8.362
	Mode-3	21.8787	27.2641	24.61
	Mode-4	29.4973	52.4998	77.98
$\alpha = 2.634$ $\beta = 2.608 \times 10^{-6}$	Mode-1	2.7723	2.8316	2.139
	Mode-2	10.4225	11.2947	8.368
	Mode-3	21.8780	27.2641	24.62
	Mode-4	29.4663	52.4998	78.17
$\alpha = 3.2925$ $\beta = 2.608 \times 10^{-6}$	Mode-1	2.7707	2.8316	2.198
	Mode-2	10.4207	11.2947	8.387
	Mode-3	21.8760	27.2641	24.63
	Mode-4	29.4634	52.4998	78.19
$\alpha = 3.84125$ $\beta = 2.608 \times 10^{-6}$	Mode-1	2.7693	2.8316	2.25
	Mode-2	10.4192	11.2947	8.403
	Mode-3	21.8742	27.2641	24.64
	Mode-4	29.4610	52.4998	78.2
$\alpha = 4.39$ $\beta = 2.608 \times 10^{-6}$	Mode-1	2.7679	2.8316	2.301
	Mode-2	10.4177	11.2947	8.418
	Mode-3	21.8725	27.2641	24.65
	Mode-4	29.4585	52.4998	78.22

It is observed from the Table 4.65 that with the increment of the value of mass proportional constant and by keeping original value of stiffness proportional constant, the percentage of difference of damped frequencies does not change more. It is also observed that change in fourth and third modes of damped natural frequencies is a little bit more significant with the un-damped natural frequencies than the first and second modes.

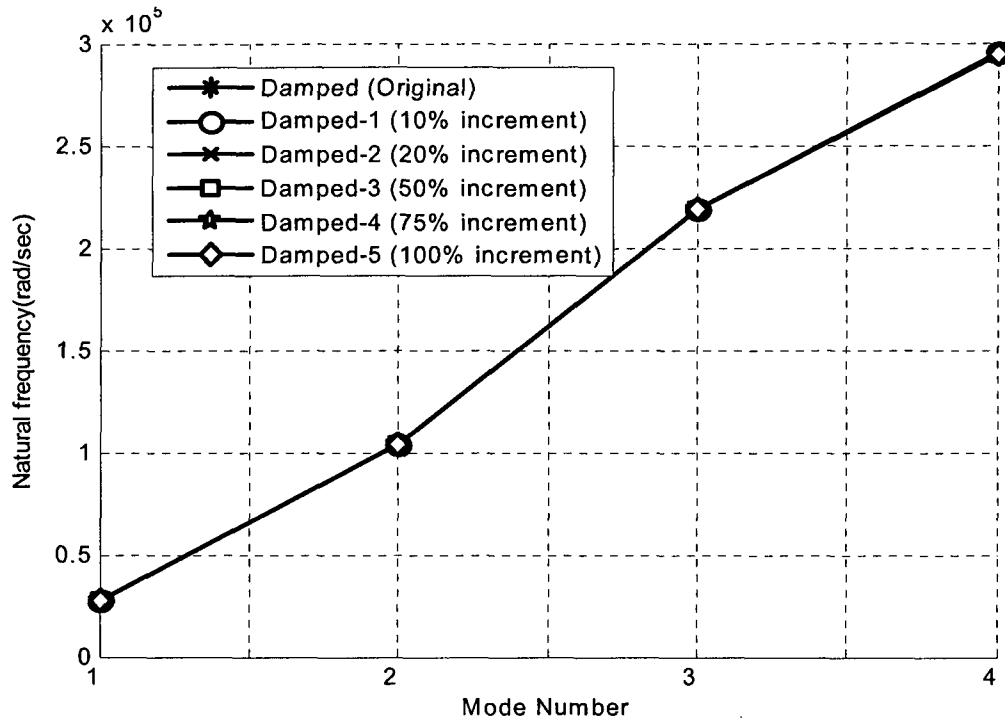


Figure 4. 20 Effect of damping properties on lowest four natural frequencies for fixed-free boundary condition of beam with taper configuration-D for case-2

One can observe the effect of different values of mass proportional constant while stiffness proportional constant is kept original value on damped natural frequencies of beam with taper configuration-D for fixed-free boundary condition from the Figure 4.20. The results obtained for different increment of mass proportional constant show that changes in damped natural frequencies is very very less; even it cannot be distinguished from the Figure 4.20.

Table 4. 66 Comparison of natural frequencies ($\times 10^4$ rad/sec) of beam with taper configuration-D for fixed-free boundary condition for case-3

α and β	Mode No.	Damped	Un-damped	% of difference
$\alpha = 2.195$ $\beta = 2.608 \times 10^{-6}$	Mode-1	2.7790	2.8316	1.893
	Mode-2	10.4295	11.2947	8.296
	Mode-3	21.8861	27.2641	24.57
	Mode-4	29.4780	52.4998	78.1
$\alpha = 2.195$ $\beta = 2.869 \times 10^{-6}$	Mode-1	2.7737	2.8316	2.087
	Mode-2	10.3391	11.2947	9.243
	Mode-3	21.2737	27.2641	28.16
	Mode-4	28.0811	52.4998	101.3
$\alpha = 2.195$ $\beta = 3.130 \times 10^{-6}$	Mode-1	2.7683	2.8316	2.287
	Mode-2	10.2478	11.2947	10.22
	Mode-3	20.6431	27.2641	32.07
	Mode-4	26.1698	52.4998	100.6
$\alpha = 2.195$ $\beta = 3.913 \times 10^{-6}$	Mode-1	2.7522	2.8316	2.885
	Mode-2	9.9689	11.2947	13.3
	Mode-3	18.6237	27.2641	46.39
	Mode-4	24.8641	52.4998	111.1
$\alpha = 2.195$ $\beta = 4.565 \times 10^{-6}$	Mode-1	2.7387	2.8316	3.392
	Mode-2	9.7304	11.2947	16.08
	Mode-3	16.7560	27.2641	62.71
	Mode-4	23.3772	52.4998	124.6
$\alpha = 2.195$ $\beta = 5.217 \times 10^{-6}$	Mode-1	2.7252	2.8316	3.904
	Mode-2	9.4859	11.2947	19.07
	Mode-3	14.6520	27.2641	86.08
	Mode-4	21.9110	52.4998	139.6

It is observed from the Table 4.66 that with the increment of the value of stiffness proportional constant and mass proportional constant is kept constant the percentage of difference of damped frequencies does not change linearly. It is also observed that change in fourth and third modes of damped natural frequencies is a little bit more significant with undamped natural frequencies than the first and second modes.

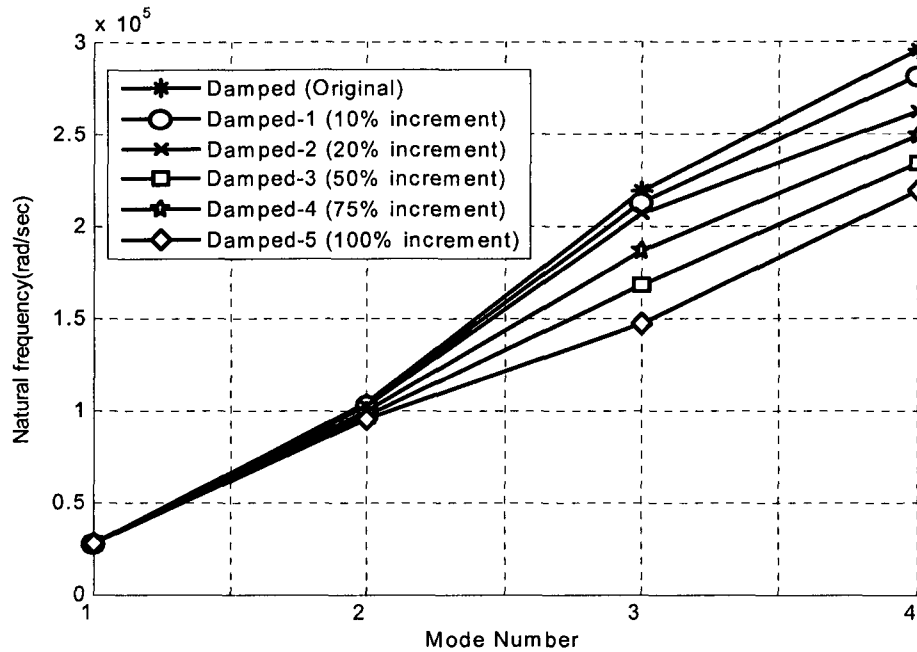


Figure 4. 21 Effect of damping properties on lowest four natural frequencies for fixed-free boundary condition of beam with taper configuration-D for case-3

One can observe the effect of different values of stiffness proportional constant while mass proportional constant is kept constant on damped natural frequencies of beam with taper configuration-D for fixed-free boundary condition from the Figure 4.21. The results obtained for the beam with different values of stiffness proportional constant while mass proportional constant is kept constant show that damped natural frequencies obtained considering different values of stiffness proportional constant are almost same up to 2nd mode but difference among the 3rd and 4th modes are little bit more.

4.9 Conclusion and discussion

In this chapter, free vibration analysis of beams with different types of taper configuration such as taper configurations-A, B, C, and D has been carried out using conventional finite element, higher-order finite element and Rayleigh-Ritz method. The first four lowest natural frequencies are obtained using different methods and compared with each other. From observation of results for natural frequencies, one can see that the first four natural frequencies calculated using different finite elements and Rayleigh-Ritz methods are converging well for different meshes and number of terms.

Several examples have been solved for different laminate configurations, various values of taper angles, and different length-ratios and for different boundary conditions. The effects of applied axial static force and damping on natural frequencies of tapered composite beam have also been investigated. From the tables and figures given in different sections, one can conclude the following:

- The results obtained for different types of taper configuration show that natural frequencies obtained for taper configuration-D gives the highest values; then taper configurations-B, C and A ranked second, third and fourth respectively.
- The results obtained for different types of laminate configuration show that natural frequencies obtained for laminate configuration LC-3 (that has $[0_4 / \pm 45_7]_s$ configuration at thick section and $[0_4 / \pm 45]_s$ configuration at thin section) gives the highest values; then laminate configuration LC-1 (that has $[0/90]_{9s}$ configuration at thick section and $[0/90]_{3s}$ configuration at thin section) ranked second and laminate configuration LC-2 (that has $[\pm 45]_{9s}$ configuration at thick section and $[\pm 45]_{3s}$ configuration at thin section) gives the lowest values.

- Natural frequencies obtained for highest taper angle value are the highest and lowest taper angle gives the lowest values of frequencies. The frequency is increasing with the increasing of taper angle, because the length of the beam decreases which makes it stiffer that results in higher natural frequency and vice versa.
- The results obtained for different values of length ratio show that natural frequencies obtained for highest length ratio are the highest and lowest length ratio gives the lowest values of frequencies.
- Beam with fixed-fixed boundary condition gives the highest natural frequency that means for this boundary condition the beam gets highest stiffness and beam with (thin end) fixed-(thick end) free boundary condition gives the lowest natural frequency that means for this boundary condition the beam gets lowest stiffness. Then beam with simply supported, (thick end) fixed-(thin end) free boundary conditions ranked second and third positions. Beam with (thick end) fixed-(thin end) hinged and (thick end) hinged-(thin end) fixed boundary conditions give almost the same natural frequencies.
- Natural frequencies of beam with tensile axial force are higher than the natural frequencies of beam without axial force for all taper configurations with all boundary conditions. The percentage difference of natural frequencies does not change much with the increment of the value of axial force.
- Un-damped natural frequencies of beam are higher than the natural frequencies with damping effect included for all boundary conditions for tapered composite beam. The percentage difference of damped frequencies does not change linearly with the increment of the value of mass proportional constant and stiffness proportional constant. It is observed that stiffness proportional constant has more effect than mass proportional constant.

Chapter-5

Forced vibration analysis of tapered composite beams

5.1 Introduction

Excitation is more often encountered in engineering structures. Mechanical structures are forced to vibrate at the same frequency as that of excitation. This excitation may be undesirable if large vibration amplitude develops. Service operation of structures may be disturbed or the safety of the structures may reach to a risk of failure. When forcing frequency matches the natural frequency of the system, resonance can be occurred and the amplitude will be at its maximum. So accurate prediction of forced response characteristics of tapered composite structures should be undertaken to prevent failure as use of such composite structures is growing day by day.

The design of a tapered structure (laminate which formed a thick section, a tapered section and a thin section) involves consideration of ply orientations in laminate, length ratios, taper angle, etc. The length of tapered section depends on the taper angle and usually is much smaller than the lengths of the other two sections. Free vibration analyses of tapered composite beams are explained in detail in chapter 4 using conventional finite element and higher-order finite element modeling procedures and Rayleigh-Ritz method. In this chapter these developed formulations are employed for a comprehensive parametric study of forced vibration analysis of different types of composite beams with taper configuration.

The material chosen is NCT/301 graphite-epoxy. The properties of the material are given in the introduction of section 5.2. The specifications of composite laminate (ply orientations) and geometric properties (total number of plies in different sections, taper angle and length) are given in detail in each example. Symmetric laminate is considered in all problems.

5.2 Effect of taper configuration on transverse displacement and rotation

In this section a set of examples is solved using conventional finite element, higher-order finite element and Rayleigh-Ritz method to investigate the forced response in terms of displacement and rotation of composite beam with different types of taper configurations. Mechanical properties of the graphite-epoxy material are: E_1 is 113.9 GPa, E_2 is 7.9856 GPa, Poisson's ratio ν_{21} is 0.0178, ν_{12} is 0.288, shear modulus G_{12} is 3.138 GPa, and density ρ is 1480 kg/m³. Elastic modulus of epoxy resin (E_r) is 3.902 GPa and Poisson's ratio (ν) is 0.37.

5.2.1 Beam with taper configuration-A

Example 5.2.1

Beam with taper configuration-A subjected to applied force and moment is shown in Figure 5.1. The beam is made of 36 plies at thick section and after dropping off 24 plies, it ends with 12 plies at thin section. The configuration of the thick section is $[0/90]_{9s}$ and it is $[0/90]_{3s}$ at thin section. The geometric properties of the beam are: length L is 0.0345 m (corresponding to fixed taper angle and beam thickness), individual ply thickness (t_k) is 0.000125 m, width (b) is unity, and taper angle (ϕ) is 2.5°. The beam is meshed with 12 elements of equal length.

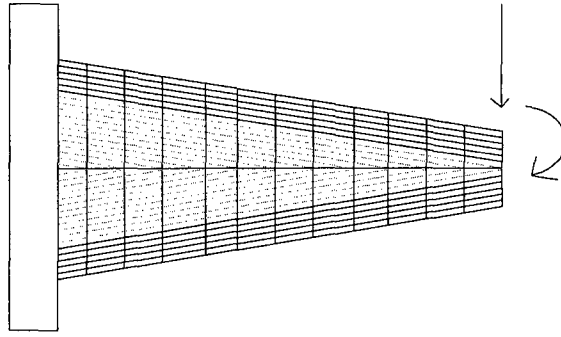


Figure 5. 1 Fixed-free composite beam with taper configuration-A

A sinusoidal force of magnitude 2 N and a sinusoidal moment of magnitude 2 N-m with excitation frequency ω are applied at free end of cantilever beam. By using the properties described already at the beginning of the present subsection, the problem is solved to calculate the forced response in terms of transverse displacement and rotation of beam at the free end of beam. The forced response in terms of the magnitude of sinusoidal transverse displacement and the magnitude of sinusoidal rotation are obtained considering 12-elements mesh for both conventional and higher-order finite element methods and 5-terms for Rayleigh-Ritz method, and presented in Figures 5.2 and 5.3.

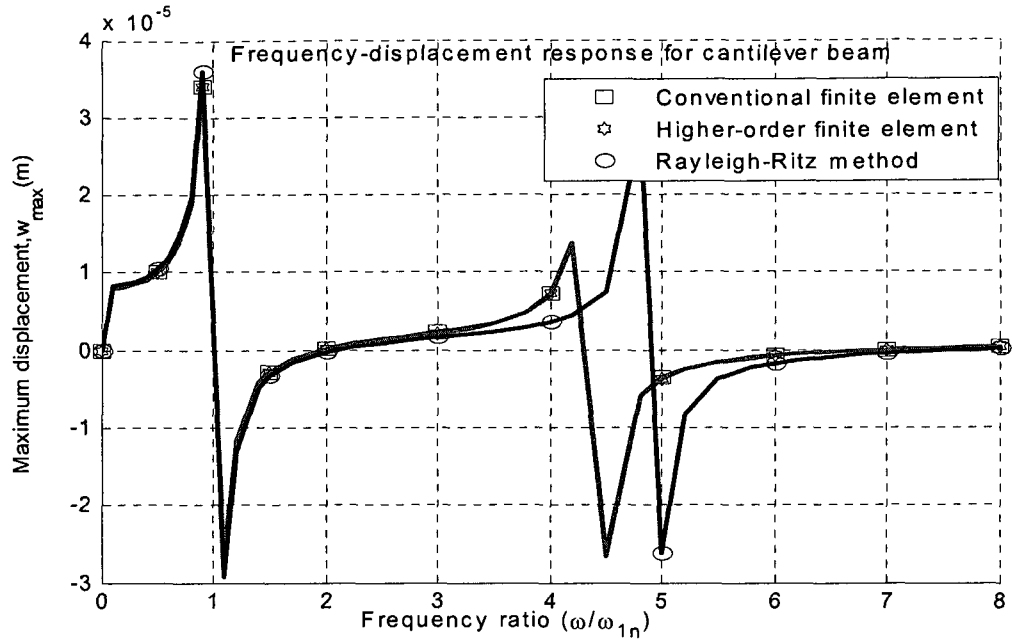


Figure 5. 2 Frequency-displacement plot of beam with taper configuration-A

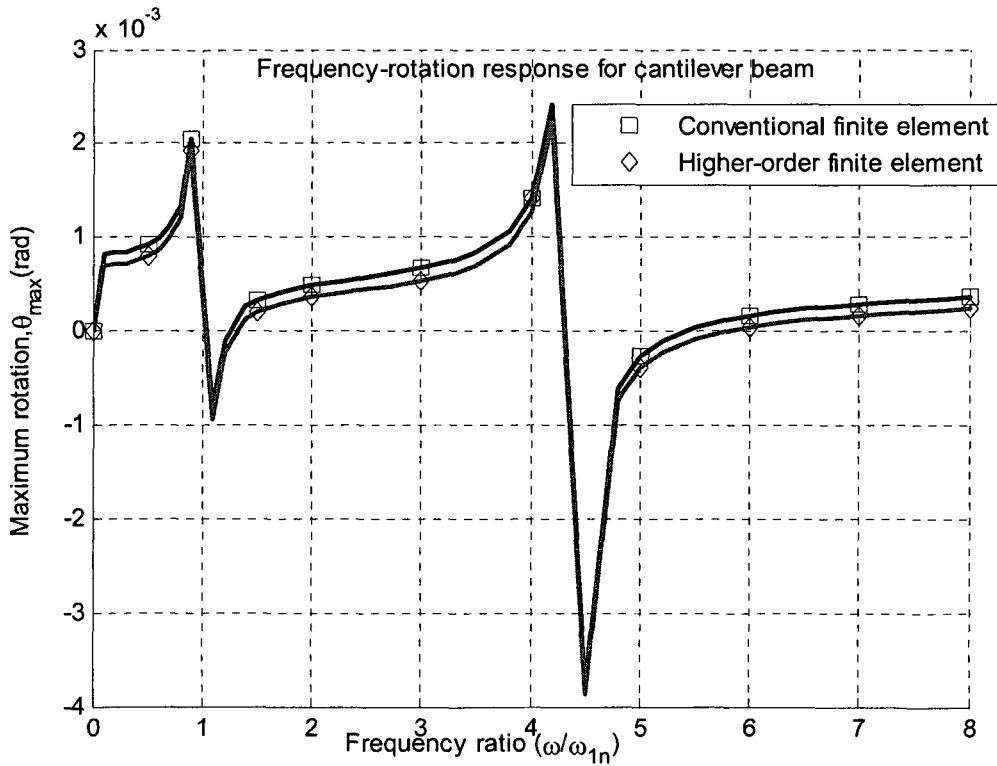


Figure 5. 3. Frequency-rotation plot of beam with taper configuration-A

Figures 5.2 and 5.3 show that forced response in terms of transverse displacement and rotation calculated using different finite element methods for beam with taper configuration-A for fixed-free boundary condition converge well where first lowest natural frequency ω_{1n} is 2.6107×10^4 rad/sec.

The forced response in terms of the magnitude of sinusoidal transverse displacement and the magnitude of sinusoidal rotation are also obtained considering different meshes using higher-order finite element for beam with taper configuration-A, and presented in Figures 5.4 and 5.5.

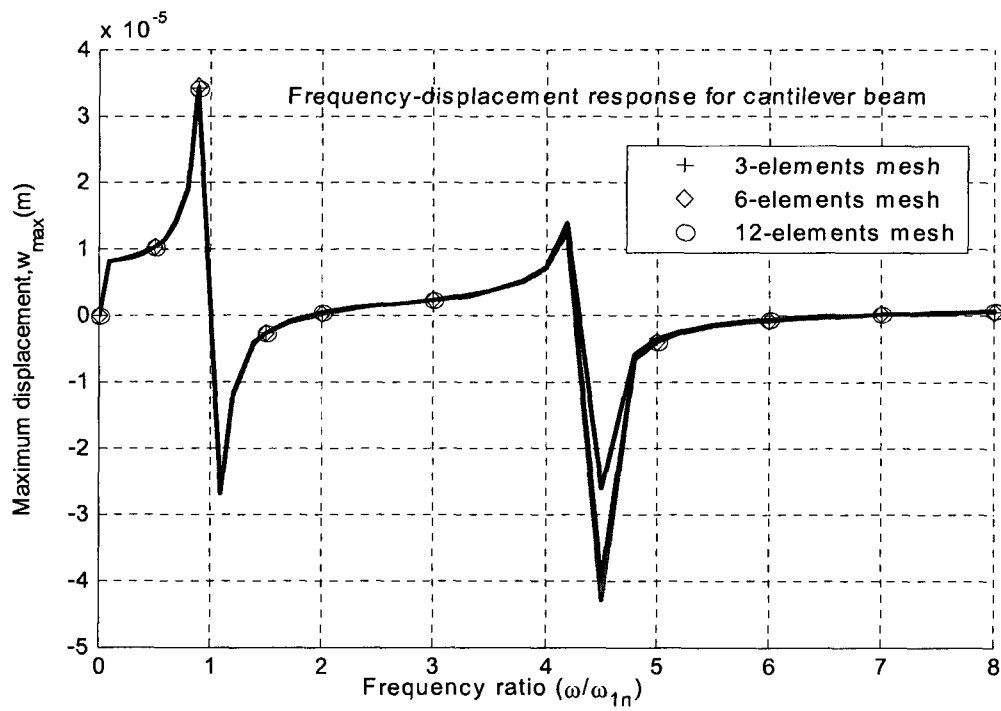


Figure 5. 4 Frequency-displacement plot of beam with taper configuration-A

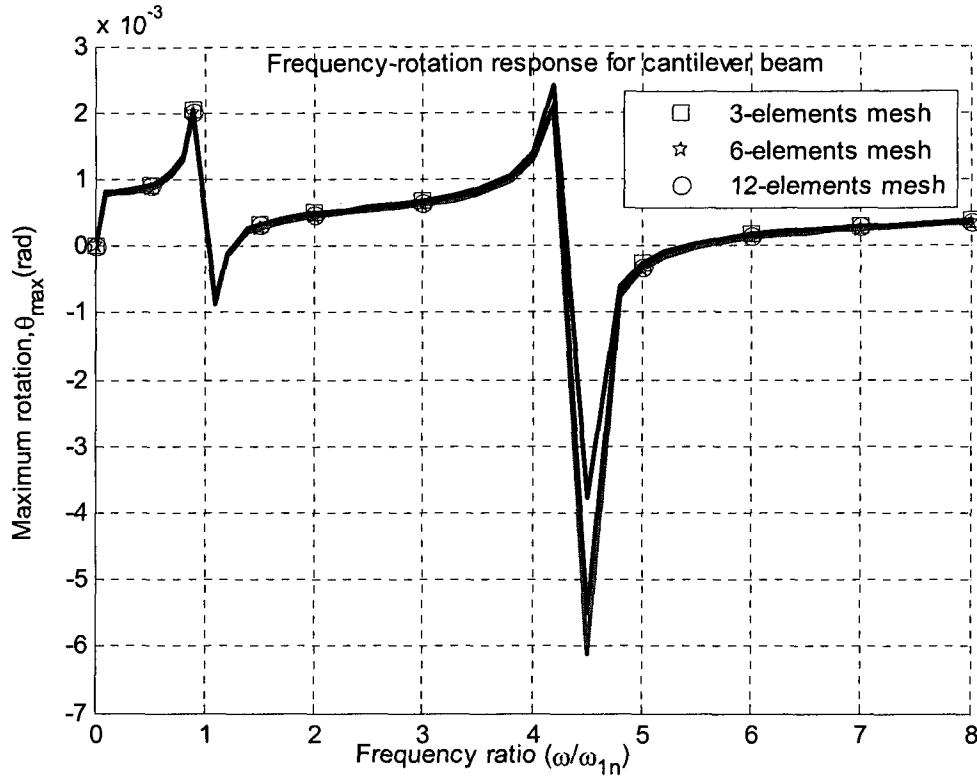


Figure 5. 5 Frequency-rotation plot of beam with taper configuration-A

Figures 5.4 and 5.5 show that forced response in terms of transverse displacement and rotation calculated using different elements mesh for beam with taper configuration-A for fixed-free boundary condition converge well where first lowest natural frequency ω_{1n} is 2.6107×10^4 rad/sec.

5.2.2 Beam with taper configuration-B

Example 5.2.2

Example 5.2.2 is solved for beam with taper configuration-B as shown in Figure 5.6. The beam is made of 36 plies at thick section and after dropping off 24 plies, it ended up with 12 plies at thin section. Plies drop-off occur consistently from top to bottom in a staircase arrangement. Dropped-off plies are replaced by resin pocket; resin pocket is divided into imaginary layers in each element with the same thickness of lamina. Integration limits for

different calculations are considered according to appropriate position of imaginary ply ending.

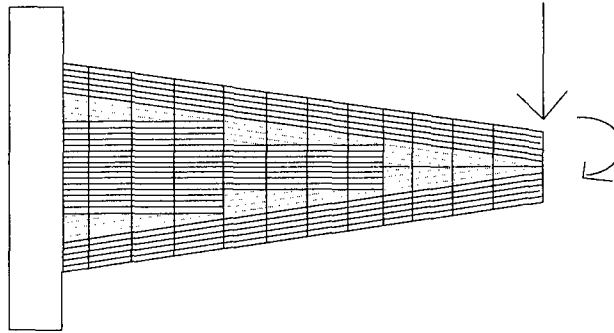


Figure 5. 6 Fixed-free composite beam with taper configuration-B

A sinusoidal force of magnitude 2 N and a sinusoidal moment of magnitude 2 N-m with excitation frequency ω are applied at free end of cantilever beam. By using the properties described already at the beginning of the present subsection, the problem is solved to calculate the forced response in terms of transverse displacement and rotation of beam at the free end of beam. The forced response in terms of the magnitude of sinusoidal transverse displacement and the magnitude of sinusoidal rotation are obtained considering 12-elements mesh for both conventional and higher-order finite element methods and 5-terms for Rayleigh-Ritz method, and presented in Figures 5.7 and 5.8.

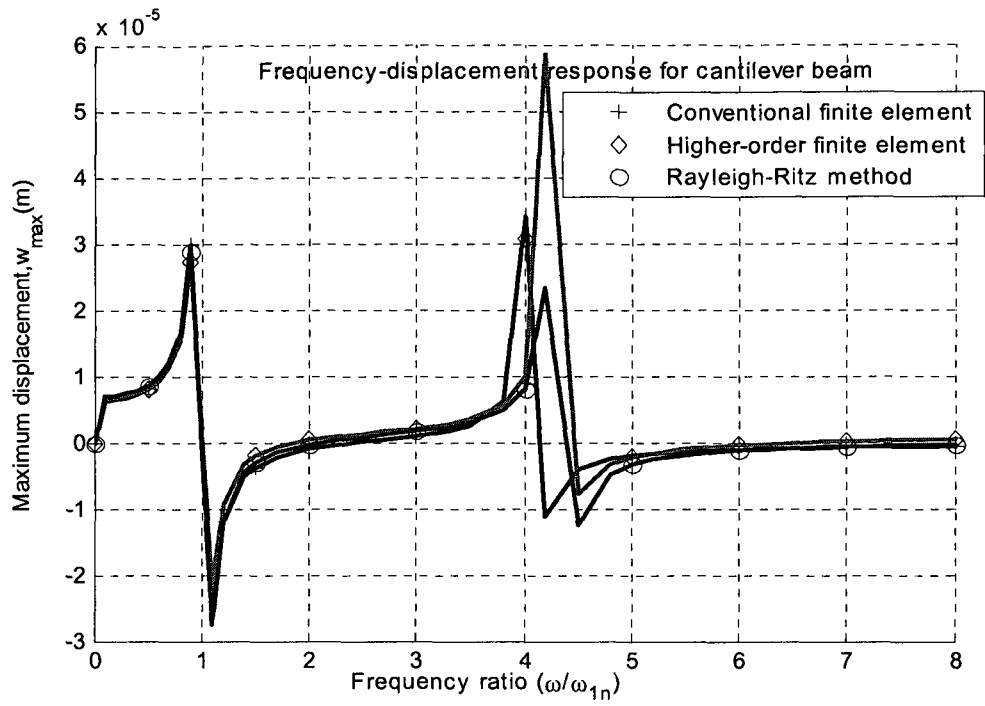


Figure 5. 7 Frequency-displacement plot of beam with taper configuration-B

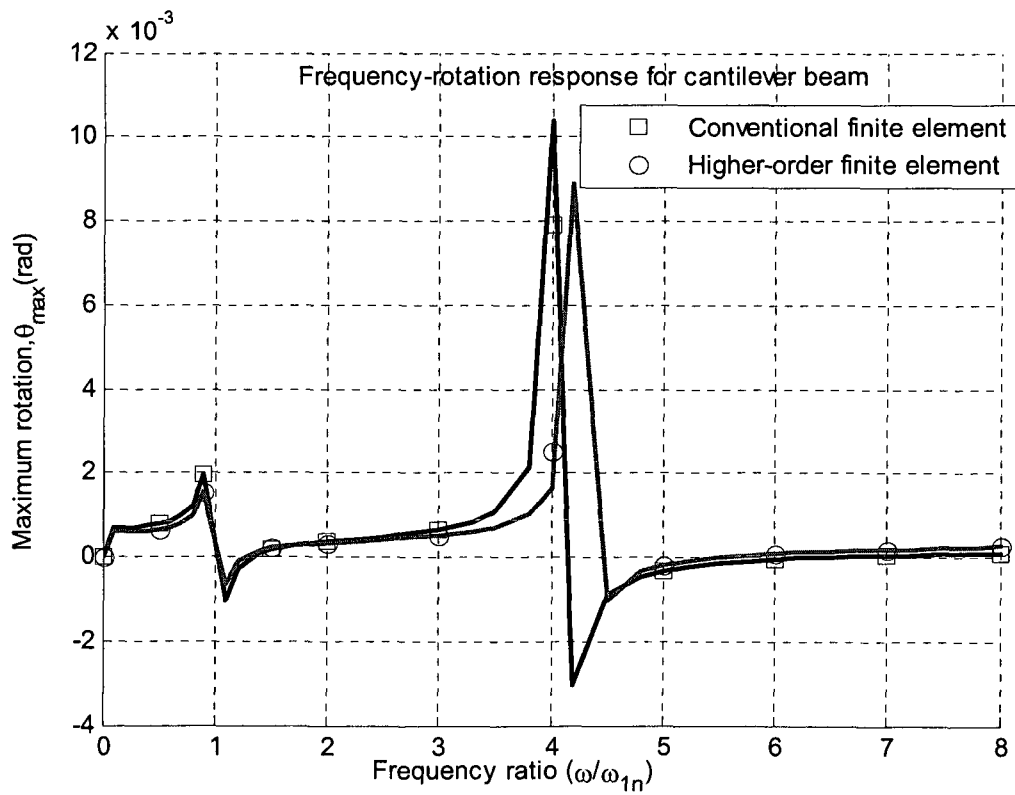


Figure 5. 8 Frequency-rotation plot of beam with taper configuration-B

As from the Figures 5.7 and 5.8, one can see that the forced response in terms of transverse displacement and rotation calculated using different finite element methods for beam with taper configuration-B for fixed-free boundary condition converge well where first lowest natural frequency, ω_{1n} is 2.8647×10^4 rad/sec.

5.2.3 Beam with taper configuration-C

Example 5.2.3

Example 5.2.3 is solved for beam with taper configuration-C as shown in Figure 5.9. The beam is meshed into twelve elements of equal length for analysis, plies drop-off occur near the middle line of beam. Dropped-off plies are replaced by resin pocket; resin pocket is divided into imaginary layers in each element with the same thickness of laminate. Again integration limits for different calculations are considered according to appropriate position of imaginary ply ending.

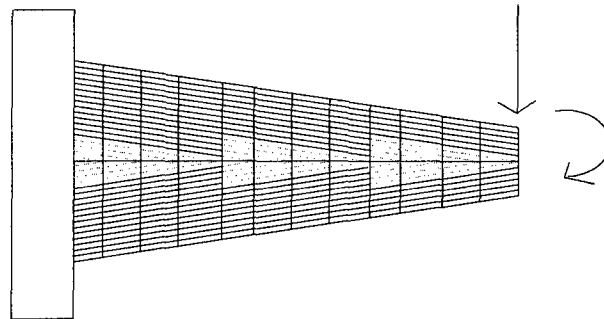


Figure 5. 9 Fixed-free composite beam with taper configuration –C

A sinusoidal force of magnitude 2 N and a sinusoidal moment of magnitude 2 N-m with excitation frequency ω are applied at free end of cantilever beam. By using the properties described already at the beginning of the present subsection, the problem is solved to calculate the forced response in terms of transverse displacement and rotation of beam at the

free end of beam. The forced response in terms of the magnitude of sinusoidal transverse displacement and the magnitude of sinusoidal rotation are obtained considering 12-elements mesh for both conventional and higher-order finite element methods and 5-terms for Rayleigh-Ritz method, and presented in Figures 5.10 and 5.11.

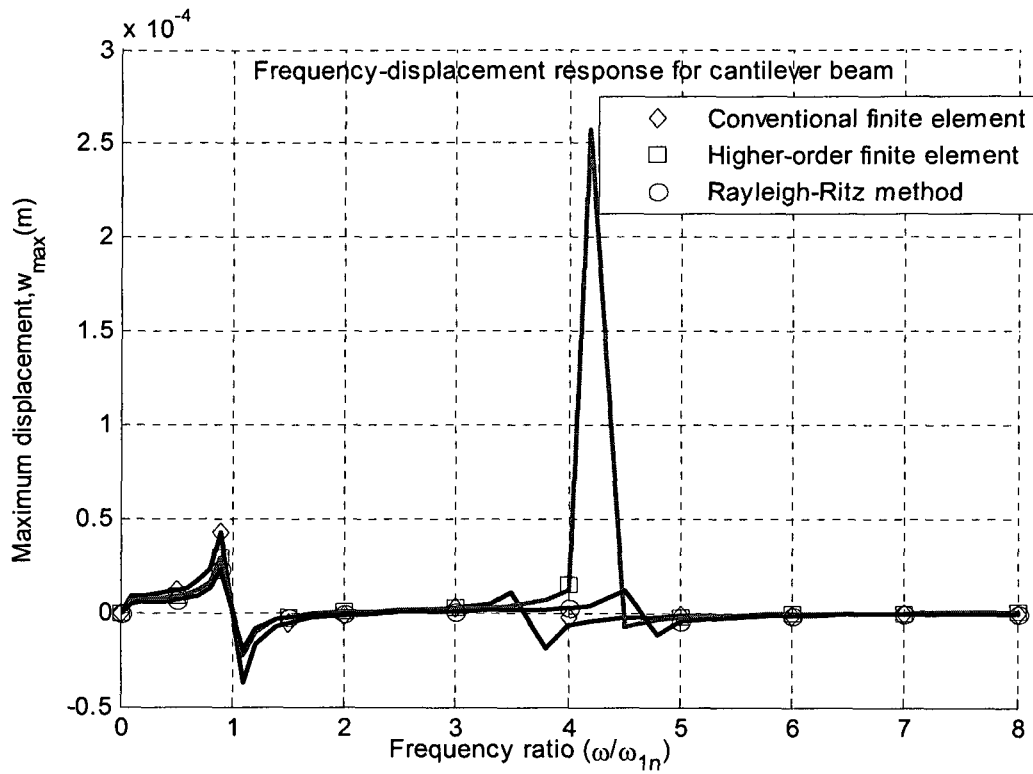


Figure 5. 10 Frequency-displacement plot of beam with taper configuration-C

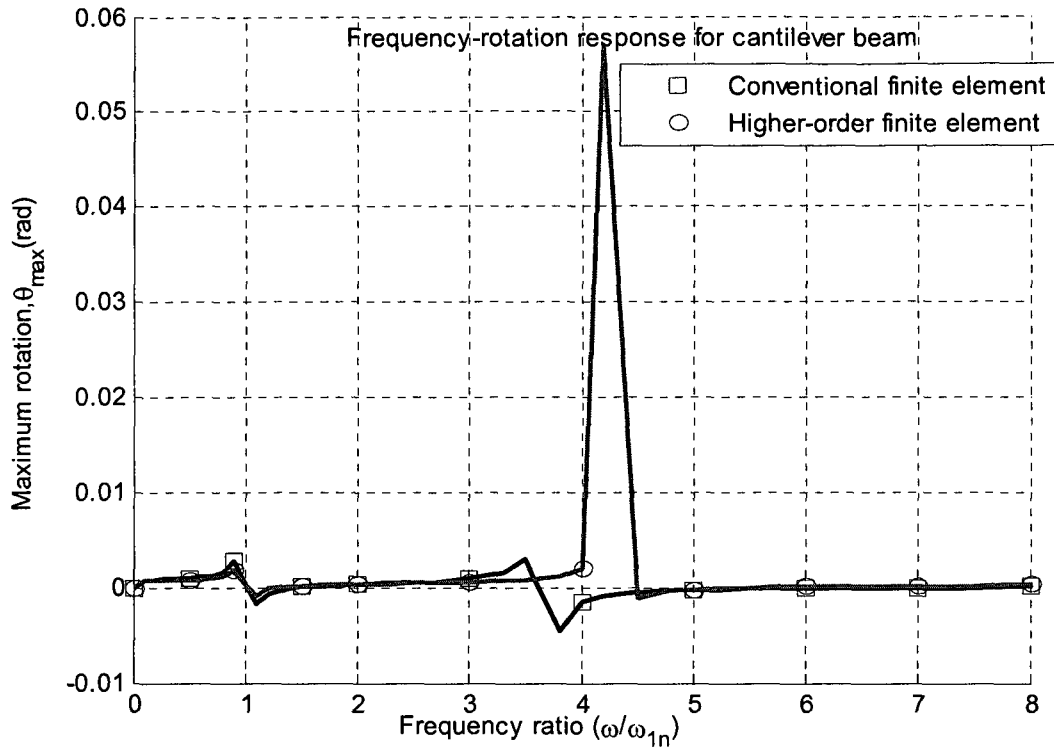


Figure 5. 11 Frequency-rotation plot of beam with taper configuration- C

As from the Figures 5.10 and 5.11, one can see that the transverse displacement and rotation (forced response) calculated by using different finite element methods for beam with taper configuration-C for fixed-free boundary condition converge well where first lowest natural frequency, ω_{1n} is 2.8244×10^4 rad/sec.

5.2.4 Beam with taper configuration-D

Example 5.2.4

Example 5.2.4 is solved for beam with taper configuration-D as shown in Figure 5.12. The beam is made of 36 plies in thick section and after dropping off 24 plies; it ends with 12 plies in thin section. The beam is symmetric and meshed into twelve elements of equal length for analysis. Ply drop-off pattern looks like that of taper configuration-B except that there is a ply difference above the resin pocket corresponding to specific element.

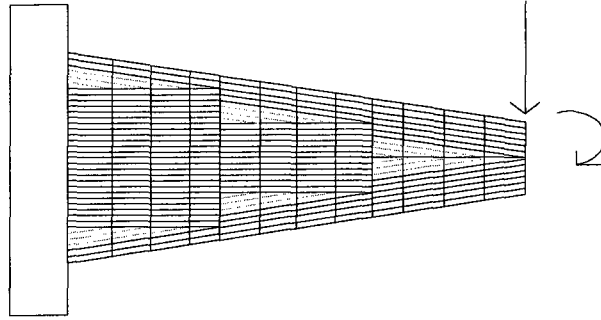


Figure 5. 12 Fixed-free composite beam with taper configuration -D

A sinusoidal force of magnitude 2 N and a sinusoidal moment of magnitude 2 N-m with excitation frequency ω are applied at free end of cantilever beam. By using the properties described already at the beginning of the present subsection, the problem is solved to calculate the forced response in terms of transverse displacement and rotation of beam at the free end of beam. The forced response in terms of the magnitude of sinusoidal transverse displacement and the magnitude of sinusoidal rotation are obtained considering 12-elements mesh for both conventional and higher-order finite element methods and 5-terms for Rayleigh-Ritz method, and presented in Figures 5.13 and 5.14.

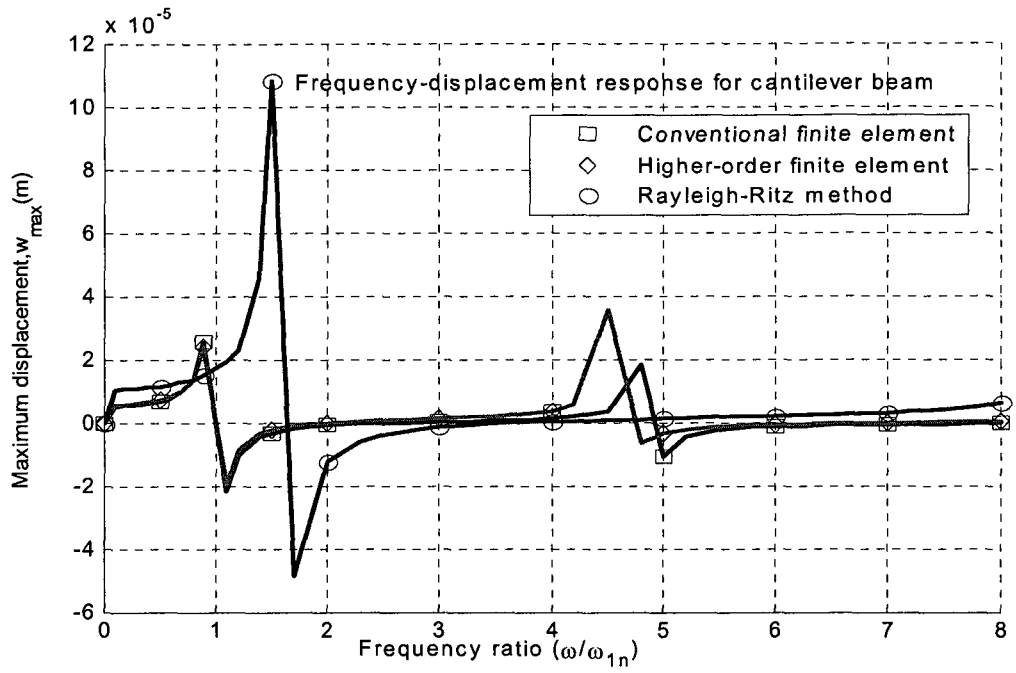


Figure 5. 13 Frequency-displacement plot of beam with taper configuration-D

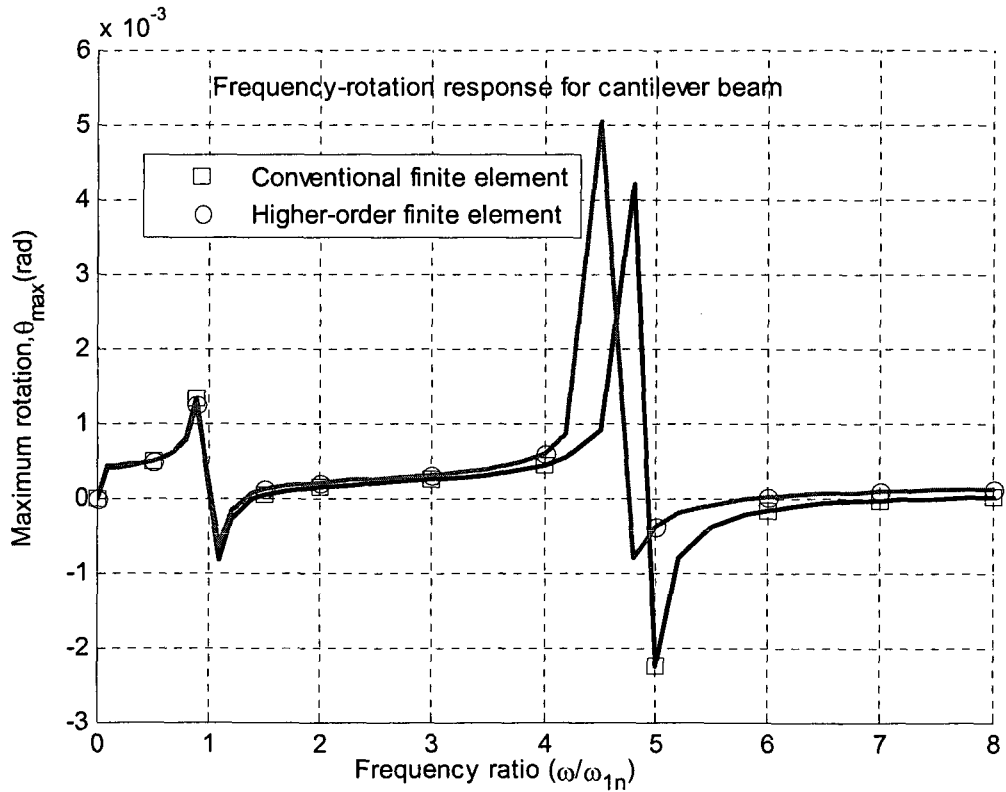


Figure 5. 14 Frequency-rotation plot of beam with taper configuration-D

As from the Figures 5.13 and 5.14, one can see that the forced response in terms of transverse displacement and rotation calculated by using different finite element methods for beam with taper configuration-D for fixed-free boundary condition converge well where first lowest natural frequency, ω_{in} is 2.8816×10^4 rad/sec.

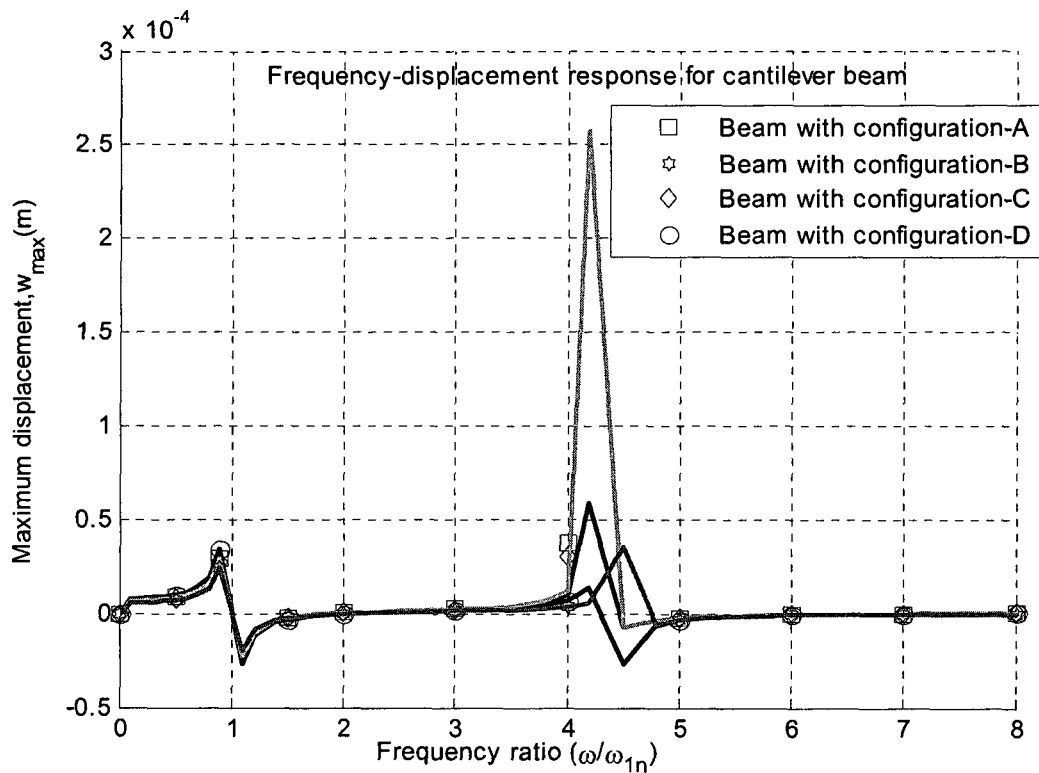


Figure 5. 15 Effects of taper configuration on frequency-displacement response

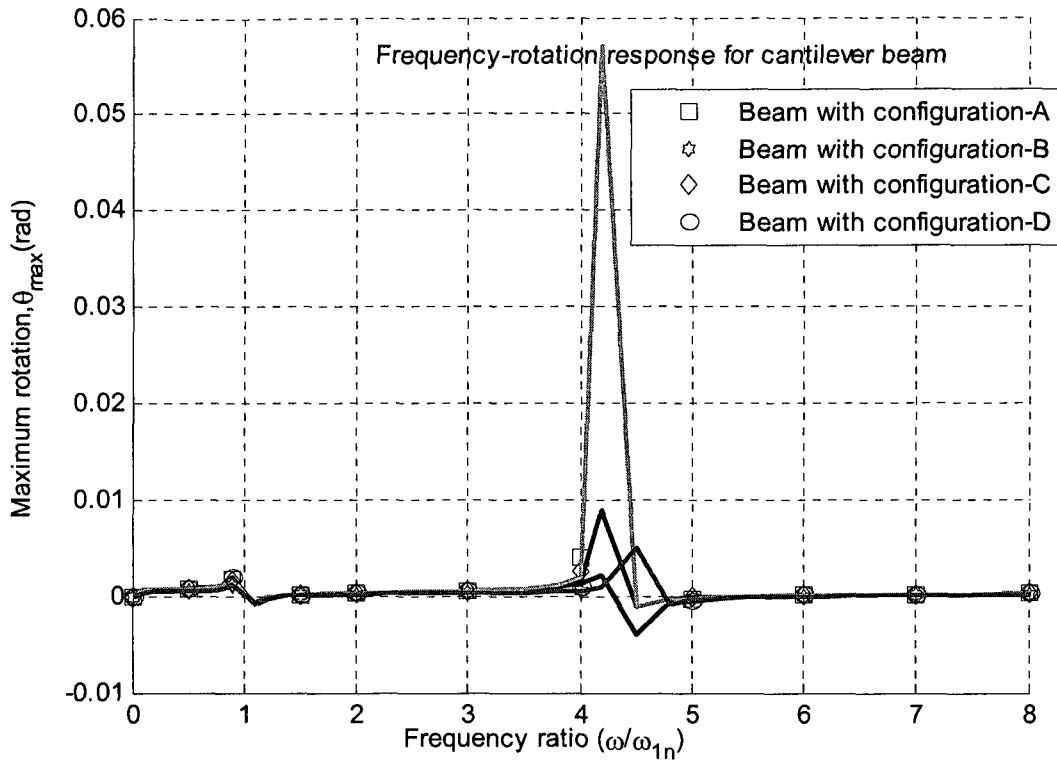


Figure 5. 16 Effects of taper configuration on frequency-rotation response

One can observe forced response in terms of transverse displacement and rotation for all taper beam configurations for fixed-free boundary condition from the Figures 5.15 and 5.16 at a glance. Here first lowest natural frequency ω_{1n} has been considered for each respective taper configuration beam in the calculation. The results obtained considering 12-elements mesh using higher-order finite element method for different types of taper configurations show that transverse displacement and rotation obtained for taper configuration-D gives the lowest values in terms of response. Taper configurations-B, C and A ranked second, third and fourth respectively. This difference in transverse displacement and rotation is expected from the inside geometry variation and the location of plies drop-off. The transverse displacement and rotation calculated for different taper configurations depend on the stiffness of the beam that is dependent on D_{11} . Again D_{11} is dependent on mechanical

properties and height of the ply from the mid-plane of the beam. As different taper configuration composite beams are considered according to plies drop-off at different locations, these are giving different stiffness values. Configuration-D is the stiffest due to more uniform plies in different elements. Then taper configuration-B gives second highest stiffness. Taper configuration-A gives the lowest stiffness compared to others as it is made with a big resin pocket. Forced response in terms of transverse displacement and rotation of taper configuration-C are in between the response given by taper configurations-B and A due to plies drop-off near mid-plane of beam.

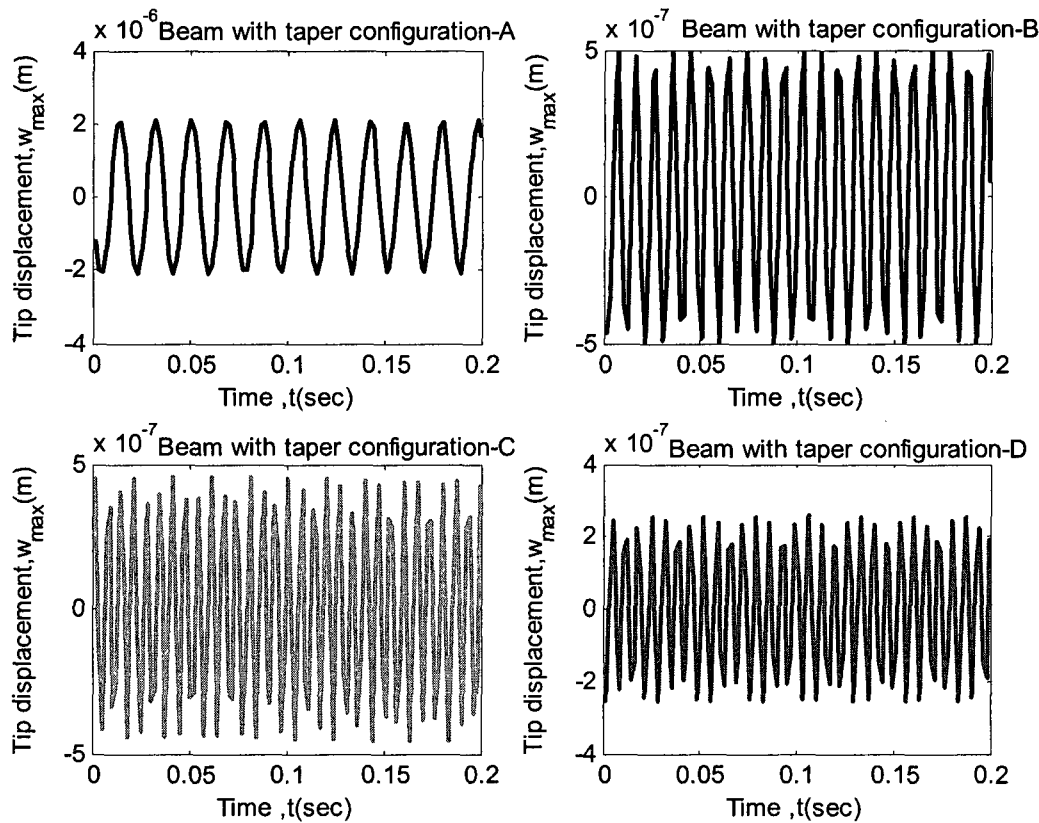


Figure 5. 17 Steady state response curves for beam with different taper configurations

Steady state response curves of different taper configurations beam at frequency ratio 2 are shown in Figure 5.17. One can observe the tip transverse displacement of beam with different taper configurations at a glance. It is clear from the figure that the tip displacement of beam with taper configuration-A is highest whereas that of beam with taper configuration-D is lowest.

5.3 Effect of laminate configuration on transverse displacement and rotation

Beams with taper configurations-C and D are considered to investigate the effects of different laminate configurations on forced response (transverse displacement and rotation). The beam is made with 36 and 12 plies at thick and thin section respectively, which results in 24 drop-off plies. The laminate configurations considered are: (i) LC-1 that has $[0/90]_{9s}$ configuration at thick section and $[0/90]_{3s}$ configuration at thin section; (ii) LC-2 that has $[\pm 45]_{9s}$ configuration at thick section and $[\pm 45]_{3s}$ configuration at thin section; (iii) LC-3 that has $[0_4/\pm 45_7]_s$ configuration at thick section and $[0_4/\pm 45]_s$ configuration at thin section.

Example 5.3.1

A sinusoidal force of magnitude 2 N and a sinusoidal moment of magnitude 2 N-m with excitation frequency ω are applied at free end of cantilever beam. Mechanical properties as described in the section 5.2 are used in this example. The problem is solved to calculate the forced response in terms of transverse displacement and rotation of beam at the free end of beam. The forced response in terms of the magnitude of sinusoidal transverse displacement and the magnitude of sinusoidal rotation are obtained considering 12-elements mesh using higher-order finite element method for beam with taper configuration-C, and presented in Figures 5.18 and 5.19.

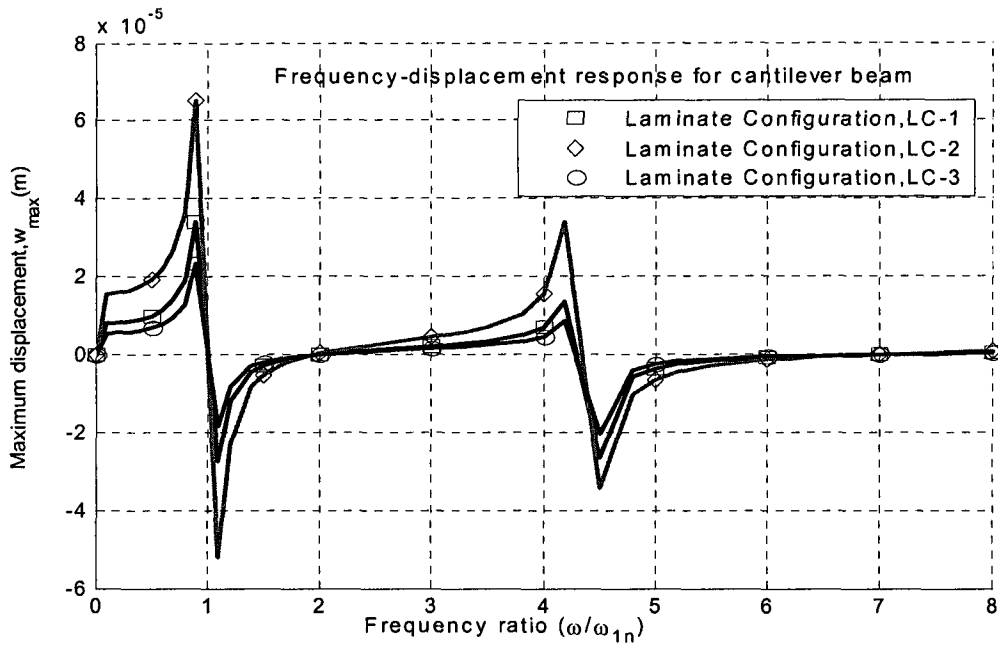


Figure 5. 18 Frequency-displacement plot of beam with taper configuration-C

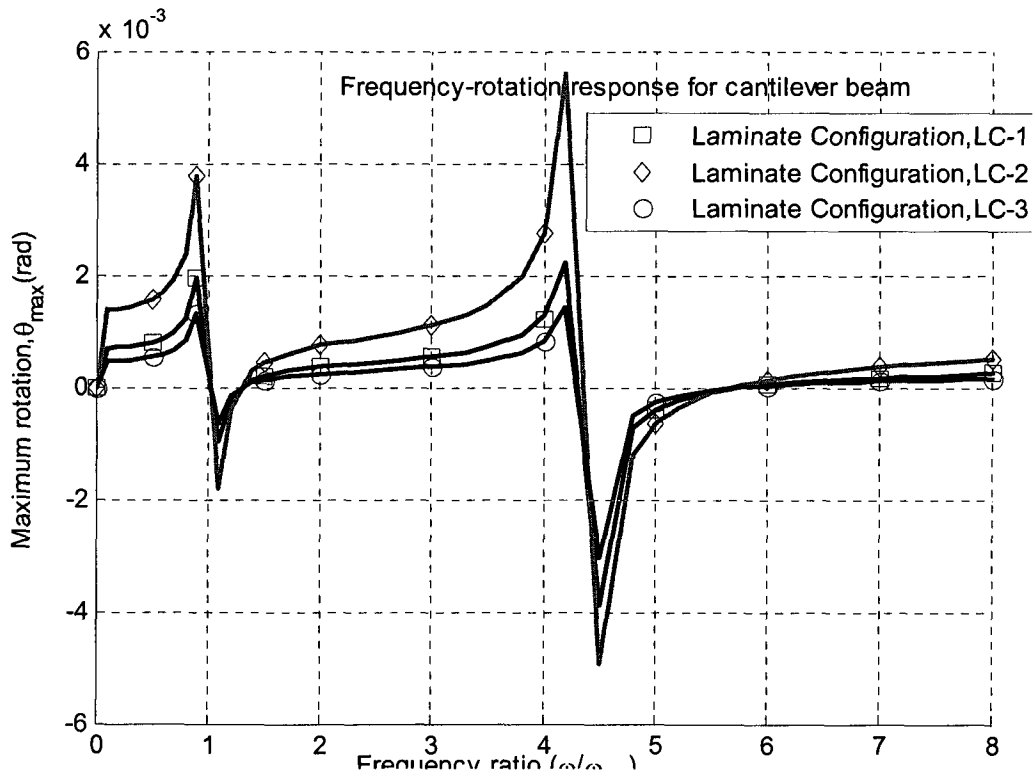


Figure 5. 19 Frequency-rotation plot of beam with taper configuration-C

It can be observed from Figures 5.18 and 5.19 that the transverse displacement and rotation of LC-3 laminate configuration are lowest and for LC-2 they are highest for beam with taper configuration-C. Here first lowest natural frequency ω_{1n} has been considered for each respective laminate configuration (given in Table 4.14) in the calculation.

Example 5.3.2

A sinusoidal force of magnitude 2 N and a sinusoidal moment of magnitude 2 N-m with excitation frequency ω are applied at free end of cantilever beam. Mechanical properties as described in the section 5.2 are used in this example. The example 5.3.2 is solved to calculate the forced response in terms of transverse displacement and rotation of beam at the free end of beam. The forced response in terms of the magnitude of sinusoidal transverse displacement and the magnitude of sinusoidal rotation are obtained considering 12-elements mesh using higher-order finite element method for beam with taper configuration-D and presented in Figures 5.20 and 5.21.

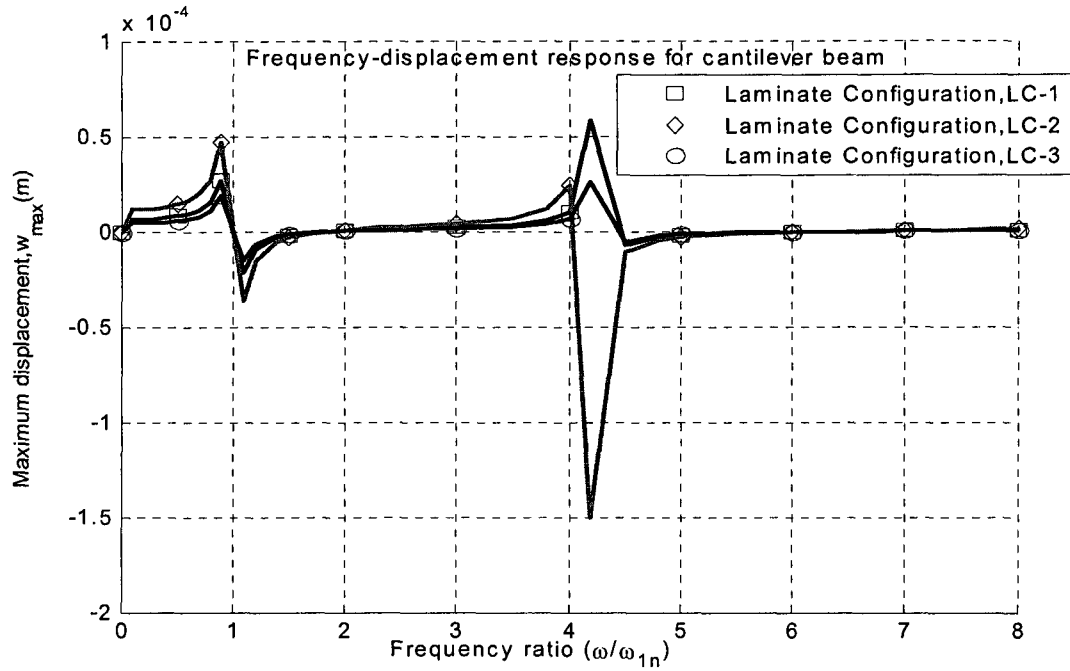


Figure 5. 20 Frequency-displacement plot of beam with taper configuration-D

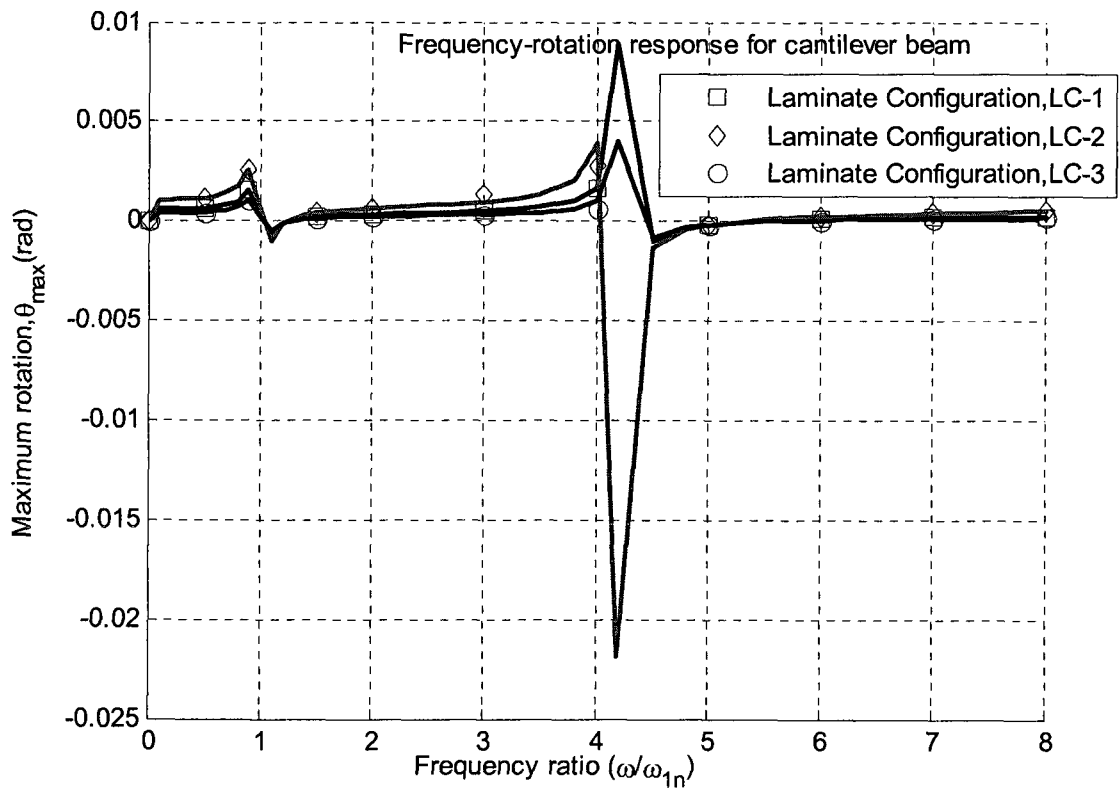


Figure 5. 21 Frequency-rotation plot of beam with taper configuration-D

Figures 5.20 and 5.21 show that transverse displacement and rotation of LC-3 laminate configuration are lowest and that of LC-2 are highest. Here first lowest natural frequency ω_{1n} has been considered for each respective laminate configuration (given in Table 4.17) in the calculation. Laminate configuration LC-1 ranked second in terms of forced response for fixed-free boundary condition of beam with taper configuration-D. This difference in response is expected for different laminate configurations because transverse displacement and rotation calculated for different laminate configurations depend on the stiffness of the beam. The stiffness of the beam depends upon D_{11} which is directly related with Q_{11} of the ply. Different laminate configurations of composite beams give the different stiffnesses according to ply orientations in the laminate.

5.4 Effect of Taper angle on transverse displacement and rotation

To investigate the effects of taper angle on forced response in terms of transverse displacement and rotation, beams with taper configurations-C and D are considered. The geometric properties of the beams are: Beam is considered with 36 and 12 plies at thick and thin sections respectively, which results in 24 drop-off plies, height at thick section (h_1) is 0.0045m, height at thin section (h_2) is 0.0015m, individual ply thickness (t_k) is 0.000125m, and width (b) is unity. Values of taper angle (ϕ) for tapered section have been set in the range of 1^0 to 3^0 . Since the thickness ratio is kept constant, therefore increasing the taper angle results in decreasing the length of tapered section. The tapered section of beam is meshed with twelve equal length elements.

Example 5.4.1

A sinusoidal force of magnitude 2 N and a sinusoidal moment of magnitude 2 N-m with excitation frequency ω are applied at free end of cantilever beam. Mechanical properties as described in the section 5.2 are used in this example. The example 5.4.1 is solved to calculate the forced response in terms of transverse displacement and rotation of beam at the free end of beam. The forced response in terms of the magnitude of sinusoidal transverse displacement and the magnitude of sinusoidal rotation are obtained considering 12-elements mesh using higher-order finite element method for beam with taper configuration-C and presented in Figures 5.22 and 5.23.

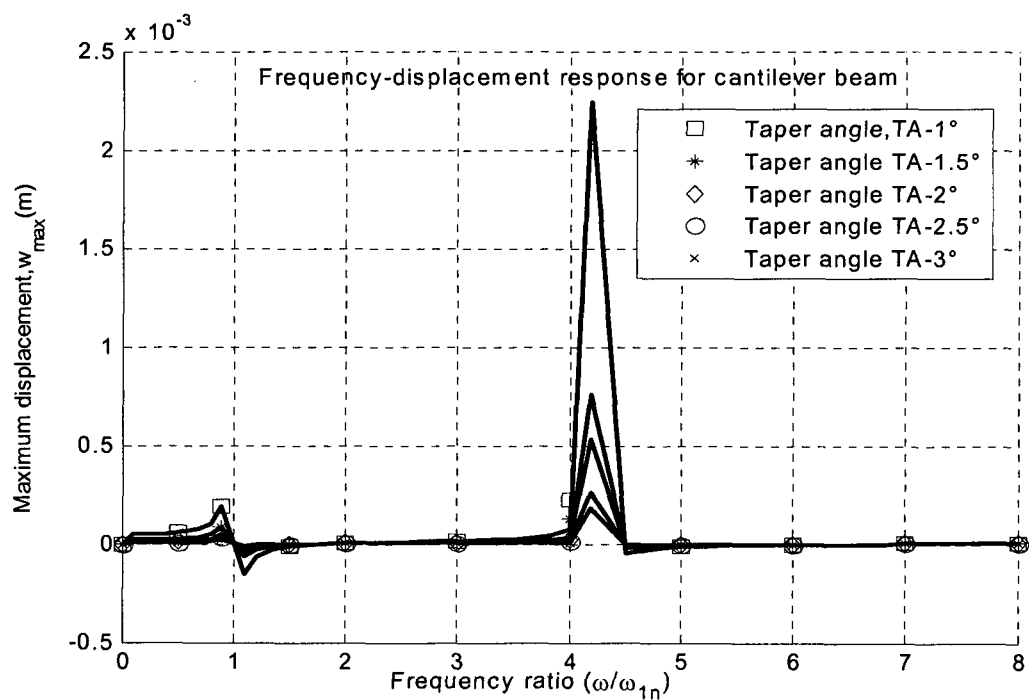


Figure 5. 22 Frequency-displacement plot of beam with taper configuration-C

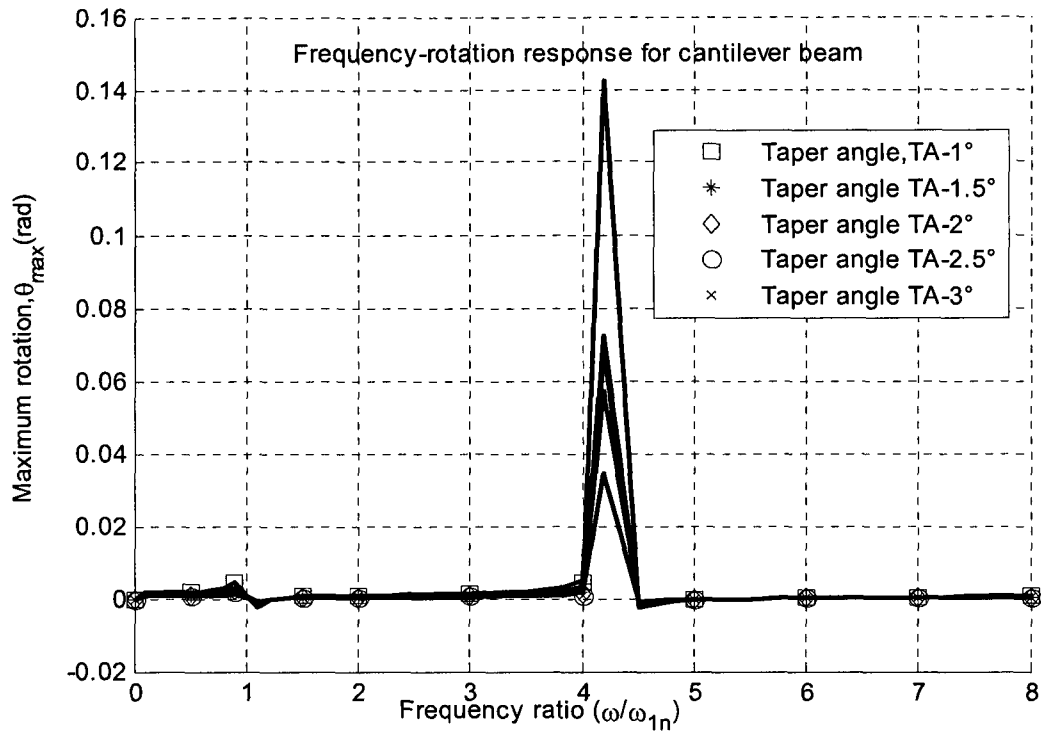


Figure 5. 23 Frequency-rotation plot of beam with taper configuration-C

The effect of taper angle on forced response (transverse displacement and rotation) of beam with taper configuration-C for fixed-free boundary condition is shown in Figures 5.22 and 5.23. Here first lowest natural frequency ω_{1n} has been considered for each respective taper angle of the beam (given in Table 4.20) in the calculation. The results obtained for different values of taper angle show that the transverse displacement and rotation (forced response) obtained from lowest taper angle are the highest and further, the highest taper angle gives the lowest response.

Example 5.4.2

A sinusoidal force of magnitude 2 N and a sinusoidal moment of magnitude 2 N-m with excitation frequency ω are applied at free end of cantilever beam. Mechanical properties as described in the section 5.2 are used in this example. The example 5.4.2 is

solved to calculate the forced response in terms of transverse displacement and rotation of beam at the free end of beam. The forced response in terms of the magnitude of sinusoidal transverse displacement and the magnitude of sinusoidal rotation are obtained considering 12-elements mesh using higher-order finite element for beam with taper configuration-D and presented in Figures 5.24 and 5.25.

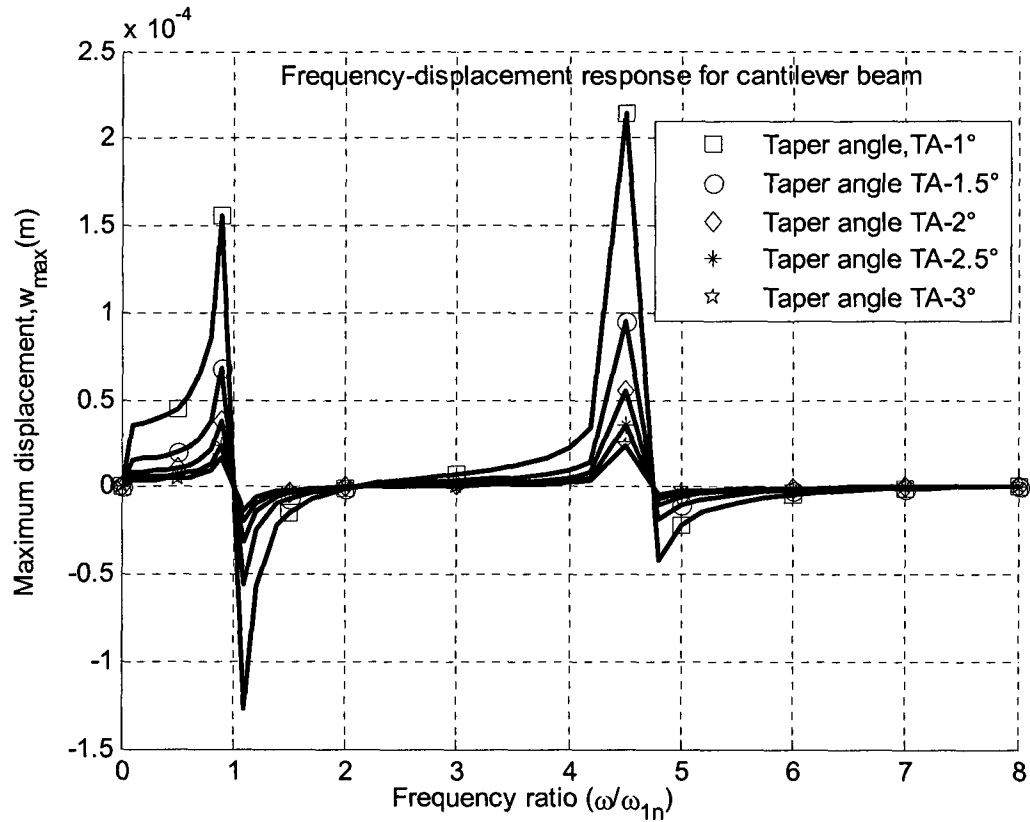


Figure 5. 24 Frequency-displacement plot of beam with taper configuration-D

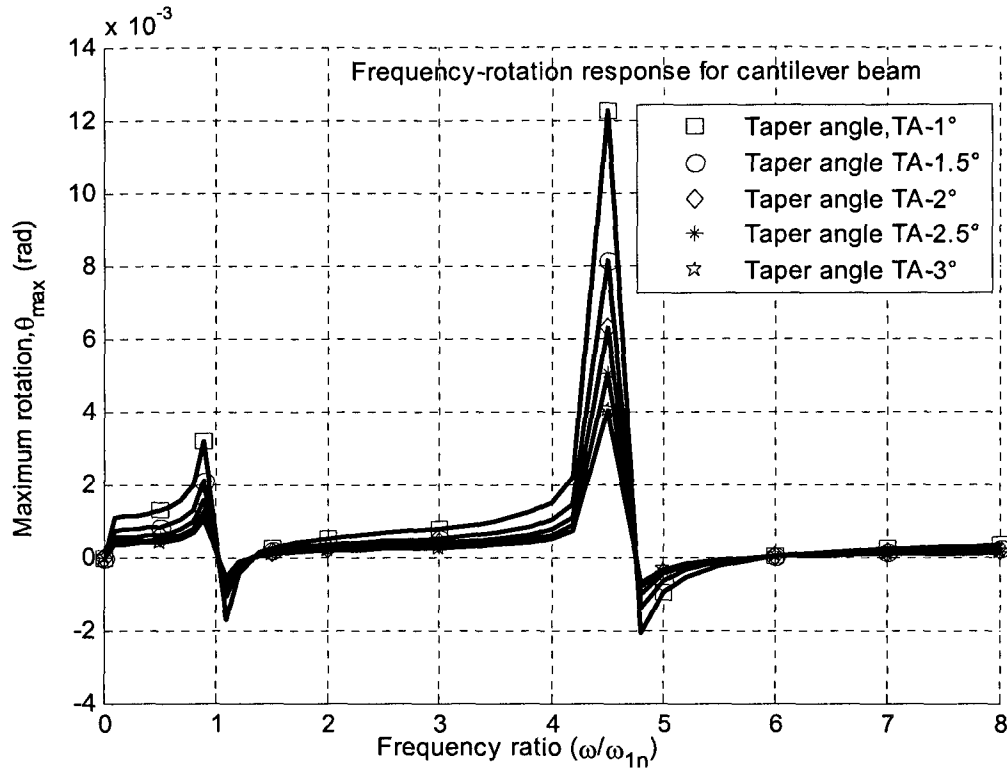


Figure 5. 25 Frequency-rotation plot of beam with taper configuration-D

The effect of taper angle on forced response (transverse displacement and rotation) of beam with taper configuration-D for fixed-free boundary condition is shown in Figures 5.24 and 5.25. Here first lowest natural frequency ω_{1n} has been considered for each respective taper angle of the beam (given in Table 4.23) in the calculation. The results obtained for different values of taper angle show that forced response in terms of transverse displacement and rotation obtained for lowest taper angle values are the highest and further, the highest taper angle value gives the lowest response. It is because of the effect of increasing beam length that makes it less stiff and vice versa.

5.5 Effect of length ratio on transverse displacement and rotation

To study the length ratio (L_{thick} / L_{thin}) effect on forced response in terms of transverse displacement and rotation, beams with taper configurations-C and D are considered as shown in Figures 4.8 and 4.10. The ply of composite beam is made of NCT/301 graphite-epoxy material and the beam consists of 36 plies. The configuration of the thick section is $[0/90]_{9s}$, and that of thin section is $[0/90]_{3s}$. The beam is considered with 36 and 12 plies at thick and thin sections respectively, which results in 24 drop-off plies. The beam is meshed using 9-elements and the length of each element subsection is 0.0115m, total length of the beam is 0.1035m, height at thick section (h_1) is 0.0045m, height at thin section (h_2) is 0.0015m, individual ply thickness (t_k) is 0.000125m, and width (b) is unity. Taper angle (ϕ) for tapered section is considered as 2.5° .

Since the thickness ratio, taper angle and total length are kept constant, changing length ratio is adjusted by using changing lengths of thick and thin sections. When length ratio is 2, it is that length of thick section is twice that of thin section. When length ratio is $\frac{1}{2}$, it is that length of thick section is half of the length of thin section. When length ratio is 1, the length of thick section is equal to the length of thin section.

Example 5.5.1

A sinusoidal force of magnitude 2 N and a sinusoidal moment of magnitude 2 N-m with excitation frequency ω are applied at free end of cantilever beam. Mechanical properties as described in the section 5.2 are used in this example. The example 5.5.1 is solved to calculate the forced response in terms of transverse displacement and rotation of beam at the free end of beam. The forced response in terms of the magnitude of sinusoidal transverse displacement and the magnitude of sinusoidal rotation are obtained using higher-

order finite element of beam with taper configuration-C for fixed-free boundary condition and presented in Figures 5.26 and 5.27.

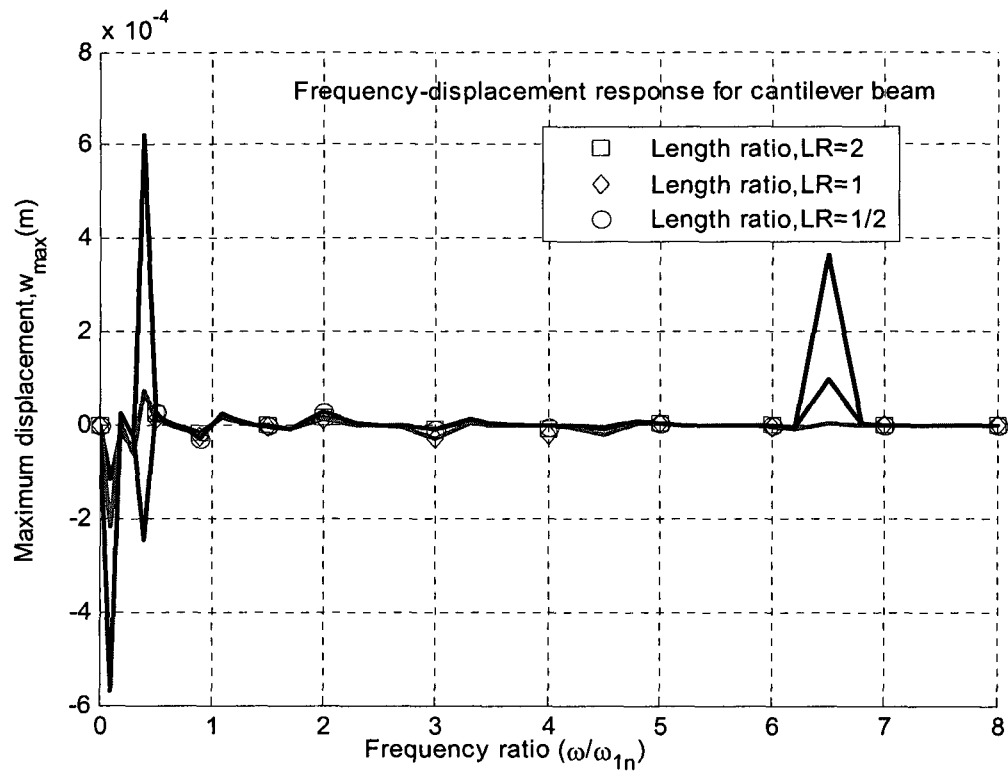


Figure 5. 26 Frequency-displacement plot of beam with taper configuration-C

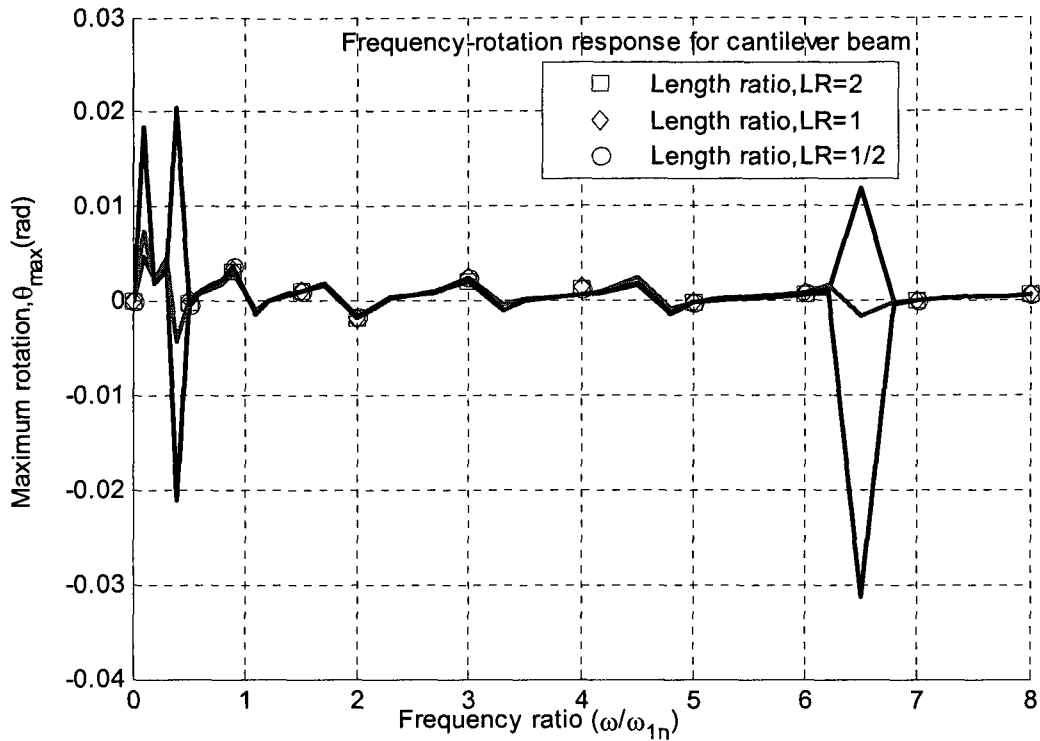


Figure 5. 27 Frequency-rotation plot of beam with taper configuration-C

As one can observe from the Figures 5.26 and 5.27, transverse displacement and rotation of beam with higher length ratio are lower and they are higher for beam with lower length ratio for fixed-free boundary condition of beam with taper configuration-C. Here first lowest natural frequency ω_{1n} has been considered for each respective length ratio of the beam (given in Table 4.26) in the calculation.

Example 5.5.2

A sinusoidal force of magnitude 2 N and a sinusoidal moment of magnitude 2 N-m with excitation frequency ω are applied at free end of cantilever beam. Mechanical properties as described in the section 5.2 are used in this example. The example 5.5.2 is solved to calculate the forced response at the free end of the beam. The forced response in terms of the magnitude of sinusoidal transverse displacement and the magnitude of sinusoidal rotation are

obtained using higher-order finite element of beam with taper configuration-D for fixed-free boundary condition and presented in Figures 5.28 and 5.29.

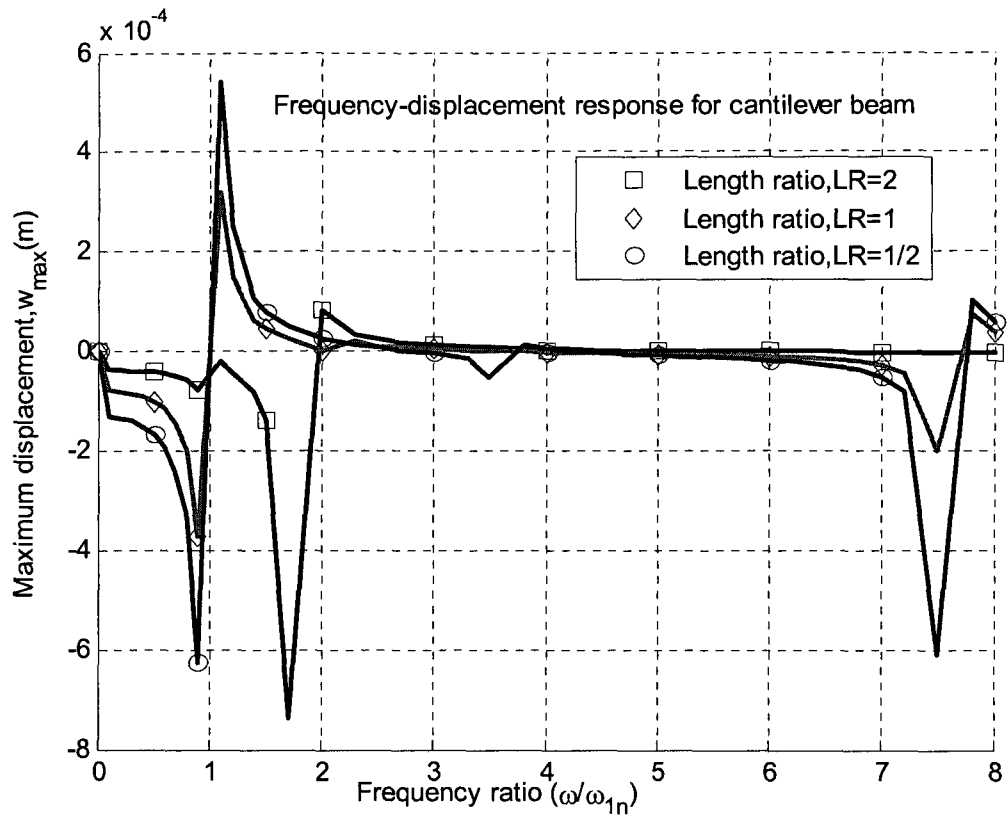


Figure 5. 28 Frequency-displacement plot of beam with taper configuration-D

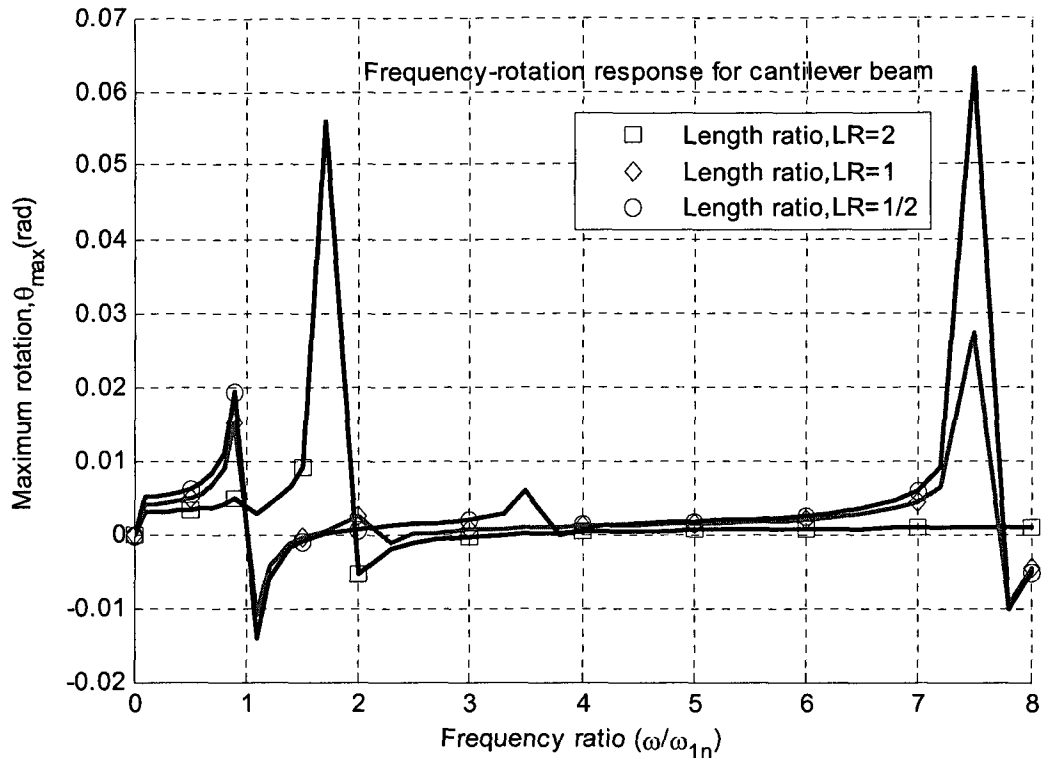


Figure 5.29 Frequency-rotation plot of beam with taper configuration-D

As one can observe from the Figures 5.28 and 5.29, transverse displacement and rotation of beam with higher length ratio are lower and they are higher for beam with lower length ratio for fixed-free boundary condition of beam with taper configuration-D. Here first lowest natural frequency ω_{1n} has been considered for each respective length ratio of the beam (given in Table 4.29) in the calculation. The results obtained for different values of length ratio show that, transverse displacement and rotation obtained from highest length ratio are the lowest and further the lowest length ratio gives the highest values. The transverse displacement and rotation are decreasing with the increasing of length ratio, because the length of thick section increases, which makes it stiffer that results in lower response in terms of transverse displacement and rotation and vice versa.

5.6 Effect of boundary condition on transverse displacement and rotation

To study the boundary condition effects on forced response in terms of transverse displacement and rotation, beams with taper configurations C and D are considered. The ply of composite beam is made of NCT/301 graphite-epoxy material and the beam consists of 36 plies. The configuration of the thick section is $[0/90]_{9s}$ and it is $[0/90]_{3s}$ at thin section.

The geometric properties of the beams are: Beam is considered with 36 and 12 plies at thick and thin section respectively, which results in 24 drop-off plies, it is considered with 12-elements mesh of equal length and the length the beam is 0.0345m, height at thick section (h_1) is 0.0045m, height at thin section (h_2) is 0.0015m, individual ply thickness (t_k) is 0.000125m, width (b) is unity, and taper angle (ϕ) is 2.5°.

Example 5.6.1

By using the mechanical properties as described in the section 5.2, the example 5.6.1 is solved to find the forced response in terms of transverse displacement and rotation of beam with taper configuration-C for simply supported, (thick end) fixed- (thin end) free or cantilever, fixed-fixed, (thick end) free-(thin end) fixed, (thick end) fixed- (thin end) hinged and (thick end) hinged-(thin end) fixed boundary conditions as shown in Figure 5.32 but for taper configuration-D. A sinusoidal force of magnitude 2 N and a sinusoidal moment of magnitude 2 N-m with excitation frequency ω are applied at midpoint of beam span for simply supported, fixed-fixed, (thick end) fixed- (thin end) hinged and (thick end) hinged-(thin end) fixed and at free end of (thick end) fixed- (thin end) free or cantilever, (thick end) free- (thin end) fixed boundary conditions. The forced response in terms of the magnitude of sinusoidal transverse displacement and the magnitude of sinusoidal rotation are obtained (at the place where force is applied) considering 12-elements mesh using higher-order finite

element of beam with taper configuration-C for all boundary conditions and presented in Figures 5.30 and 5.31.

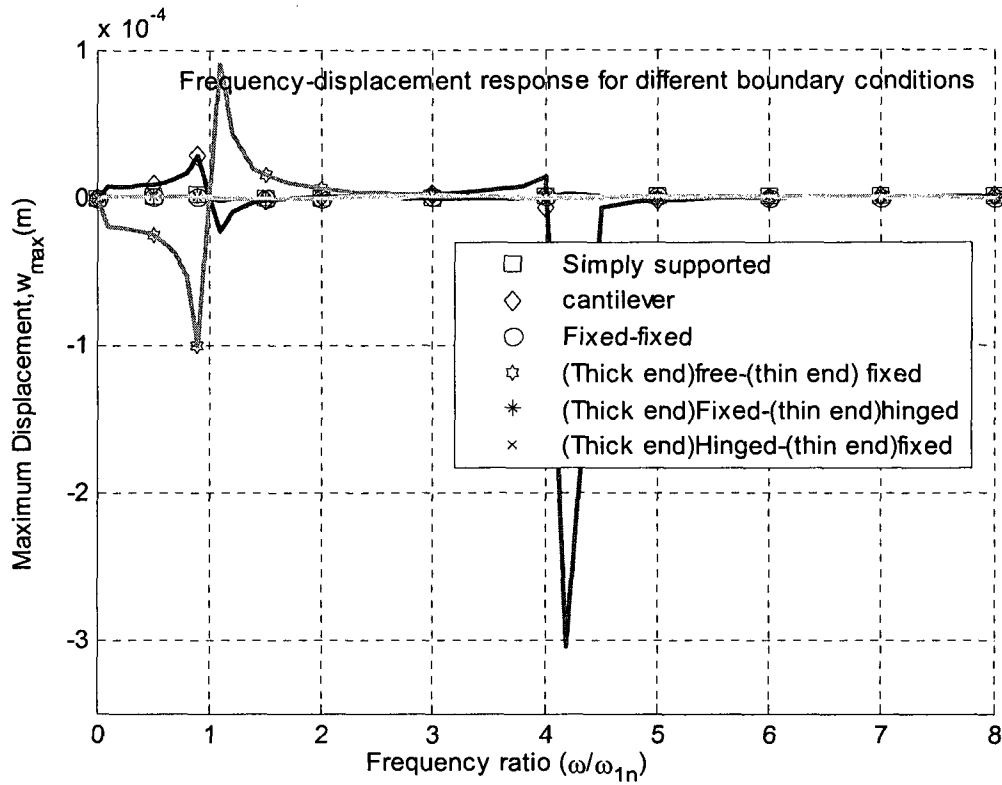


Figure 5. 30 Frequency-displacement plot of beam with taper configuration-C

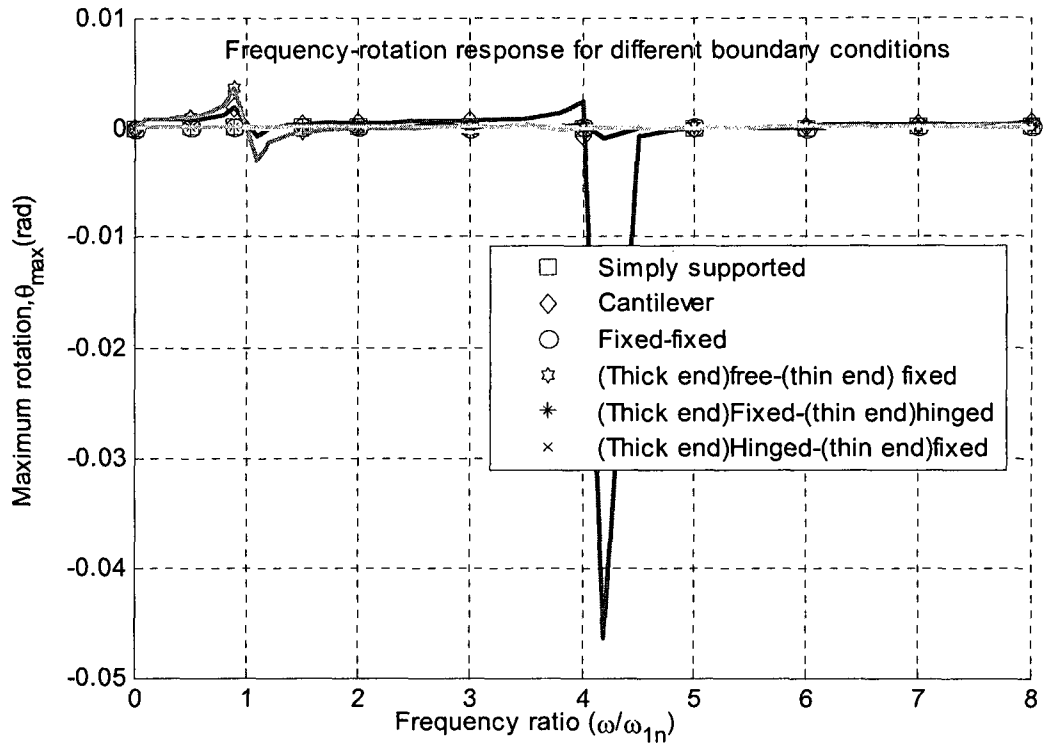


Figure 5.31 Frequency-rotation plot of beam with taper configuration-C

One can observe the effect of boundary conditions on transverse displacement and rotation of beam with taper configuration-C from the Figures 5.30 and 5.31. Here first lowest natural frequency ω_{1n} has been considered for each respective boundary condition (ω_{1n} is 4.4752×10^4 rad/sec for simply supported, ω_{1n} is 2.8244×10^4 rad/sec for cantilever, ω_{1n} is 10.4273×10^4 rad/sec for fixed-fixed, ω_{1n} is 0.1331×10^4 rad/sec for (thick end) free- (thin end) fixed, ω_{1n} is 1.3259×10^4 rad/sec for (thick end) fixed- (thin end) hinged, ω_{1n} is 0.9998×10^4 rad/sec for (thick end) hinged- (thin end) fixed) beam) in the calculation. It shows that beam with (thick end) free- (thin end) fixed boundary condition gives the highest transverse displacement and rotation that means at this boundary condition the beam gets lowest stiffness and beam with fixed-fixed boundary condition gives the lowest transverse

displacement and rotation that means at this boundary condition the beam gets highest stiffness.

Example 5.6.2

By using the mechanical properties as described in the section 5.2, the example 5.6.2 is solved to calculate the forced response of beam with taper configuration-D with simply supported, (thick end) fixed- (thin end) free or cantilever, fixed-fixed, (thick end) free- (thin end) fixed, (thick end) fixed- (thin end) hinged and (thick end) hinged- (thin end) fixed boundary conditions as shown in Figure 5.32. A sinusoidal force of magnitude 2 N and a sinusoidal moment of magnitude 2 N-m with excitation frequency ω are applied at midpoint of beam span for simply supported, fixed-fixed, (thick end) fixed- (thin end) hinged and (thick end) hinged- (thin end) fixed and at free end of (thick end) fixed- (thin end) free, (thick end) free- (thin end) fixed boundary conditions. The forced response in terms of the magnitude of sinusoidal transverse displacement and the magnitude of sinusoidal rotation are obtained (at the place where force is applied) considering 12-elements mesh using higher-order finite element for all boundary conditions and presented in Figures 5.33 and 5.34.

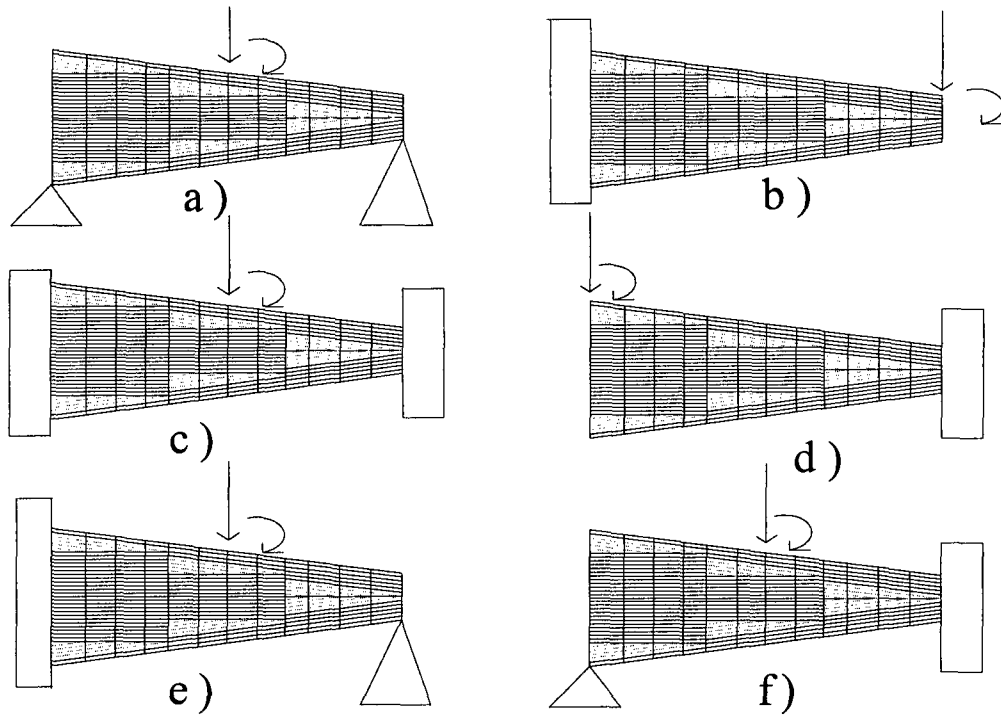


Figure 5.32 Force applied on beam with taper configuration-D a) at mid-point of simply supported beam, b) at free end of (thick end) fixed- (thin end) free or cantilever beam, c) at mid-point of fixed-fixed beam, d) at free end of (thick end) free- (thin end) fixed beam, e) at mid-point of (thick end) fixed- (thin end) hinged beam, and f) at mid-point of (thick end) hinged-(thin end) fixed beam.

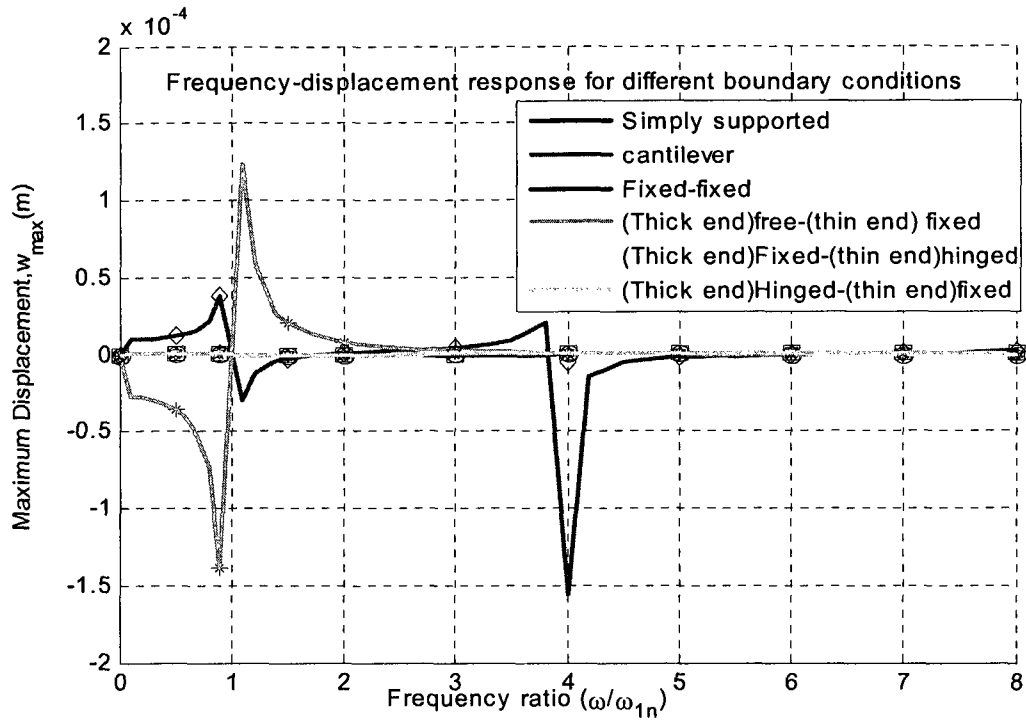


Figure 5.33 Frequency-displacement plot of beam with taper configuration-D

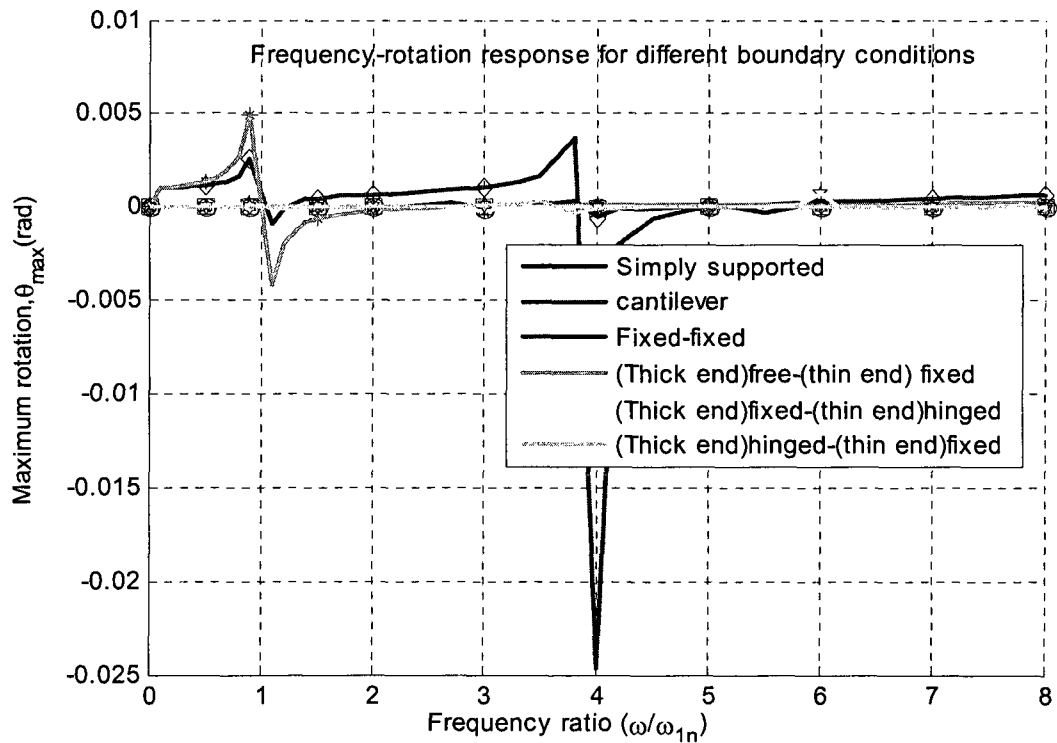


Figure 5.34 Frequency-rotation plot of beam with taper configuration-D

One can observe the effect of boundary conditions on transverse displacement and rotation of beam with taper configuration-D from the Figures 5.33 and 5.34. Here first lowest natural frequency ω_{1n} has been considered for each respective boundary condition (ω_{1n} is 5.1732×10^4 rad/sec for simply supported, ω_{1n} is 2.8816×10^4 rad/sec for cantilever, ω_{1n} is 11.6828×10^4 rad/sec for fixed-fixed, ω_{1n} is 0.1525×10^4 rad/sec for (thick end) free- (thin end) fixed, ω_{1n} is 1.2796×10^4 rad/sec for (thick end) fixed- (thin end) hinged, ω_{1n} is 1.0325×10^4 rad/sec for (thick end) hinged- (thin end) fixed beam) in the calculation. It shows that beam with (thick end) free-(thin end) fixed boundary condition gives the highest transverse displacement and rotation that means at this boundary condition the beam gets lowest stiffness and beam with fixed-fixed boundary condition gives the lowest transverse displacement and rotation that means at this boundary condition the beam gets highest stiffness. Then beam with (thick end) fixed-(thin end) free, and simply supported ranked second, and third position for highest response. Beam with (thick end) fixed-(thin end) hinged and (thick end) hinged-(thin end) fixed boundary conditions give almost the same transverse displacement and rotation though it is very hard to distinguish from the figures due to a large difference with the response for(thick end) free-(thin end) fixed or (thick end) fixed-(thin end)free or cantilever boundary conditions.

5.7 Effect of axial force on transverse displacement and rotation

To investigate the effects of applied axial force on forced response in terms of transverse displacement and rotation, beams with taper configurations A, B, C and D are considered. The ply of composite beam is made of NCT/301 graphite-epoxy material and the beam consists of 36 plies at the thick section. The configuration of the thick section is

$[0/90]_{9s}$, and it is $[0/90]_{3s}$ at thin section. The geometric properties of the beam are with 36 and 12 plies at thick and thin section respectively, which results in 24 drop-off plies, it is considered with 12-element mesh of equal length and the length the beam is 0.0345m, height at thick section (h_1) is 0.0045m, height at thin section (h_2) is 0.0015m, individual ply thickness (t_k) is 0.000125m, width (b) is unity, and taper angle (ϕ) is 2.5° . Concentrated axial tensile (and compressive) force of 10000 N (less than the critical buckling load for any type of taper configurations for any boundary condition) is applied at both ends of the beam and axially distributed tensile force of $10x$ N/m is applied over the beam span.

Example 5.7.1

A sinusoidal force of magnitude 2 N and a sinusoidal moment of magnitude 2 N-m with excitation frequency ω are applied at free end of cantilever beam. By using the mechanical properties as described in the section 5.2, the example 5.7.1 is solved to find the forced response in terms of transverse displacement and rotation of beam with taper configuration-A at the free end of beam. The forced response in terms of the magnitude of sinusoidal transverse displacement and the magnitude of sinusoidal rotation for all types of axial force are obtained considering 12-elements mesh using higher-order finite element and presented in Figures 5.35 and 5.36.

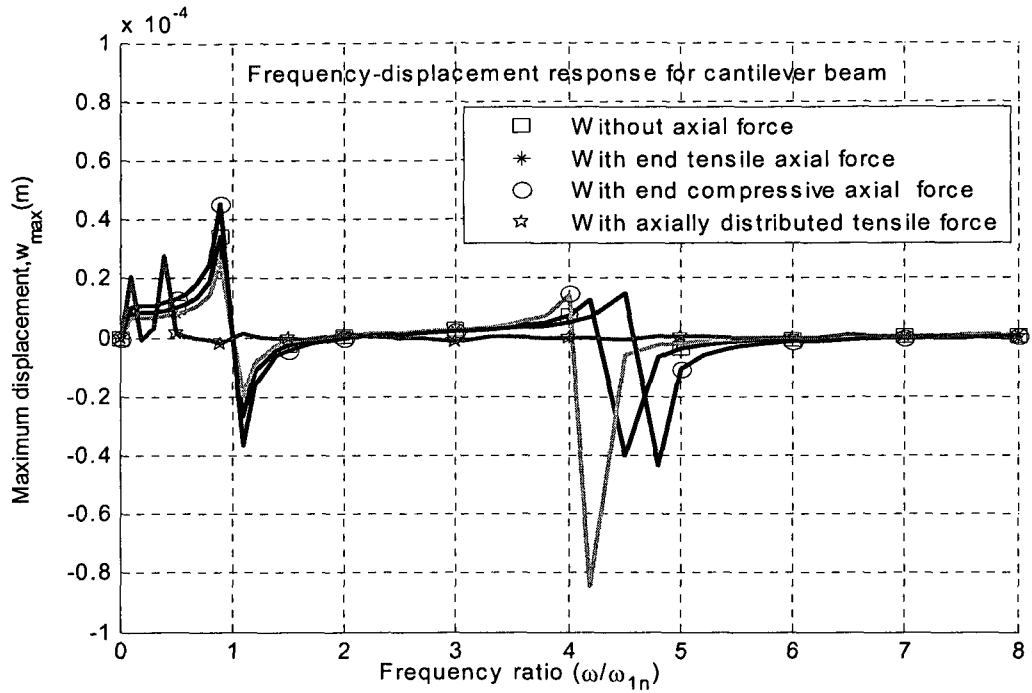


Figure 5. 35 Frequency-displacement plot of beam with taper configuration-A

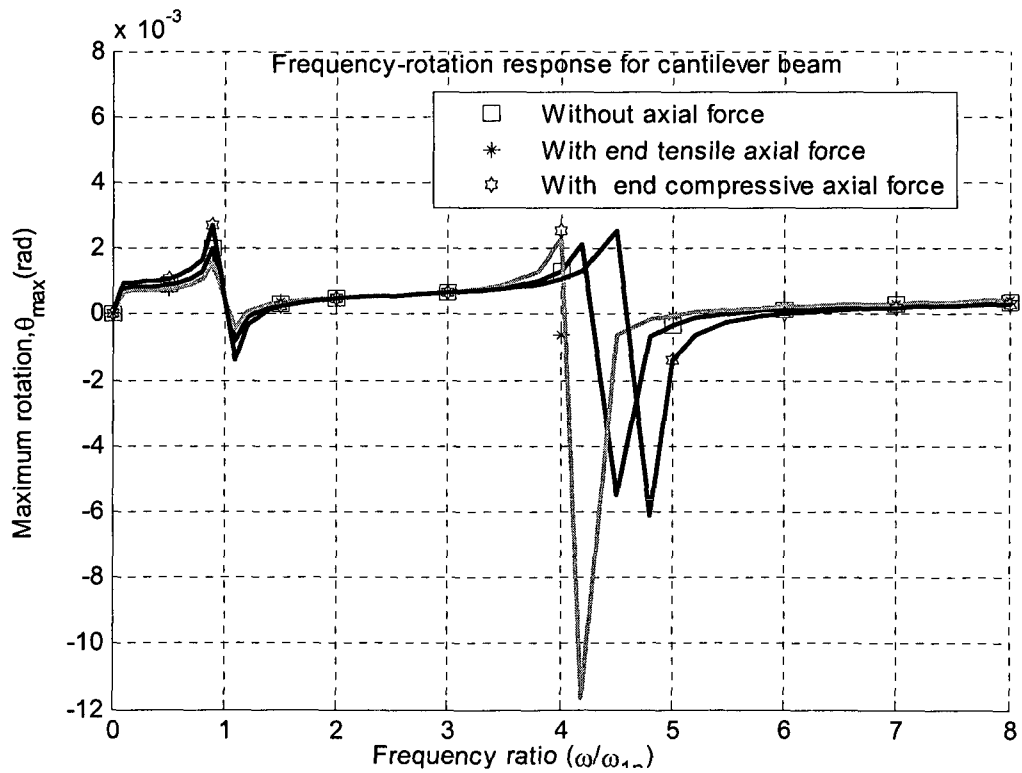


Figure 5. 36 Frequency-rotation plot of beam with taper configuration-A

One can observe the effect of applied axial force on transverse displacement and rotation of beam with taper configuration-A from the Figures 5.35 and 5.36. Here first lowest natural frequency ω_{1n} has been considered for each respective axial force effect of the beam (given in Table 4.34) in the calculation. The results obtained show that the forced response in terms of transverse displacement and rotation obtained considering end tensile axial force and axially distributed tensile force are less than the forced response (transverse displacement and rotation) obtained without axial force (With end compressive axial force, they are more).

Example 5.7.2

A sinusoidal force of magnitude 2 N and a sinusoidal moment of magnitude 2 N-m with excitation frequency ω are applied at free end of cantilever beam. By using the mechanical properties as described in the section 5.2, the example 5.7.2 is solved to calculate the forced response of beam with taper configuration-B at the free end of beam. The forced response in terms of transverse displacement and rotation for all types of axial force are obtained considering 12-elements mesh using higher-order finite element and presented in Figures 5.37 and 5.38.

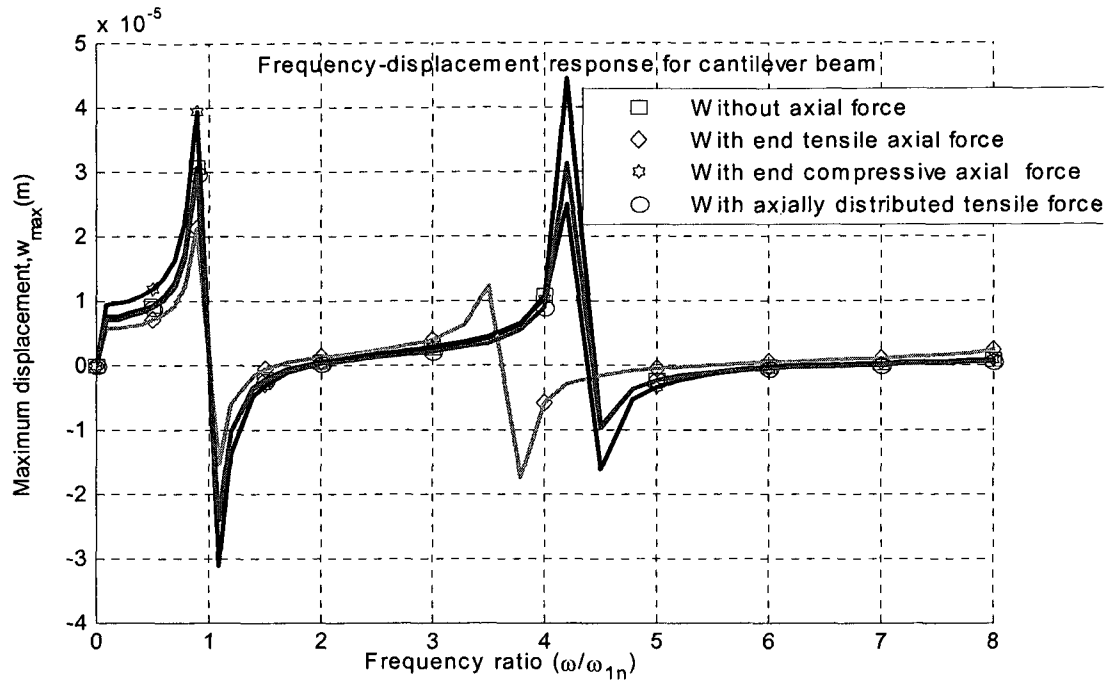


Figure 5.37 Frequency-displacement plot of beam with taper configuration-B

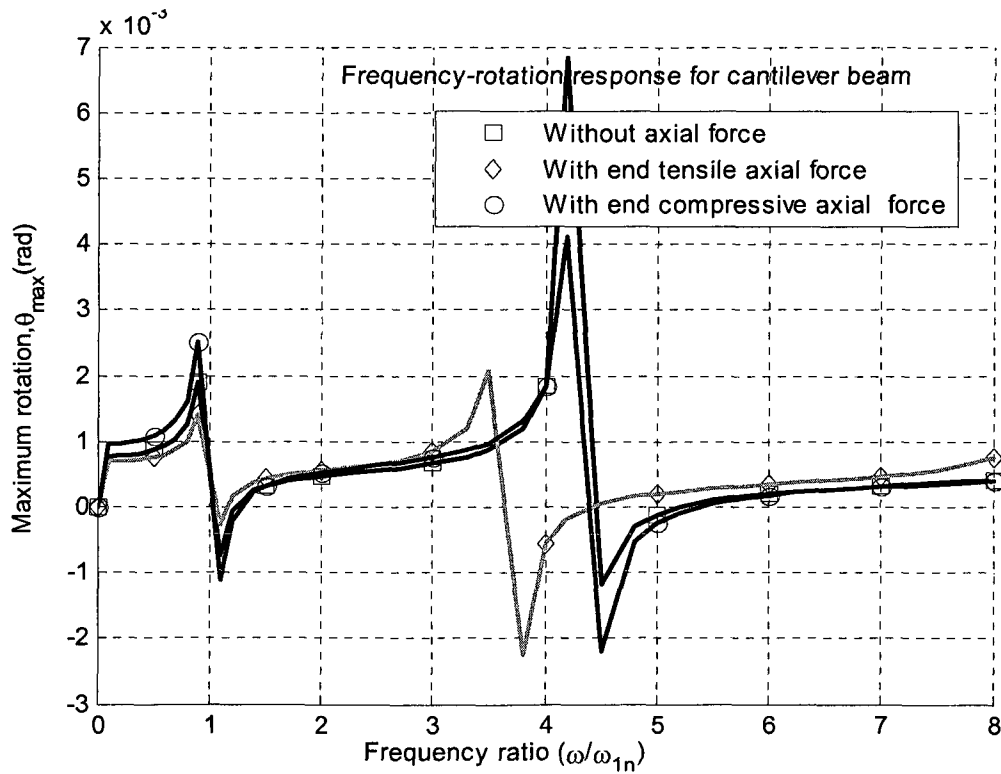


Figure 5.38 Frequency-rotation plot of beam with taper configuration-B

One can observe the effect of applied axial force on transverse displacement and rotation (forced response) of beam with taper configuration-B at fixed-free boundary condition from the Figures 5.37 and 5.38. Here first lowest natural frequency ω_{1n} has been considered for each respective axial force effect of the beam (given in Table 4.37) in the calculation. The results obtained show that the forced response in terms of transverse displacement and rotation obtained considering end tensile axial force and axially distributed tensile force are less than the forced response (transverse displacement and rotation) obtained without axial force (With end compressive axial force, they are more).

Example 5.7.3

A sinusoidal force of magnitude 2 N and a sinusoidal moment of magnitude 2 N-m with excitation frequency ω are applied at free end of cantilever beam. By using the mechanical properties as described in the section 5.2, the example 5.7.3 is solved to calculate the transverse displacement and rotation (forced response) of beam with taper configuration-C at the free end of beam. The forced response in terms of the magnitude of sinusoidal transverse displacement and the magnitude of sinusoidal rotation for all types of axial force are obtained considering 12-elements mesh using higher-order finite element and presented in Figures 5.39 and 5.40.

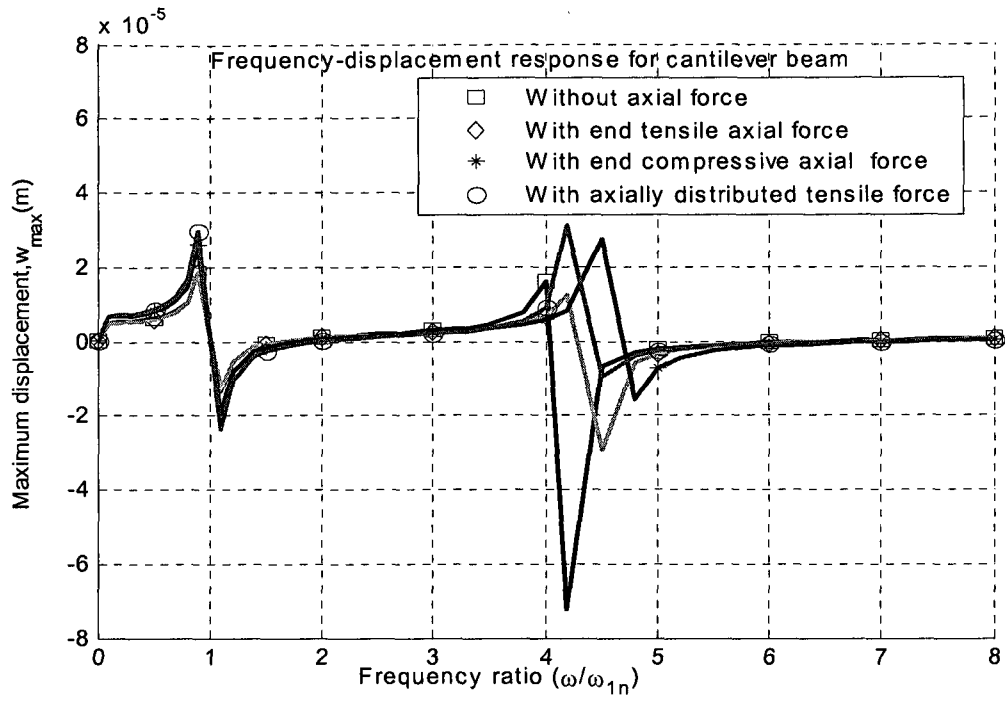


Figure 5. 39 Frequency-displacement plot of beam with taper configuration-C

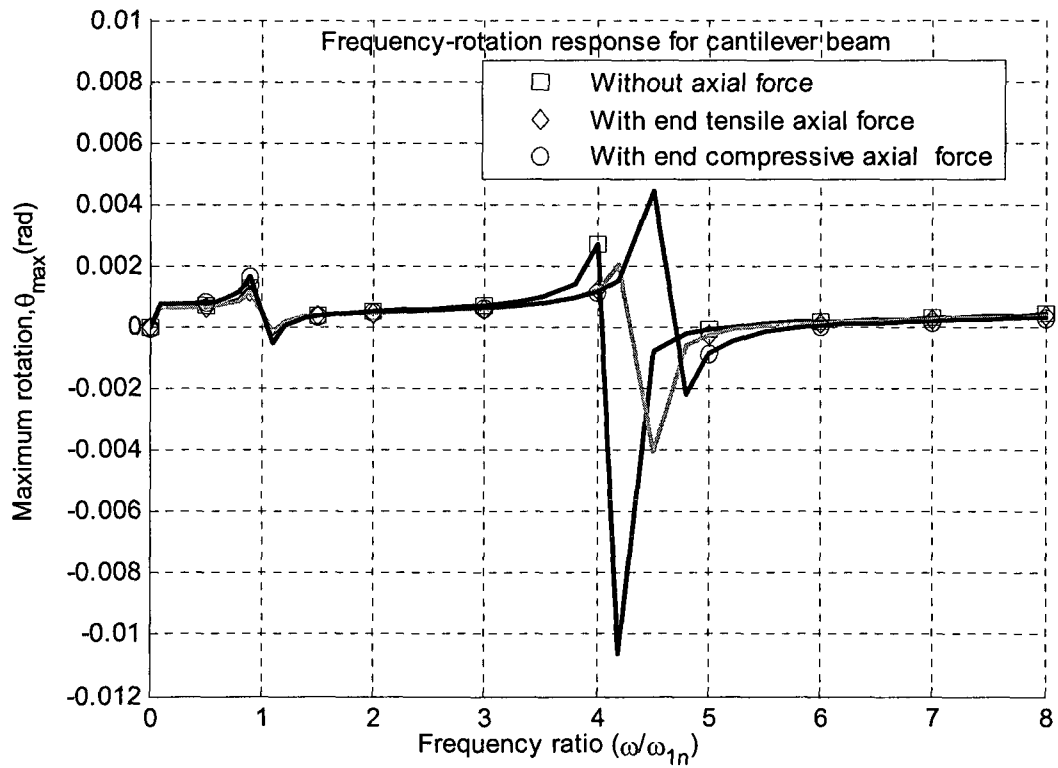


Figure 5. 40 Frequency-rotation plot of beam with taper configuration-C

One can observe the effects of applied axial force on transverse displacement and rotation of beam with taper configuration-C from the Figures 5.39 and 5.40. Here first lowest natural frequency ω_{1n} has been considered for each respective axial force effect of the beam (given in Table 4.40) in the calculation. The results obtained show that the forced response in terms of transverse displacement and rotation obtained considering end tensile axial force and axially distributed tensile force are less than the forced response (transverse displacement and rotation) obtained without axial force (With end compressive axial force, they are more).

Example 5.7.4

A sinusoidal force of magnitude 2 N and a sinusoidal moment of magnitude 2 N-m with excitation frequency ω are applied at free end of cantilever beam. By using the mechanical properties as described in the section 5.2, the example 5.7.4 is solved to calculate the transverse displacement and rotation (forced response) of beam with taper configuration-D at the free end of beam. The forced response in terms of the magnitude of sinusoidal transverse displacement and the magnitude of sinusoidal rotation for all types of axial force are obtained considering 12-elements mesh using higher-order finite element and presented in Figures 5.41 and 5.42.

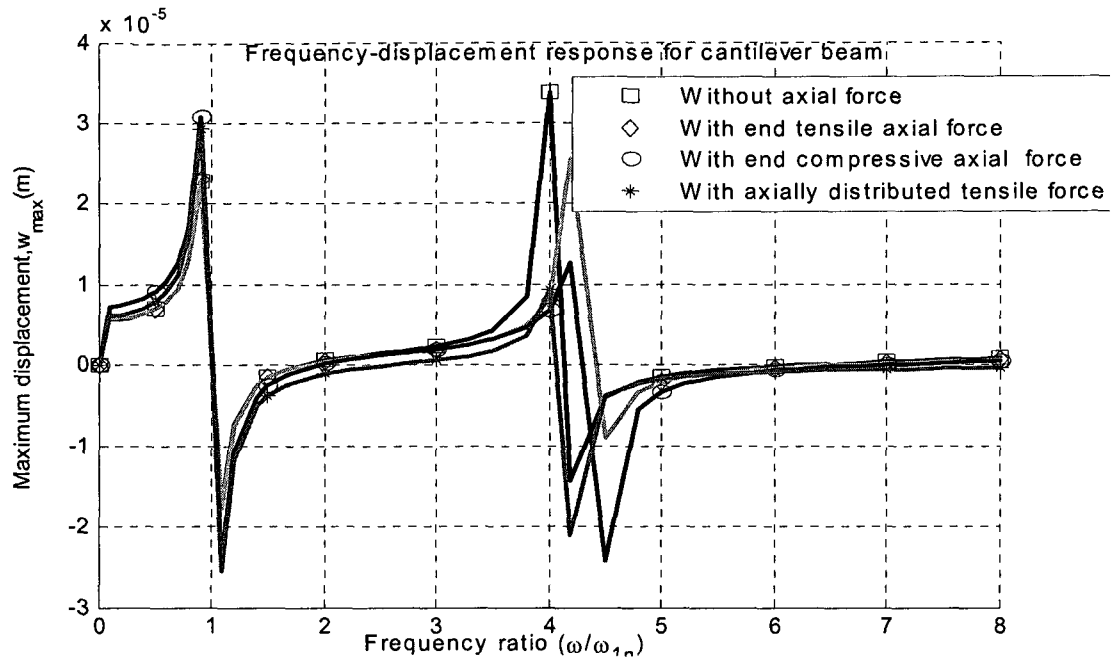


Figure 5.41 Frequency-displacement plot of beam with taper configuration-D

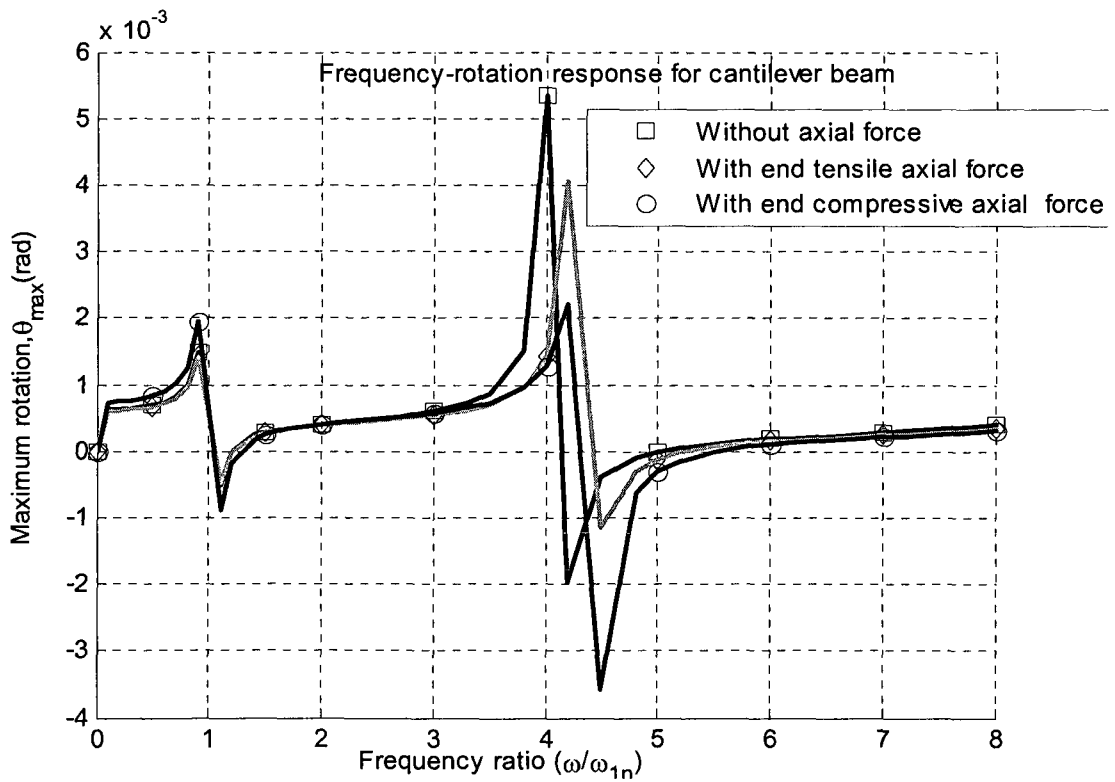
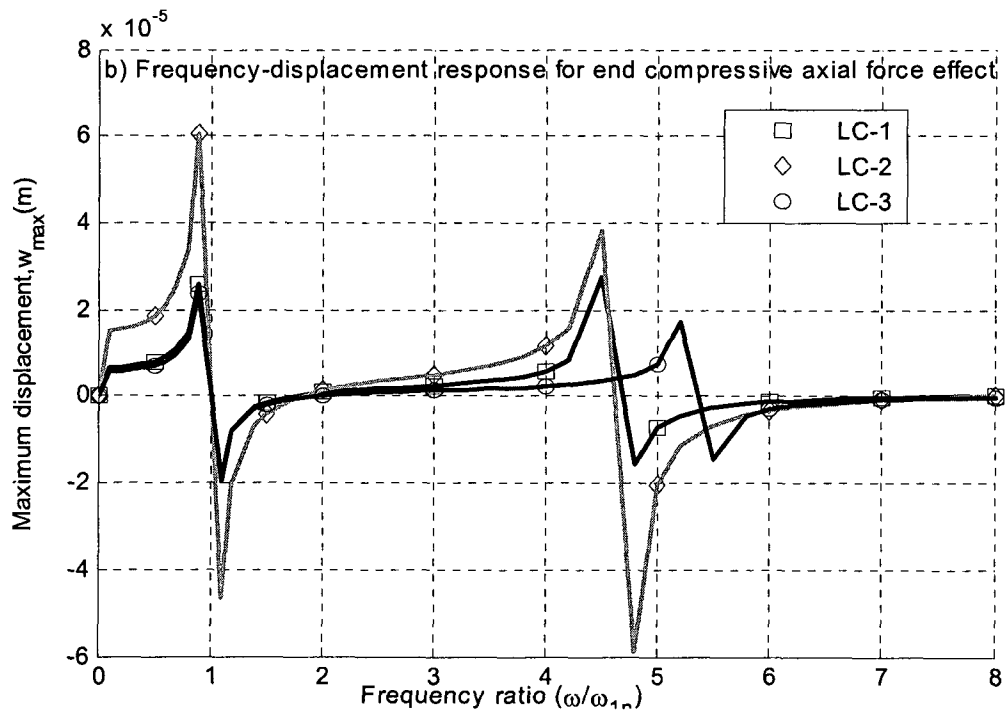
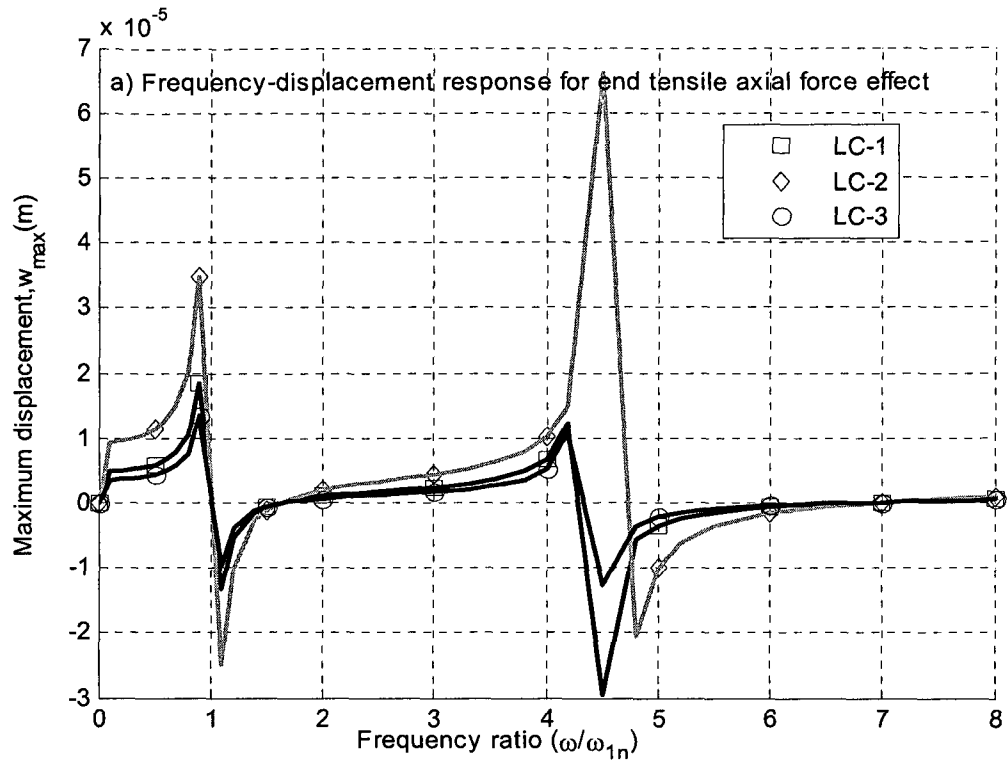


Figure 5.42 Frequency-rotation plot of beam with taper configuration-D

One can observe the effect of applied axial force on forced response in terms of transverse displacement and rotation of beam with taper configuration-D at fixed-free boundary conditions from the Figures 5.41 and 5.42. Here first lowest natural frequency ω_{1n} has been considered for each respective axial force effect of the beam (given in Table 4.43) in the calculation. The results obtained show that the forced response in terms of transverse displacement and rotation obtained considering end tensile axial force and axially distributed tensile force are less than the forced response (transverse displacement and rotation) obtained without axial force (With end compressive axial force, they are more).

Example 5.7.5

A sinusoidal force of magnitude 2 N and a sinusoidal moment of magnitude 2 N-m with excitation frequency ω are applied at free end of cantilever beam. By using the mechanical properties as described in the section 5.2, the example 5.7.5 is solved to calculate the forced response of different laminate configurations of beam with taper configuration-C at the free end of beam. The forced response in terms of the magnitude of sinusoidal transverse displacement and the magnitude of sinusoidal rotation for fixed-free boundary condition for all types of axial force are obtained considering 12-elements mesh using higher-order finite element and presented in Figures 5.43 and 5.44.



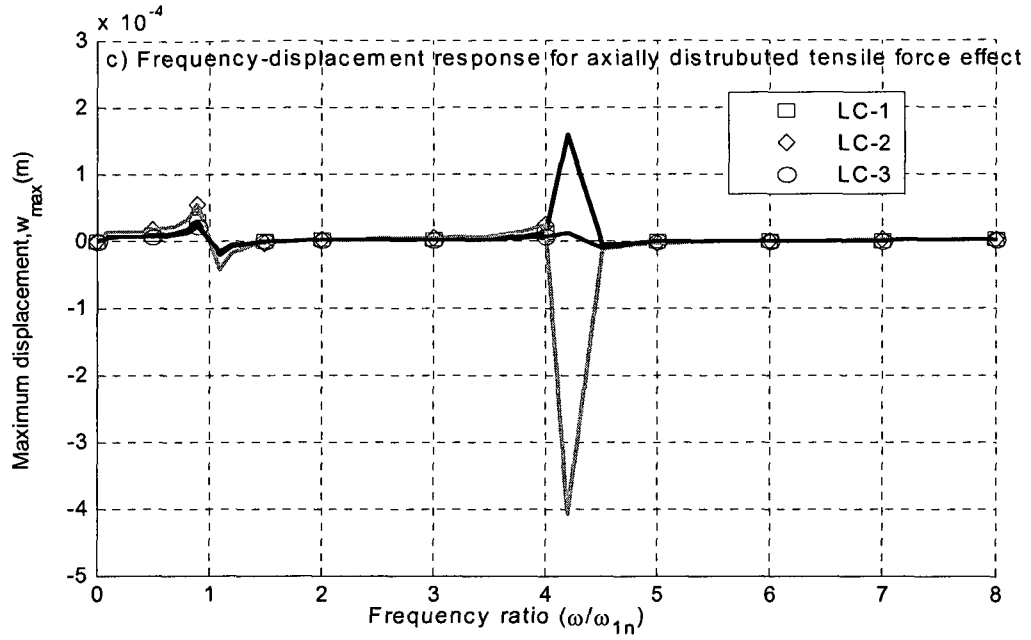
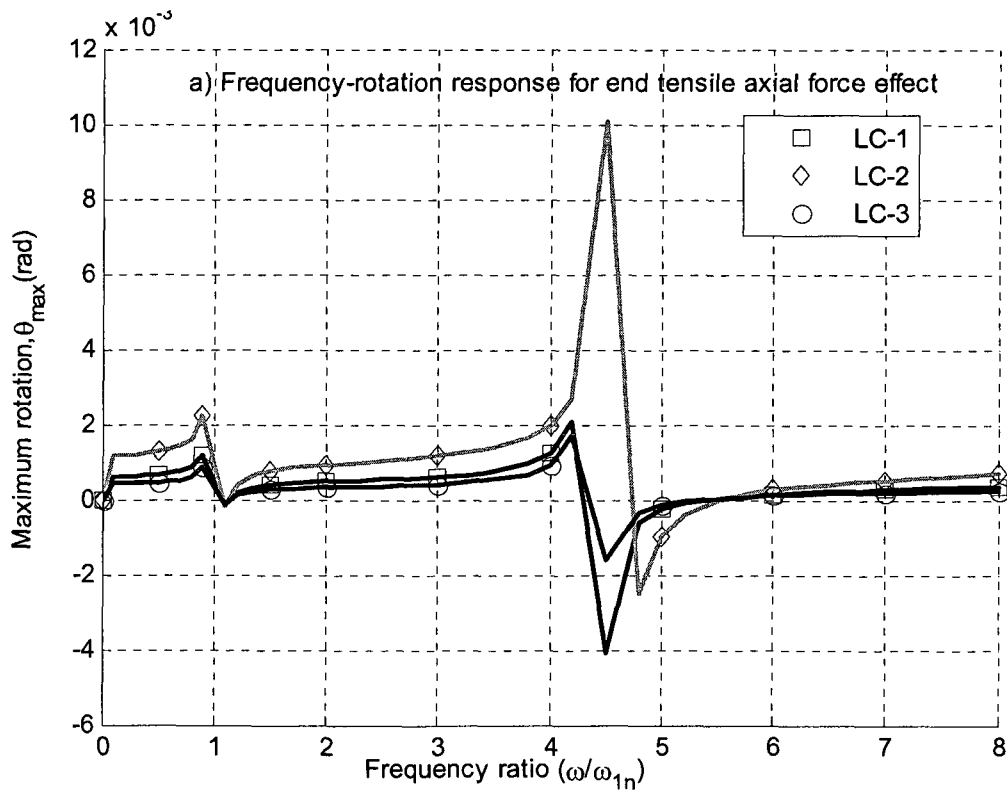


Figure 5. 43 Frequency-displacement plot of beam with taper configuration-C for fixed-free boundary condition with a) Tensile axial force, b) Compressive axial force, and c) Axially distributed tensile force



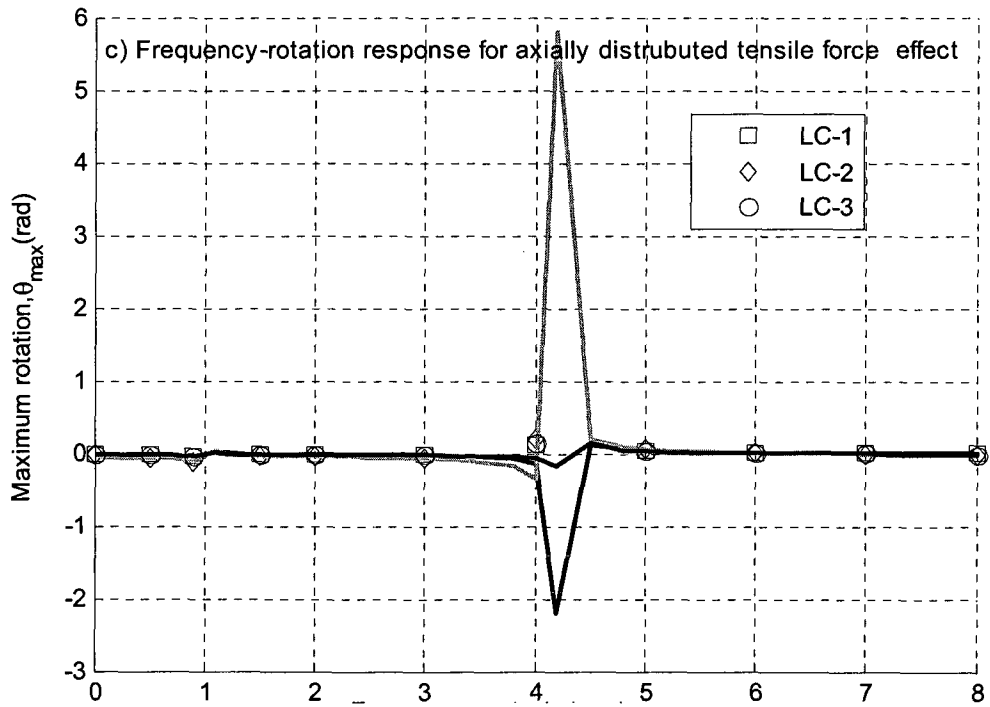
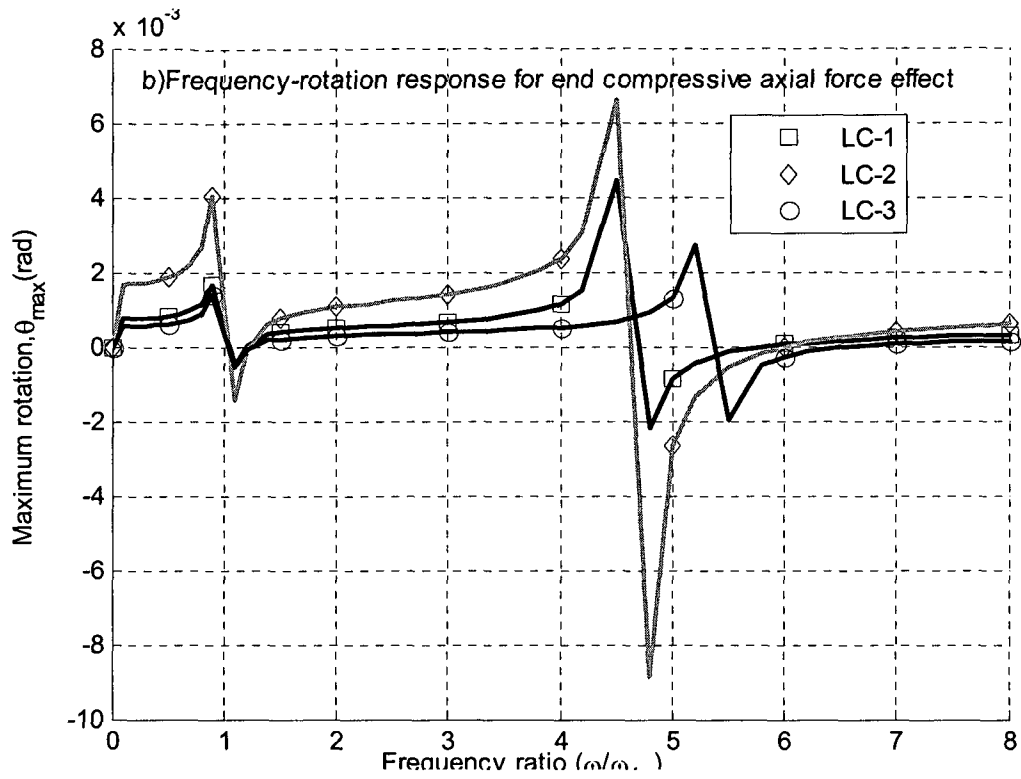


Figure 5. 44 Frequency-rotation plot of beam with taper configuration-C with a) Tensile axial force, b) Compressive axial force, and c) Axially distributed tensile force

One can observe the effects of applied axial force on transverse displacement and rotation for different laminate configurations of beam with taper configuration-C from the Figures 5.43 and 5.44 (a), b), and c)). Here first lowest natural frequency ω_{1n} has been considered for each respective laminate configuration under respective axial force effect of the beam in the calculation. It is obvious from the plotting that LC-2 is more sensitive in terms of forced response. The results in Figures 5.43 and 5.44 (a) show that the forced response obtained from considering tensile axial force are less than forced response obtained without axial force effect but the nature of response among the laminates are similar to response without axial force effect. The results in Figures 5.43 and 5.44 (b) show that forced response obtained from considering compressive axial force are more than the forced response obtained without axial force effect but the nature of response among the laminates are similar to response without axial force effect. The results in Figures 5.43 and 5.44 (c) show that forced response obtained from considering axially distributed force are less than the forced response obtained without axial force effect but the nature of response among the laminates are similar to response of without axial force effect.

Example 5.7.6

A sinusoidal force of magnitude 2 N and a sinusoidal moment of magnitude 2 N-m with excitation frequency ω are applied at free end of cantilever beam with taper configuration-D. By using the mechanical properties as described in the section 5.2, the example 5.7.6 is solved to calculate the forced response in terms of transverse displacement and rotation for different magnitudes of tensile axial force at the free end of the beam. The forced response in terms of the magnitude of sinusoidal transverse displacement and the

magnitude of sinusoidal rotation for fixed-free boundary condition are obtained considering 12-elements mesh using higher-order finite element and presented in Figures 5.45 and 5.46.

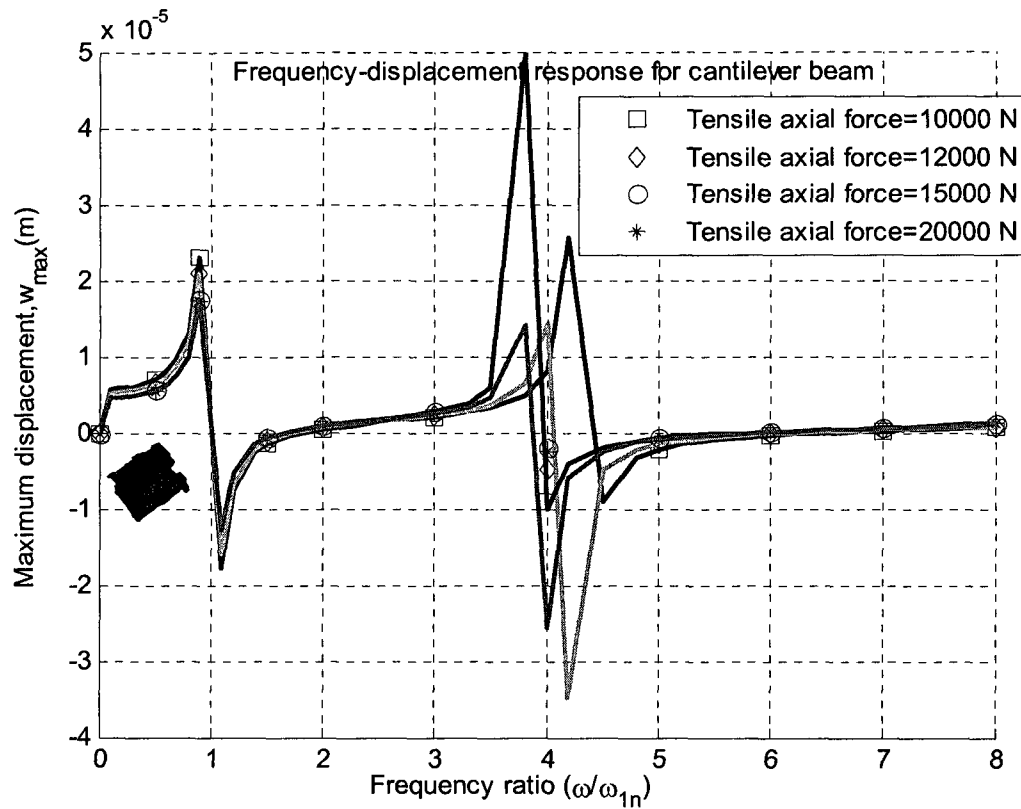


Figure 5. 45 Frequency-displacement plot of beam with taper configuration-D

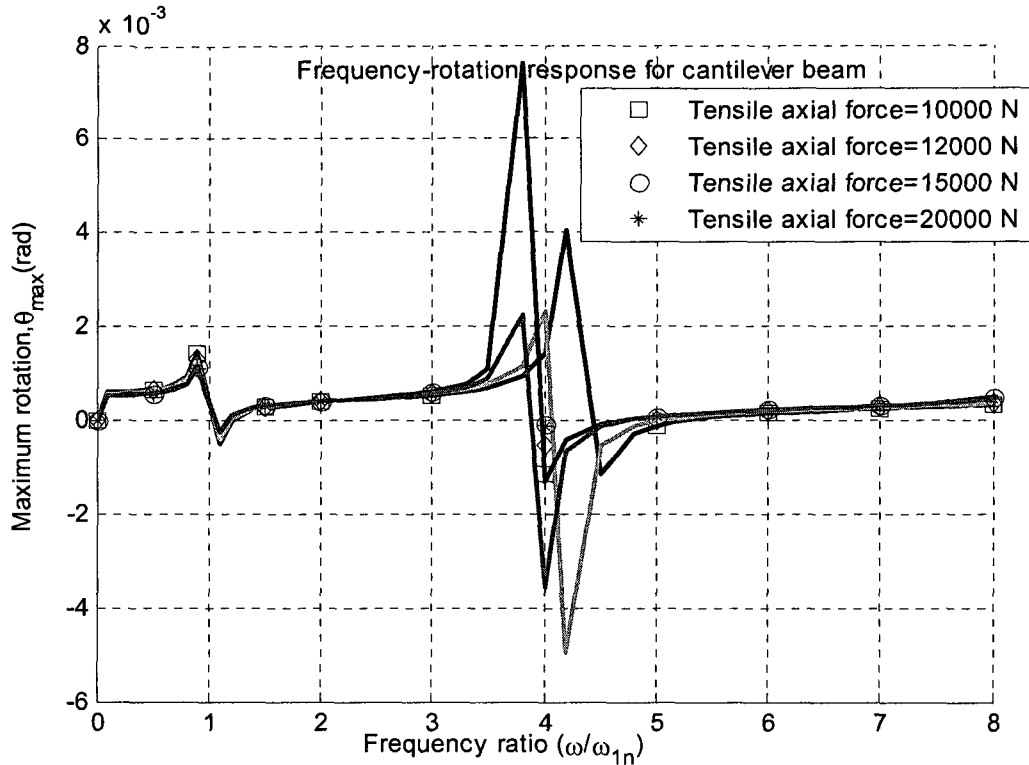


Figure 5.46 Frequency-rotation plot of beam with taper configuration-D

One can observe the effect of magnitude of tensile axial force on both transverse displacement and rotation of beam with taper configuration-D for fixed-free boundary condition from the Figures 5.45 and 5.46. Here first lowest natural frequency ω_{1n} has been considered for each respective amount of end tensile axial force of the beam in the calculation. It shows that with increasing of tensile axial force the response is decreasing respectively as the beam is getting stiffer with the addition of tensile axial force.

5.8 Effect of damping on transverse displacement and rotation

To investigate the effects of damping loss factor on forced response in terms of transverse displacement and rotation, beams with taper configurations A, B, C and D are considered. The ply of composite beam is made of NCT/301 graphite-epoxy material and the

beam consists of 36 plies at the thick section. The configuration of the thick section is $[0/90]_{9s}$ and it is $[0/90]_{3s}$ at thin section.

The geometric properties of the beams are: The beam is considered with 36 and 12 plies at thick and thin section respectively, which results in 24 drop-off plies. The beam is considered with 12-element of equal length and the length the beam is 0.0345m, height at thick section (h_1) is 0.0045m, height at thin section (h_2) is 0.0015m, individual ply thickness (t_k) is 0.000125m, width (b) is unity, and taper angle (ϕ) is 2.5°. The mass proportional constant (α) and stiffness proportional constant (β) are 2.195 and 2.6085×10^{-6} respectively. Here first lowest natural frequency ω_{1n} has been considered for each respective taper configuration of the beam in the calculation.

Example 5.8.1

A sinusoidal force of magnitude 2 N and a sinusoidal moment of magnitude 2 N-m with excitation frequency ω are applied at free end of cantilever beam with taper configuration-A. By using the mechanical properties as described in the section 5.2, the example 5.8.1 is solved to calculate the forced response in terms of transverse displacement and rotation at the free end of the beam. The forced response in terms of the magnitude of sinusoidal transverse displacement and the magnitude of sinusoidal rotation are obtained considering 12-elements mesh using higher-order finite element and presented in Figures 5.47 and 5.48.

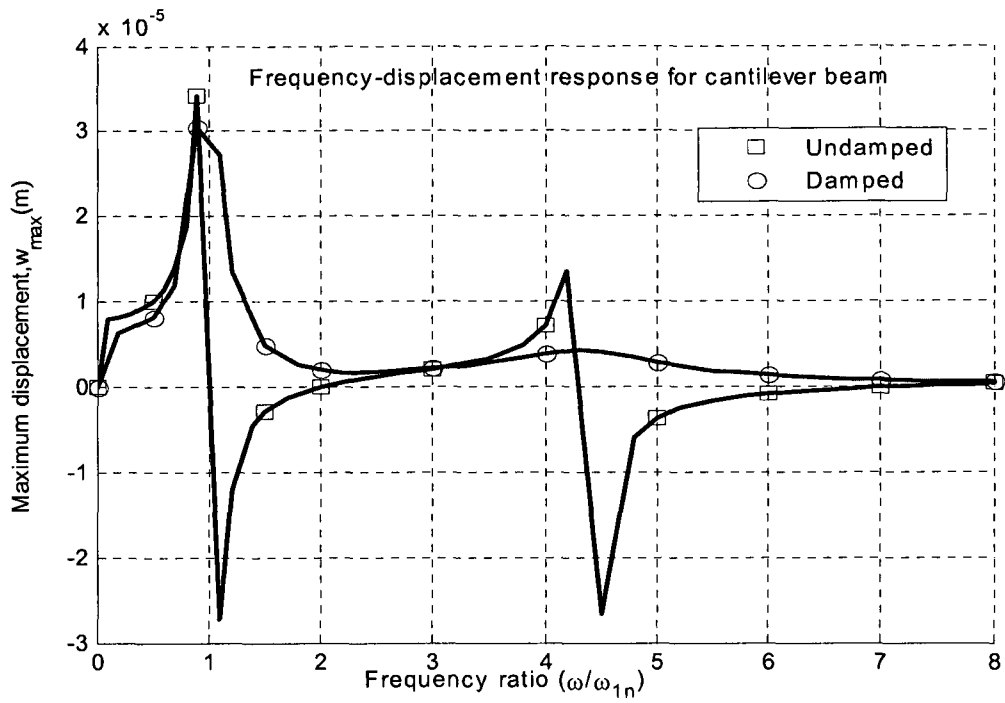


Figure 5.47 Frequency-displacement plot of beam with taper configuration-A

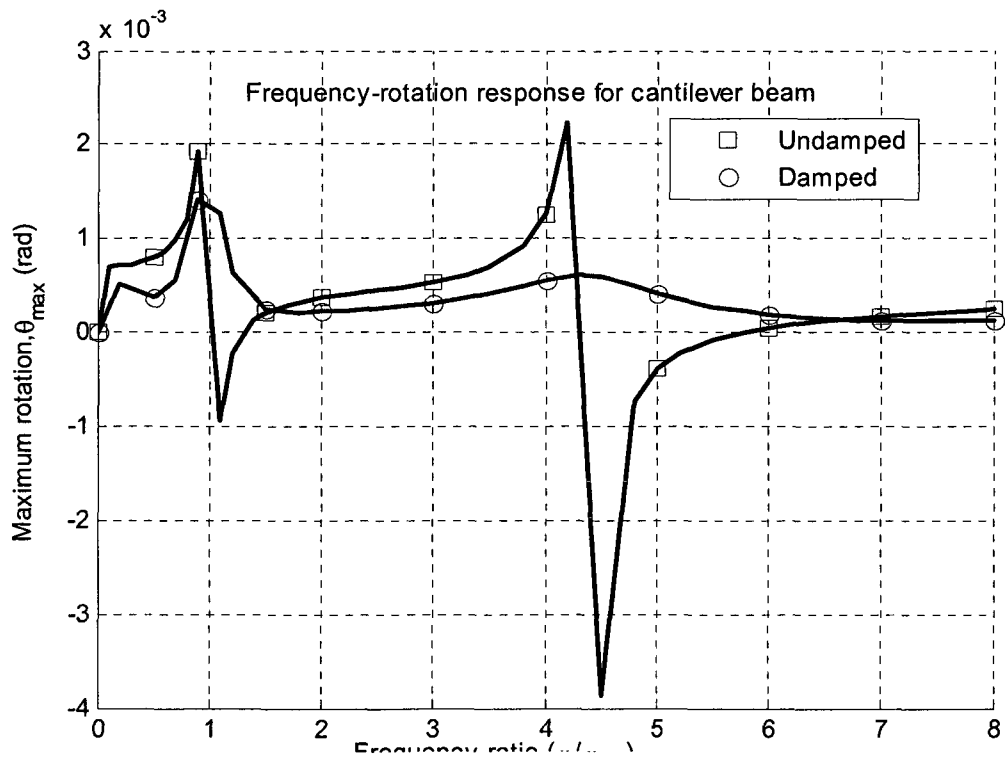


Figure 5.48 Frequency-rotation of beam with taper configuration-A

One can observe the effect of damping loss factor on transverse displacement and rotation (forced response) of beam with taper configuration-A for fixed-free boundary condition from the Figures 5.47 and 5.48. Transverse displacement and rotation obtained from considering damping loss are less than the transverse displacement and rotation obtained without damping loss.

Example 5.8.2

A sinusoidal force of magnitude 2 N and a sinusoidal moment of magnitude 2 N-m with excitation frequency ω are applied at free end of cantilever beam with taper configuration-B. By using the mechanical properties as described in the section 5.2, the example 5.8.2 is solved to calculate the forced response in terms of transverse displacement and rotation at the free end of the beam. The forced response in terms of the magnitude of sinusoidal transverse displacement and the magnitude of sinusoidal rotation are obtained considering 12-elements mesh using higher-order finite element and presented in Figures 5.49 and 5.50.

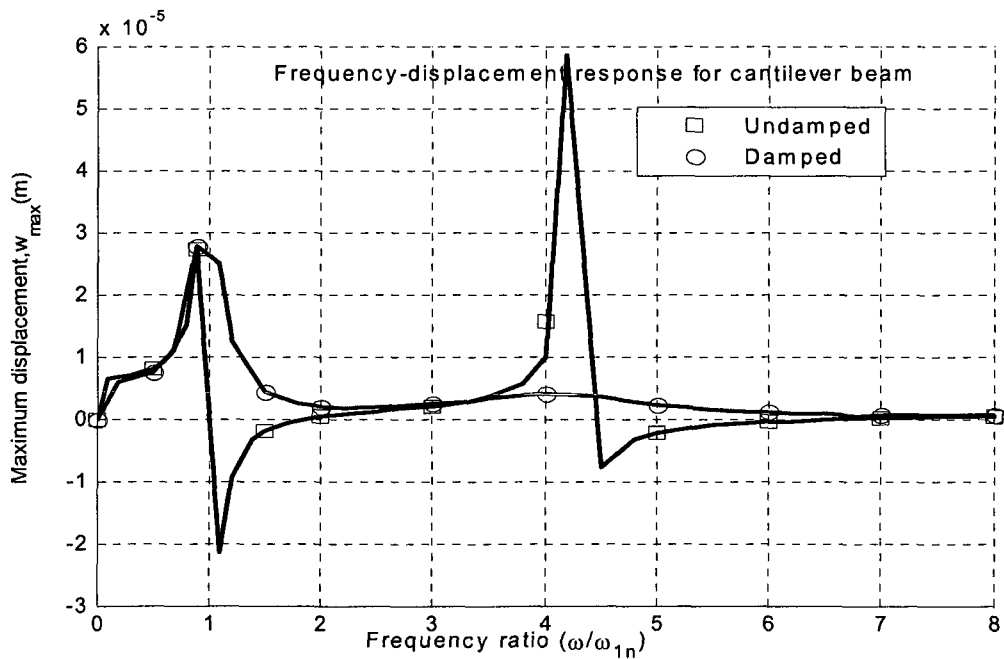


Figure 5.49 Frequency-displacement plot of beam with taper configuration-B

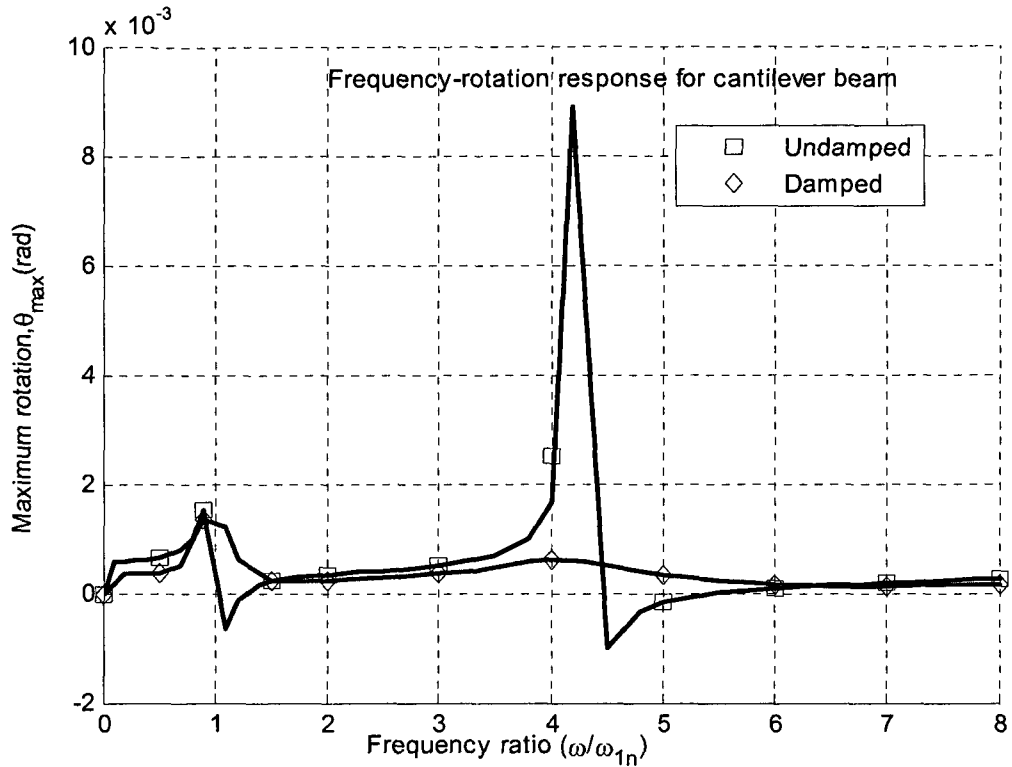


Figure 5.50 Frequency-rotation plot of beam with taper configuration-B

One can observe the effect of transverse displacement and rotation (forced response) of beam with taper configuration-B for fixed-free boundary condition from the Figures 5.49 and 5.50. Transverse displacement and rotation obtained from considering with damping loss are less than the transverse displacement and rotation obtained without damping loss.

Example 5.8.3

A sinusoidal force of magnitude 2 N and a sinusoidal moment of magnitude 2 N-m with excitation frequency ω are applied at free end of cantilever beam with taper configuration-C. By using the mechanical properties as described in the section 5.2, the example 5.8.3 is solved to calculate the forced response in terms of transverse displacement and rotation at the free end of the beam. The forced response in terms of the magnitude of sinusoidal transverse displacement and the magnitude of sinusoidal rotation are obtained

considering 12-elements mesh using higher-order finite element and presented in Figures 5.51 and 5.52.

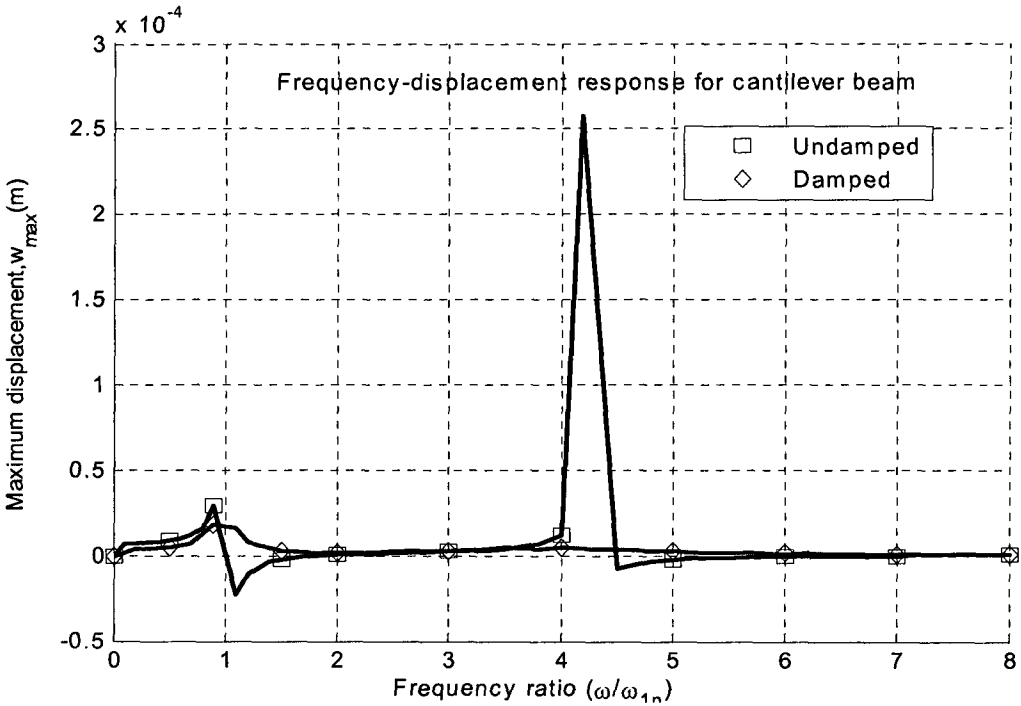


Figure 5. 51 Frequency-displacement plot of beam with taper configuration-C

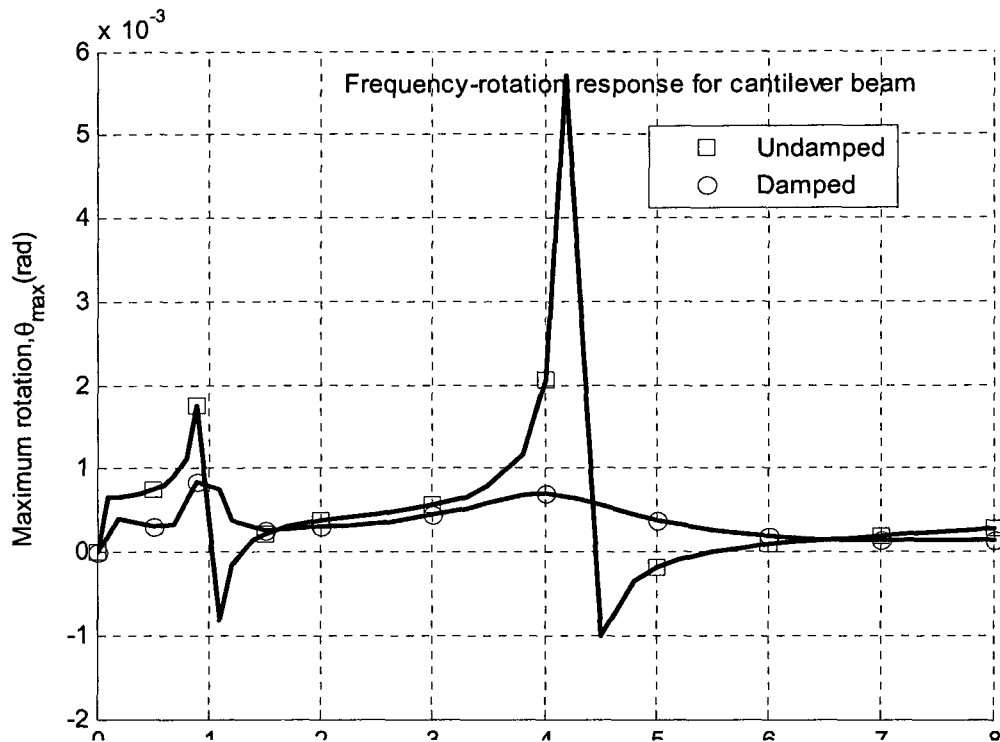


Figure 5.52 Frequency-rotation plot of beam with taper configuration-C

One can observe the effect of damping loss factor on transverse displacement and rotation (forced response) of beam with taper configuration-C for fixed-free boundary condition from the Figures 5.51 and 5.52. Transverse displacement and rotation obtained from considering with damping loss are less than the transverse displacement and rotation obtained without damping loss.

Example 5.8.4

A sinusoidal force of magnitude 2 N and a sinusoidal moment of magnitude 2 N-m with excitation frequency ω are applied at free end of cantilever beam with taper configuration-D. By using the mechanical properties as described in the section 5.2, the example 5.8.4 is solved to calculate the forced response in terms of transverse displacement and rotation at the free end of the beam. The forced response in terms of the magnitude of sinusoidal transverse

displacement and the magnitude of sinusoidal rotation are obtained considering 12-elements mesh using higher-order finite element and presented in Figures 5.53 and 5.54.

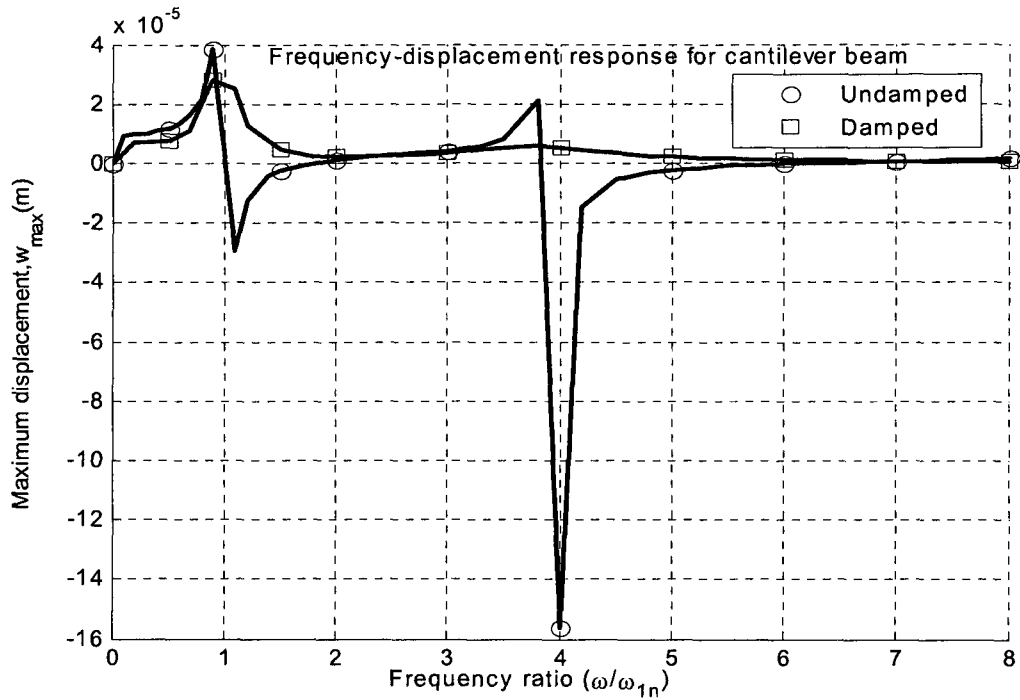


Figure 5. 53 Frequency-displacement plot of beam with taper configuration-D

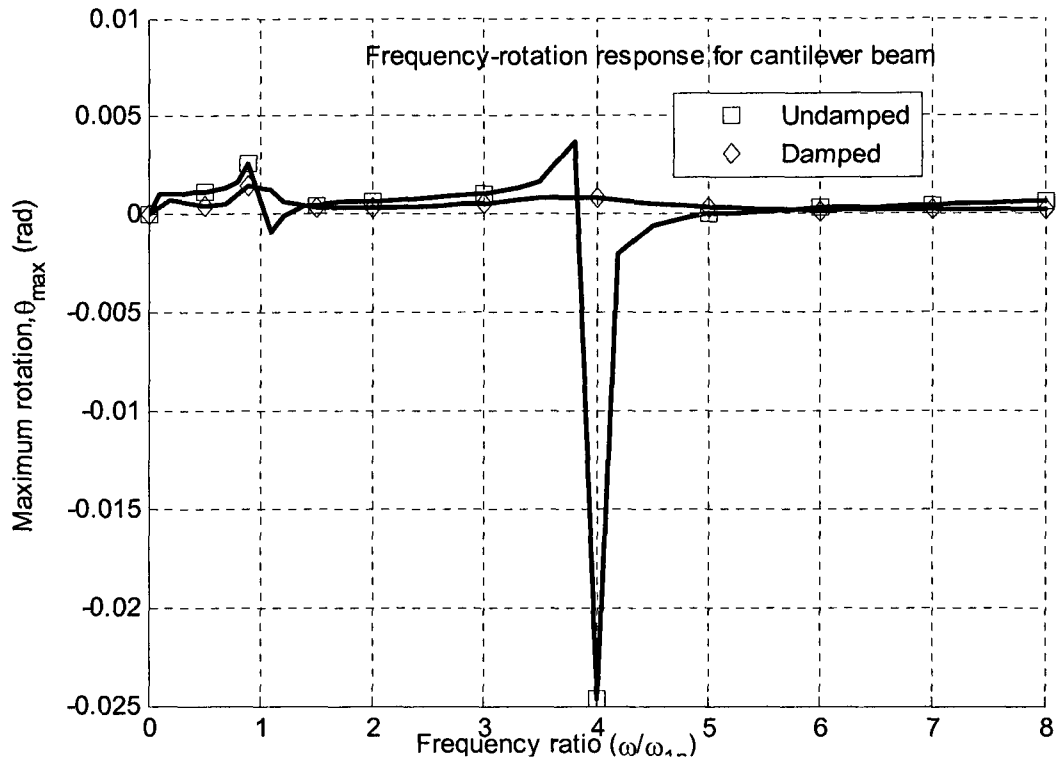


Figure 5.54 Frequency-rotation plot of beam with taper configuration-D

One can observe the effect of damping on transverse displacement and rotation of beam with taper configuration-D for fixed-free boundary condition from the Figures 5.53 and 5.54. Transverse displacement and rotation obtained from considering with damping loss are less than the transverse displacement and rotation obtained without damping loss.

Example 5.8.5

A sinusoidal force of magnitude 2 N and a sinusoidal moment of magnitude 2 N-m with excitation frequency ω are applied at free end of cantilever beam with taper configuration-C. By using the mechanical properties as described in the section 5.2, the example 5.8.5 is solved to calculate the effect on the forced response in terms of transverse displacement and rotation of different laminate configurations at the free end of the beam. The forced response in terms of the magnitude of sinusoidal transverse displacement and the

magnitude of sinusoidal rotation for fixed-free boundary condition are obtained considering 12-elements mesh using higher-order finite element and presented in Figures 5.55 and 5.56.

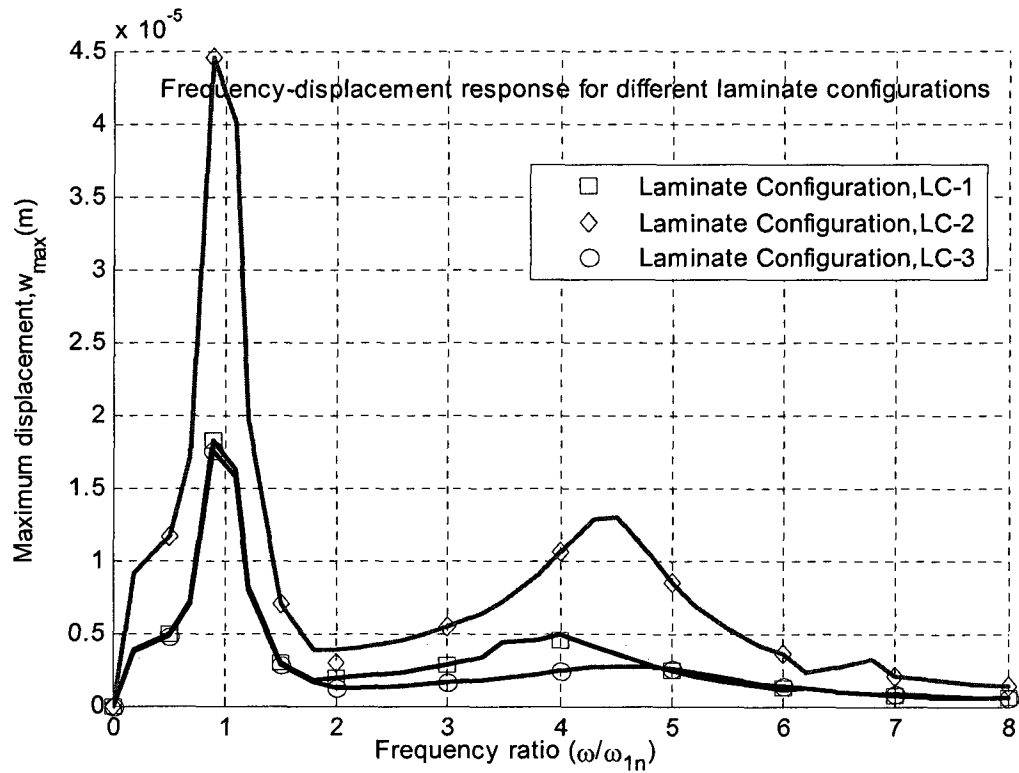


Figure 5. 55 Frequency-displacement plot of beam with taper configuration-C

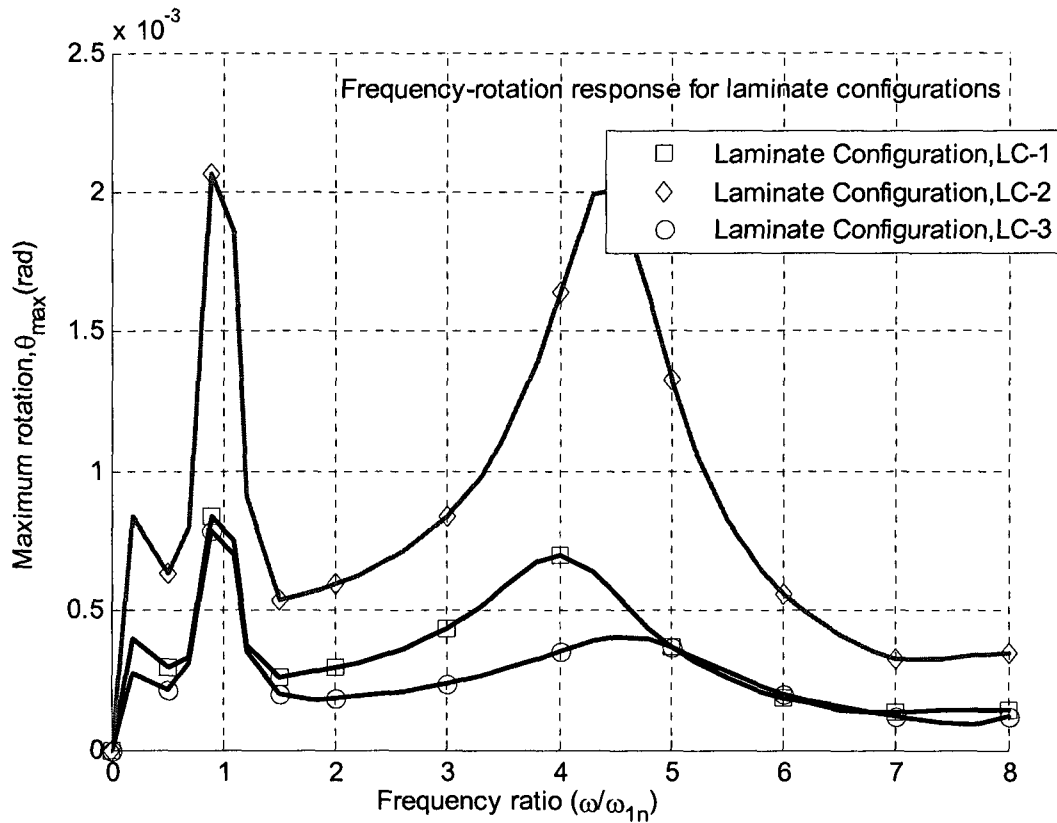


Figure 5. 56 Frequency-rotation plot of beam with taper configuration-C for cantilever boundary condition

One can observe the effect of damping loss factor on forced response in terms of transverse displacement and rotation for different laminate configurations of beam with taper configuration-C at fixed-free boundary condition from the Figures 5.55 and 5.56. The forced response in terms of transverse displacement and rotation for LC-2 are highest and the response for the other two laminate configurations are very close to each other except where frequency ratio (excitation frequency to first natural frequency) is in the range of 2 to 5.

Example 5.8.6

A sinusoidal force of magnitude 2 N and a sinusoidal moment of magnitude 2 N-m with excitation frequency ω are applied at free end of cantilever beam with taper configuration-D. By using the mechanical properties as described in the section 5.2, the example 5.8.6 is solved to calculate the forced response in terms of transverse displacement and rotation with the variation of damping properties of beam with taper configuration-D for fixed-free boundary condition. The values of the mass proportional constant, (α) and stiffness proportional constant (β) were increased by 20%, 50%, and 100%, and the other two cases are when mass proportional constant is increased by 50% of original value and stiffness constant is kept constant, and when stiffness proportional constant is increased by 50% of original value and mass proportional constant is kept constant. These are assigned names as damped case-1, damped case-2, damped case-3, damped case-4, and damped case-5 respectively and the effect on damped forced response was observed. The forced response in terms of the magnitude of sinusoidal transverse displacement and the magnitude of sinusoidal rotation are obtained considering 12-elements mesh using higher-order finite element and presented in Figures 5.57 and 5.58

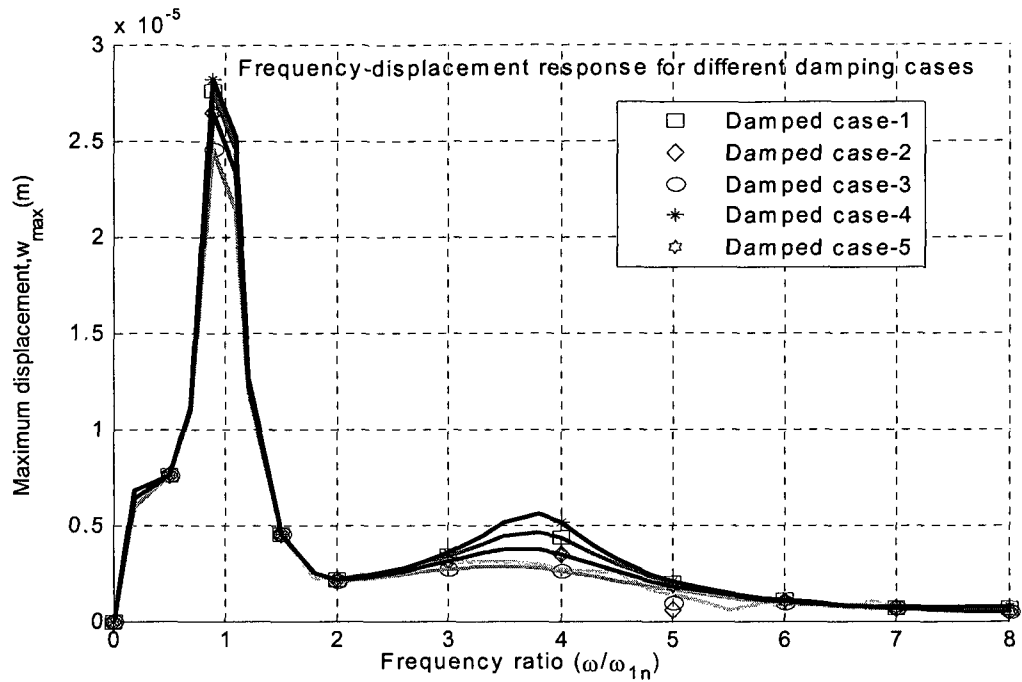


Figure 5.57 Frequency-displacement plot of beam with taper configuration-D

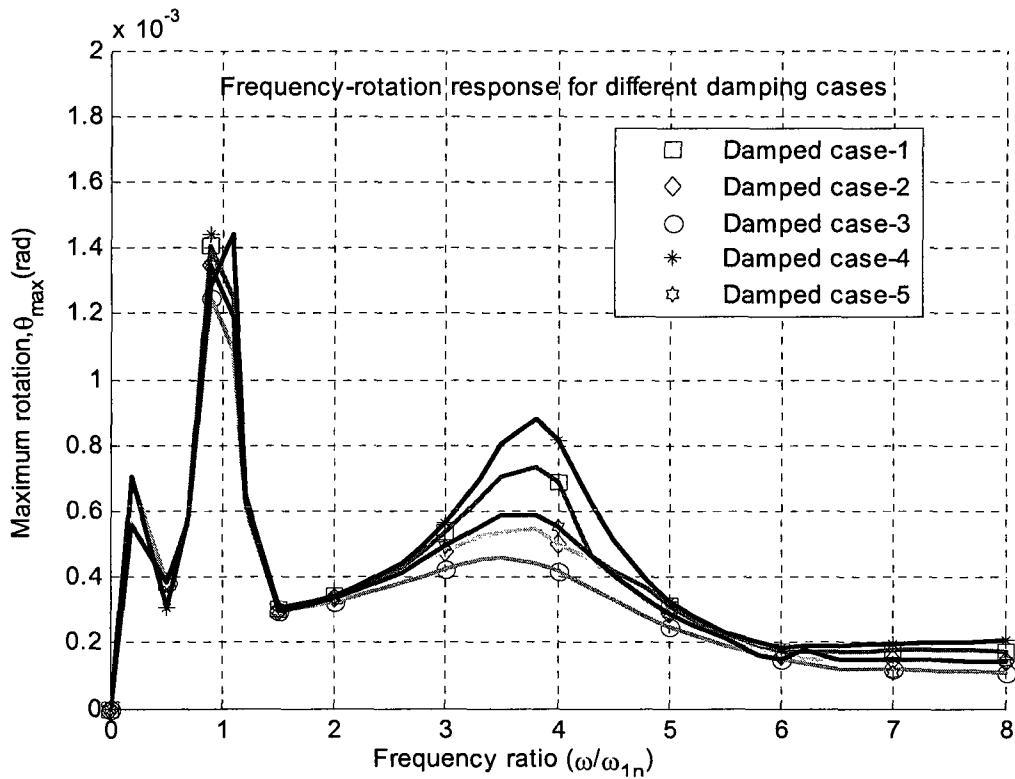


Figure 5.58 Frequency-rotation plot of beam with taper configuration-D

One can observe the effect of damping loss factor on forced response in terms of transverse displacement and rotation with the variation of damping properties of beam with taper configuration-D for fixed-free boundary condition from the Figures 5.57 and 5.58. The results obtained for different values of damping loss factor show that transverse displacement and rotation (forced response) obtained from considering the highest damping loss are less than transverse displacement and rotation obtained from considering the lowest damping loss respectively. It is also observed that stiffness proportional constant has more effect on transverse displacement and rotation (forced response) than mass proportional constant. The transverse displacement and rotation (forced response) are less when stiffness proportional constant is increased by 50% of original value (and value of mass proportional constant is kept constant) than when mass proportional constant is increased by 50% of original value (and value of stiffness proportional constant is kept constant).

5.9 Conclusion and discussion

In this chapter, forced vibration analysis for different types of tapered laminated composite beam are performed using conventional finite element, higher-order finite element and Rayleigh-Ritz method. Four different types of taper laminate configurations (taper configurations-A, B, C, and D) are considered in the analysis. Forced response results in terms of transverse displacement and rotation obtained from conventional finite element and higher-order finite element methods are compared with Rayleigh-Ritz method and that shows a good agreement.

A parametric study has been conducted in terms of different laminate configurations, various taper angles and different length-ratios using fixed-free boundary condition. The effects of additionally applied axial force and damping on forced response for transverse displacement and rotation of taper composite beam have also been investigated. Following observations are made after studying all the above-mentioned parameters and comparing results:

- The results obtained for different types of taper configuration show that transverse displacement and rotation (forced response) obtained for taper configuration-D are the lowest; then taper configurations-B, C and A ranked second, third and fourth in terms of lowest response respectively.
- The results obtained for different types of laminate configurations show that transverse displacement and rotation (forced response) obtained from laminate configuration LC-3 (that has $[0_4 / \pm 45_7]_s$ configuration at thick section and $[0_4 / \pm 45]_s$ configuration at thin section) gives the lowest values; then laminate configuration LC-1 (that has $[0/90]_{9s}$ configuration at thick section and $[0/90]_{3s}$ configuration at thin section) ranked second and laminate configuration LC-2 (that has $[\pm 45]_{9s}$ configuration at thick section and $[\pm 45]_{3s}$ configuration at thin section) gives the highest values.
- Transverse displacement and rotation (forced response) obtained from highest taper angle are the lowest and lowest taper angle gives the highest response. The transverse displacement and rotation (forced response) are decreasing with the increasing of taper angle values, because the length of the beam decreases with the increasing of taper angle which makes it stiffer that results in lower transverse displacement and rotation (forced response) and vice versa.

- The results obtained for different values of length ratio show that transverse displacement and rotation (forced response) obtained from highest length ratio are the lowest and lowest length ratio gives the highest response.
- Beam with fixed-fixed boundary condition gives the lowest transverse displacement and rotation (forced response) that means at this boundary condition the beam gets highest stiffness and beam with (thick end) free-(thin end) fixed boundary condition gives the highest transverse displacement and rotation that means at this boundary condition the beam gets lowest stiffness. Then beam with (thick end) fixed-(thin end) free and simply supported ranked second and third position in terms of highest response respectively. Beam with (thick end) fixed-(thin end) hinged and (thick end) hinged-(thin end) fixed boundary condition gives almost the same transverse displacement and rotation respectively.
- Forced response in terms of transverse displacement and rotation of beam with end tensile axial force are lower than the transverse displacement and rotation without axial force effect at fixed-free boundary condition. With increasing of tensile axial force the response is decreasing, as the beam is getting stiffer with the addition of tensile axial force. Forced response in terms of transverse displacement and rotation of beam with end compressive axial force are higher than the transverse displacement and rotation without axial force at fixed-free boundary condition. With increasing of compressive axial force the response is increasing as the beam is losing stiffness with the addition of compressive axial force.
- Forced response in terms of transverse displacement and rotation of un-damped beam are higher than the transverse displacement and rotation with damping at fixed-free boundary condition. It is also observed that stiffness proportional constant has more effect on both transverse displacement and rotation than mass proportional constant.

Chapter-6

Conclusion

In the present thesis, free and forced vibration analyses of composite beams have been conducted using conventional finite element, higher-order finite element and Rayleigh-Ritz methods. The free and forced vibration analyses of uniform-thickness beam and different types of tapered configuration composite beams have been conducted. Equations have been derived for energy method based on Euler-Bernoulli beam theory and adapted to free and forced vibration analysis with and without damping of one-dimensional composite beam. Some experimental work was done to get the mechanical properties and damping loss factor. Several specimens from a laminated plate were used to get the damping loss factor of NCT-301 graphite-epoxy composite material using modal testing. Damping loss factor (η) is extracted from the FRF plots by using half power bandwidth method.

The conventional finite element, higher-order finite element and Rayleigh-Ritz method formulations have been derived in detail to bring out the efficiency and accuracy very systematically. Formulations have been developed for free and forced vibrations of tapered composite beams considering axial concentrated and distributed forces. Effects of different types of laminate configuration such as cross-ply and angle ply and different types of boundary conditions have been investigated on natural frequencies and modal displacement and rotation.

The conventional finite element model for composite beam structure is considered with two degrees of freedom per node; displacement and slope that satisfy the geometric boundary conditions. The higher-order finite element model is considered with four degrees of freedom per node; displacement, slope, curvature and gradient of curvature. Higher-order finite

element method has removed the disadvantages of conventional finite element method that needs large number of elements to achieve accurate results as well as the linear variation of curvature along the length of the element. It has also removed the limitations of the advanced finite element developed in ref. [29] (wherein shear force and bending moment were used as additional degrees of freedom rather than curvature and gradient of curvature) for forced vibration analysis. Comparisons between the results obtained using the conventional and higher-order finite elements are inherent. Results obtained by using higher-order finite element method are also validated by using the approximate solution given by Rayleigh-Ritz method. The formulation enhances the capability of the element by increasing the degree of the approximate (polynomial) functions.

The code of programming, involving numerical and symbolic computations is written in MATLAB software. The element properties such as stiffness matrix, mass matrix and force matrix are computed numerically using individual subprograms.

A detailed parametric study has been conducted using the above-mentioned theoretical developments to determine the influence of the material properties, geometric properties and applied axial force on the natural frequencies and maximum modal displacement and rotation response. The effects of taper configuration, taper angle, length ratio, boundary conditions, and laminate configuration, axial concentrated and distributed forces and damping on natural frequencies and modal displacement and rotation response are studied.

The study done in this thesis is of great importance to the researcher and mechanical designer who does research and design composite structure to withstand dynamic loads. The most important and principal contributions of this thesis that has provided some conclusion

on the design and analysis of uniform-thickness and tapered composite beams with dynamic loads are given below:

1) Experimental work for determination of mechanical properties and damping loss factor is done for NCT-301 graphite-epoxy composite beams using uni-axial and modal testing respectively. Calculated damping properties is used to calculate average proportional mass and stiffness constants that are used in the finite element analysis to form a Rayleigh damping matrix [C] as a linear combination of mass and stiffness matrices.

2) It has been shown that more accurate results can be obtained by increasing the number of degrees of freedom than that have the same or lower degrees of freedom. Then a finite element considers both the primary (deflection and slope) and secondary (curvature and gradient of curvature) variables at each node of the beam element.

3) From the observation of results and analyses, it is found that tapered beam made with taper configuration-D has the highest stiffness and configuration-A has the lowest stiffness. Correspondingly taper configuration-D has the highest natural frequencies and configuration-A has the lowest. Beam with configuration-B and that with configuration-C ranked in 2nd and 3rd respectively for both stiffness and natural frequencies. Observation of the plots of the magnitudes of sinusoidal displacement and sinusoidal rotation response verses frequency ratio for individual boundary conditions for all configuration beams shows that higher transverse deflection and rotation occur for taper configuration-A. Configuration-C, configuration-B and configuration-D show the lower response respectively.

4) Observation for different boundary conditions shows that fixed-fixed beam has the highest natural frequencies and the simply supported and cantilever beams have the lower frequencies respectively. Cantilevered and (Thick end) free- (thin end) fixed beam always

show highest values for both transverse displacement and rotation response when force and moment were applied at free end of beam. The natural frequencies and forced response in terms of displacement and rotation for (thick end) fixed-(thin end) hinged and (thick end) hinged-(thin end) fixed boundary conditions of beam are also observed. Beam with (thick end) fixed-(thin end) hinged and (thick end) hinged-(thin end)fixed boundary conditions give almost the same natural frequencies and forced response in terms of transverse displacement and rotation.

5) Comparison of the results for natural frequencies and forced response in terms of transverse displacement and rotation obtained by using different finite elements with that of Rayleigh-Ritz method is done. The results found with 5 to 7 trial functions of Rayleigh-Ritz method matched well with the results calculated by using conventional and higher-order finite elements for uniform-thickness and all tapered beams for all types of boundary conditions.

6) It is concluded from the parametric study that first four natural frequencies of LC-3 (that has $[0_4 / \pm 45_7]_s$ configuration at thick section is and $[0_4 / \pm 45]_s$ configuration at thin section) laminate configuration are highest among that of different laminate configurations and lowest for LC-2 (that has $[\pm 45]_{9s}$ configuration at thick section and $[\pm 45]_{3s}$ configuration at thin section) for all types of taper composite beam configurations. LC-2 always shows the maximum displacement and rotation and LC-3 shows comparatively less value than the others laminate configuration. LC-1 (that has $[0/90]_{9s}$ configuration at thick section and $[0/90]_{3s}$ configuration at thin section) is in between among different laminate configurations both in free and forced vibration response.

7) Free and forced vibration analysis for different taper angles of composite beams shows that lower values of taper angle leads to higher natural frequencies and lower forced response whereas higher taper angle always shows lower natural frequencies and maximum displacement and rotation for all boundary conditions.

8) It has been concluded from the parametric study among three considered length ratios that high length ratio leads to higher natural frequencies whereas lower length ratio leads to lower natural frequencies for all boundary conditions. Comparison for forced vibration analysis shows that the maximum displacement and rotation occur for lower length ratio and vice versa.

9) It was observed that natural frequencies obtained considering the axial force acting at the end of uniform-thickness and taper beam with all boundary conditions are more for tensile force and less for compressive axial force than the frequencies obtained when it is considered without any axial force. Forced response in terms of transverse displacement and rotation obtained considering the axial compressive force are more and they are less for the axial tensile force acting at the end of uniform-thickness and taper beam than the transverse displacement and rotation obtained considering without any axial force effect. With the increasing of tensile axial force, the forced response is decreasing as the beam is getting stiffer with the addition of tensile axial force and with the increasing of compressive axial force, the forced response is increasing as the beam is losing stiffness with the addition of compressive axial force.

10) By observing the results of parametric study conducted with and without damping effects, natural frequencies are less when considering damping than that obtained without damping for all boundary conditions. Forced response in terms of transverse displacement

and rotation are less considering damping than that obtained without damping. It is also observed that stiffness proportional constant has more effect on natural frequencies and forced response in terms of more response than mass proportional constant.

The study of free and forced vibration of tapered composite beam can be continued in the future studies on these following recommendations:

1. Forced vibration analyses using both conventional and higher-order finite elements and Rayleigh-Ritz method presented in this thesis can be extended for Timoshenko beam.
2. Forced vibration analyses using both conventional and higher-order finite element methods presented in this thesis can be formulated with other finite element methods such as hierarchical finite element method.
3. Free and forced vibration analyses of tapered composite beam using both conventional and higher-order finite elements and Rayleigh-Ritz method presented in this thesis can be extended to transient and random vibrations.
4. Free and forced vibration analysis using both conventional and higher-order finite element methods presented in this thesis can be extended for free and forced vibration analysis of curved beam, plates and shell.

References

- [1] S.S.Rao, "Vibration of continuous systems", Hoboken, N.J. Wiley, 2007.
- [2] O.O. Ochoa and J.N. Reddy, Finite Element Analysis of Composite laminates, 1992, Kluwer Academic Publishers.
- [3] Y.W. Know and H. Bang, "The Finite Element Method Using Matlab", 1997, CRC Press.
- [4] A.W.Leissa, "The historical bases of the Rayleigh and Ritz methods", Journal of Sound and Vibration, Vol.287, 2005, pp. 961-978.
- [5] Ibrahim,MD, "Effect of notch size on the reliability of composite laminates based on stochastic finite element analysis and experimental investigation", M.A.Sc.Thesis, 2000, Concordia university, Montreal, Canada.
- [6] S.A.Suarez, R.F.Gibson, L.R.Deobald, "Random and impulse techniques for measurement of damping in composite materials", Experimental Techniques, 1984, pp.19-24.
- [7] W.D. Morison, "The prediction of material damping of laminated composites", Journal of Canadian Aeronautics and Space, 28(4), 1982, pp.372-382.
- [8] S.V.Hoa and P.Ouellette, " Damping of composite materials", Polymer Composite, 5(4) 1984, pp.334-337.
- [9] R.F.Gibbson, "Dynamical mechanical properties of advanced composite materials and structures: A review", Shock and Vibration Digest, 19(7), 1978,pp13-22.
- [10] R.D Adams and D.G.C. Bacon, " Effect of fiber orientation and laminate geometry on the dynamic properties of CFRP", Journal of Composite materials, 7(4), 1973,pp.402-428.

- [11] Zabaraz, N. and Pervez, T, "Viscous damping approximation of laminated anisotropic composite plates using the finite element method." *Computer methods in applied mechanics and engineering*, Vol.81 1990, pp. 291-316.
- [12] Wei, C.Y. and Kukureka, S.N. " Evaluation of Damping and Elastic Properties of Composite and Composite Structures by the Resonance Technique", *Journal of Materials science*, Vol.35, 2000,pp. 378-392.
- [13] Adams, R.D. and Maheri, M.R., " Damping in Advanced polymer-matrix composite", *Journal of Alloys and Composite*, Vol.355, 2003, pp. 126-130.
- [14] Sefaroni, Y and Bertholet, J.M. " Temperature Effect on the Damping Properties of Unidirectional Glass-fiber Composite", *Journal of Composite Part: B*, Vol.37, 2006, pp.346-355.
- [15] Colakoglu, M. " Damping and Vibration Analysis of Polyethylene Fiber Composite under Varied Temperature", *Turkish Journal of Engineering and Environmental Science*, Vol.30, 2006, pp. 351-357.
- [16] J. Thomas and E. Dokumaci , " Improved finite elements for vibration analysis of tapered beam", *Aeronautical Quarterly*, Vol-24 1973 pp. 39-46.
- [17] C.W.S.To, " Higher order tapered beams finite elements for vibration analysis" *Journal of Sound and Vibration*, Vol.63,1979, pp. 33-50.
- [18] Balasubramaniam, TS. And Subramanian, G, "On the performance of a four-degree-of-freedom per node element for stepped beam analysis and higher frequency estimation.", *Journal of Sound and Vibration*, Vol. 99. 1985, pp. 563-567.

- [19] Heyliger P R, Reddy J N , “ A higher order beam finite element for bending and vibration problems.” Journal of Sound and Vibration, Vol. 126. 1988, pp.309-326.
- [20] Gupto R.S. and Rao. S.S., “ Finite element vibration analysis of tapered and twisted Timoshenko beams.” Journal of Sound and Vibration, Vol. 56. 1978, pp.178-200.
- [21] S.R. Marur and Kant,T . “A higher order finite element model for the vibration analysis of laminated beams”, Journal of vibration and Acoustics, ASME Vol.120 No.3 pp.822-4.
- [22] Yuan, F and miller, R.E., “A higher order finite element for Laminate Composite Beams”, Computers and Structures, Vol.31, 1990,pp.125-150.
- [23] Manjunatha,B.S. and Kant,T., “New theories of for symmetric and Unsymmetrical composite and sandwich beams with C^0 Finite element “, Composite Structures, Vol.23, 1993,pp.61-73.
- [24] Prathap,G and Vinayak, R.U., “ Vibrations of laminated beams using higher-order theory”, Advanced Composite structure. Vol.6, No.1, pp 33-50.
- [25] Shi,G and Lam, K.Y., “ Finite element vibration analysis of composite beams based on higher –order beam theory”, Journal of sound and vibration Vol.219, No.4, pp707-721.
- [26] Cleghorn, W.L and Tabarrok, B., “Finite Element Formulations of a Tapered Timoshenko Beam for Free Vibration Analysis.” Journal of sound and vibration Vol152, No.3,1997, pp461-470.

- [27] Rao, Ramalingeswara, S. and Ganesan, N., "Dynamic Response of Tapered Composite beam Using Higher Order Shear deformation Theory", Journal of sound and vibration Vol.187, No.5, 1995 pp737-756.
- [28] Nigam, Amit, "Dynamic Analysis of Composite Beams Using Hierarchical Finite Element Formulations." M.A.Sc.Thesis, 2000,Concordia University, Montreal, Canada.
- [29] Zabihollah, A, "Vibration and Buckling Analysis of tapered Composite Beams using Conventional and Advanced Finite Element Formulations", M.A.Sc.Thesis, 2003, Concordia University, Montreal, Canada.
- [30] Abarcar,R.B. and Cunniff, P.F., "The vibration of cantilevered Beam of Fibre Reinforced Material", Journal of Composite Materials, Vol.6, 1972, pp.504-516
- [31] Miller, A.K. and Adams, D.F., "An Analytical means of determining the Flexural and Torsional Resonant Frequencies of Generally Orthotropic beams", Journal of sound and vibration Vol41, 1975, pp433-449.
- [32] Cheng, A.T and Yang, T.Y., "Static and Dynamic formulation of Symmetrically Laminated Beam Finite Element for Microcomputer", Journal of Composite Materials,Vol.19, 1985, pp459-475.
- [33] Chandrashekhara, K., Krisnamurthy, K. and Roy, S., " Free Vibrations of Composite beams including Rotary Inertia and Shear Deformation", Composite Structure, Vol.14, 1990, pp. 269-279.
- [34] Hodges, Dewey H., Atilgan, Ali R., Fulton Mark V and Rehfield L.W., " Free vibration of Composite beams" ,Journal of American Helicopter Society, Vol.36(3) 1991,pp.36-47.

- [35] Krishanaswamy, S. Chandrashekhara, K. and Wu, W.Z.B., “ Analytical Solutions to Vibration of Generally Layered Composite Beams”, *Journal of Sound and Vibration*, Vol.159 (1), 1992,pp.85-99.
- [36] Zeng, P., “Composite element method for vibration analysis of structure, Part II: C¹ element (beam)”, *Journal of Sound and Vibration*, Vol.218 (4), 1992,pp.659-696.
- [37] Khedeir,A.A.,and Reddy, J.N. “ Free vibration of cross-ply Laminated Beams with Arbitrary Boundary Conditions” ,*International Journal of Engineering*, Vol.32(12), 1994,pp. 1971-1980.
- [38] Abramovich, H and Livshits, A., “Free vibration of Non-symmetric Cross-ply Laminated Composite beams”, *Journal of Sound and Vibration*, Vol.176 (5), 1994, pp.596-612.
- [39] Houmat, A., “Vibration of Temoshenko Beams by Variable order Finite Elements”, *Journal of Sound and Vibration*, Vol.187, 1995, pp. 841-849.
- [40] Singh, M. P. and Abdelnassar, A.S., “Random response of Symmetric Cross-ply Composite beams with Arbitrary Boundary Conditions”, *AIAA Journal*, Vol.30 (4), 1992,pp.1081-1088.
- [41] Chen, J.K. and Sun, C.T., “Dynamic Large Deflection Response of Composite Laminate Subjected to Impact”, *Journal of Composite Structures*, Vol.4, 1985, pp. 59-73.
- [42] Lips, J.A., Kasper, E.P., and Welsh, J.S., “Finite Element Methods for the Frequency Response Prediction of Bonded Composite Structures”, *Journal of Composite Structures*, Vol.40, 2005, pp.1175-1192

- [43] Amit. K. O., Yadav, D., “Forced nonlinear vibration of laminated composite plates with random material properties ”, *Journal of Composite Structures*, Vol.70, 2005, pp.334-342
- [44] Asghar N, Rakesh K K and J N Reddy, “Forced vibration and low-velocity impact of laminated composite plates” *Journal of Computational Mechanics*, Vol.13, 1994, pp.360–379,
- [45] Cheung, Y.K. and Zhou, D, “ Vibration analysis of symmetrically laminated rectangular plates with intermediate line supports”, *Journal of Computers and Structures*, Vol. 79, 2001, pp.33.41
- [46] Kadivar, M.H. and Mohebpour, S.R., “ Forced vibration of unsymmetrical laminated composite beams under the action of moving loads”, *Journal of Composites Science and Technology*, Vol. 58, 1998, *pp.* 1675-1684
- [47] Beytullah T, Farouk, F.C. and Naki T. “ Forced vibration of composite cylindrical helical rods”, *International Journal of Mechanical Science*, Vol.45, 2005, pp.998-1022.
- [48] Azrar,I, Benamar, R and White R.G., “ A Semi-analytical approach to the non-linear dynamic response problem of S-S and C-C beams at large vibration amplitudes Part I: General theory and Application to the single mode approach to free and forced vibration analysis”, *Journal of Sound and Vibration*, Vol.224 (2), 1999, pp.183-207.
- [49] Faruk, F.C , “ Free and forced vibrations of non-uniform composite beams”, *Journal of Composite Structures*, 2008, article in press.

- [50] ASTM E 756-98, "Standard Test Method for Measuring Vibration-Damping Properties of materials".
- [51] Gowtesky T.G, "Advanced Composites Manufacturing", A Wiley interscience publication,1997.
- [52] Bertholet, J.M., Assarar,M., Sefrani,Y., Mahi,A.E, "Damping analysis of composite materials and structures", Composite Structures, 2007, In press.
- [53] Maher,A., Ramadan,F.,and Ferra, M., "Modeling of vibration damping in composite structures", Composite Structures, 46 (1999) 163-170.
- [54] Jones, R.M., Mechanics of Composite Materials,1975, Scripta Book Co., Washington
- [55] Reddy, J.N, Mechanics of laminated composite plates-Theory and Analysis, 1997, CRC press, U.S.A
- [56] Thomson, W.T. and Dahleh, M.D, Theory of Vibration With Applications, Fifth edition, Prentice Hall, New Jersey.
- [57] Bertholet, J.M., Composite Materials-Mechanical Behavior and Structural Analysis, 1999, Springer verlag, New York.
- [58] Kelly, S.G, Advanced Vibration Analysis, 2007, CRC Press, Taylor's and Francis group, UK
- [59] A.D Nashif, D.I.G. Jones and J.P. Henderson, Vibration damping, 1985, Wiley, New York.
- [60] Inman, D.J., Engineering Vibration, second edition, 2001, Prentice Hall, New Jersey.

Appendix

MATLAB program development for vibration analysis

In this section the MATLAB programming sequence are described which are developed to compute the natural frequency and forced response. Free and forced vibrations are carried out for both uniform-thickness and variable-thickness (Taper configuration) composite beam using finite element modeling. Detailed descriptions of different subroutines are given below:

Dmat: The function of this subroutine is to find out the value of D for specific composite beam. It takes the some geometric (ply stacking sequence) and materials properties as input data and gives the value of D for different elements.

Kt and Km: The function of these subroutines is to find out the value of K (stiffness) for individual element. It takes the value of D , shape function and geometric properties as input and gives the stiffness values for individual element.

Kmid: The function of these subroutines is to find out the value of K (stiffness) for whole taper configuration composite beam. It takes the value of K_t and K_m and some geometric properties as input and gives the stiffness values for whole tapered beam under specific taper angle.

Mmid: This subroutine function calculates the values of mass matrix for composite beam by taking some geometric values such as shape function, density, area etc. as input.

KM: The sub-function gathers the values of the stiffness and mass matrix from individual element in one program.

Free_forced: It is the main function which calls the value of stiffness and mass matrix, assemble them for whole tapered beam, apply boundary conditions, solve the Eigen value problem to give Eigen values and Eigen vectors and then solve the response for forced vibration.

Elindex: This sub-function is called in main function, which helps make index for assembling the matrices.

Elasmb1: This sub-function is used to assemble the element matrices.

Symbc: This sub-function is also called in main function to apply the beam boundary conditions.

Flow chart for MATLAB Programming

